COMPARISON AND EVALUATION OF VARIOUS MESFET MODELS

A THESIS SUBMITTED TO
THE GRADUATE SCHOOL OF NATURAL AND APPLIED SCIENCES
OF
MIDDLE EAST TECHNICAL UNIVERSITY

BY

MİRKAN ALTAY

IN PARTIAL FULFILLMENT OF THE REQUIREMENTS
FOR
THE DEGREE OF MASTER OF SCIENCE
IN
THE DEPARTMENT OF ELECTRICAL AND ELECTRONICS
ENGINEERING

MARCH 2005

Approval of the Graduate School of Natural and Applied Sciences

Prof. Dr. Canan ÖZGEN
Director

I certify that this thesis satisfies all the requirements as a thesis for the degree of Master of Science.

Prof.Dr. İsmet ERKMEN
Head of Department

This is to certify that we have read this thesis and that in our opinion it is fully adequate, in scope and quality, as a thesis for the degree of Master of Science.

Prof. Dr. Canan TOKER
Supervisor

Examining Committee Members

Prof. Dr. Nilgün GÜNALP (METU,EE)

Prof. Dr. Canan TOKER (METU,EE)

Prof. Dr. Gönül TURHAN SAYAN (METU,EE)

Asst. Prof. Dr. Şimşek DEMİR (METU,EE)

Asst. Prof. Dr. Yeşim YÜKSEL (Dokuz Eylül Uni,EE)

I hereby declare that all information in this document has been obtained and presented in accordance with academic rules and ethical conduct. I also declare that, as required by these rules and conduct, I have fully cited and referenced all material and results that are not original to this work.

ABSTRACT

COMPARISON AND EVALUATION OF VARIOUS MESFET MODELS

ALTAY, Mirkan
M.Sc., Department of Electrical and Electronics Engineering
Supervisor : Prof. Dr. Canan TOKER

March 2005, 179 pages

There exist various models for Microwave MESFET equivalent circuit representations. These models use different mathematical models to describe the same MESFET and give similar results. However, there are some differences in the results when compared to the experimental measurements. In this thesis, various theoretical models are applied to the same MESFET and comparison made with measured data. It is shown that some models worked better on some parameters of the MESFET, while the others were more effective on other parameters. Altogether eight models were examined and data optimized to fit these theoretical models. In using optimization algorithms MATLAB FMINSEARCH and GENETIC ALGORITHM CODE were used alternatively to solve the initial value problem.

Keywords: MESFET Modeling, Large-signal parameters

ÖZ

DEĞİŞİK MESFET MODELLERİNİN KARŞILAŞTIRILMALARI VE DEĞERLENDİRİLMESİ

ALTAY, Mirkan
Yüksek Lisans, Elektrik ve Elektronik Mühendisliği Bölümü
Tez Yöneticisi : Prof. Dr. Canan TOKER

Mart 2005, 179 sayfa

Mikrodalga MESFET'ler için bir çok eşdeğer devre gösterimi vardır. Bunlar aynı MESFET için değişik matematik modeller kullanmaktadırlar ve benzer sonuçlar vermektedirler. Ancak bu modeller, deneysel sonuçlarla karşılaştırıldığında farklı sonuçlar alınmaktadır. Bu tezde, değişik modeller aynı MESFET için uygulanmış ve bir karşılaştırma yapılmıştır. Bu çalışma sonucunda bazı modellerin bazı parametreler için daha iyi sonuç verdiği görülmüştür. Toplam sekiz model üzerinde çalışma yapılmış ve parametreler eniyileştirme yöntemleriyle ölçüm değerlerine yaklaştırılmaya çalışılmıştır. Eniyileştirme yöntemleri olarak MATLAB FMINSEARCH ve GENETIC ALGORITHM CODE programları birlikte kullanılarak, başlangıç değerleri ile ilgili olarak ortaya çıkan problemler aşılmaya çalışılmıştır.

Anahtar Kelimeler: MESFET Modelleme, Büyük işaret parametreleri

ACKNOWLEDGMENTS

I would like to express my deepest gratitude to Prof. Dr. Canan TOKER for his guidance, advice, encouragements, insight and mostly his patient during the study.

I would also like to thank Prof. Dr. Gönül TURHAN SAYAN for her valuable suggestions concerning the GENETIC ALGORITHM CODE..

I thank my parents and my sister without whose love, support, and guidance none of this would have been possible.

And I am also geatful to Asst. Prof. Dr. Yeşim YÜKSEL as she came from İzmir to Ankara inspite of her tiring studies.

Finally, I thank my best friends; Mesture, Önder and Kutlu for their valuable helps.

TABLE OF CONTENTS

PLAGIARISM iii

ABSTRACT iv

ÖZ v

ACKNOWLEDGMENTS vi

TABLE OF CONTENTS vii

LIST OF TABLES x

LIST OF FIGURES xi

CHAPTER

1. INTRODUCTION 1

2. METAL SEMICONDUCTOR FIELD EFFECT TRANSISTORS (MESFETS) 4

2.1 MESFET Principle of Operation 5

2.2 MESFET Description 10

2.3 I-V Characteristics of MESFET 11

2.4 Transconductance and Output Resistance 14

2.5 Capacitance- Voltage characteristics 16

3. DEVİCE MODELS 22

3.1 Small Signal Model 23

3.1.1 Physical Significance of Equivalent Circuit Element Values 24

3.1.1.1 Parasitic Inductances Ls, Lg, and Ld 24

3.1.1.2 Parasitic Resistances R_s, R_g, and R_d 26

3.1.1.3 Capacitances C_{gs}, C_{gd}, and C_{ds} 26

3.1.1.4 Transconductance g_m 26

3.1.1.5 Output Resistance, R_{ds} (Output Conductance, g_{ds}) 27

3.1.1.6 Transconductance Delay, τ 28

3.1.1.7 Charging Resistance, R_i 28

3.2 Large Signal Models....29

4. PARAMETER EXTRACTION....32

4.1 DC Data Measurements....33

4.1.1 Forward Bias Gate Measurements....35

4.1.2 Current-Voltage Behavior....35

4.1.3 Parasitic Resistances....37

4.2 Extraction of Small Signal Equivalent Circuits....38

4.2.1 Direct Extraction of Intrinsic Elements....39

4.2.2 Capacitance Extraction....42

4.2.3 Output Conductance and Transconductance Extraction....42

4.2.4 Extraction of τ and R_i....43

4.2.5 Comparison of Measured and Modeled S-parameter Data....44

4.2.6 Parasitic Inductance Extraction....44

4.3 Large-Signal Extraction....46

4.3.1 Non-linear Unconstrained Optimization....47

4.3.2 Fundamentals of Unconstrained Optimization....47

4.3.3 A large-Signal Parameter Extraction Methodology....50

5. MEASURED VALUES AND APPLICATION TO MODELS....53

5.1Measured Values....53

5.1.1 Forward-Bias gate Measurements....53

5.1.2 Breakdown Voltage Measurement....55

5.1.3 Pinch-off Voltage V_t Measurements....56

5.1.4 S-Parameters Measurements for Extrinsic Elements....56

5.1.5 $V_{ds} - I_{ds}$ Measurements....57

5.2 Large-Signal Models....58

5.2.1 Tajima Model [7]....60

5.2.2 Materka&Kacprzak Model [8] [9]....72

5.2.3 Curtice&Ettenberg Model [12]....82

5.2.4 Statz Model [10]....91

5.2.5 Curtice Model [3], [4], [5]....101

5.2.6 TriQuint's Own Model (TOM) [11] 111
5.2.7 Angelov Model [14]... 120
5.2.8 TriQuint's Own Model -2 (TOM-2) [13]................................... 131
6. CONCLUSION... 142
REFERENCES 148
APPENDICES
A. RESULTS OF DC I-V MEASUREMENTS 150
A.1 V-I data of 2x50 MESFET …………………………….......……... 144
A.2 V-I data of 2x150 MESFET …………………………..………..… 145
A.3 V-I data of 4x50 MESFET …………..………………………..……... 145
A.4 V-I data of 4x75 MESFET …….……………………………..……... 146
A.5 V-I data of 4x100 MESFET ……….…………………………...…… 146
A.6 V-I data of 4x125 MESFET …………..………………………...…… 147
A.7 V-I data of 4x150 MESFET ……………..……………………...….... 147
A.8 V-I data of 4x175 MESFET ………………..…………………...….... 148
A.9 V-I data of 6x50 MESFET ……………………..……………...……... 148
A.10 V-I data of 6x150 MESFET ……………………..……………...…... 149
B. MATLAB SCRIPTS.. 156

LIST OF TABLES

TABLES

5.1 $V_{gs} - I_g$ data obtained for source-short / drain open case [1] 54

5.2 $V_{gs} - I_g$ data obtained for drain -short / source-open case [1] 55

5.3 Pinch-off voltage values for various V_{ds} voltage levels. [1]........................56

5.4 Model Parameters extracted from the S-parameters Measurements for the Extrinsic circuit elements [1]..57

5.5 Parameter values for Tajima large-signal model 64

5.6 Results for Materka&Kacprzak large-signal model...................................74

5.7 Parameter results of Curtice and Ettenberg Large Signal Model.................84

5.8 Results for Large-Signal Statz Model 100

5.9 The parameter values extracted by using MATLAB program for Curtice Model 110

5.10 Results for TOM Large Signal Model...113

5.11 Parameter results of Angelov Large Signal Model 130

5.12 Results for TOM-2 Large Signal Model..141

LIST OF FIGURES

FIGURES

2-1 I-V characteristics of an n-type GaAs layer with two ohmic contacts. [16]..........5

2-2 I-V characteristics of an n-type GaAs layer with two ohmic contacts and a metal contact as gate [16]..........6

2-3 Equivalent Circuit of a MESFET 7

2-4 Physical Origin of the circuit elements of MESFET [16]..........7

2-5 $V_{ds} - I_{ds}$ Representation with respect to V_{gs} [16] 8

2-6 $V_{ds} - I_{ds}$ Representation with respect to V_{gs} 9

2-7 $V_{ds} - I_{ds}$ Representation with respect to V_{gs} [16] 9

2-8 Cross-sectional view of a MESFET 10

2-9 Important physical dimensions of MESFET..........11

2-10 I-V characteristics of ideal MESFETs..........13

2-11 Measured I_{ds} as a function of V_{ds} for several V_{gs} levels..........13

2-12 Measured output resistance of MESFET as a function of V_{ds} 15

2-13 Measured Microwave Transconductance..........16

2-14 Depletion region shapes for various applied bias levels..........17

2-15 Measured microwave gate-source capacitance 20

2-16 Measured Gate-drain Capacitance of a MESFET as a function of gate-drain voltage 21

3-1 MESFET small-signal model including parasitic elements..........25

3-2 MESFET small-signal model showing physical origin of elements 25

3-3 A typical equivalent circuit for a MESFET Large Signal model[17]..........29

4-1 Illustration of the relationships between characterization, parameter extraction, and modeling of microwave MESFETs.[17]..........34

4-2 A DC Model of a MESFET 35

4-3 Minimal FET Equivalent circuit..........39

4-4 MESFET Small Signal Model without parasitic inductances [17] 39

4-5 3-port representation of MESFET 41

5-1 Forward-gate Bias Measurement of MESFET Circuit 54
5-2 Extraction process of Extrinsic device parameters..57
5-3 FET equivalent circuit of Tajima Large-signal model 62
5-4 Transconductance of 4x150 MESFET for Tajima Large Signal Model.............65
5-5 Output Conductance of 4x150 MESFET for Tajima Large Signal Model..........65
5-6 Comparison of Vds-Ids characteristics of Tajima Model with measured (solid lines) and theoretical values (dashed lines) 66
5-7 Comparison of Vds-Ids characteristics of Tajima Model with measured (solid lines) and theoretical values (dashed lines) 66
5-8 Comparison of Vds-Ids characteristics of Tajima Model with measured (solid lines) and theoretical values (dashed lines) 67
5-9 Comparison of Vds-Ids characteristics of Tajima Model with measured (solid lines) and theoretical values (dashed lines) 67
5-10 Comparison of Vds-Ids characteristics of Tajima Model with measured (solid lines) and theoretical values (dashed lines) 68
5-11 Comparison of Vds-Ids characteristics of Tajima Model with measured (solid lines) and theoretical values (dashed lines) 68
5-12 Comparison of Vds-Ids characteristics of Tajima Model with measured (solid lines) and theoretical values (dashed lines) 69
5-13 Comparison of Vds-Ids characteristics of Tajima Model with measured (solid lines) and theoretical values (dashed lines) 69
5-14 Comparison of Vds-Ids characteristics of Tajima Model with measured (solid lines) and theoretical values (dashed lines) 70
5-15 Comparison of Vds-Ids characteristics of Tajima Model with measured (solid lines) and theoretical values (dashed lines) 70
5-16 Parameter characteristics wih respect to MESFET Types 71
5-17 Large Signal Equivalent Circuit of Materka-Kacprzak FET Model 73
5-18 Transconductance of 4x150 MESFET for Materka&Kacprzak Large Signal Model 75
5-19 Output Conductance of 4x150 MESFET for Materka&Kacprzak Large Signal Model 75
5-20 Comparison of Vds-Ids characteristics of Materka&Kacprzak Model with measured (solid lines) and theoretical values (dashed lines)............................76

5-21 Comparison of Vds-Ids characteristics of Materka&Kacprzak Model with measured (solid lines) and theoretical values (dashed lines)............................76
5-22 Comparison of Vds-Ids characteristics of Materka&Kacprzak Model with measured (solid lines) and theoretical values (dashed lines)............................77
5-23 Comparison of Vds-Ids characteristics of Materka&Kacprzak Model with measured (solid lines) and theoretical values (dashed lines)............................77
5-24 Comparison of Vds-Ids characteristics of Materka&Kacprzak Model with measured (solid lines) and theoretical values (dashed lines)............................78
5-25 Comparison of Vds-Ids characteristics of Materka&Kacprzak Model with measured (solid lines) and theoretical values (dashed lines)............................78
5-26 Comparison of Vds-Ids characteristics of Materka&Kacprzak Model with measured (solid lines) and theoretical values (dashed lines)............................79
5-27 Comparison of Vds-Ids characteristics of Materka&Kacprzak Model with measured (solid lines) and theoretical values (dashed lines)............................79
5-28 Comparison of Vds-Ids characteristics of Materka&Kacprzak Model with measured (solid lines) and theoretical values (dashed lines)............................80
5-29 Comparison of Vds-Ids characteristics of Materka&Kacprzak Model with measured (solid lines) and theoretical values (dashed lines)............................80
5-30 Parameter characteristics wih respect to MESFET Types...............................81
5-31 Equivalent circuit model of the Curtice&Ettenberg Model.............................83
5-32 Transconductance of 4x150 MESFET for Curtice&Ettenberg Large Signal Model 85
5-33 Output Conductance of 4x150 MESFET for Curtice&Ettenberg Large Signal Model 85
5-34Comparison of Vds-Ids characteristics of Curtice&Ettenberg Model with measured (solid lines) and theoretical values (dashed lines)............................86
5-35 Comparison of Vds-Ids characteristics of Curtice&Ettenberg Model with measured (solid lines) and theoretical values (dashed lines)............................86
5-36 Comparison of Vds-Ids characteristics of Curtice&Ettenberg Model with measured (solid lines) and theoretical values (dashed lines)............................87
5-37 Comparison of Vds-Ids characteristics of Curtice&Ettenberg Model with measured (solid lines) and theoretical values (dashed lines)............................87
5-38 Comparison of Vds-Ids characteristics of Curtice&Ettenberg Model with

measured (solid lines) and theoretical values (dashed lines)............................88
5-39 Comparison of Vds-Ids characteristics of Curtice&Ettenberg Model with measured (solid lines) and theoretical values (dashed lines)............................88
5-40 Comparison of Vds-Ids characteristics of Curtice&Ettenberg Model with measured (solid lines) and theoretical values (dashed lines)............................89
5-41 Comparison of Vds-Ids characteristics of Curtice&Ettenberg Model with measured (solid lines) and theoretical values (dashed lines)............................89
5-42 Comparison of Vds-Ids characteristics of Curtice&Ettenberg Model with measured (solid lines) and theoretical values (dashed lines)............................90
5-43 Comparison of Vds-Ids characteristics of Curtice&Ettenberg Model with measured (solid lines) and theoretical values (dashed lines)............................90
5-44 Parameter characteristics wih respect to MESFET Types...............................91
5-45 Transconductance of 4x150 MESFET for Statz Large-Signal Model..............94
5-46 Output Conductance of 4x150 MESFET for Statz Large Signal Model...........95
5-47 Comparison of Vds-Ids characteristics of Statz Model with measured (solid lines) and theoretical values (dashed lines)..95
5-48 Comparison of Vds-Ids characteristics of Statz Model with measured (solid lines) and theoretical values (dashed lines)..96
5-49 Comparison of Vds-Ids characteristics of Statz Model with measured (solid lines) and theoretical values (dashed lines)..96
5-50 Comparison of Vds-Ids characteristics of Statz Model with measured (solid lines) and theoretical values (dashed lines)..97
5-51 Comparison of Vds-Ids characteristics of Statz Model with measured (solid lines) and theoretical values (dashed lines)..97
5-52 Comparison of Vds-Ids characteristics of Statz Model with measured (solid lines) and theoretical values (dashed lines)..98
5-53 Comparison of Vds-Ids characteristics of Statz Model with measured (solid lines) and theoretical values (dashed lines)..98
5-54 Comparison of Vds-Ids characteristics of Statz Model with measured (solid lines) and theoretical values (dashed lines)..99
5-55 Comparison of Vds-Ids characteristics of Statz Model with measured (solid lines) and theoretical values (dashed lines)..99
5-56 Comparison of Vds-Ids characteristics of Statz Model with measured (solid

lines) and theoretical values (dashed lines) 100
5-57 Parameter characteristics wih respect to MESFET Types 101
5-58 Equivalent Circuit for Large Signal Curtice Model of GaAs MESFET..........102
5-59 Transconductance of 4x150 MESFET for Curtice Large Signal Model 104
5-60 Output Conductance of 4x150 MESFET for Curtice Large Signal Model......104
5-61 Comparison of Vds-Ids characteristics of Curtice Model with measured (solid
lines) and theoretical values (dashed lines) 105
5-62 Comparison of Vds-Ids characteristics of Curtice Model with measured (solid
lines) and theoretical values (dashed lines) 105
5-63 Comparison of Vds-Ids characteristics of Curtice Model with measured (solid
lines) and theoretical values (dashed lines) 106
5-64 Comparison of Vds-Ids characteristics of Curtice Model with measured (solid
lines) and theoretical values (dashed lines) 106
5-65 Comparison of Vds-Ids characteristics of Curtice Model with measured (solid
lines) and theoretical values (dashed lines) 107
5-66 Comparison of Vds-Ids characteristics of Curtice Model with measured (solid
lines) and theoretical values (dashed lines) 107
5-67 Comparison of Vds-Ids characteristics of Curtice Model with measured (solid
lines) and theoretical values (dashed lines) 108
5-68 Comparison of Vds-Ids characteristics of Curtice Model with measured (solid
lines) and theoretical values (dashed lines) 108
5-69 Comparison of Vds-Ids characteristics of Curtice Model with measured (solid
lines) and theoretical values (dashed lines) 109
5-70 Comparison of Vds-Ids characteristics of Curtice Model with measured (solid
lines) and theoretical values (dashed lines) 109
5-71 Parameter characteristics wih respect to MESFET Types 110
5-72 Transconductance of 4x150 MESFET for TOM Large Signal Model 114
5-73 Output Conductance of 4x150 MESFET for TOM Large Signal Model 114
5-74 Comparison of Vds-Ids characteristics of TOM Model with measured (solid
lines) and theoretical values (dashed lines) 115
5-75 Comparison of Vds-Ids characteristics of TOM Model with measured (solid
lines) and theoretical values (dashed lines) 115
5-76 Comparison of Vds-Ids characteristics of TOM Model with measured (solid

lines) and theoretical values (dashed lines) 116
5-77 Comparison of Vds-Ids characteristics of TOM Model with measured (solid lines) and theoretical values (dashed lines) 116
5-78 Comparison of Vds-Ids characteristics of TOM Model with measured (solid lines) and theoretical values (dashed lines) 117
5-79 Comparison of Vds-Ids characteristics of TOM Model with measured (solid lines) and theoretical values (dashed lines) 117
5-80 Comparison of Vds-Ids characteristics of TOM Model with measured (solid lines) and theoretical values (dashed lines) 118
5-81 Comparison of Vds-Ids characteristics of TOM Model with measured (solid lines) and theoretical values (dashed lines) 118
5-82 Comparison of Vds-Ids characteristics of TOM Model with measured (solid lines) and theoretical values (dashed lines) 119
5-83 Comparison of Vds-Ids characteristics of TOM Model with measured (solid lines) and theoretical values (dashed lines) 119
5-84 Parameter characteristics wih respect to MESFET Types 120
5-85 Equivalent Circuit model for Angelov Large Signal Model...........................121
5-86 Transconductance of 4x150 MESFET for Angelov Large-Signal Model 124
5-87 Output Conductance of 4x150 MESFET for Angelov Large Signal Model....124
5-88 Comparison of Vds-Ids characteristics of Angelov Model with measured (solid lines) and theoretical values (dashed lines) 125
5-89 Comparison of Vds-Ids characteristics of Angelov Model with measured (solid lines) and theoretical values (dashed lines) 125
5-90 Comparison of Vds-Ids characteristics of Angelov Model with measured (solid lines) and theoretical values (dashed lines) 126
5-91 Comparison of Vds-Ids characteristics of Angelov Model with measured (solid lines) and theoretical values (dashed lines) 126
5-92 Comparison of Vds-Ids characteristics of Angelov Model with measured (solid lines) and theoretical values (dashed lines) 127
5-93 Comparison of Vds-Ids characteristics of Angelov Model with measured (solid lines) and theoretical values (dashed lines) 127
5-94 Comparison of Vds-Ids characteristics of Angelov Model with measured (solid lines) and theoretical values (dashed lines) 128

5-95 Comparison of Vds-Ids characteristics of Angelov Model with measured (solid lines) and theoretical values (dashed lines) 128
5-96 Comparison of Vds-Ids characteristics of Angelov Model with measured (solid lines) and theoretical values (dashed lines) 129
5-97 Comparison of Vds-Ids characteristics of Angelov Model with measured (solid lines) and theoretical values (dashed lines) 129
5-98 Parameter characteristics wih respect to MESFET Types 131
5-99 A simple Large Signal Equivalent Circuit of TOM-2 MESFET Model 132
5-100 Transconductance of 4x150 MESFET for TOM-2 Large Signal Model 134
5-101 Output Conductance of 4x150 MESFET for TOM-2 Large Signal Model ... 135
5-102 2x50 Comparison of Vds-Ids characteristics of TOM-2 Model with measured (solid lines) and theoretical values (dashed lines) 135
5-103 2x150 Comparison of Vds-Ids characteristics of TOM-2 Model with measured (solid lines) and theoretical values (dashed lines) 136
5-104 4x50 Comparison of Vds-Ids characteristics of TOM-2 Model with measured (solid lines) and theoretical values (dashed lines) 136
5-105 4x75 Comparison of Vds-Ids characteristics of TOM-2 Model with measured (solid lines) and theoretical values (dashed lines) 137
5-106 4x100 Comparison of Vds-Ids characteristics of TOM-2 Model with measured (solid lines) and theoretical values (dashed lines) 137
5-107 4x125 Comparison of Vds-Ids characteristics of TOM-2 Model with measured (solid lines) and theoretical values (dashed lines) 138
5-108 4x150 Comparison of Vds-Ids characteristics of TOM-2 Model with measured (solid lines) and theoretical values (dashed lines) 138
5-109 4x175 Comparison of Vds-Ids characteristics of TOM-2 Model with measured (solid lines) and theoretical values (dashed lines) 139
5-110 6x50 Comparison of Vds-Ids characteristics of TOM-2 Model with measured (solid lines) and theoretical values (dashed lines) 139
5-111 6x150 Comparison of Vds-Ids characteristics of TOM-2 Model with measured (solid lines) and theoretical values (dashed lines) 140
5-112 Parameter characteristics wih respect to MESFET Types 140

CHAPTER 1

INTRODUCTION

Modeling means a representation of a system, process or device to make a description or analogy. This thesis is concerned with the modeling of the *metal-semiconductor field effect transistor* (MESFET). The MESFET is mostly used in microwave engineering. The modeling can be divided into two categories based on the way of representation: analytical modeling and equivalent circuit modeling. The former one is formed by mathematical equations, which represent or describe electron/hole transportation in the device.

In a signal-level categorization, more than one model may be used to represent the same device depending on the level of the excitation of signal. Typically, two models are used for a device: small-signal model and large-signal model. A small-signal model represents the behavior of the device under low level of input excitation. This model is useful in small-signal amplifier designs. In contrast, a large-signal model represents the behavior of the device under large level of input excitation. This model is usually used in the design of such circuit having large voltages propagating through it such as: power amplifiers and oscillators. The large-signal model is vital for calculations of nonlinear information: harmonic content, intermodulation distortion, saturation…etc.

Since 1980s many researches developed many different models to represent the MESFET characterization conveniently. This thesis includes some of these models and their representations with respect to the measured data of MESFET, which is taken experimentally by Çelebi in 2000 [1].

For all models, the circuit consists of some elements (resistances, capacitors, inductors, sources). Our basic task is to calculate those elements (parameters) from device measurements.

Usually, the small-signal model is the corner stone of the large-signal model. If an accurate large-signal model is required, an accurate small-signal model should

be devised first. In order to extract a large-signal model, small-signal model parameters should be extracted at different bias points throughout the region of interest. Those parameters should fit bias dependent equations to represent the dependence of the device on the bias point.

The main focus of this study is devoted to extract an accurate large-signal model from measured data taken among the models discussed in Chapter 5 [3-5,7-14]. All models have been derived from the same measurements; S-parameter measurements, $I_{ds} - V_{ds}$ measurements with various V_{gs} values, DC measurements. The small-signal parameters, extracted at different bias points, are used to derive a large-signal model for the drain-source current.

It is obvious that the accuracy of the model determines the accuracy of the design analysis. An accurate model is essential for quick design and fabrication process development. The inaccuracy in the model results in many trials before getting a working design or a successful process. Moreover, modern communication systems require more sophisticated monolithic microwave integrated circuits (MMICs) with smaller and smaller sizes. The miniaturization of MMICs and increasing the chip density emphasized the need of accurate models to minimize the number of design and fabrication cycles.

When we talk about the modeling of GaAs MESFETs, we also have to talk about the uses and applications of GaAs MESFET itself. MESFET has been used in the microwave industry for many years. The use of MESFET found many applications in the military, commercial, research fields for its low noise performance in the microwave range. The MESFET has been used since the beginning of the 1970s when it showed promising properties of low noise amplification. The demand for the lowest possible noise figure at higher frequencies has encouraged research on the physics of the device and has had a great impact on its technology. Fabrication of MESFETs is also compatible with the industry of monolithic circuitry. This advantage reinforced the development and interest of the MESFET technology; it also ensures that MESFET devices will continue to serve the communication industry for some time. The MESFET is used as the active device for low noise and power amplifiers as well as for transfer switches, attenuators, oscillators and mixers.

There exist various models for Microwave MESFET equivalent circuit

representations. These models use different mathematical models to describe the same MESFET and give similar results. However, there are some differences in the results when compared to the experimental measurements. In this thesis, various theoretical models are applied to the same MESFET and comparison made with measured data. It is shown that some models worked better on some parameters of the MESFET, while the others were more effective on other parameters. Altogether eight models were examined and data optimized to fit these theoretical models. In using optimization algorithms MATLAB FMINSEARCH and GENETIC ALGORITHM CODE were used alternatively to solve the initial value problem.

In chapter 2, generally GaAs MESFET is defined; the structure, principles of operation, equivalent circuit and the circuit elements are defined.

In chapter 3, the device models; small signal and large signal models are discussed. And the physical origin of the models is defined briefly.

In chapter 4, the parameter extraction process is described theoretically. The procedure of parameter extraction, which includes DC measurements, S-parameter measurements for extrinsic and intrinsic circuit elements is described. In the last section the large signal model and its parameter extraction algorithm is described.

In chapter 5, results of measurements, which are taken from Celebs's study [1], are tabulated. Each large-signal model is defined together with their relevant model parameters and the models are evaluated by utilizing the measured data. The results of all models, the comparison of modeled and measured data, the parameters that are extracted by optimization process for each model and for each type of MESFET, are presented in figures and tables with the measured results on the same graph.

In chapter 6, conclusion and further study to improve the modeling are discussed.

CHAPTER 2

METAL SEMICONDUCTOR FIELD EFFECT TRANSISTORS (MESFETs)

MESFET, HEMT and HBT have been the most important subject of the microwave industry for the last two decades. The MESFET is used as the active device for both low noise and power amplifiers as well as for transfer switches, attenuators, oscillators, and mixers.

MESFET is a three terminal device in which the current through two terminals is controlled using the third terminal. Unlike the BJT, MESFET is controlled by a voltage at the third terminal rather than by a current. Another difference is that the MESFET is a unipolar device; that is the current involves only majority carriers.

So there are several advantages of MESFET (FET) over the BJT; Voltage gain in addition to current gain, higher efficiency, lower noise figure, an operating frequency of up to X-Band, and very high input resistance (up to several Mega ohms) are among these advantages[15].

Monolithic integration of circuits on semi-insulating substrates enables device isolation with low parasitic capacitance, low-loss interconnections, and high packaging density.

In 1969 Middelhoek realized a Silicon MESFET with 1-µm gate length by projection masking. This FET had a 12-Ghz maximum frequency of oscillation, which was considerably higher than for previously known FETs.

The next significant step was the fabrication of 1-µm MESFETs on GaAs. In 1971 FETs with f_{max} of 50-GHz and useful gain up to 18GHz became available.

In 1972 it became apparent that GaAs MESFETs are capable of very low noise amplification, Noise figure of 3.5-dB with 6.6-dB associated gain at 10GHz.

MESFET structure may have two or more gates than the usual one having one. This type of structure gives higher gain and a lower feedback capacitance than

the single-gate counterpart. For a dual gate MESFET, the gain can be controlled over a wide range (44dB) by varying the DC bias of the second gate. This feature can be used for automatic gain control in amplifiers. The gain modulation response is very fast. Pulse-amplitude modulation of an RF carrier with less than 100-ps fall and rise times has been demonstrated.

The GaAs-MESFET is not limited to small signal low-noise applications. The first power MESFETs appeared in 1973 [16].

The MESFETs have been the most successful among the microwave FETs in low noise and in power amplification above 2GHz. The reasons for these are easy realization on GaAs and the fact that the two critical dimensions, the gate length and channel thickness, can be accurately controlled.

2.1 MESFET Principle of Operation

The current-voltage characteristics of a thin n-type GaAs layer in which electrons are carrying the current are plotted in Figure 2.1.

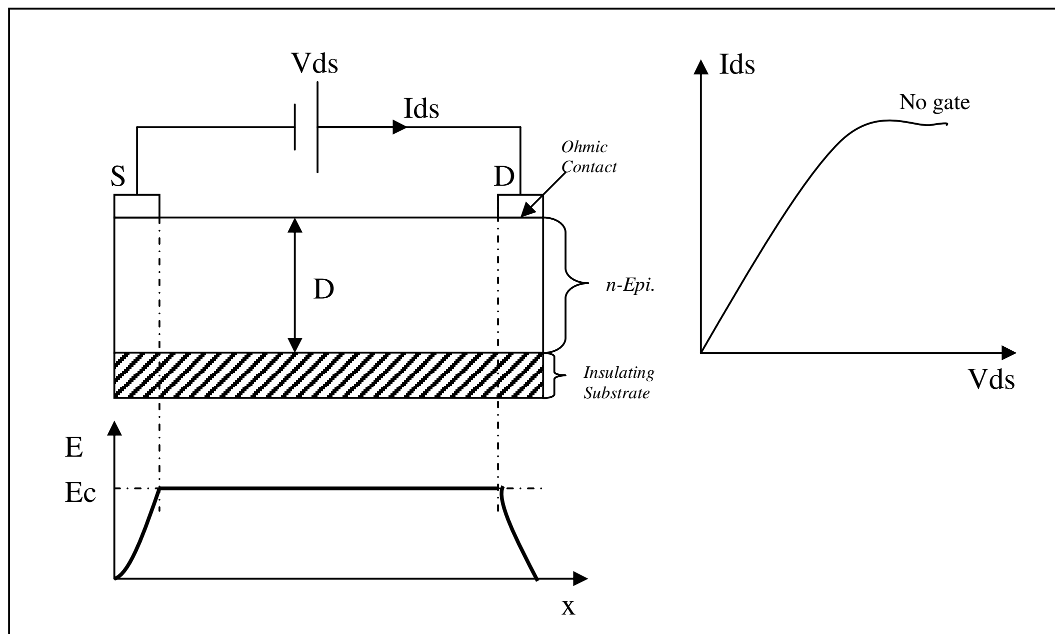

Figure 2-1 I-V characteristics of an n-type GaAs layer with two ohmic contacts [16].

This layer is supported by an insulating GaAs substrate. At the surface

of the conducting layer, two ohmic contacts are made, called the source and drain. A cross section of this device is shown in Figure 2.1. If a positive voltage V_{ds} is applied to the drain, electrons will flow from source to drain. Hence the source acts as the origin of carriers and the drain as a sink. For small voltages, the GaAs layer behaves like a linear resistor. For larger voltages, the electron drift velocity does not increase at the same rate as the electric field *E*. As a result, the current-voltage characteristic falls below the initial resistor line. As V_{ds} is further increased, *E* reaches a critical field, E_c for which the electrons reach a maximum velocity, v_s. At this drain voltage, the current starts to saturate.

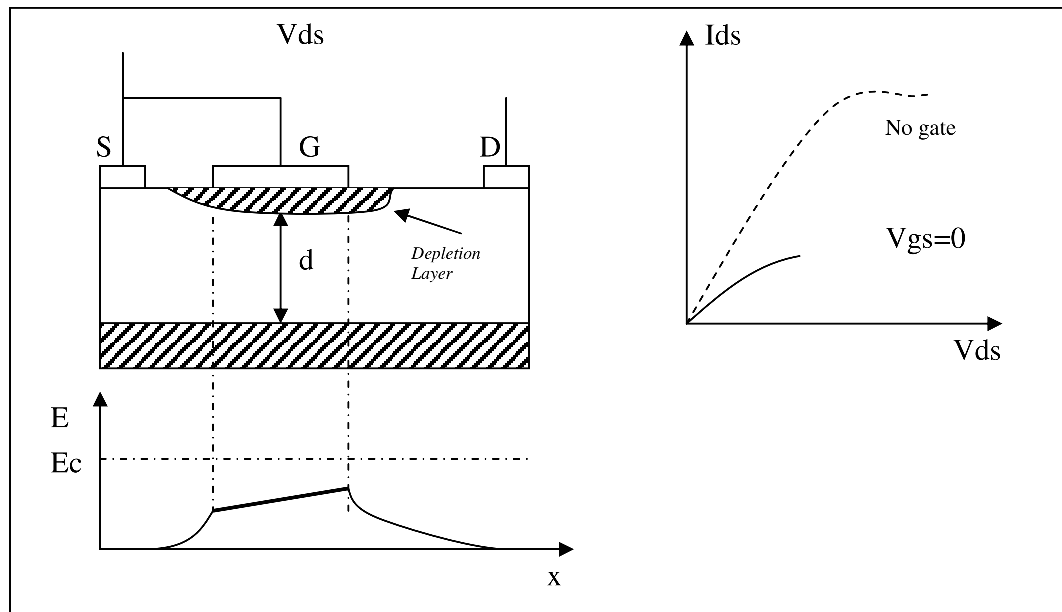

Figure 2-2 I-V characteristics of an n-type GaAs layer with two ohmic contacts and a metal contact as gate [16].

In Figure 2.2, a metal-to-semiconductor contact, called the gate, has been added between source and drain. This contact creates a layer in the semiconductor that is completely depleted of free-carrier electrons. This depletion layer acts like an insulating region and constricts the cross section available for current flow in the n-layer. The width of the depletion region depends on the voltage applied between the semiconductor and the gate. In Figure 2.2, the gate is shorted to the source and a small drain voltage is applied. Under these conditions, the depletion layer has a finite width and the conductive channel beneath has a smaller cross section *d* than in

Figure 2.1. Consequently, the resistance between source and drain is larger.

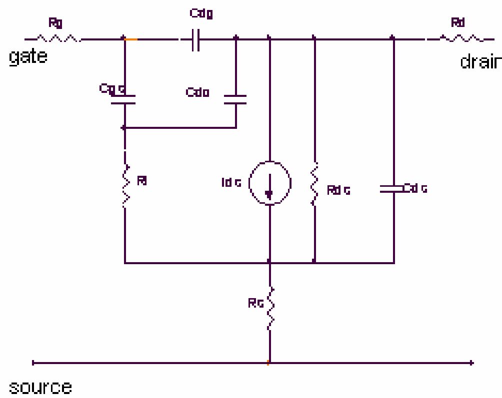

Figure 2-3 Equivalent Circuit of a MESFET

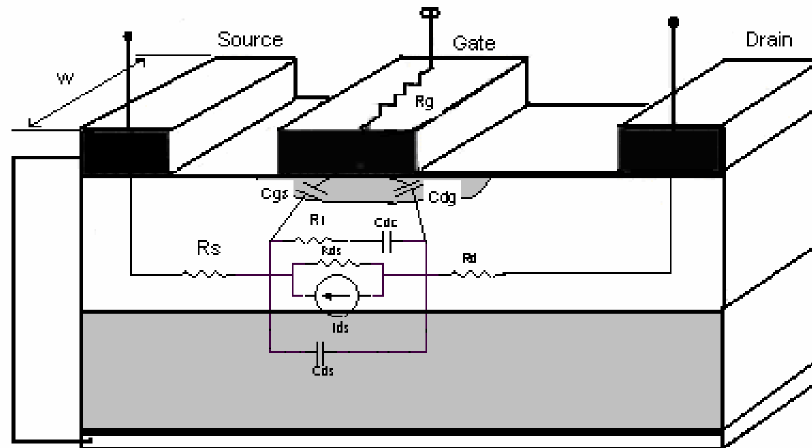

Figure 2-4 Physical Origin of the circuit elements of MESFET [16]

If the drain voltage is increased beyond V_{Dsat}, the depletion region widens toward the drain. The point x_1, where the electrons reach the limiting velocity, moves slightly toward the source (Figure 2.6). As x_1 moves closer to the source, the voltage at x_1 decreases. Consequently, the conductive cross section d_1 widens and more current is injected into the velocity-limited region. This results in a positive slope of the I_{DS} curve and a finite drain-to-source resistance beyond current saturation. The effect is particularly pronounced in microwave MESFETs with short gate lengths.

Proceeding from x_l toward the drain, the channel potential increases, the depletion layer widens, and the channel cross section d becomes narrower than d_l.

Since the electron velocity is saturated, the change in channel width must be compensated for by a change in carrier concentration to maintain constant current. An electron accumulation layer forms between x_l and x_2 , where d is smaller than d_l. At x_2 the channel cross section is again d_l and the negative space charge changes to a positive space charge to preserve constant current.

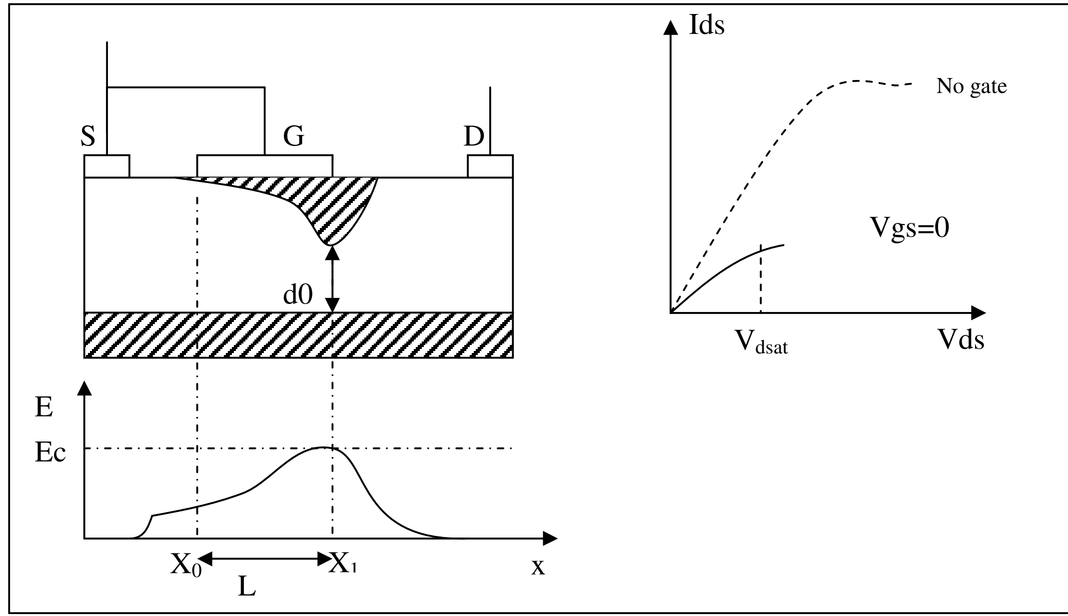

Figure 2-5 $V_{ds} - I_{ds}$ Representation with respect to V_{gs} [16]

The positive space charge is caused by partial electron depletion. The electron velocity remains saturated between x_2 and x_3 due to the field added by the negative space charge. In short, the drain voltage applied in excess of V_{Dsat} forms a dipole layer in a channel that extends beyond the drain end of the gate.

When a negative voltage is applied to the gate (Figure 2.7), the gate-to-channel junction is reverse biased, and the depletion region grows wider. For small values of V_{DS}, the channel will act as a linear resistor, but its resistance will be larger due to a narrower cross section available for current flow. As V_{DS} is increased, the critical field is reached at a lower drain current than in the $V_{GS} = 0$ case, due to the larger channel resistance. For a further increase in V_{DS}, the current remains saturated. In essence, the MESFET consists of a semiconducting channel whose thickness can be varied by widening the depletion region under the metal-to-semiconductor junction. The depletion region widening is the effect of a field or voltage applied between gate and channel of the transistor [16],[18],[19].

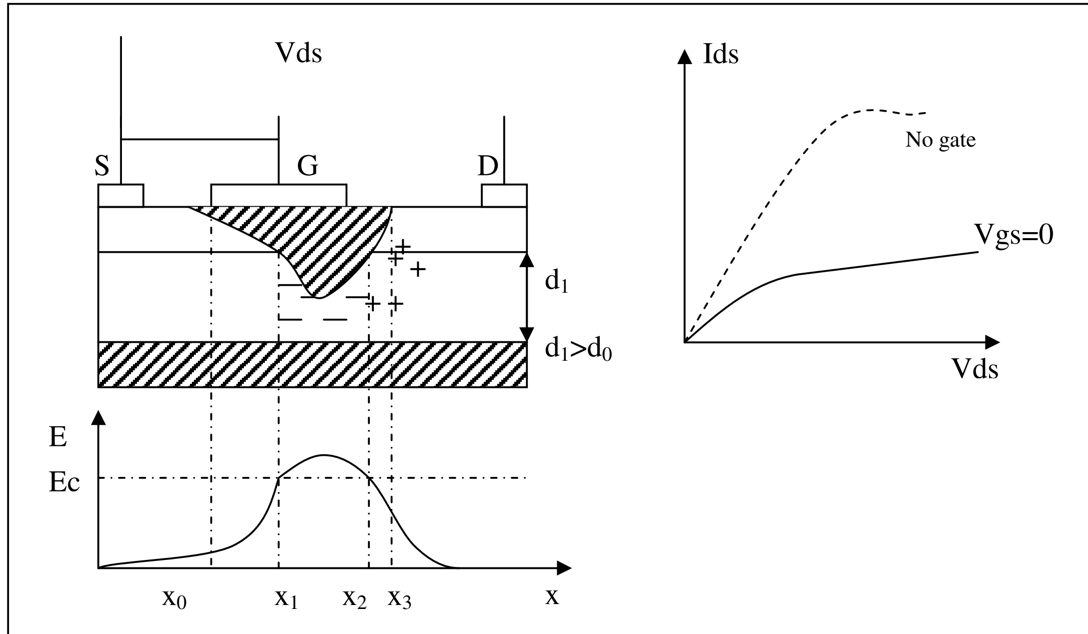

Figure 2-6 $V_{ds} - I_{ds}$ Representation with respect to V_{gs}

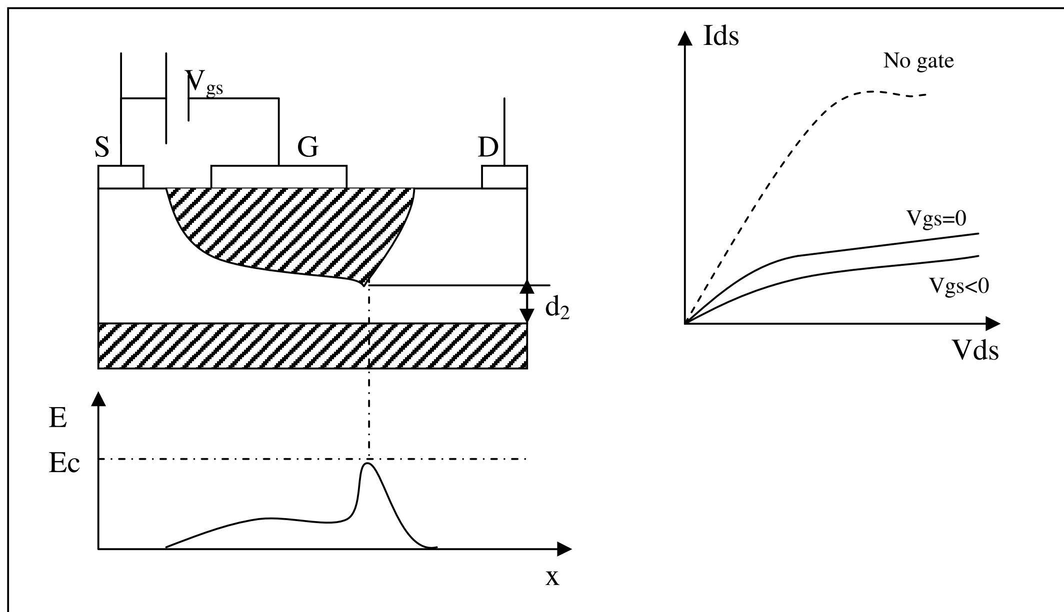

Figure 2-7 $V_{ds} - I_{ds}$ Representation with respect to V_{gs} [16]

2.2 MESFET Description

After explaining the principles of MESFET Operation, now let's discuss the MESFET and its structure completely.

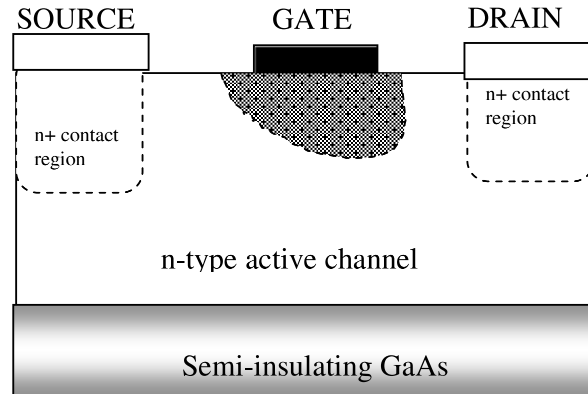

Figure 2-8 Cross-sectional view of a MESFET

The cross section of a MESFET device is shown in Figure 2.8. Three metal electrode contacts are made to a thin semiconductor active channel layer. The contacts are labelled, as explained before, "Source", "Gate", and "Drain". For microwave applications, the thin active layer is almost always *n*-type GaAs material. The active channel is fabricated by utilising ion implantation of donor atoms into semi-insulating material or epitaxial growth of doped material. Doping concentrations are often varied intentionally with depth to achieve specific performance. Regions of highly doped material beneath the source and drain contacts such as those shown in the figure are often incorporated into the structure to reduce unwanted contact resistance. These regions are produced using an additional implant or diffusion process. The active channel lies on top of semi-insulating GaAs.

Figure 2.9 presents another perspective of the MESFET Device with geometric dimensions. The most important dimension that characterises the MESFET physical structure is the gate length, "L". This dimension is critical in determining the maximum frequency limits for MESFET devices. The gate width, "w", is another physical dimension that is of primary importance in the determination of device behaviour.

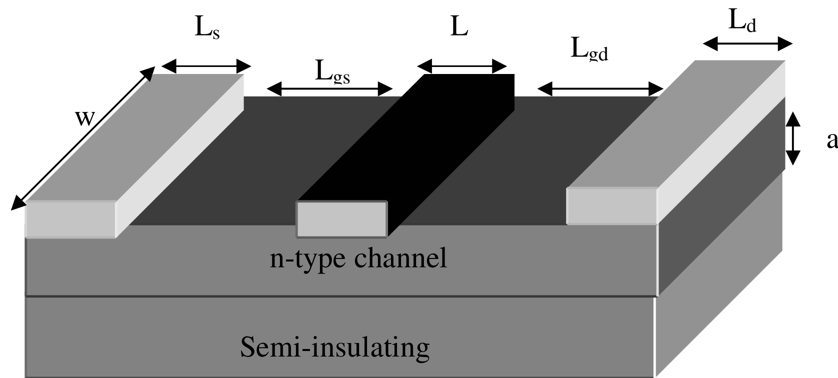

Figure 2-9 Important physical dimensions of MESFET

In fact, MESFETs are often described only in terms of the gate dimensions. A device is referred as a 0.5x300-μm device when the gate length is 0.5μm and the gate width is 300μm. Other characteristic dimensions include the epi-thickness, *a*; the gate-to-source and gate-to-drain terminal spacings, L_{gs} and L_{gd}; and the drain and the source terminal lengths, L_d and L_s.

A microwave device typically has a gate length in the 0.1- to 1.0-μm range. The epi-thickness is approximately 0.2 to 0.3 times the gate length dimension. Terminal spacings are on the order of one to four times the gate length. The gate width can vary significantly, ranging from about 100 to 2000 times that of the gate length. Note that the device current is directly proportional to gate width because the cross-sectional area available for channel current is proportional to w. For low noise, low-current applications, therefore, relatively small-gate-width devices are utilised. In contrast, large gate-width devices are typically used in power applications[17],[19].

2.3 I-V Characteristics of MESFET

As described in Section 2.2 the source and drain terminals are ohmic contacts. Most MESFET devices are *Depletion Mode* Devices. This means that in the absence of applied reverse gate bias, current can flow between the source and drain contacts. *Enhancement Mode* Devices do not conduct current between the drain and source unless forward gate bias is applied. For depletion mode devices, when low

bias potentials are applied between the source and the drain contacts, a current flows through the channel. The current is linearly related to the voltage across the terminals. Thus, for small biases, the source-drain terminals behave similar to a linear resistor. For higher drain-source bias levels, the electrons in the semiconductor material will attain their maximum carrier.

The gate contact in a MESFET device is a Schottky barrier. The energy band bending produced by making Schottky barrier contact with the semiconductor creates a layer beneath the gate that is completely depleted of free charge carriers. As no free carriers exist in this depletion layer, no current can flow through it. The available cross-sectional area for current flow between the source and drain is reduced by the existence of this depletion layer. As reverse bias is applied to the gate, the depletion layer penetrates deeper into the active channel. These further reductions in cross-sectional area result in further current reductions. The gate bias, then, acts as a mechanism for limiting the maximum amount of source-drain current that can flow. When enough reverse bias is applied, the depletion region will extend across the entire active channel and allow essentially no current to flow. The gate-source potential required to accomplish this, is termed as the "Pinch-off potential" or "Pinch-off voltage".

The current-voltage relationship expected from an ideal MESFET as described above is illustrated in Figure 2.10.

In Figure 2.10, the channel current is plotted as a function of applied drain-source potential for several different gate-source voltage levels. The *Saturated Current Level* achieved when V_{gs}=0 is commonly expressed as I_{dss}. Saturated current levels for other gate-source bias conditions are then expressed in terms of $\%I_{dss}$. The magnitude of the current for a given drain-source bias will be directly proportional to the gate width of the device. For that reason, drain current at a particular bias point is often discussed in terms of the current per unit gate width, I_{ds}/w.

The current-voltage characteristics of actual MESFET devices are similar to these ideal characteristics, with the important exception that the slope of the curves remains slightly positive even after semiconductor-limited velocity has been reached. Figure 2.11 presents measured I_{ds}-V_{ds} characteristics for a GaAs MESFETs[1].

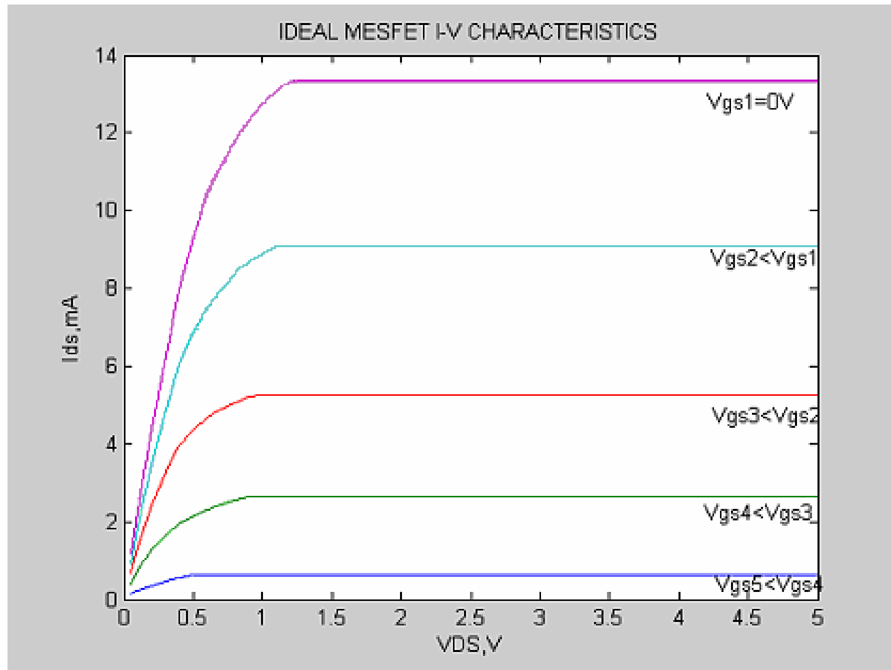

Figure 2-10 I-V characteristics of ideal MESFETs

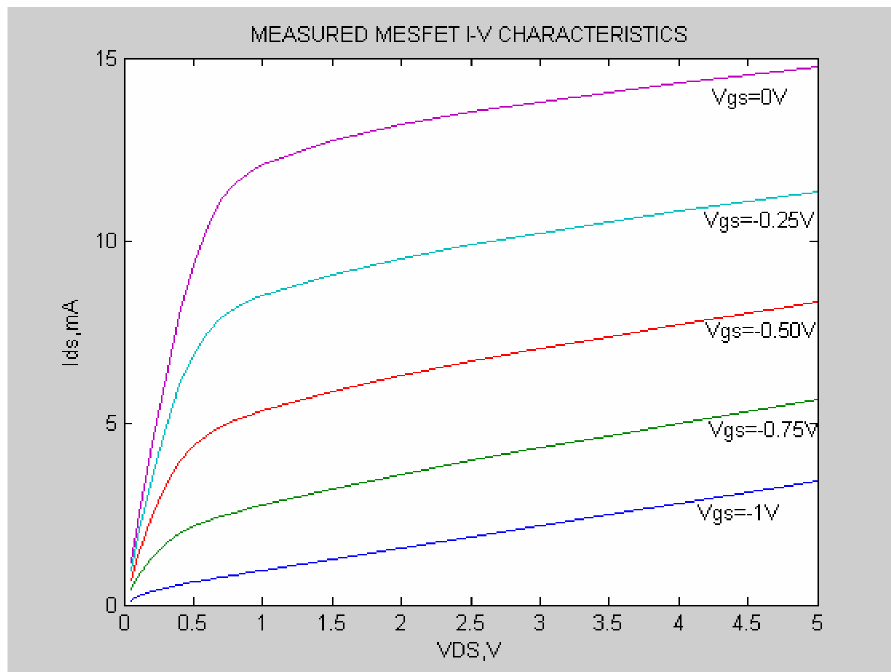

Figure 2-11 Measured I_{ds} as a function of V_{ds} for several V_{gs} levels

2.4 Transconductance and Output Resistance

For analog applications, the plot of current-voltage characteristics such as shown in Figure 2.10 and Figure 2.11 do not reveal as much about device performance as do the derivatives of these curves. Both device output conductance and transconductance are defined in terms of derivatives of the curves presented in Figure 2.11.

The derivative of the drain-source current with respect to drain-source voltage while gate-source voltage is held constant is defined as the output conductance of the device. Note that the output characteristics of the device are often more conveniently expressed in terms of output resistance. These quantities are related simply as the inverse of each other. Mathematically, the output conductance and resistance are given by

$$g_{ds} = \frac{1}{r_{ds}} = \left.\frac{dI_{ds}}{dV_{ds}}\right|_{V_{gs}=\text{constant}} \tag{2.1}$$

The output conductance of the device is an important characteristic in analog applications. It plays a significant role in determining the maximum voltage gain attainable from the device and is extremely important for determining optimum output matching properties. In general, for a device to have a low value output conductance is desirable, or, equivalently, an extremely high output resistance.

Figure 2.12 shows measured microwave output resistance for a MESFET device. As expected from figure 2.11, the output resistance is low at low drain-source bias levels and increases dramatically as the device reaches saturation. This is true for all the curves presented except for a gate bias level of –1V. At this bias level, the active channel is nearly pinched-off by the depletion region.

Device dimensions and channel material properties both affect output resistance of the MESFET. As in the case of channel current, the magnitude of the device output conductance (the inverse of the resistance) is directly proportional to device gate width. For devices with equivalent gate widths, short gate lengths typically result in lower output resistances. The output resistance can also be reduced by increasing channel doping concentrations, N_d, or the device epi-thickness, a.
The device transconductance is defined as the slope of the I_{ds}-V_{gs} characteristics with the drain-source voltage held constant.

$$g_m = \left. \frac{dI_{ds}}{dV_{gs}} \right|_{V_{ds}=\text{constant}} \quad (2.2)$$

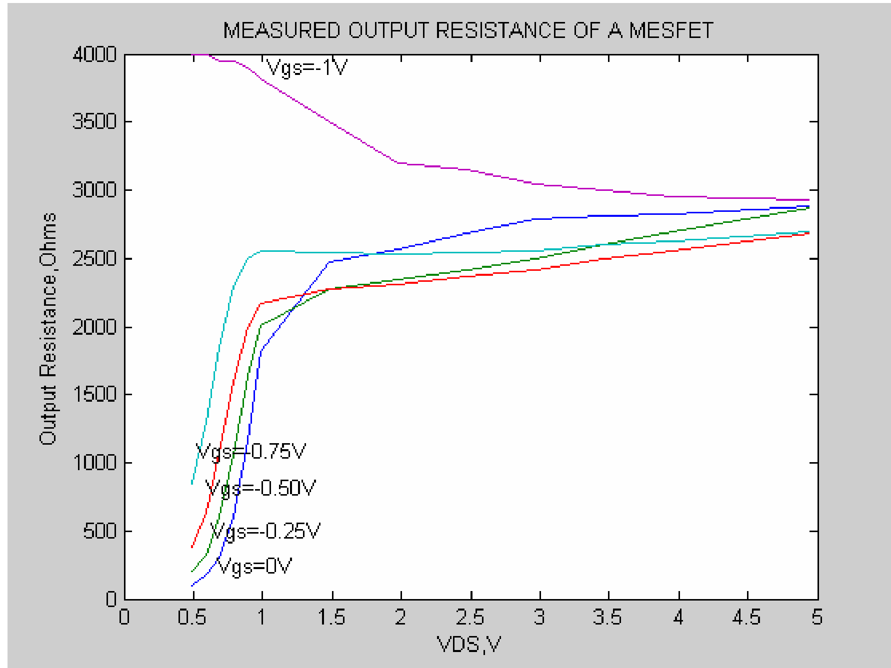

Figure 2-12 Measured output resistance of MESFET as a function of V_{ds}

The transconductance of the device is one of the most important indicators of device quality for microwave applications. When all other characteristics are equal, a device with high transconductance will provide greater gains and superior high-frequency performance.

Figure 2.13 presents the measured microwave transconductance of a 0.5x300-μm gate length device as a function of gate-source voltage. The characteristics presented in the figure are in agreement with what is expected from Figure 2.11 and equation (2.3).

The transconductance is essentially zero for gate bias levels below the pinch-off voltage. As the reverse bias on the gate is reduced toward zero, the transconductance increases monotonically. This is characteristic of GaAs MESFET behaviour.

The device transconductance is greatly affected by device dimensions and channel material properties. As with channel current and output conductance, MESFET transconductance is directly proportional to gate width. For this reason,

comparisons between devices are often made by examining the transconductance per unit gate width, g_m/w [17][18][19].

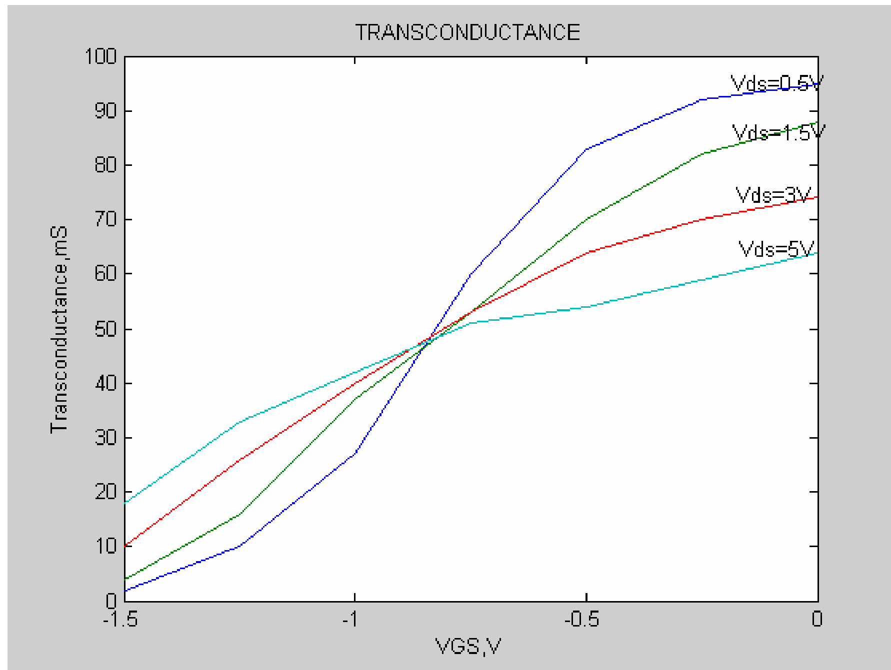

Figure 2-13 Measured Microwave Transconductance

2.5 Capacitance- Voltage characteristics

As reviewed in the previous discussions, the extent and dimensions of the depletion region beneath the gate of the MESFET are determined by the bias applied to the device terminals. Both the gate-to-source potential and gate-to-drain potential affect the charge distribution in the channel.

Figure 2.14 illustrates three different depletion region shapes that can be realised in the device. Figure 2.14(a) represents the symmetric bias case in which the gate-to-drain bias is equal to the gate-to-source bias. The illustration also assumes that the gate terminal is located directly in the middle of the gap between the drain and source terminals. The resulting depletion region is symmetric with respect to the source and drain. The case in which the gate-drain reverse bias is greater than the gate-source reverse bias is illustrated in Figure 2.14(b). For these circumstances, the depletion region is deeper at the drain end of the gate than at the source end of the gate, and it extends closer to the drain than to the source. This simulation represents the normal MESFET operating region in most amplifier, mixer, and oscillator

applications. Figure 2.14(c) represents the case in which the gate-source reverse bias is greater than the gate-drain reverse bias. This situation is the mirror image of the case shown in Figure 2.14(b).

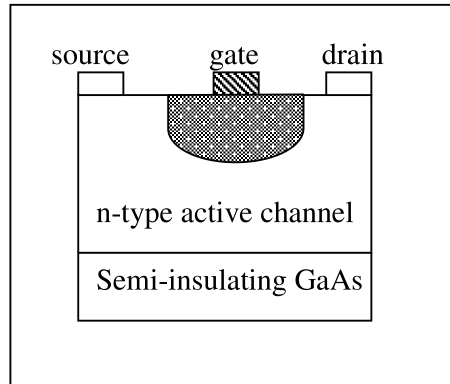

(a) gate-source voltage is equal to gate-drain voltage

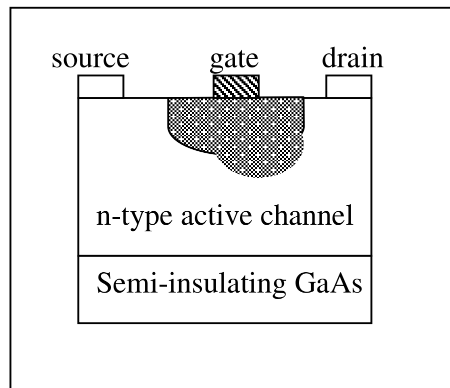

(b) reverse bias applied to gate-drain is greater than the bias applied to gate source.

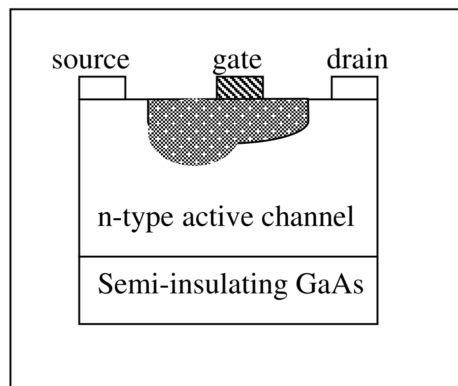

(c) reverse bias applied to gate-source is greater than the bias applied to gate-drain.

Figure 2-14 Depletion region shapes for various applied bias levels

Because the charge is redistributed with changing gate-source and gate-drain voltages, two important capacitances can be defined from the general definition of capacitance $C = {dQ}/{dV}$, where Q is the total charge involved in transition and V is the applied voltage. This definition is easily applied to two terminal devices such as parallel plate capacitors or simple *p-n* junctions. Because in a MESFET only one region of depletion charge is shared between gate-source and gate-drain capacitances, these quantities must be defined more carefully. The gate-source capacitance may be defined as

$$C_{gs} = \left. \frac{dQ_g}{dV_{gs}} \right|_{V_{gd}=\text{constant}} \tag{2.3}$$

In equation 2.3, Q_g is the depletion region charge beneath the gate. Similarly, the gate-drain capacitance can be defined as:

$$C_{gd} = \left. \frac{dQ_g}{dV_{gd}} \right|_{V_{gs}=\text{constant}} \tag{2.4}$$

The definitions expressed by equations (2.3-2.4) are not the only possible definitions applied to the MESFET capacitance problem. Under typical operating conditions, the MESFET source terminal is grounded. A negative bias is applied to the gate and a positive bias to the drain. Therefore, it is the gate-source and drain-source DC bias voltages that are directly controlled. For this reason, the gate source capacitance is often defined as

$$C_{gs} = \left. \frac{dQ_g}{dV_{gs}} \right|_{V_{ds}=\text{constant}} \tag{2.5}$$

Equations 2.3 and 2.5 are not equivalent, but describe slightly different quantities. The distinction is usually minor, but can be significant if calculations are based on a physically based model. When capacitance is determined by measurements or derived from empirical models, however, the capacitance definitions given by equations 2.3, 2.4 and 2.5 are not applied. Instead, the capacitance values are defined in terms of an equivalent circuit and the values required of the equivalent circuit elements to predict device behaviour accurately.

The gate source capacitance is important for microwave applications because

it has a significant impact on both device input impedance and ultimate frequency performance. To first order, the input impedance of a MESFET in a standard common source configuration, with typical bias levels applied, is simply the impedance of the gate-source capacitance in series with a few ohms of resistance. At high enough frequencies, the gate-source capacitance represents nearly a short circuit. The higher the C_{gs} value, the lower the frequency at which this situation occurs. At such frequencies, the device will not produce useful gain. To increase the high frequency characteristics of GaAs MESFETs, therefore, the reduction of gate-source capacitance is desirable.

Figure 2.15 represents measured gate-source capacitance for a 0.5x300-μm device. The figure shows capacitance increasing monotonically as gate-source voltage is increased from pinch-off toward zero bias. This general trend is true for all drain-source bias levels and is a typical of MESFET performance. The characteristics observed for this device are nearly linear with gate source voltage. This linear relationship is not unusual, but is not common to all MESFETs. Some devices exhibit gate-source capacitance characteristics that increase at greater than linear rates.

As the gate dimensions of a device are altered, the depletion region underneath the gate is also changed. This directly affects gate-source capacitance. Thus, the value of C_{gs} is proportional to both gate length and gate width. But note that although the gate length of a device has doubled, the value of C_{gs} is not doubled. The depletion region is composed of charge located both directly underneath the gate electrode as well as fringing charge in the gate-drain and gate-source spacing (see figure 2.8). This fringing charge does not scale directly with gate length, but remains nearly constant. Thus, gate-source capacitance does not scale in a strictly linearly manner with gate length.

Gate-source capacitance is also affected by channel doping density. Higher values of doping density cause higher values of C_{gs} to be observed. In practice, device technology advances that have allowed the production of shorter gate length devices have also required higher doping densities in the channel for optimum scaling. While shorter gate lengths produce smaller C_{gs} values, higher doping densities result in higher capacitance. These two trends have tended to cancel each other, resulting in a gate-source capacitance to gate-width ratio, C_{gs}/w, for microwave

devices that has remained nearly constant at a value near 1pF/mm.

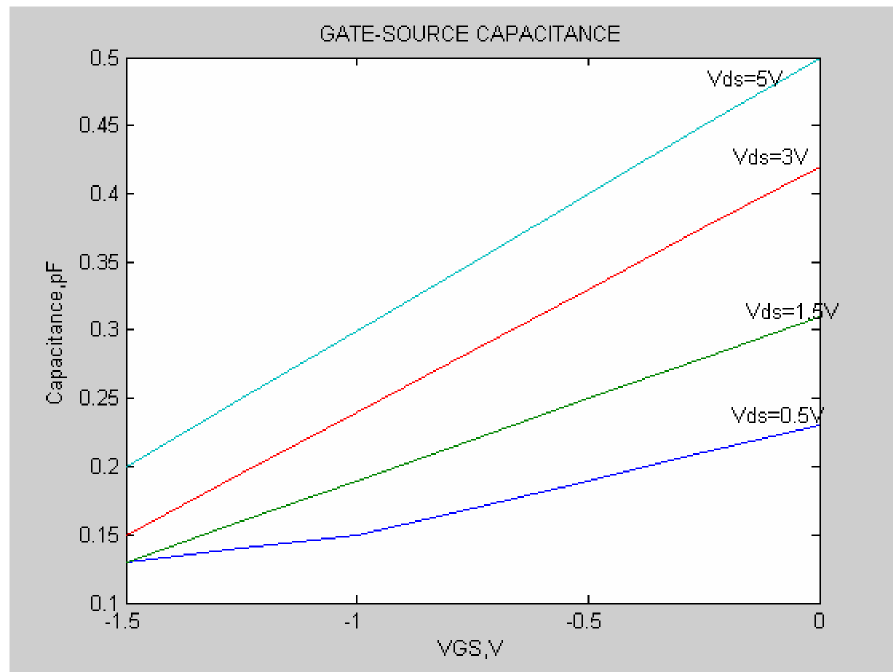

Figure 2-15 Measured microwave gate-source capacitance

The gate-drain capacitance of the MESFET is clearly closely related to the gate-source capacitance. In the normal mode of operation for amplifiers and oscillators, the primary characteristic affected by C_{gd} is the reverse isolation of the device. The smaller the gate-source capacitance, the greater the isolation.

Figure 2.16 presents measured microwave gate-drain capacitance as a function of gate-drain voltage. The bias levels presented in the figure represent the range of the bias levels for typical amplifier, oscillator, and frequency converter applications.

As in the case of gate-source capacitance, the value of C_{gd} is directly proportional to gate width. A similar relationship to gate length and doping density is also observed [17][18][19].

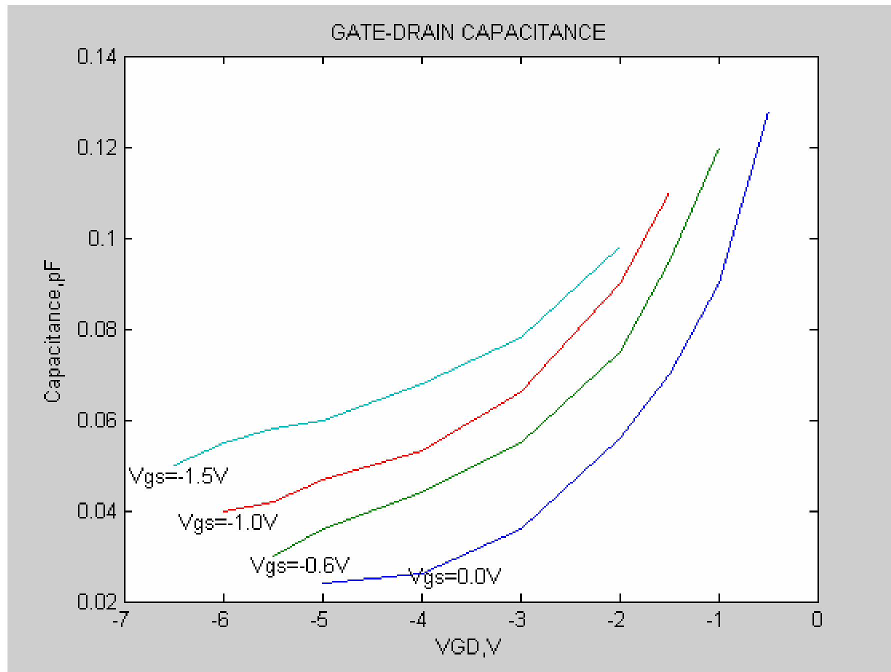

Figure 2-16 Measured Gate-drain Capacitance of a MESFET as a function of gate-drain voltage

CHAPTER 3

DEVICE MODELS

In a typical application, models are used to predict or estimate performance information that is not available or easily obtainable by direct measurement. Small-signal, large-signal and noise models are utilized to obtain information about device characteristics. *Small-signal models* can offer the designer the ability to predict performance of devices with gate width dimensions that have been scaled from previously measured devices. Another use of these models is to interpolate or extrapolate measured data to frequencies not covered by measurements. *Noise models* are used to predict the noise figure for arbitrary circuit topologies, which incorporate a particular device, or to predict the ultimate noise performance of a device. A *large-signal model* provides a means of obtaining performance information concerning nonlinear operation of a device or device-circuit combination.

Models are classified according to how they are derived. Empirical models are derived from describing observed characteristics with arbitrary functions. Physically based models are derived from the physical principles that apply to the device structure. And many models have aspects of both empirical and physical derivations.

Physically based models are useful to circuit and device designers who have some control over the fabrication process because they allow simultaneous optimization of both the devices and the circuits in which they are to be used. Additionally, a physical model is useful for predicting the effects of process variations on the electrical behavior of a device. If the statistical distribution of the process parameters is known, yield predictions can also be obtained. Using such an approach, performance prediction information may be obtained purely from physical data describing the device (i.e., device geometry and semiconductor material properties). No electrical characterization of individual devices is required. But

purely physical models are not as accurate as required for most circuit design applications. The inaccuracies arise from the assumptions and approximations required to perform the device analysis. Even the most sophisticated multidimensional numerical device simulation techniques make simplifying assumptions that can severely limit their accuracy. For example, surface state effects, traps, non-homogeneous interfaces, etc., are typically neglected in these analyses. Yet these phenomena have a significant effect on the microwave performance of modern devices. A second problem with physically based models is that information concerning the physical design of the device can often be difficult or impossible to obtain-especially for the circuit designer utilizing purchased devices. This problem may be solved by extracting the physical parameter values from measured data in the same way that empirical parameter values are determined.

In contrast, empirical models are capable of prediction accuracies that approach measurement capability. The primary difficulty with this approach is that large amounts of tedious characterization data are often required to obtain such accuracy. In addition, minor changes in the device geometry or material require the performance of complete recharacterizations. Such models are also of questionable value when performing design centering or yield analyses because the empirical parameter distributions do not vary independently. Because physical models are typically less accurate than their empirical counterparts, one attractive implementation is to use an empirical model to simulate nominal device performance and then use the physically based model to predict the deviations about this nominal behavior resulting from process parameter variations.

In this chapter, we will give some details of several models. The chapter is divided into two sections according to the type of performance predictions for which the models are used – small signal model and large signal model. Small signal is described mostly in this chapter. Because of the thesis subject, the large signal model will be disscussed in chapter 5 detailed.

3.1 Small Signal Model

The small-signal MESFET model is extremely important for active microwave circuit work. This model provides a vital link between measured

S-parameters and the electrical processes occurring within the device. Each of the elements in the equivalent circuit provides a lumped element approximation to some aspect of the device physics. A properly chosen topology, in addition to being physically meaningful, provides an excellent match to measured S-parameters over a very wide frequency range. When element values are properly extracted, the model is valid above the frequency range of the measurements, providing the possibility of extrapolating device performance to frequencies beyond some equipment's measurement capabilities. In addition, equivalent circuit element values can be scaled with gate width, thereby enabling the designer to predict the S-parameters of different size devices from a given foundry. The ability to include device gate width scaling as part of the circuit design process is important in MMIC design applications.

3.1.1 Physical Significance of Equivalent Circuit Element Values

A standard MESFET equivalent circuit topology is shown in figure 3.1. Although other circuit topologies involving additional elements, the topology of figure 3.1 has been shown to provide an excellent match to measured S-parameters through 26GHz. This topology has the additional advantage that the elements can be uniquely extracted. In figure 3.2, the same equivalent circuit is shown superimposed on a device cross section, indicating the physical origin of the equivalent circuit. A brief discussion follows of each equivalent circuit element and its role in modeling the device physics.

3.1.1.1 Parasitic Inductances Ls, Lg, and Ld

The parasitic inductances arise primarily from metal contact pads deposited on the device surface. So these values are dependent on the surface features of the device. For modern short gate length devices, the gate inductance is usually the largest of the three, although this is a function of the particular layout employed. Typically, L_g, and L_d are on the order of 5 to 10 pH. The source inductance is often is small, ~1 pH, especially for devices utilizing via hole grounds. Note that these inductances exist in addition to any parasitic bond wire inductances or parasitic package inductances, which must also be accounted for in the circuit model. In many cases, bonding inductances are on the order of 0.1 to 0.3 nH and dominates the

device parasitics [17].

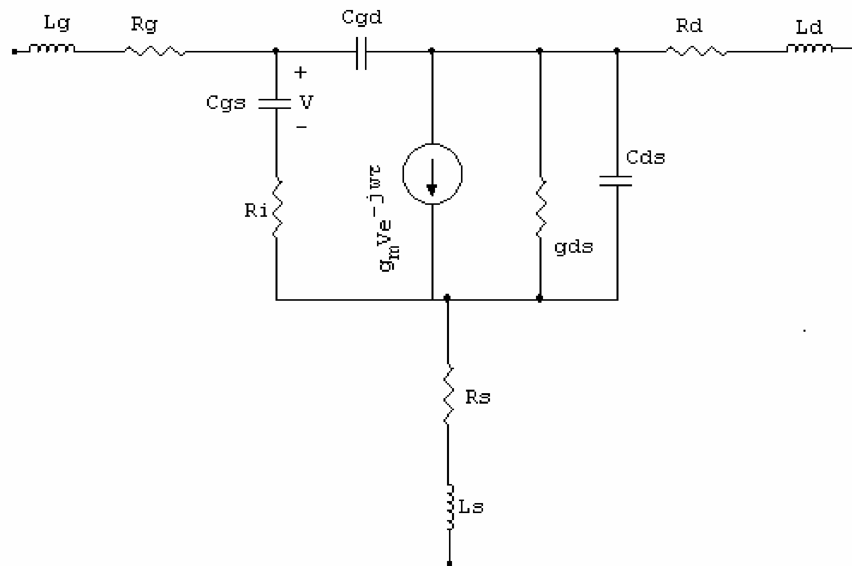

Figure 3-1 MESFET small-signal model including parasitic elements

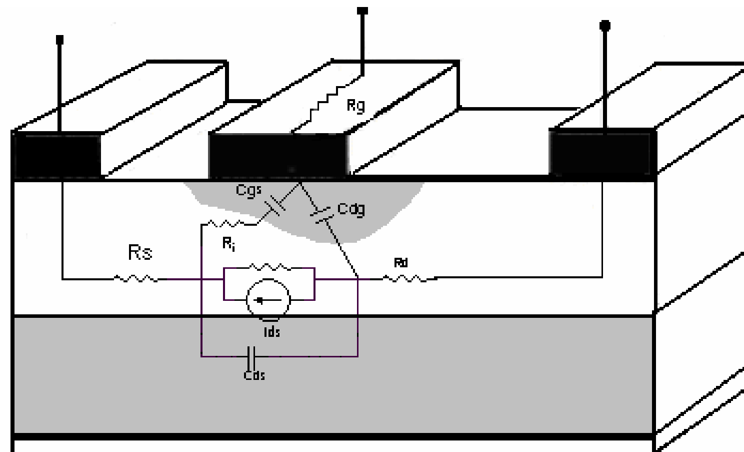

Figure 3-2 MESFET small-signal model showing physical origin of elements

3.1.1.2 Parasitic Resistances R_s, R_g, and R_d

The resistances R_s and R_d are included to account for the contact resistance of the ohmic contacts as well as any bulk resistance leading up to the active channel. The gate resistance R_g results from the metalization resistance of the gate schottky contact. All three resistances are on the order of 1 Ω for a modern microwave device. Although measurements indicate a slight bias dependence in the values, they are held constant in the large-signal models commonly available in circuit simulators today. These resistance values can be estimated either from forward conduction measurements or directly from the s-parameters using an optimization technique.[17]

3.1.1.3 Capacitances C_{gs}, C_{gd}, and C_{ds}

As discussed in Chapter 2, the capacitances C_{gs} and C_{gd} model the change in the depletion charge with respect to the gate-source and gate-drain voltages respectively. Under typical amplifier or oscillator bias conditions, the gate-source capacitance is the larger quantity because it models the change in depletion charge resulting from fluctuations in gate-source voltage. Under these normal bias conditions, the gate-drain capacitance C_{gd} is considerably smaller in magnitude than C_{gs} but nevertheless critical to obtaining accurate S-parameter predictions. The drain-source capacitance C_{ds} is included in the equivalent circuit to account for geometric capacitance effects between the source and drain electrodes. It is usually not considered to be bias dependent for the purposes of device modeling. Values for C_{gs} are typically on the order of 1pF/mm gate width under normal amplifier bias conditions. The values of C_{gd} and C_{ds} are about 1/10 of the value of C_{gs}. Because of symmetry, C_{gs} and C_{gd} are approximately equal for $V_{ds} = 0$ and reverse roles for inverted drain-source bias conditions ($V_{ds} < 0$) [17][18].

3.1.1.4 Transconductance g_m

The intrinsic gain mechanism of the FET is provided by the transconductance. The

transconductance $\mathbf{g_m}$ is a measure of the incremental change in the output current I_{ds} for a given change in input voltage V_{gs}. The internal input voltage is the voltage across the gate source junction. In other words, the device transconductance is defined as the slope of the I_{ds}-V_{gs} characteristics with the drain-source voltage held constant. The mathematical statement of this definition can be expressed as:

$$g_m = \left.\frac{\partial I_{ds}}{\partial V_{gs}}\right|_{V_{ds}=constant} \tag{3.1}$$

The transconductance of the device is one of the most important indicators of the device quality for microwave and millimeter wave applications. When all other characteristics are equal, a device with high transconductance will provide greater gains and superior high frequency performance. The transconductance suffers from what is called low frequency dispersion. The low frequency dispersion is the phenomenon of a parameter variation at low frequencies. The low frequency dispersion takes place as a result of the deep levels in the device structure. So, it significantly depends on the semiconductor material quality and fabrication processes.

The transconductance varies with frequency below a frequency of about 1MHz. Transconductance values vary directly with gate width and inversely with gate length for MESFETs [17][18].

3.1.1.5 Output Resistance, R_{ds} (Output Conductance, g_{ds})

The output resistance R_{ds} is the incremental resistance between drain and source, and it is more convenient to be explained in terms of its reciprocal, the output conductance g_{ds}. The output conductance is a measure of the incremental change in output current I_{ds} with the output voltage V_{ds}. So, it can be defined as the slope of the $I_{ds} - V_{ds}$ characteristics with the gate-source voltage held constant. Mathematically, the output conductance and resistance can be defined by:

$$g_{ds} = \frac{1}{R_{ds}} = \left.\frac{\partial I_{ds}}{\partial V_{ds}}\right|_{V_{gs}=constant} \tag{3.2}$$

The output conductance of the device is an important characteristic in analog applications. It plays a significant role in determining the maximum voltage gain attainable from a device and is extremely important for determining optimum output matching properties. In general, it is desirable to have a device with extremely high output resistance, or equivalently, low output conductance. Values of g_{ds} are on the order of 1mS/mm gate width at typical MESFET amplifier biases. Also, as gate length is reduced, output conductance tends to increase. The low frequency dispersion is more significant in output conductance than in the transconductance. The RF output conductance can be more than 100% higher than the DC output conductance. The RF values for both transconductance and output conductance are of primary concern for small-signal modeling applications while both RF and DC values are important for accurate large-signal modeling [17][18].

3.1.1.6 Transconductance Delay, τ

Transconductance cannot respond instantaneously to changes in gate voltage. The delay inherent to this process is described by the transconductance delay, τ. Physically, the transconductance delay represents the time it takes for the charge to redistribute itself after a fluctuation of gate voltage. Typical values of τ are on the order of 1pS for microwave MESFETs.[17]

3.1.1.7 Charging Resistance, R_i

The charging resistance is included in the equivalent circuit primarily to improve the match to S_{11}. For many devices, however, the presence of R_g is sufficient to match the real part of S_{11}. In either case, R_i is difficult to extract and is of questionable physical significance. The inclusion of R_i also complicates the large-signal analysis[17].

3.2 Large Signal Models

Several researchers have developed empirical models that describe the operational characteristics of the GaAs MESFET. All of these models are analytical and all are capable of describing the large-signal properties of microwave MESFETs with some success. The MESFET models discussed in this section are available in many of the popular large-signal circuit simulation packages used by microwave engineers. For any given device and application, the optimal choice of models depends on many considerations including model availability, computational efficiency, and prediction accuracy.

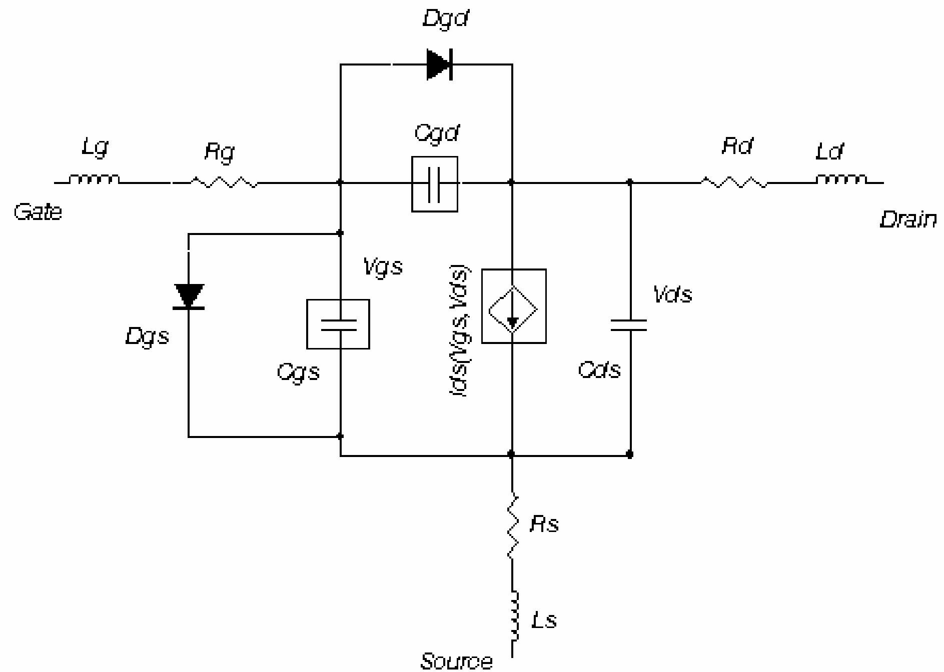

Figure 3-3 A typical equivalent circuit for a MESFET Large Signal model[17].

The general empirical modeling approach is to first examine the measured device characteristics and then look for a mathematical function that behaves in the same manner. The mathematical function includes adjustable parameters that, when assigned proper values, will cause the function to approximate the measured data

closely. Figure 3.3 is an equivalent circuit corresponding to a typical large-signal model. Analytical large-signal models approximate the nonlinear properties of a device using a unique set of analytical equations. These nonlinear properties can be related to elements of the equivalent circuit. The main nonlinear elements of the circuit of figure 3.3 are as follows:

(1) The drain-source current I_{ds} controlled by voltages V_{gs} and V_{ds} from which the transconductance and output conductance are derived.

(2) The gate-source capacitance C_{gs}

(3) The gate-drain capacitance C_{gd}

(4) The diode D_{gs}, which is important in the modeling of forward-bias gate current (or breakdown under conditions of inverted drain-source bias),

(5) The diode D_{gd}, which is important in the modeling of drain-gate avalanche current (or forward conduction under conditions of inverted drain-source bias)

The difference between the various large-signal empirical models presented here is the way in which they approximate the current-voltage or capacitance-voltage relationships. To first order, the development of empirical capacitance-voltage relationships is independent of the development of the current-voltage relationships.
The forward conduction in the gate diodes and is typically modeled using the Shockley Equation:

$$I_{df} = I_s[e^{V_d/(nV_t)} - 1] \qquad (3.3)$$

Where V_d is the voltage across the junction, V_t is the thermal voltage (kT/q), I_s is the reverse saturation current, and n is the ideality factor. The diode parameters I_s and n can be obtained from forward-bias DC measurements.

Breakdown characteristics can also be modeled by utilizing the diode elements. The excess device current due to avalanche breakdown is given to first order by the expression:

$$I_{dr} = I_s[e^{-(V_d + V_{br})/(nV_t)}] \quad \text{for } V_d < -V_{br} \tag{3.4}$$

where V_{br} is the device breakdown voltage.

Although there are too many Large-signal models present, we are dealing with a few of them.

Large-signal models which have importance in microwave, will be discussed in Chapter-5.

CHAPTER 4

PARAMETER EXTRACTION

Before any device model can be used, values for the parameters required of the model must be determined. This parameter extraction process must be closely related to both the obtained characterization data and the actual model used. The small signal equivalent circuit models are determined as an intermediate step toward large-signal model determination.

There are several parameters to be determined in a MESFET model. These parameters are either the values of the linear circuit elements of the equivalent circuit or the constants in the analytical expressions with the optimized variables are to converge to the measured data.

In practice all parameters are never optimized at the same time, since too many variables tend to slow down the optimization and make convergence more difficult, if impossible. Instead of optimizing all the parameters at once, parameters that can be derived from direct measurements are obtained and given to optimizations as constants.

Figure 4.1 illustrates the general reationship between device characterization, parameter extraction, device modeling, and circuit simulation for one approach to the microwave circuit design problem. The processes described by figure 4.1 apply to small-signal and large signal modeling applications referring to DC and S-parameter measurements. The outputs of the optimizations using the data obtained by these measurements are directly the model parameters or the equivalent circuit elements, which are then processed to reach to the parameters defining these elements. That is to say, at the end of the stated measurements we get some of the model parameters or the equivalent circuit elements. The rest of the model parameters are obtained from

these element values.

The procedure to obtain model parameters follows:

1- DC Measurements, get the parameters that are directly obtainable from the data of these measurements. The order is;

- Breakdown voltage measurements
- Pinch-off voltage measurements
- Forward bias gate measurements in 'source-short drain-open' and 'source-open drain-short' cases
- Drain-source voltage versus drain-source current measurements for various gate-source voltage levels

The breakdown voltage parameter VBR is directly obtained once the relevant measurement is done.

2- From the S-parameter measurements for extrinsic circuit elements, the parasitic inductances and the resistances are obtained.

3- Utilizing the DC parameters obtained in the first step and the parasitic resistances found in step 2, the parameters characterizing the analytical expression that is to fit to the measured $V_{ds} - I_{ds}$ data are obtained.

4- Once the extrinsic elements are found, using the relevant S-parameters, the elements of the intrinsic part of the equivalent circuit are obtained. Some of these elements are directly model parameters while others are used as data in optimizing the analytical expressions containing the model parameters to converge to these elements values.

5- From the S-parameters measured at various bias levels, the bias dependent large signal elements are designated and the parameters characterizing this dependence are obtained.

4.1 DC Data Measurements

Although DC Measurements alone are not sufficient to describe the RF behavior of MESFETs, these measurements are easily performed and provide information that may be used to determine some of the important device parameters. Figure 4.2 illustrates the DC equivalent circuit for a MESFET. The DC data may be used to extract the DC output conductance, DC transconductance, and the parasitic resistances[1].

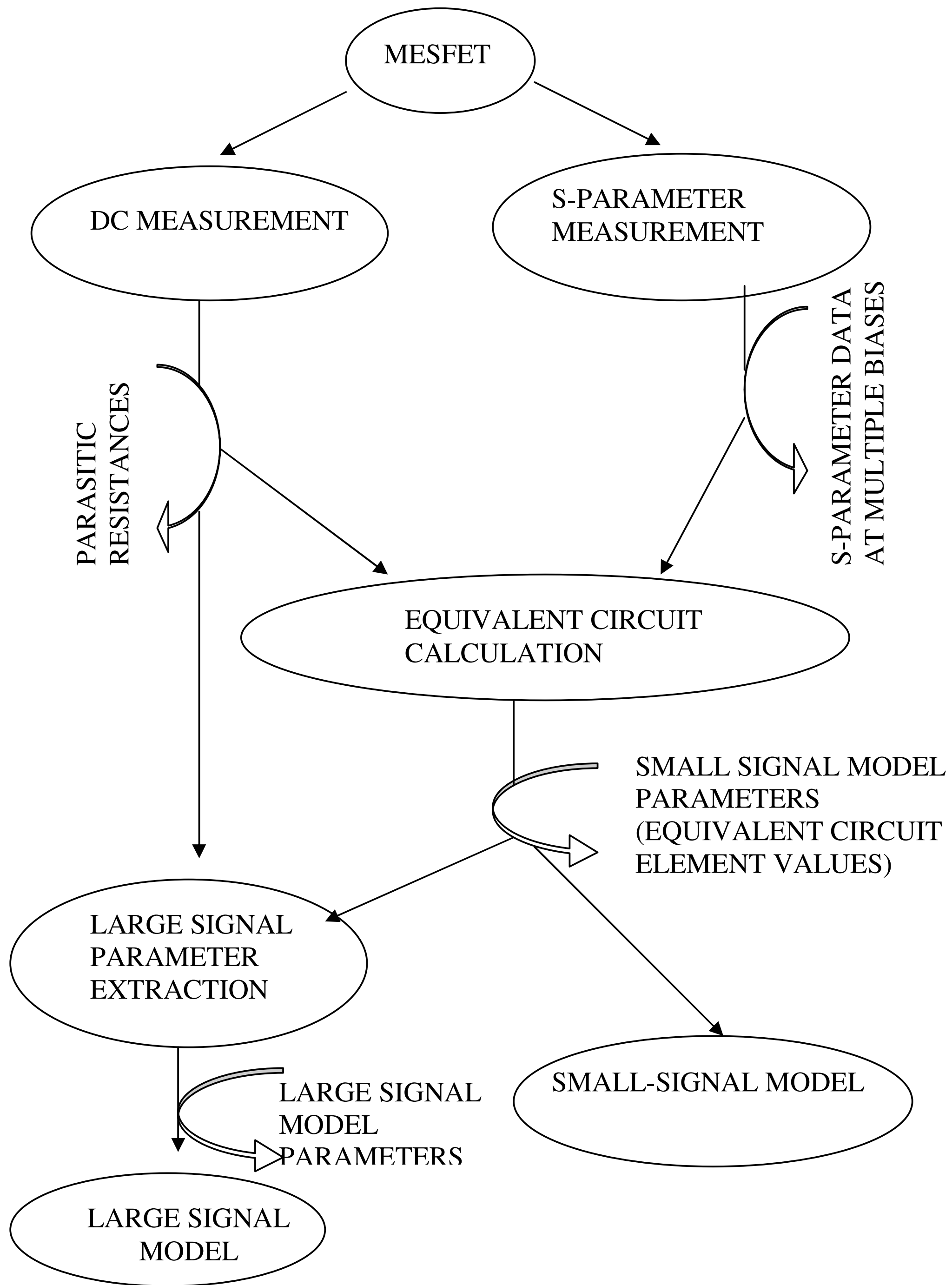

Figure 4-1 Illustration of the relationships between characterization, parameter extraction, and modeling of microwave MESFETs.[17]

In addition, the forward bias characteristics and DC breakdown properties of the gate source and gate-drain diodes may be evaluated.

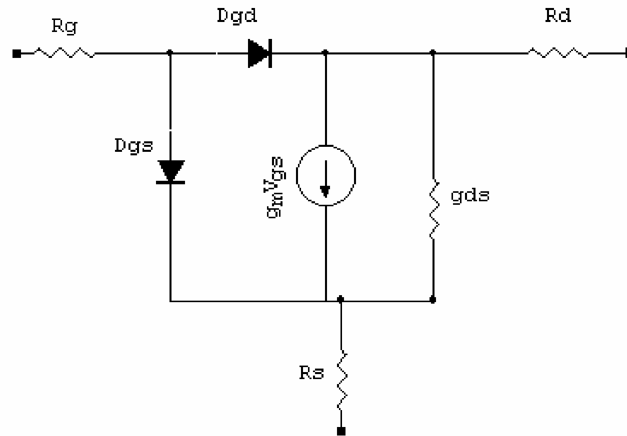

Figure 4-2 A DC Model of a MESFET

4.1.1 Forward Bias Gate Measurements

The assumed equivalent DC circuit model for a MESFET is illustrated in Figure 4.2. At low forward gate voltages, the gate-drain and gate-source junctions operate as ideal forward biased diodes producing a gate current of;

$$I_g = 2I_s(e^{V_g/N.v_t} - 1) \tag{4.1}$$

where V_g is the forward gate voltage, I_g the gate current, v_t is the built-in potential, here I_s and N are model parameters.

Due to the symmetry, ideal currents are expected in two cases, which are 'source-short/drain-open' and 'drain-short/source-open'.

Expressing the given relationship in terms of the applied forward potential, we can easily notice that the linear relationship between the applied voltage and the logarithm of the gate current [1][15][17][18].

4.1.2 Current-Voltage Behavior

The large signal models relate the I_{ds} and device capacitances to the bias voltages. Although DC measured data are not easily applied to device capacitance relationships, they can be related directly to device current. One method of

extracting the parameter values required of these models is to apply optimization of the modeled values of I_{ds} to the measured values at several bias points.

The optimization process involves the minimization of a specified error function by adjustment of the model parameter values.

One such error function that can be used in the optimization of the model to DC data is:

$$E_{I_{ds}} = \sum_{i=1}^{N} \frac{(I_{\mathrm{mod}\,i} - I_{measi})^2}{I_{measi}^2} \tag{4.2}$$

Where $I_{\mathrm{mod}\,i}$ is the modeled I_{ds} current at bias point i,

I_{measi} is the measured current at bias point i,

N is the number of bias points considered.

Two other parameters that may be of interest are the output conductance and the transconductance of the device.

$$g_{ds} = \frac{1}{r_{ds}} = \left.\frac{dI_{ds}}{dV_{ds}}\right|_{V_{gs}=\text{constant}} \tag{4.3}$$

$$g_{m} = \left.\frac{dI_{ds}}{dV_{gs}}\right|_{V_{ds}=\text{constant}} \tag{4.4}$$

Optimization of the model to the measured I_{ds} indirectly affects g_{ds} and g_m values. For analog applications, however, these parameters are of particular interest.

Investigations have shown that DC characterization in itself does not provide sufficient information to describe accurately the RF behavior of the device. The g_{ds} and g_m of these devices are dispersive, thus models optimized to only DC data do not accurately describe the RF performance. Because of the g_{ds} and g_m have significant impact on the performance of most microwave circuits, these DC extracted models are not acceptable for use in the design of microwave circuits. By using a combination of DC and RF measurements, accurate models can be developed

[1][15][17][18].

4.1.3 Parasitic Resistances

Determination of parasitic resistances is an important step in parameter extraction process for small-signal, large-signal models. Independent determination of these resistance values reduces the number of element values requiring optimization. This reduction makes the small-signal optimization process faster and more reliable. The parasitic resistances of the gate, drain and source of a MESFET may be determined by measuring the gate current as a function of gate voltage for the configuration.

The measurements are made under three conditions:

a) Source grounded

b) Drain grounded

c) Both source and drain grounded.

The series resistance values obtained for these three configurations may be related to the parasitic resistances as follows:

a) $R_a = R_{ser} = R_g + R_s$ (Source grounded) (4.5a)

b) $R_b = R_{ser} = R_g + R_d$ (Drain grounded) (4.5b)

c) $R_c = R_{ser} = R_g + {R_d R_s}/{(R_d + R_s)}$ (Source and drain both grounded) (4.5c)

These applications may be solved for R_g, R_d and R_s in terms of R_a, R_b, R_c.

$$\begin{aligned} R_g &= R_c - [R_c^2 - R_c(R_a + R_b) + R_a R_b]^{1/2} \\ R_d &= R_b - R_g \\ R_s &= R_a - R_g \end{aligned} \qquad (4.6)$$

The values of the parasitic resistances determined in this way can be slightly sensitive to the bias conditions.

These results show that the source and drain resistance values for a MESFET

are fairly constant, except for a decrease at lower gate voltages.

The gate resistance shows much greater dependence on V_g. This bias dependence is not typically included in microwave device models, making it difficult to specify a unique value of resistance from the DC measurement. In some circumstances, the value of R_g obtained from these measurements may not be acceptable for a value of modeled gate resistance is often 10 to 50% higher than a value determined using this measurement method.

One criticism of this method is that the resistance values are obtained under forward-bias conditions, while most designers desire the resistance values of the reverse-biased gate. Although the bias conditions of the measurement do not match the typical bias conditions of operation, these measurements at least give good estimates of the desired resistance values- particularly for the R_s and R_d resistances.

Other methods of extracting parasitic resistance values involve optimization to measured S-parameters, and the optimized values may be sensitive to the initial value choices, as well as to the optimization technique used. None of these methods, DC or S-parameter, directly determines the resistances, thus ascertaining the most accurate approach is difficult. Differences between the resistances derived using the various methods may be on the order of 25% [1][15][17][18].

4.2 Extraction of Small Signal Equivalent Circuits

From these equivalent circuits, the bias dependent RF element values of output conductance $g_{ds}(V_{ds},V_{gs})$, transconductance $g_m(V_{ds},V_{gs})$, gate-source capacitance $C_{gs}(V_{ds},V_{gs})$, gate-drain capacitance $C_{gd}(V_{ds},V_{gs})$ can be obtained.

The other intrinsic element values; C_{ds}, R_i, and τ are also extracted in this process, although their bias dependence is much weaker than the other four elements. Typically, these element values are held constant at their $I_{dss}/2$ value or some other bias in the saturation region.

This section describes techniques that can be used to extract the intrinsic element values as well as the parasitic inductance values from each set of S-parameters [17].

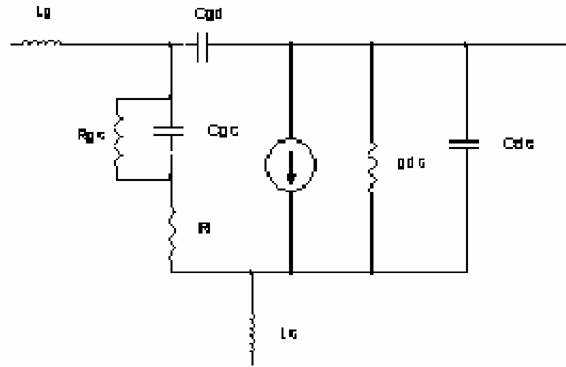

Figure 4-3 Minimal FET Equivalent circuit

4.2.1 Direct Extraction of Intrinsic Elements

The intrinsic FET topology is such that a Y-parameter analysis of the equivalent circuit results in relatively simple expressions that can be equated to measured Y-parameter data.

For this analysis, the equivalent circuit of Figure 4.4 is referenced.

Initially, the inductances will be neglected, and these elements will be discussed in the next section.

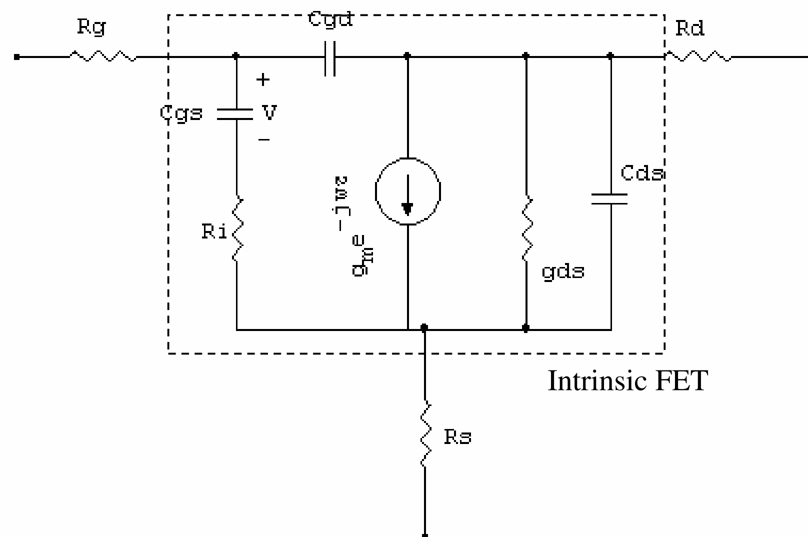

Figure 4-4 MESFET Small Signal Model without parasitic inductances [17]

In addition, we assumed that parasitic resistances have been determined using one of the techniques described in section 4.1.3 or some other technique.

- The first step in extraction process is the conversion of the measured S-parameters to Z-parameters using the following:

$$Z'_{11_{meas}} = \frac{(1+S_{11})(1-S_{22})+S_{12}S_{21}}{\Delta} \quad (4.7)$$

$$Z'_{12_{meas}} = \frac{2S_{12}}{\Delta} \quad (4.8)$$

$$Z'_{21_{meas}} = \frac{2S_{21}}{\Delta} \quad (4.9)$$

$$Z'_{22_{meas}} = \frac{(1-S_{11})(1+S_{22})+S_{12}S_{21}}{\Delta} \quad (4.10)$$

Where $\Delta = (1-S_{11})(1-S_{22}) - S_{21}S_{12}$ and the (‘) prime denotes normalized (to Z_0) Z-parameters. From the denormalized extrinsic Z-parameters, the parasitic resistance values can be de-embedded to obtain *the intrinsic Z-parameters***.**

$$z_{11_{meas}} = Z_{11_{meas}} - (R_g + R_s) \quad (4.11)$$

$$z_{12_{meas}} = Z_{12_{meas}} - R_s \quad (4.12)$$

$$z_{21_{meas}} = Z_{21_{meas}} - R_s \quad (4.13)$$

$$z_{22_{meas}} = Z_{22_{meas}} - (R_d + R_s) \quad (4.14)$$

where the known extrinsic values are denoted by upper-case letters (*Z*) and the intrinsic values are denoted by lower-case letters (*z*).

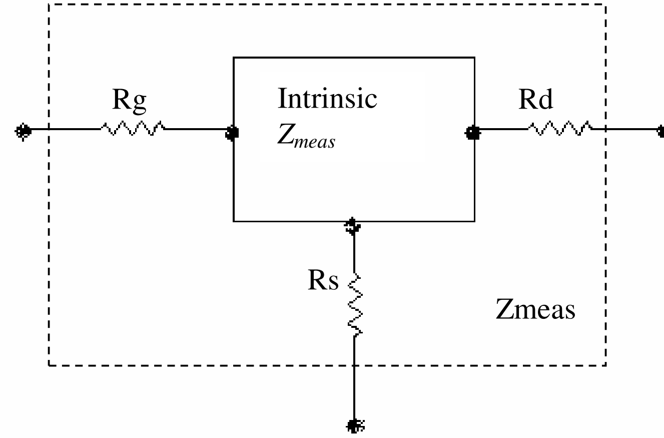

Figure 4-5 3-port representation of MESFET

- We now convert these z-parameter data into y-parameter data:

[$(Z_{ext} - R) \rightarrow z_{\text{int}} \rightarrow y_{\text{int}}$]

$$y_{11_{meas}} = \frac{z_{22_{meas}}}{(|z|Z_0)} \tag{4.15}$$

$$y_{12_{meas}} = \frac{-z_{12_{meas}}}{(|z|Z_0)} \tag{4.16}$$

$$y_{21_{meas}} = \frac{-z_{21_{meas}}}{(|z|Z_0)} \tag{4.17}$$

$$y_{22_{meas}} = \frac{z_{11_{meas}}}{(|z|Z_0)} \tag{4.18}$$

where $|z| = z_{11_{meas}} z_{22_{meas}} - z_{12_{meas}} z_{21_{meas}}$ these above equations provide de-embedded y-parameter data from the measured S-parameters. From the equivalent circuit in Figure 4.4, the exact analytical form of the intrinsic y-parameters can be derived:

$$y_{11} = \left.\frac{I_1}{V_1}\right|_{V_2=0} = \frac{R_i C_{gs}^2 w^2}{D} + jw(\frac{C_{gs}}{D} + C_{gd}) \tag{4.19}$$

$$y_{12} = -jwC_{gd} \tag{4.20}$$

$$y_{21} = \{\frac{g_m e^{-jw\tau}}{(1 + jR_i C_{gs} w)}\} - jwC_{gd} \tag{4.21}$$

$$y_{22} = g_{ds} + jw(C_{gd} + C_{gs}) \tag{4.22}$$

where $D = 1 + w^2 C_{gs}^2 R_i^2$, from these 4 equations, closed form expressions for extracting the element values from y-parameter data can be developed [1][15][17].

4.2.2 Capacitance Extraction

From equations given above we can calculate the capacitances as follows:[17]

$$C_{gd} = \frac{-\text{Im}\{y_{12}\}}{w} \tag{4.23}$$

$$C_{ds} = \frac{\text{Im}\{y_{22}\}}{w} - C_{gd} \tag{4.24}$$

$$C_{gs} = \frac{\text{Im}\{y_{11}\}}{w} - C_{gd} \tag{4.25}$$

4.2.3 Output Conductance and Transconductance Extraction

$$g_{ds} = \text{Re}\{y_{22}\} \tag{4.26}$$

Although $\text{Re}\{y_{22meas}\}$ falls off at high frequency, the value of g_{ds} computed from low frequency $\text{Re}\{y_{22meas}\}$ data provides a reliable value for matching the S-parameters over frequency. The data are fairly flat in the low frequency range, so g_{ds} may be computed from either a single point or from the average of a few points [1][17].

$$g_m e^{-jw\tau} = g_{mr} + jg_{mi} \tag{4.27}$$

where,

$$g_{mr} = \text{Re}\{y_{21}\} - \text{Im}\{y_{21}\} R_i C_{gs} w - w^2 C_{gd} C_{gs} R_i \tag{4.28}$$

and

$$g_{mi} = \text{Re}\{y_{21}\} R_i C_{gs} w + \text{Im}\{y_{21}\} + w C_{gd} \tag{4.29}$$

The transconductance is simply the magnitude of these two components:

$$g_m = (g_{mr}^2 + g_{mi}^2)^{\frac{1}{2}} \tag{4.30}$$

For a typical low noise device at low frequencies (≈2GHz) $\text{Re}\{y_{21}\}$ is assumed as the only term of significance and g_m is well approximated as:

$$g_m \approx \text{Re}\{y_{21}\} \tag{4.31}$$

As with output conductance, the $\text{Re}\{y_{21meas}\}$ data are smooth, and g_m can be computed from either a single point or from an average of a few points [1][15][17].

4.2.4 Extraction of τ and R_i

τ is primarily a parameter that affects the high frequency phase of s_{21}, it is logical to extract it in this frequency range. Any expression for τ will include an R_i dependence. Because R_i primarily affects s_{11}, a more reliable method for extracting it may be to optimize it to match s_{11} after the other elements have been extracted.

The primary effects of R_i on the equivalent circuit behavior are to increase the real portion of the modeled device input impedance and the time required for the channel current to respond to gate voltage fluctuations. However the resistor R_g also increases the real part of the modeled input impedance, and the element τ increases the channel current to gate voltage response time.

$$R_i = \frac{1 - \left(1 - \frac{4\,\text{Re}^2\{y_{11}\}}{w^2 C_{gs}^2}\right)^{\frac{1}{2}}}{2\,\text{Re}\{y_{11}\}} \tag{4.32}$$

$$\tau = -\frac{1}{w}\tan^{-1}\left(\frac{g_{mi}}{g_{mr}}\right) \tag{4.33}$$

where, g_{mr} and g_{mi} are represented in equations 4.28 and 4.29 [17].

4.2.5 Comparison of Measured and Modeled S-parameter Data

Although the small-signal equivalent circuit elements are extracted from Y-parameter data, the objective is to match measured S-parameters as closely as possible to an equivalent circuit. To evaluate the quality of the fit to measured data, definition of an *error term* is convenient.

$$E_{ij} = \frac{1}{n}\sum_{k=1}^{n}\frac{\left|s_{ij\,meas}^{k} - s_{ij\,\mathrm{mod}}^{k}\right|}{\left|s_{ij\,meas}^{k}\right|} \tag{4.34}$$

where *n* is the number of discrete frequencies used [17].

4.2.6 Parasitic Inductance Extraction

The inclusion of parasitic inductances in the model is critical to accurate modeling of MESFET high frequency RF behavior. The method requires measurement of the device S-parameters at 0V drain-source bias ($V_{ds} = 0\mathrm{V}$). This presents an extra step in the characterization process.

In MMIC devices, the parasitic inductances result from metalization strips at the gate and drain terminals of the device. The metalization inductance is a function of the semiconductor properties, which are significantly different under zero- or forward-bias condition than they are under reverse bias.

The method outlined in this section, obtains the parasitic inductance from the same S-parameter measurements from which the intrinsic elements are extracted. The method is fast and equally valid for either MMIC or Packaged Devices.

The extrinsic device Z-parameters can be expressed in terms of the intrinsic parameters as follows:

$$Z_{11} = z_{11} + (R_g + R_s) + jw(L_g + L_s) \tag{4.35}$$

$$Z_{12} = z_{12} + R_s + jwL_s \tag{4.36}$$

$$Z_{21} = z_{21} + R_s + jwL_s \tag{4.37}$$

$$Z_{22} = z_{22} + (R_d + R_s) + jw(L_d + L_s) \tag{4.38}$$

where the extrinsic device parameters are denoted by uppercase letters (Z). The key to this extraction technique lies in the fact that at sufficiently low frequencies, the inductances have a minimal effect on the response of the small-signal model.

Because the intrinsic elements are extracted at low frequencies, the assumption is valid that intrinsic elements extracted in the absence of parasitic inductances are close to the actual values for the complete model. From equations above, the inductances can be computed at high frequencies by evaluating imaginary components of the measured and modeled data.

$$\mathrm{Im}\{Z_{11meas}\} - \mathrm{Im}\{z_{11\mathrm{mod}}\} = \Delta Z_{11} = w(L_g + L_s) \tag{4.39}$$

$$\mathrm{Im}\{Z_{12meas}\} - \mathrm{Im}\{z_{12\mathrm{mod}}\} = \Delta Z_{12} = wL_s \tag{4.40}$$

$$\mathrm{Im}\{Z_{21meas}\} - \mathrm{Im}\{z_{21\mathrm{mod}}\} = \Delta Z_{21} = wL_s \tag{4.41}$$

$$\mathrm{Im}\{Z_{22meas}\} - \mathrm{Im}\{z_{22\mathrm{mod}}\} = \Delta Z_{22} = w(L_d + L_s) \tag{4.42}$$

The inductance values are then easily obtained from the ΔZ_{ij} data as follows:

(1) L_s from ΔZ_{12} or ΔZ_{21}

(2) L_g from ΔZ_{11}

(3) L_d from ΔZ_{22}

Successively better approximations to both the intrinsic and extrinsic element values can be obtained by repeating this extraction procedure, but de-embedding the inductance found in the previous iteration in all subsequent iterations. Diminishing returns in increased accuracy are usually achieved after two or three iterations. The algorithm for the extraction of intrinsic elements and parasitic inductors is as follows:

1- Convert measured S-parameters to z-parameters using equations (4.7) through (4.10).
2- Evaluate inductances from equations (4.39) through (4.42) (inductors set to zero for first iteration)
3- De-embbed parasitics to obtain low frequency intrinsic z-parameters using equations (4.35)-(4.38).
4- Convert the intrinsic z-parameters to y-parameters using equations (4.15) through (4.18).
5- Evaluate intrinsic elements; for capacitances from equations (4.23) through (4.25), for output conductance equation (4.26), for transconductance equation (4.31), for R_i and τ equations (4.32) and (4.33)
6- Compute intrinsic modeled z-parameters from circuit elements found in step 5.
7- Compute extrinsic modeled z-parameters from equations (4.35) through (4.58) using known parasitic resistance values and inductances found in step 2.
8- Convert extrinsic modeled z-parameters back to S-parameters
9- Compute modeling error, E_{mod} from equation 4.34
10- If $E_{\mathrm{mod}} < E_{tol}$ then go to 11, otherwise go to 2.
11- Stop.

Note the large decrease in modeling error resulting from the inclusion of parasitic inductances [17].

4.3 Large-Signal Extraction

The empirical and physical parameters contained in large-signal device models are rarely known when devices are fabricated or acquired by the circuit or device designer. These parameters define the electrical characteristics unique to an individual device and must be extracted for use in a large-signal circuit simulation. The parameter values are defined by fitting measured data to modeled data. The measured data can include measured physical parameters such as device geometry or doping density, or electrical parameters such as I-V characteristics or S-parameters. The problem of which measurements to make in order to characterize fully a device

in terms of large-signal behavior is significant. Currently, small-signal S-parameters over a varied bias range and harmonic content in the output signal have been used with good success.

Some parameters required for a large-signal MESFET model can be determined from direct analytical and graphical techniques. Section 4.1 presents methods to obtain parasitic resistance values in MESFETs and Schottky diode parameters for MESFETs using such techniques. Extraction of most other required parameters, however, is significantly more difficult. The process of determining these other parameters is greatly simplified by using nonlinear optimization techniques. The development of multidimensional optimization routines is a task that requires familiarity with many specialized concepts.

This section first presents a general introduction of some optimization terminology and methods, then applies these methods to the particular problem of large-signal model parameter extraction [1][15][17][18].

4.3.1 Non-linear Unconstrained Optimization

Nonlinear optimization is the process of finding the minimum and maximum of a nonlinear function of one or several independent variables. The function being maximized or minimized is called the **objective function**.

If the problem is solved by allowing the independent variables to assume any value, then it is an **unconstrained problem**; otherwise it is a **constrained problem** and confining conditions are called **constraints**. For most cases, large-signal parameter extraction is solved using unconstrained optimization [17].

4.3.2 Fundamentals of Unconstrained Optimization

Firstly, let us describe some important functions:

n→number of independent variables

$$x=\begin{bmatrix} x_1 \\ x_2 \\ . \\ . \\ x_n \end{bmatrix} \rightarrow \text{Vector form of variables}$$

$F(x_1, x_2, ..., x_n) \rightarrow$ Objective function

The ultimate goal of optimization is to find the global minimum of the objective function. In terms of large-signal parameter extraction problems, the error function defining the difference between the measured and modeled data is minimized. The set of parameters at the minimum is called the minimizer. The minimizer of a function can take on several forms and is usually expressed as x^*.

If the error $x^k - x^*$ exists, then the pth order rate of convergence is defined by the limit

$$\beta = \lim_{k\to\infty} \frac{\left\| x^{k+1} - x^* \right\|}{\left\| x^k - x^* \right\|^p} \tag{4.43}$$

where x^k represents the kth iteration and x^* is the minimum the term β $(0 \le \beta < 1)$ is known as the convergence ratio. The most important cases are p=1 (1st order or linear convergence) and p=2 (2nd order or quadratic convergence).

The most important part of setting up an optimization problem is defining the objective function. The choice of objective function affects both the numerical efficiency of the routine and, more importantly, the validity of the final solution. For large-signal parameter extraction, the primary concern is to match measured to modeled data. Which measured data to use, however, is not obvious. The DC data, small-signal RF data, load-pull contours, large-signal S-parameters, and harmonic signal content as a function of input power have all been used by some investigators.

The formulated function uses measured and modeled drain current, transconductance, and output conductance. These quantities can be easily measured and are easily modeled using any large-signal models drain current expression and derivatives.

The function is then minimized using an appropriate optimization method. The error is defined in the form of a sum of the squares of nonlinear functions.

$$F(x)=\sum_{i=1}^{m}\left[\sum_{j=1}^{p} r_{i,j}^{2}(x)\right] \text{ for } i=1:1:m \text{ and j=1:1:p} \tag{4.44}$$

$r_{i,j}$ represents the difference between measured and modeled drain current, transconductance, and output conductance;

m→total number of data points

p→number of nonlinear device properties to be optimized

(i.e., drain current, transconductance, output conductance etc.)

x→the group of n variables (model parameters such as α, β, V_{TO} etc.) to be optimized.

The $r_{i,j}$ are known as residuals and are expressed as:

$$r_{i,j}=y_{i,j}-M(x,z_i) \text{ for } i=1:1:m,\ j=1:1:p \tag{4.45}$$

$y_{i,j}$→ represent the measured properties

$M(x,z_i)$→represents the model equations, which are a function of both the model parameters x and terminal voltages z_i.

Varying importance can be placed on the nonlinear device properties by applying scalar quantities called weighting factors. The resulting function to be minimized is then given as:

$$F(x)=\sum_{i=1}^{m}\left[\sum_{j=1}^{p} w_j r_{i,j}^{2}(x)\right] \text{ for } i=1:1:m \text{ and j=1:1:p} \tag{4.46}$$

w_i represents the weighting factors. The minimization of functions of this kind is called weighted nonlinear least squares. The objective function can be formulated in many other ways, however, the form presented works well in practice.

Here is we show a random optimization technique algorithm below [17]:

1- Set N= number of variables
2- Set Tol= routine termination value

3- Bracket each variable by determining a maximum and minimum value for each variable
4- Loop
5- Set n=random number between 0 and 1.
6- For i=1 to N
7- Set $x_i = x_{\min} + (x_{\max} - x_{\min}) * n$
8- Next i
9- Evaluate $F^k(x) \rightarrow F^{k+1}(x)$
10- If $F^{k+1}(x) < F^k(x)$ then save x.
11- Until $F^{k+1}(x) < \text{Tol}$

4.3.3 A large-Signal Parameter Extraction Methodology

Various methods exist for determining the large-signal model parameters for MESFET. A more efficient method is to use DC and small-signal S-parameter measurements to determine large-signal device behavior.

Large signal device behavior is approximated by measuring S-parameters over many bias voltages from the linear through the saturation regions of device operation. Static DC measurements are also made at the bias points where the S-parameters are measured. The nonlinear equivalent circuit element values are extracted at all bias voltages, thereby creating an equivalent circuit for the device at each bias point. The parasitic resistances, inductances, and drain-source capacitance C_{ds} are considered linear elements and remain constant for all bias voltages. A compression of data is realized from the S-parameters to the equivalent circuit. The importance of the data compression is apparent when the parameter extraction problem is solved using explicitly defined optimization goals.

The technique described above offers several advantages over many other large-signal parameter extraction methods. It eliminates the need for time-consuming, expensive, and demanding measurements, while providing excellent agreement between measured and modeled characteristics. Load-pull measurements, pulsed I-V measurements, and transient or harmonic output power measurements all require significant expenditures of time or capital. The complexity of these

measurements also often reduces their accuracy. The DC and S-parameter data required of this method are easily taken using equipment commonly available in any microwave laboratory. An extremely useful by-product of the procedure described above is that small-signal equivalent circuit models are obtained for a number of bias levels. These models can be scaled to describe devices with arbitrary gate widths and used in small-signal simulations.

The extraction problem is defined by first obtaining the DC measurements and nonlinear equivalent circuit elements over bias from measured S-parameters. The device model parameters are then adjusted by using the optimization program. This fits the measured nonlinear elements g_m and g_{ds} ($1/r_{ds}$) , and the measured DC drain-source current I_{ds} to the modeled values obtained using a device model. Using this technique, the device model can be used to simulate both the DC and frequency-dependent large-signal characteristics. In a similar manner, the nonlinear gate-source capacitance C_{gs} and gate-drain capacitance C_{gd} parameters can be determined using a capacitance model of choice. The extraction of the capacitance-voltage model parameters is therefore independent of the extraction of other model parameters.

The objective function is termed the error magnitude unit (EMU) and is defined by equation below. (This formula is typical of a nonlinear weighted least-squares problem.)

$$EMU = \frac{EMU^{'}}{3n} \tag{4.47}$$

where n→number of bias points and

$$EMU^{'} = \sum_{i=1}^{n} \left[E_{I_{ds}}(i).WF_{I_{ds}} + E_{g_m}(i).WF_{g_m} + E_{g_{ds}}(i).WF_{g_{ds}} \right].100 \tag{4.48}$$

and

$$E(i) = \frac{\left[meas(i) - \text{mod}(i) \right]^2}{meas(i)^2}, \text{ for } I_{ds},\ g_m, \text{ and } g_{ds} \tag{4.49}$$

with $WF_{I_{ds}}$, WF_{g_m}, and $WF_{g_{ds}}$ as normalized weighting factors for I_{ds}, g_m, and g_{ds} respectively.

The above EMU equation is used to determine all model parameter values except capacitance parameters. Capacitance parameters can be determined independently and a capacitance EMU is easily defined by

$$EMU_{cap} = \frac{EMU_{cap}'}{2n} \tag{4.50}$$

where n→number of bias points and

$$EMU_{cap}' = \sum_{i=1}^{n}\left[E_{C_{gs}}(i).WF_{C_{gs}} + E_{C_{gd}}(i).WF_{C_{gd}}\right].100 \tag{4.51}$$

and

$$E(i) = \frac{\left[meas(i) - \text{mod}(i)\right]^2}{meas(i)^2}, \text{ for } I_{ds},\ g_m,\ \text{and } g_{ds} \tag{4.52}$$

Parameters typically required of a physically based MESFET model include semiconductor layer thickness, gate dimensions, dimensions of other surface features such as terminal spacing, doping densities, and transport properties such as electron mobility and saturated velocity. Unfortunately for the circuit designer, device manufacturers and foundries typically consider such information proprietary. Thus, the physical characteristics of the device are not often known when the design process begins.

An attractive alternative to making direct measurements of the physical characteristics of a finished device is to make electrical measurements of device behavior and then extract physical properties. Using this technique, the physical dimensions and material properties of the device are treated as model parameters.

In addition to predicting large-signal device performance, large-signal models can also be used to estimate small-signal S-parameters. This may be useful when measured S-parameters are only available for a limited number of bias points or in order to achieve data compression when storing data for a large number of devices [1][15][17][18].

CHAPTER 5

MEASURED VALUES AND APPLICATION TO MODELS

In the previous chapters we have defined MESFET structure, MESFET models, and how to model these structures to have nearly the best results. As we know from the previous chapters there are a few different large-signal MESFET models. In this chapter we will compare these different large signal models by using the measured data for different size of MESFETs.

We used the small signal model parameters obtained by Çelebi [1], which are needed in obtaining the large signal model parameters. In the following lines the relevant parameters transconductance, output conductance and nonlinear capacitance, for large signal $V_{ds} - I_{ds}$ curves, will be discussed.

5.1 Measured Values

Following measurements refers to the Figure 5.1.

5.1.1 Forward-Bias gate Measurements

The gate voltage is increased from 0.300V up to 0.825V with 0.025V increments, and at each voltage level the gate current is taken [1]. These data, taken for two cases one for the source is shorted while the drain is left open and the other for the drain is shorted and the source is left open, are given in Table 5.1 and Table 5.2.

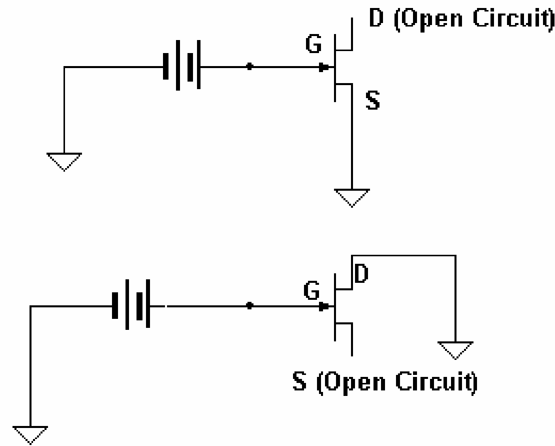

Figure 5-1 Forward-gate Bias Measurement of MESFET Circuit

Case 1: The source is shorted while the drain is left open.

Table 5–1 $V_{gs} - I_g$ data obtained for source-short / drain open case [1]

	2x50	**2x150**	**4x50**	**4x75**	**4x100**	**4x125**	**4x150**	**4x175**	**6x50**	**6x150**
V_{gs}, V	I_g, μA	I_g, μA	I_g, μA	I_g, μA	I_g, μA	I_g, μA	I_g, μA	I_g, μA	I_g, μA	I_g, μA
0.300	0.014	0.027	0.022	0.030	0.035	0.041	0.049	0.055	0.030	0.092
0.325	0.028	0.056	0.047	0.062	0.076	0.089	0.106	0.120	0.065	0.201
0.350	0.060	0.123	0.105	0.139	0.168	0.200	0.238	0.267	0.142	0.448
0.375	0.131	0.275	0.228	0.305	0.375	0.450	0.540	0.615	0.319	1.000
0.400	0.289	0.615	0.516	0.660	0.835	1.019	1.225	1.345	0.721	2.229
0.425	0.639	1.399	1.170	1.480	1.860	2.260	2.678	3.020	1.548	4.985
0.450	1.406	3.090	2.620	3.50	4.345	5.148	5.995	7.150	3.582	Kas.19
0.475	3.090	6.950	5.600	7.58	9.510	11.34	13.82	15.67	7.980	24.62
0.500	6.760	15.87	12.35	16.98	20.99	26.31	30.01	34.63	17.86	54.74
0.525	14.98	35.19	27.52	37.59	47.15	58.57	69.05	77.83	39.18	119.5
0.550	33.03	78.15	62.96	82.50	104.7	132.0	151.9	169.8	96.44	263
0.575	71.36	169.4	133.2	182	227.4	281.6	329.9	369.7	189	561
0.600	151.3	365	285.3	390	505	609	714	776	406	1160
0.625	311	728	597	810	1000	1225	1418	1526	836	2244
0.650	599	1374	1150	1559	1885	2274	2596	2845	1620	4050
0.675	1052	2319	2020	2714	3288	3919	4380	4668	2856	6570
0.700	1698	3577	3220	4355	5270	6060	6700	7160	4590	9850
0.725	2518	5170	4800	6350	7540	8700	9530	10040	6800	13730
0.750	3480	6960	6630	8720	10330	11790	12760	13380	9380	18090
0.775	4570	8960	8670	11350	13340	15010	16350	16970	12280	22870
0.800	5790	11110	11060	14170	16610	18640	20130	20960	15510	27920
0.825		13340	13270	17280	20050	22380	24080		18770	

Case 2: The drain is shorted and the source is left open.

Table 5–2 $V_{gs} - I_g$ data obtained for drain -short / source-open case [1]

	2x50	**2x150**	**4x50**	**4x75**	**4x100**	**4x125**	**4x150**	**4x175**	**6x50**	**6x150**
Vgs, V	Ig, µA	Ig, µA	Ig, µA	Ig, µA	Ig, µA	Ig, µA	Ig, µA	Ig, µA	Ig, µA	Ig, µA
0.300	0.013	0.026	0.022	0.030	0.036	0.042	0.052	0.055	0.030	0.090
0.325	0.027	0.057	0.046	0.063	0.076	0.093	0.110	0.125	0.066	0.195
0.350	0.058	0.126	0.103	0.142	0.173	0.209	0.250	0.280	0.146	0.440
0.375	0.125	0.280	0.227	0.312	0.390	0.467	0.552	0.608	0.324	0.980
0.400	0.275	0.632	0.525	0.726	0.849	1.082	1.234	1.389	0.714	2.192
0.425	0.627	1.420	1.143	1.600	1.980	2.440	2.770	3.150	1.636	4.862
0.450	1.333	3.170	2.522	3.590	4.435	5.527	6.420	7.25	3.65	10.89
0.475	3.020	7.19	5.67	7.930	9.84	12.23	14.08	16.00	8.12	24.11
0.500	6.65	16.28	12.84	17.49	21.94	28.50	31.59	35.29	17.84	53.51
0.525	14.35	36.37	27.82	39.20	48.68	60.68	70.63	79.59	39.62	118
0.550	31.82	80.36	61.71	86.57	106.3	133.7	156.5	177.0	88.22	257
0.575	70.22	172.5	135.7	190.4	235.5	295.0	342	385	192.5	557
0.600	155	362	286.3	415	505	641	725	804	428	1161
0.625	325	747	611	856	1039	1282	1460	1592	877	2310
0.650	647	1415	1210	1676	1977	2433	2750	2960	1740	4220
0.675	1240	2380	2170	2980	3480	4180	4630	4960	3135	7060
0.700	2100	3740	3590	4930	5560	6600	7240	7640	5120	10770
0.725	3330	5330	5390	7260	8060	9560	10300	10830	7790	15720
0.750	4790	7250	7570	10060	11080	13030	13790	14580	10980	20360
0.775	6540	9280	10020	13240	14290	16680	17600	18660	14530	25950
0.800	8430	11580	12720	16650	17840	20650	21660	22930	18390	32150
0.825		13800	15490	20330	21660				22540	

5.1.2 Breakdown Voltage Measurement

Breakdown voltage is defined as the gate voltage where the knee occurs before the gate current rapidly increases in the reverse bias region. Breakdown Voltage measurements are performed for two cases, as in the forward bias gate measurements. In the first case, the gate is driven by negative voltages while the drain is left open. In the second case, the source is left open, and the drain is grounded.

Results obtained for the both cases showed that, for the MESFET the breakdown voltage was obtained as –13 Volts, which is equivalent to having $V_{BR} = 13\text{V}$.

V_{BR} is a constant model parameter and throughout the extraction processes

breakdown voltage is taken as $V_{BR} = 13\text{V}$ for all transistors.

5.1.3 Pinch-off Voltage V_t Measurements

The pinch-off voltage is defined as the potential required, which extend the depletion region across the entire active channel, preventing the current from flowing from drain to source. Practically, there is a pre-defined current level and the potential at this current level is called as the pinch-off voltage. Hence, the pinch-off voltage is defined as the potential at the minimum current value obtainable from drain to source. That is the gate-to-source voltage level at a V_{ds} potential and at a minimum value of I_{ds} current value.

Table 5–3 Pinch-off voltage values for various V_{ds} voltage levels [1].

		V_{ds} (V)				
		0.5	**1.0**	**2.0**	**3.0**	**4.0**
V_t	**2x50**	-1.827	-1.855	-2.069	-2.116	-2.251
	2x150	-1.881	-1.936	-1.996	-2.101	-2.131
	4x50	-1897	-1.914	-2.024	-2.259	-2.235
	4x75	-1.870	-1.914	-1.974	-2.124	-2.218
	4x100	-1.887	-1.911	-2.017	-2.101	-2.217
	4x125	-1.850	-1.934	-2.067	-2.169	-2.239
	4x150	-1.875	-1.897	-1.974	-2.080	-2.188
	4x175	-1.880	-1.928	-2.007	-2.125	-2.199
	6x50	-1.879	-1.926	-2.023	-2.143	-2.204
	6x150	-1.864	-1.910	-2.005	-2.009	-2.225

5.1.4 S-Parameters Measurements for Extrinsic Elements

To extract the extrinsic elements, S-parameters with the drain-source voltage V_{ds} set to zero and gate under forward bias are needed. For each transistor, four S-parameters measurements at four different forward gate currents are performed. Hence, as explained, the drain voltage is set to zero, while the forward gate bias is adjusted to give four different gate currents. At each gate current, the s-parameters are measured.

The parasitic inductances are found from the imaginary parts of the Z-parameters, whereas the parasitic resistances are extracted from the real parts.

This subject has been discussed before and we are now dealing with the

results of this measurement and the values of L_g, L_d, L_s, R_g, R_d, and R_s are tabulated in the table below.

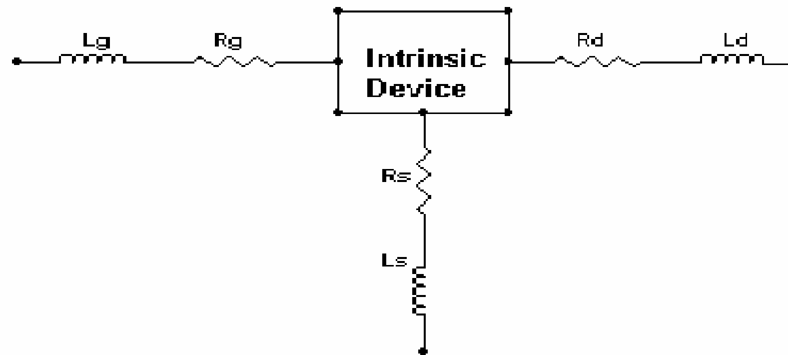

Figure 5-2 Extraction process of Extrinsic device parameters

Table 5–4 Model Parameters extracted from the S-parameters Measurements for the Extrinsic circuit elements [1]

	2x50	2x150	4x50	4x75	4x100	4x125	4x150	4x175	6x50	6x150
R_g (Ohm)	3.5	3.3	1.22	1.13	1.65	1.30	1.80	1.67	0.70	1.00
R_d (Ohm)	6.6	2.82	3.5	2.5	2.08	1.75	1.55	1.45	2.50	1.0
R_s (Ohm)	6.4	2.45	3.2	2.3	1.8	1.5	1.25	1.10	2.15	0.86
R_c (Ohm)	15	5	7.5	5	3.75	3	2.5	2.14	5	1.67
L_g (pH)	34.04	50.29	24.63	28.59	28.87	29.18	29.82	32.78	24.77	24.63
L_d (pH)	31.82	55.06	26.48	28.83	32.35	38.35	41.12	45.73	43.21	41.40
L_s (pH)	0	0	1.221	0.502	1.760	1.672	0.999	1.518	0.700	2.736

5.1.5 $V_{ds} - I_{ds}$ Measurements

The drain-source current versus drain-source voltage characteristics, at gate-source voltage levels of 0, -0.25, -0.50, -0.75, and –1.00 V, are measured.

The tables shown in Appendix A for the MESFET structures, are our main reference for the discussion of MESFET Models [1]. These results all shown in tables above will be discussed in the following section for Large-signal model parameter extraction process.

5.2 Large-Signal Models

In this section, the mostly known models for MESFETs are described briefly and the relevant parameters are extracted using MATLAB program. Several researchers have developed empirical models that describe the operational characteristics of MESFETs. All of these models are capable of describing the large signal properties of microwave MESFETs with some success.

Generally, modeling approach is started with examining the measured device characteristics, which are shown in tables above, and then look for a mathematical function that behaves in the same manner. The mathematical function includes adjustable parameters, when an available optimization is satisfied and applied to the mathematical function, this will cause the function to approximate the measured data closely.

Each model that is described in this section uses the same measured data. An algorithm is developed in matlab to obtain the model parameters for all models discussed in this chapter. This algorithm starts with by asking the model type, e.g. 2x150. After entering the type then the program will ask the model name and the relevant parameters and their initial values.

A program, called "program.m" [B1] was written to calculate the concerned parameters for each model. Each model has different numbers of parameters and those parameters were optimized using the "fminsearch.m" and "optimset.m" matlab tools, which are explained in appendices part [B3].

Generally the algorithm of program.m can be expressed as;

- At first part the model and MESFET type is asked
- Depending on the MESFET model, initial parameter values are asked. Each model has different numbers of parameters to evaluate.
- To activate the tool "fminsearch.m", the maximum number of function evaluations allowed, maximum number of iterations allowed, termination tolerance on the parameters and termination tolerance on the function value must be defined by "optimset.m" tool.
- As described in appendices part "fminsearch" uses the Nelder-Mead simplex (direct search) method. [6]
- "fminsearch.m" is an optimization tool, which resolves the function with respect to measured data by converting the initial

parameters to appropriate ones. The aim is minimization of the difference of mathematically evaluated data and measured I_{ds} data to nearest values.

- After possible minimization is applied, the evaluated $I_{ds} - V_{ds}$ data, with related new parameter values, and the measured $I_{ds} - V_{ds}$ characteristics with respect to V_{gs}, and g_m and g_{ds} are plotted as output.

As shown in the appendices part [B1], the “program.m” constitutes the problem of initial parameter assigning. The mathematical function as referred in model descriptions, which have different numbers of parameters that will be defined with initial values and then will be optimized to appropriate values to satisfy the measured values of MESFET. These initial values are randomly chosen entries, for example for most of the MESFET types and models the initial values for parameters are given as “1”. But for some models initial values do not help to optimize the mathematical function to measured data, so the initial values must be changed to obtain suitable results.

At that part of the problem we have tried different ways of evaluation of the model parameters for good approximation to measured values. The first tried and applied method is to use a different tool, “fminunc.m”, instead of “fminsearch.m”. This tool has nearly the same characteristics with fminsearch, but it takes much more time than fminsearch. Therefore this tool is not applied for optimization.

The most useful method to solve the problem of initial parameter entries was found to be “genetic algorithm code”. This code is given by Prof. Dr. Gönül Turhan SAYAN and it is applied to the MESFET model optimization. The adapted code algorithm for MESFET models, which is illustrated in appendices part [C1], provides simplicity for initial parameter entries. All entries are asked for the intervals of the parameters that are most suitable. The code tries to find the best defined parameters in the interval. The number of trials is asked in the program, increasing the number gives more suitable results for optimization. And the time for application of this code depends on the parameter values intervals and the number of the trials. Therefore this program consumes much more computer time than the fminsearch algorithm. But in some application this algorithm was very helpful to find the initial parameters, when the trials did not satisfy good approximation to measured data.

In this study, $I_{ds} - V_{ds}$ characteristics and g_m and g_{ds} characteristics are formulated and plotted with respect to various V_{gs} voltages. As described in previous chapters the capacitances, C_{gs} and C_{gd} are also described as the large signal parameters. But these parameters can be evaluated with respect to some measured values for capacitances at various voltage levels. In the previous study the capacitances are evaluated only from S-parameter measurements, which could not satisfied. We will try to define the capacitances as formulas for each model.

5.2.1 Tajima Model [7]

In the paper [7], Tajima, Wrona, and Mishima (in the discussion the model will be called as Tajima) have proposed, a technique to model the large-signal behavior of GaAs FETs. The proposed expression of *I-V* characterics for FET is applied to MESFET measured data, and the comparison of measured data and modeled data showed good approximations.

Tajima's equivalent circuit for FET under large-signal operation is shown in Figure 5.3. The element values for large-signal operation vary with time because at large driving levels they become dependent on terminal voltages. Tajima considered two of the terminal voltages to be independent and chose the set of V_{gs} and V_{ds}, V_{gs} being the voltage across the gate capacitance and V_{ds} across the drain conductance. Restriction of the interest to the signal frequency and ignoring the effects due to higher harmonic components, these voltages can be written as;

$$V_{gs} = V_{gs0} + v_{gs} \cos(wt + \phi) \qquad (5.1)$$

$$V_{ds} = V_{ds0} + v_{ds} \cos wt \qquad (5.2)$$

where V_{gs0} and V_{ds0} are the dc bias voltages, v_{gs} and v_{ds} amplitudes of signal frequency components, and ϕ the phase difference between gate and drain voltages. The equivalent circuit for the signal frequency can now be expressed as a function of

the following parameters, which are independent of time: V_{gs0}, V_{ds0}, v_{gs}, v_{ds}, w, and ϕ.

In order to avoid unnecessary complexity of calculations, Tajima has limited the nonlinear behavior to five elements, gate forward conductance G_{gf}, gate capacitance C_{gs}, gate charging resistance R_i, transconductance g_m, and drain conductance g_d. Here, G_{gf} represents the effect of the forward rectified current across the gate junction under large-signal operation. No voltage dependence was assumed for parasitic elements, i.e., lead inductances (L_g, L_d, L_s), contact resistances (R_g, R_d, R_s), and pad capacitances (C_{ge}, C_{de}). Tajima has also ignored the voltage dependence of drain channel capacitance C_{ds} and feedback capacitance C_{dg} due to their small values.

Transconductance g_m and drain conductance g_d are defined as

$$g_m = \left(\frac{i_{ds}}{v_{gs}} \right)_{v_{ds}=0} \tag{5.3}$$

$$g_d = \left(\frac{i_{ds}}{v_{ds}} \right)_{v_{gs}=0} \tag{5.4}$$

where i_{ds} is the RF drain current amplitude. The instantaneous drain current can be written using g_m and g_d as

$$I_{ds} = I_{ds0} + g_m v_{gs} \cos(wt + \phi) + g_d v_{ds} \cos wt \tag{5.5}$$

where I_{ds0} is the dc drain current. Now, a function of drain current I_{ds}, which can be simulated as a function of V_{gs} and V_{ds}, is as follows:

$$I_{ds} = I_{ds}(V_{gs}, V_{ds}) \tag{5.6}$$

Instantaneous current $I_{ds}(t)$ can be obtained by inserting equations (5.1) and (5.2) into (5.6). By multiplying $\sin wt$ to equation (5.5) and integrating over a complete

period, g_m is obtained as

$$g_m = -\frac{w/\pi}{v_{ds}\sin\phi}\int_0^{(2\pi/w)} I_{ds}\sin wtdt. \qquad (5.7)$$

Similarly, g_d is obtained as

$$g_d = \frac{w/\pi}{v_{ds}\sin\phi}\int_0^{(2\pi/w)} I_{ds}\sin(wt+\phi)dt. \qquad (5.8)$$

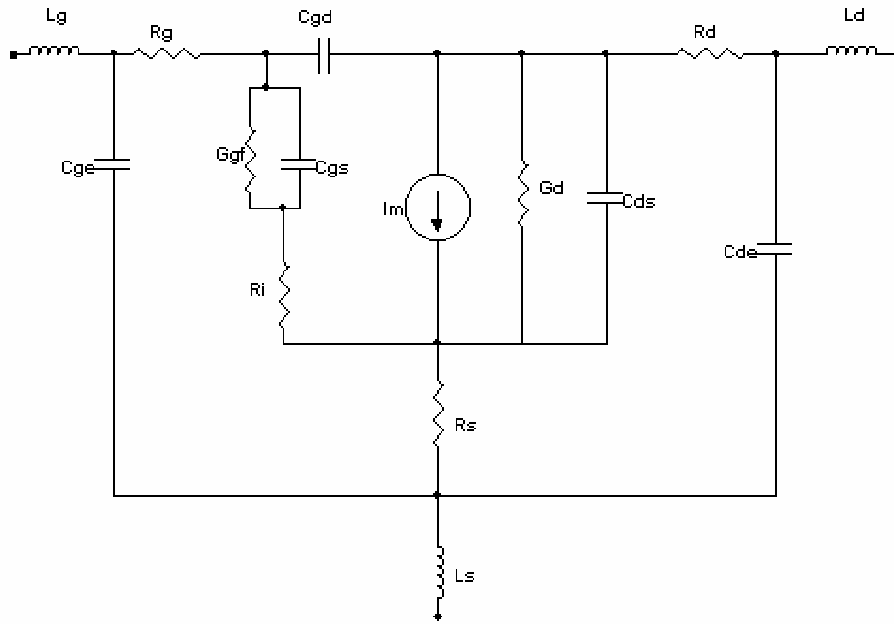

Figure 5-3 FET equivalent circuit of Tajima Large-signal model

Equations (5.7) and (5.8) are now functions of RF amplitudes v_{gs} and v_{ds}, as well as bias voltages V_{gs0} and V_{ds0}.

The equation for I_{ds} was arrived at empirically to simulate the typical dc transistor curves. Any other function that produced the *I-V* behavior could have been used.

$$I_{ds}(V_{ds}, V_{gs}) = I_{d1}\cdot I_{d2}$$

$$I_{d1} = \frac{1}{k}\left[1 + \frac{V_{gs}^{'}}{V_p} - \frac{1}{m} + \frac{1}{m}\exp\left\{-m\left(1 + \frac{V_{gs}^{'}}{V_p}\right)\right\}\right]$$

$$I_{d2} = I_{dsp}\left[1 - \exp\left\{\frac{-V_{ds}}{V_{dss}} - a\left(\frac{V_{ds}}{V_{dss}}\right)^2 - b\left(\frac{V_{ds}}{V_{dss}}\right)^3\right\}\right]$$

$$k = 1 - \frac{1}{m}\{1 - \exp(-m)\}$$

$$V_p = V_{p0} + pV_{ds} + V_\phi$$

$$V_{gs}^{'} = V_{gs} - V_\phi \tag{5.9}$$

where $V_{p0}(>0)$ is the pinch-off voltage at $V_{ds} \sim 0$, V_{dss} is the drain current saturation voltage, V_ϕ is the built-in potential of the Schottky barrier, I_{dsp} is the drain current when $V_{gs} = V_\phi$, and a, b, m, and p are fitting factors that can be varied from device to device. In addition to the fitting factors I_{dsp}, V_{p0}, V_ϕ, V_{dss} are assumed as the parameters for Tajima model. [9]

By differentiating drain current with respect to gate-source voltage and drain-source voltage, the obtained transconductance and output conductance equations for Tajima are written below:

$$g_m = \frac{\partial I_{ds}}{\partial V_{gs}} = \frac{I_{d2}}{kV_p}\left(1 - \exp\left\{-m\left(1 + \frac{V_{gs}^{'}}{V_p}\right)\right\}\right) \tag{5.10}$$

$$\begin{aligned} g_{ds} = \frac{\partial I_{ds}}{\partial V_{ds}} &= I_{d2}\frac{pV_{gs}^{'}}{V_p^2}\left[1 - \exp\left(-m\left[1 + \frac{V_{gs}^{'}}{V_p}\right]\right)\right] \\ &- I_{d1}I_{dsp}\left[\frac{1}{V_{dss}} + \frac{2aV_{ds}}{V_{dss}^2} + \frac{3bV_{ds}^2}{V_{dss}^3}\right]\exp\left\{-\frac{V_{ds}}{V_{dss}} - a\left(\frac{V_{ds}}{V_{dss}}\right)^2 - b\left(\frac{V_{ds}}{V_{dss}}\right)^3\right\} \end{aligned} \tag{5.11}$$

The parameters that have been shown in (5.9) are substituted the results are drawn in figures below. In this analysis “fminsearch.m” algorithm is used. The values were compared with the measured values, which are also shown in the same figures. The transconductance (5.10) and output conductance (5.11) equations are drawn with respect to drain-source voltage V_{ds} for 4x150 type of MESFET, the other types of MESFETs have nearly the same results with 4x150, and therefore they are not drawn here.

The obtained results for Tajima large-signal model are represented below:

Table 5–5 Parameter values for Tajima large-signal model

	V_{ϕ}	V_{PO}	p	m	I_{dsp}	V_{dss}	a	b
2x50 MESFET	0.062	-0.05	-0.0003	-1.27	0.00006	0.306	0.143	-0.011
2x150 MESFET	0.049	-0.04	-0.0005	-1.003	0.00017	0.408	1.313	-0.076
4x50 MESFET	1.7434	1.2462	0.0984	1.2143	0.1151	0.6234	2.7742	0.6511
4x75 MESFET	-0.0051	0.0101	-0.00014	-2.4519	0.0005	0.3189	-0.115	0.07725
4x100 MESFET	0.036	-0.007	-0.0017	-2.759	0.0046	0.378	0.897	-0.0712
4x125 MESFET	0.7989	1.1634	0.1175	1.4603	0.1438	0.6108	2.5096	0.2532
4x150 MESFET	0.229	1.0867	0.1503	0.8	0.1059	0.8627	6.111	-1.0814
4x175 MESFET	0.2857	1.0968	0.1269	1.7803	0.1257	0.3606	0.2246	-0.0185
6x50 MESFET	2.006	1.2909	0.0987	1.3279	0.0595	0.6916	2.7923	0.685
6x150 MESFET	0.4665	1.1237	0.1282	1.1465	0.1941	0.6411	2.0079	0.6282

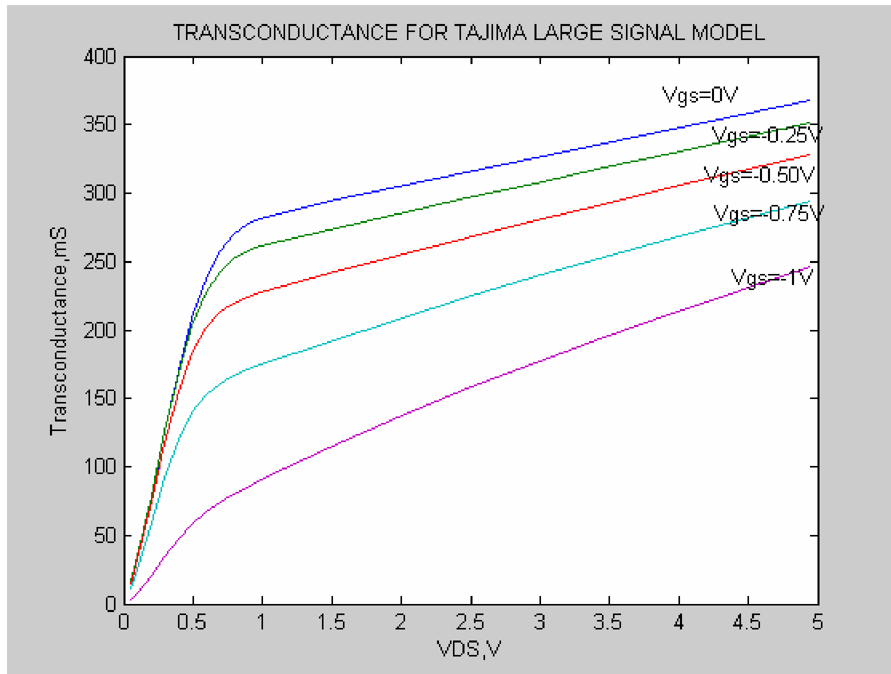

Figure 5-4 Transconductance of 4x150 MESFET for Tajima Large Signal Model

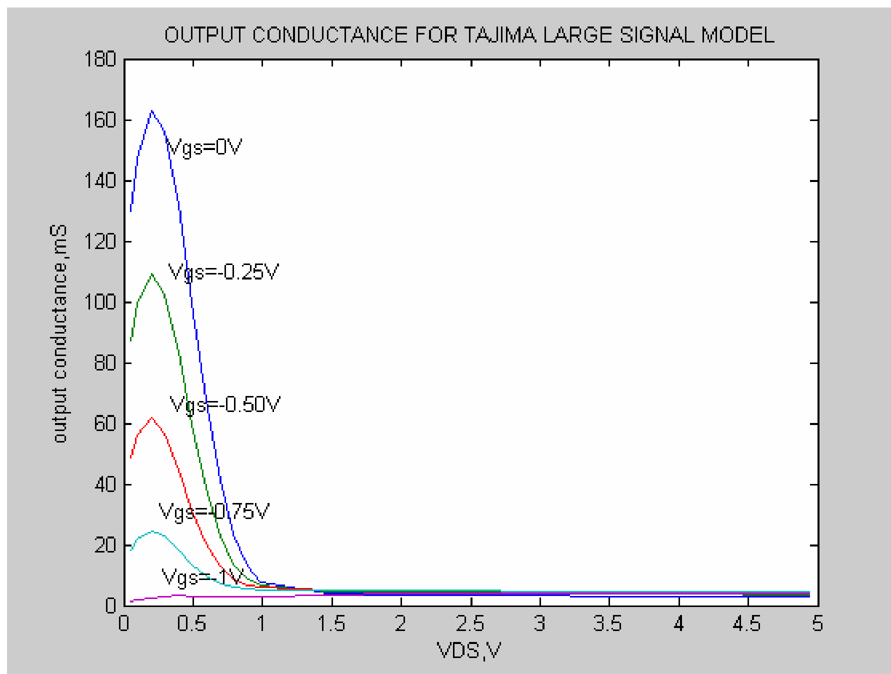

Figure 5-5 Output Conductance of 4x150 MESFET for Tajima Large Signal Model

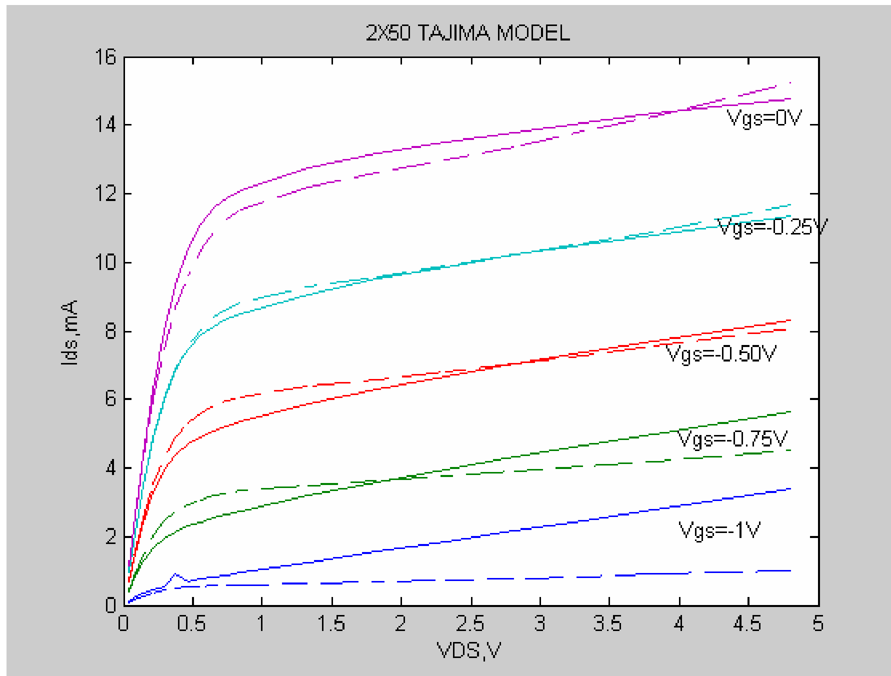

Figure 5-6 Comparison of Vds-Ids characteristics of Tajima Model with measured (solid lines) and theoretical values (dashed lines)

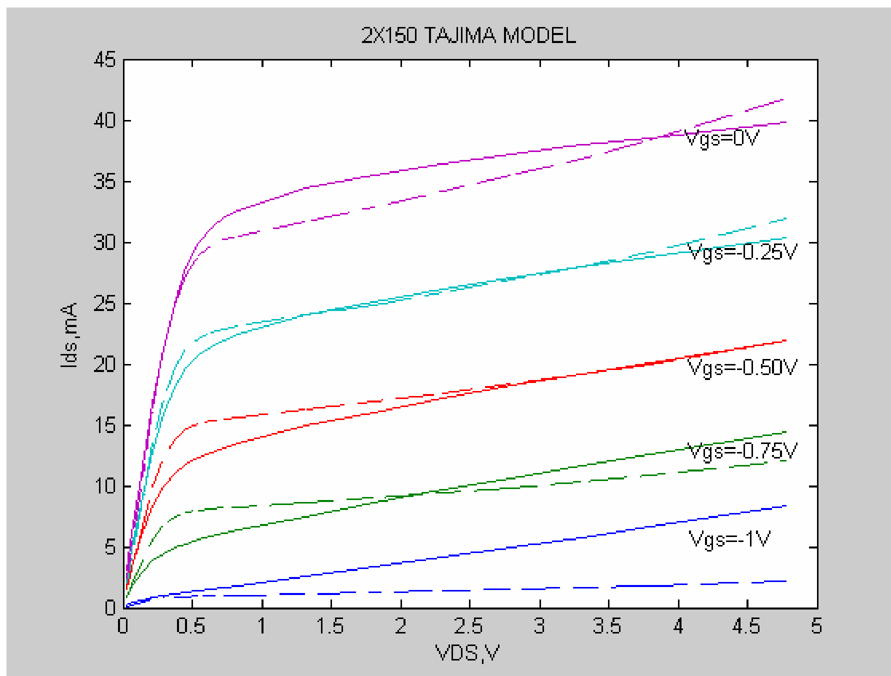

Figure 5-7 Comparison of Vds-Ids characteristics of Tajima Model with measured (solid lines) and theoretical values (dashed lines)

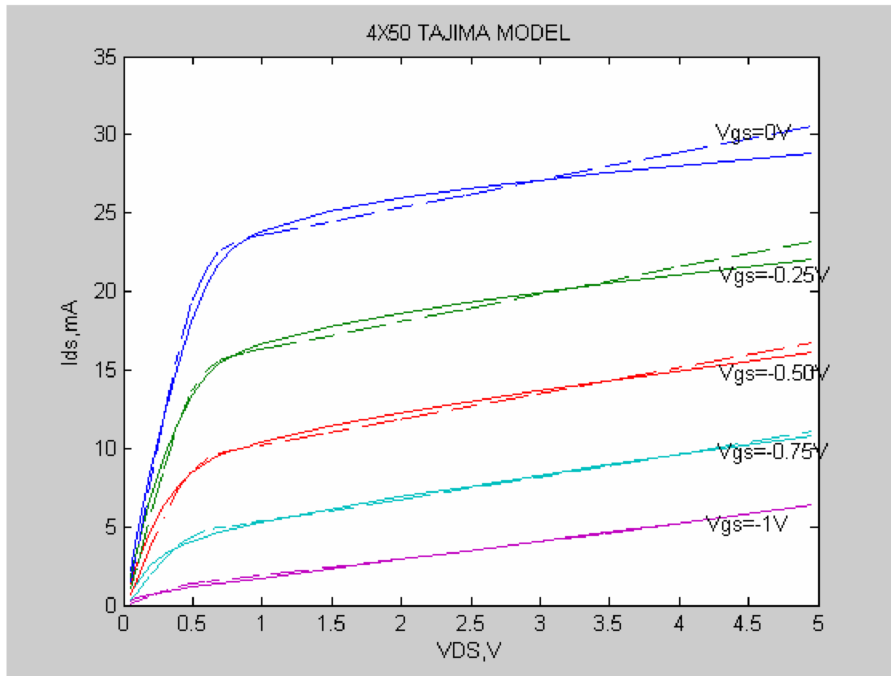

Figure 5-8 Comparison of Vds-Ids characteristics of Tajima Model with measured (solid lines) and theoretical values (dashed lines)

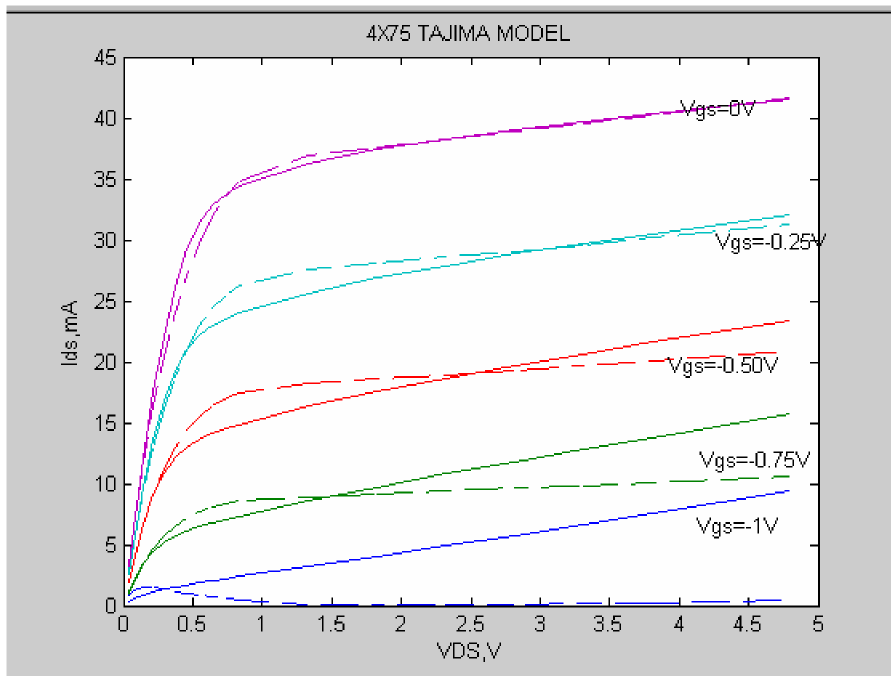

Figure 5-9 Comparison of Vds-Ids characteristics of Tajima Model with measured (solid lines) and theoretical values (dashed lines)

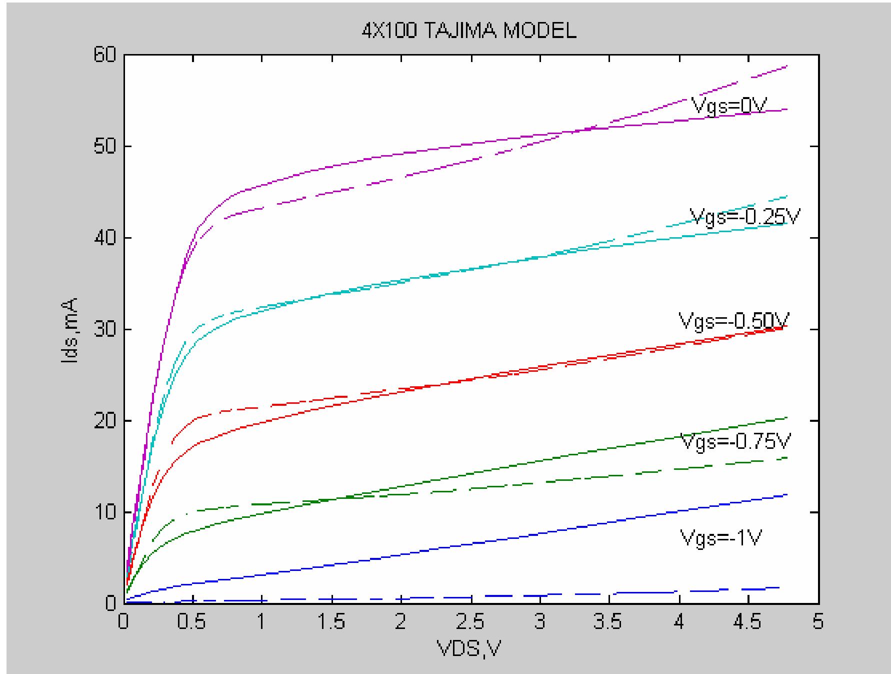

Figure 5-10 Comparison of Vds-Ids characteristics of Tajima Model with measured (solid lines) and theoretical values (dashed lines)

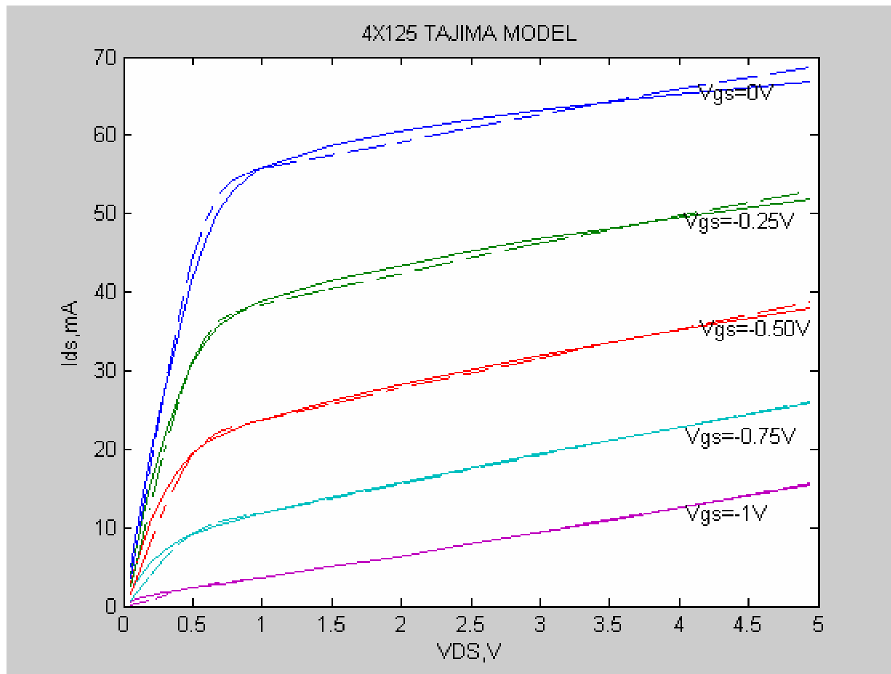

Figure 5-11 Comparison of Vds-Ids characteristics of Tajima Model with measured (solid lines) and theoretical values (dashed lines)

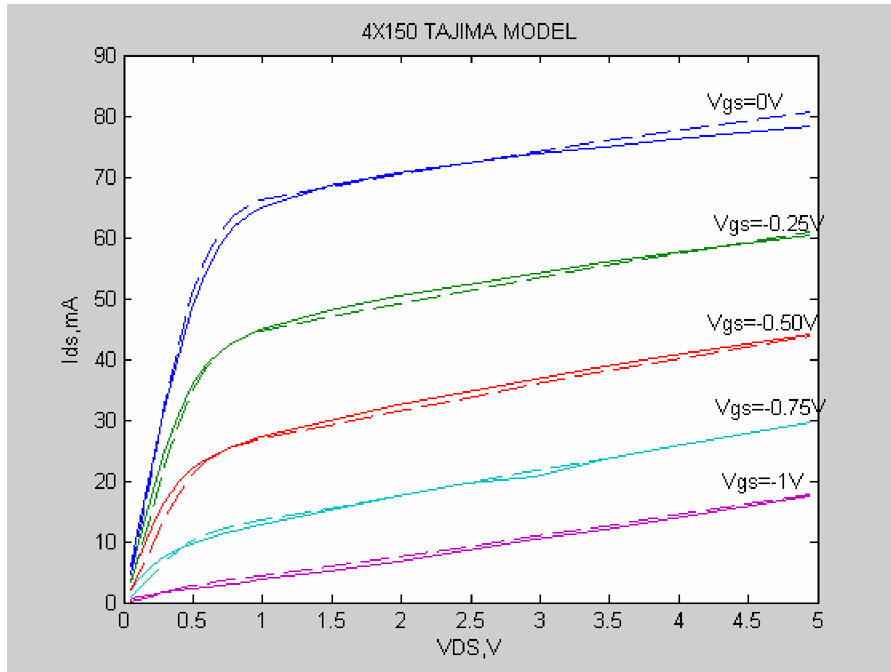

Figure 5-12 Comparison of Vds-Ids characteristics of Tajima Model with measured (solid lines) and theoretical values (dashed lines)

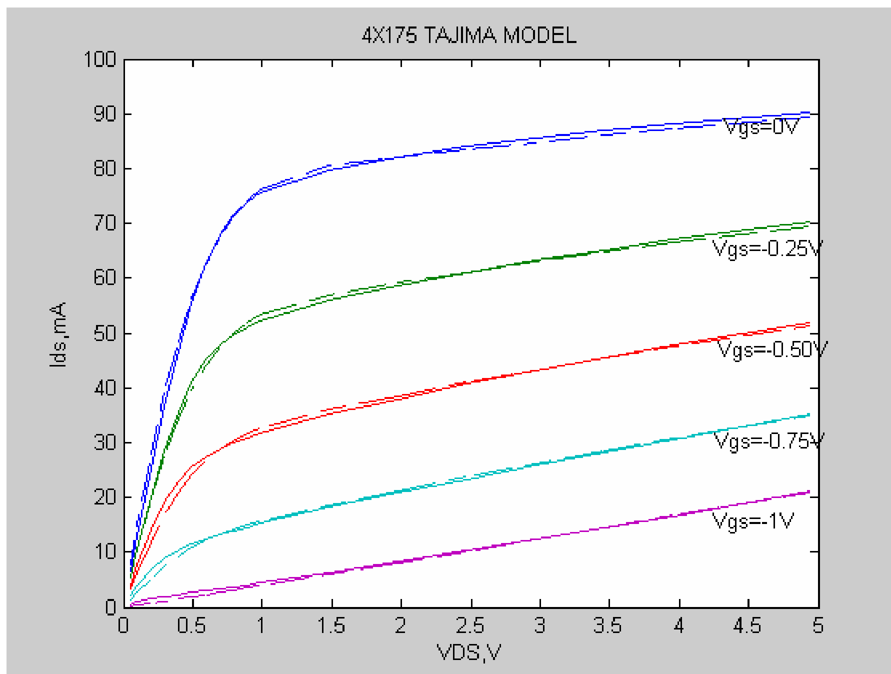

Figure 5-13 Comparison of Vds-Ids characteristics of Tajima Model with measured (solid lines) and theoretical values (dashed lines)

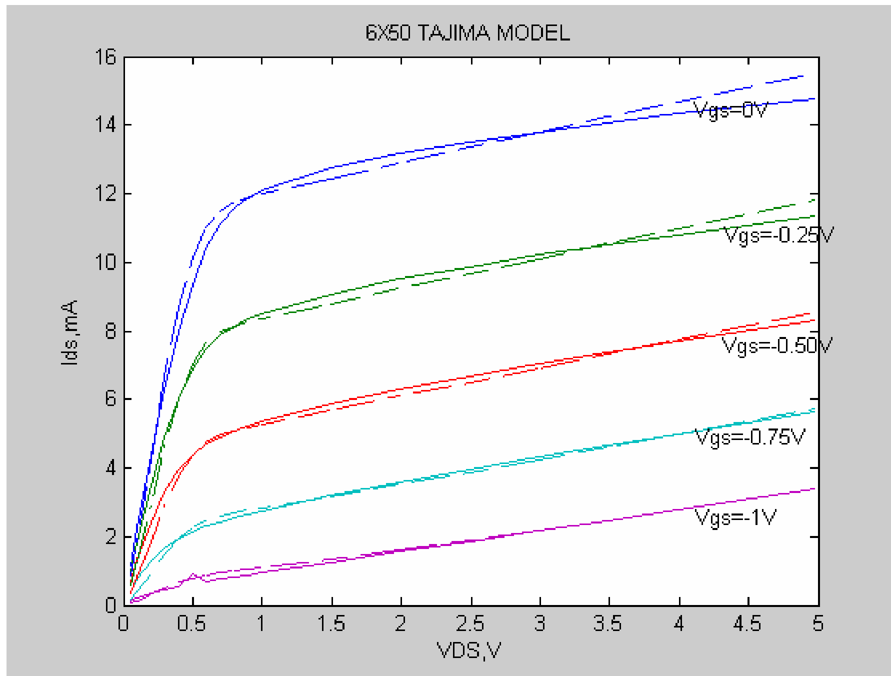

Figure 5-14 Comparison of Vds-Ids characteristics of Tajima Model with measured (solid lines) and theoretical values (dashed lines)

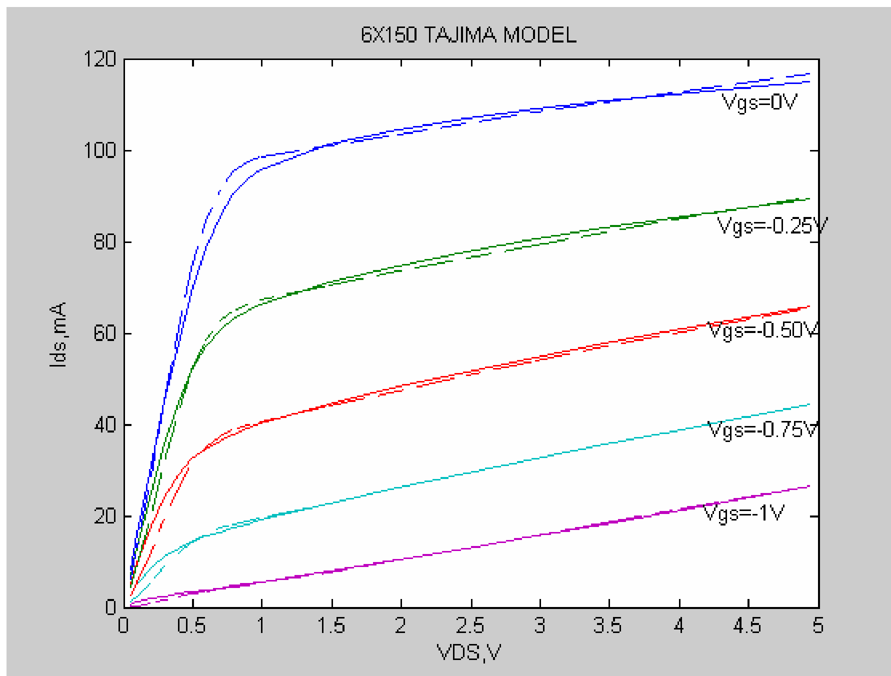

Figure 5-15 Comparison of Vds-Ids characteristics of Tajima Model with measured (solid lines) and theoretical values (dashed lines)

As shown in the figures, Tajima large-signal model presents good approximations to measured data except for 2x50, 2x150, 4x75, and 4x100 types. The other 6 types, 4x50, 4x125, 4x150, 4x175, 6x50, and 6x150, have nearly the same results with the measured data. The former four types are less accurate than the subsequent six types. Only for $V_{gs} = 0V$ the modeled data of I_{ds} (presented as dashed lines) have some errors, but if compared with the other models which are going to be discussed in this chapter, the results are better than the other models. It can be said that the Tajima large-signal model for those measured data is appropriate for some types of MESFETs. The parameter values which are tabulated in Table 5.5, shows that the differences between the types also occurs for those parameter values. The parameters of the four types of MESFETs, which are close to each other, are different than the parameters of the six types of MESFETs, which are again close to each other.

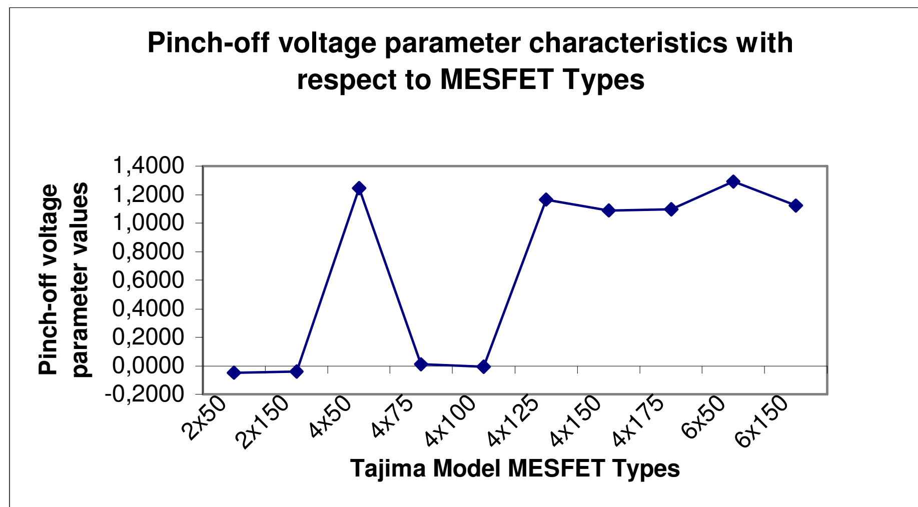

Figure 5-16 Parameter characteristics wih respect to MESFET Types

As represented in Figure 5.16 the parameter Vto is drawn. In the figure the evaluated parameter values are drawn with respect to MESFET types. As discussed before, the figure again shows that for the described 4 types of MESFETs the values of parameters are different than the other 6 types.

5.2.2 Materka&Kacprzak Model [8] [9]

The Materka-Kacprzak Model, which is a modified model of the Taki Model [21], based on experimental study of arbitrarily selected transistors, and the main nonlinear elements of the model (Figure 5.17) are as follows; the equivalent gate-to-source capacitance C_{gs}, the diode D_f, which represents the current in the gate-to-channel junction, the drain current source i_d controlled by voltage variables v_g and v_d, the diode D_r, which represents the effect of the gate–drain breakdown. The diode parameters were not chosen to describe physical phenomena but to provide the best average fit to the experimental breakdown characteristics. The remaining parameters of this model are said to be linear with their usual physical interpretation. The nonlinear gate-to-source capacitance is given by

$$C_{gs} = C_{g0}\left(1 - \frac{v_g}{V_{bi}}\right)^{-0.5}, \qquad \text{for } v_g < 0.8V_{bi} \tag{5.12}$$

and for $v_g \geq 0.8V_{bi}$, the plot of $C_{gs}(v_g)$ is approximated by a straight line with the slope equal to derivative dC_{gs}/dv_g obtained from equation (5.12) at $v_g = 0.8V_{bi}$. The parameters that appear in equation (5.12) are C_{g0}, the gate-to-source capacitance for $v_g = 0$, and V_{bi}, the built-in potential of gate function.

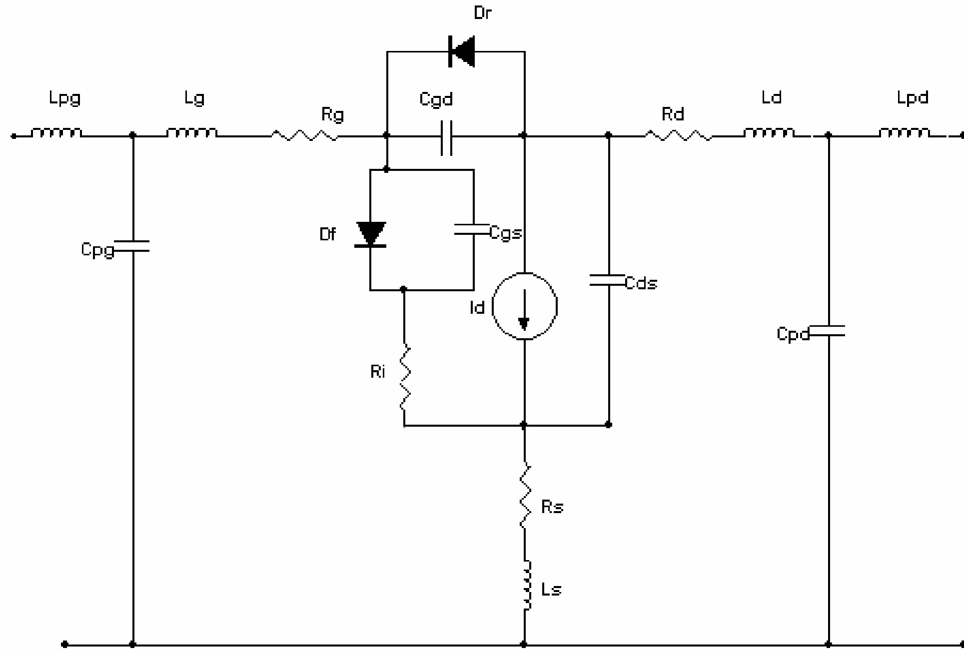

Figure 5-17 Large Signal Equivalent Circuit of Materka-Kacprzak FET Model

The voltage controlled current source i_d is described by the formulas [9]

$$I_{ds} = I_{dss}\left(1 - \frac{V_{gs}}{V_T}\right)^2 \tanh\left(\frac{\alpha V_{ds}}{V_{gs} - V_T}\right) \qquad (5.13)$$

$$V_T = V_{TO} + \gamma V_{ds} \qquad (5.14)$$

where I_{dss}, V_{TO}, α, and γ are the model parameters. In order to take into account the time delay between drain current and gate voltage, the instantaneous current $i_d(t)$ is calculated from equation (5.13) with $v_g = v_g(t-\tau)$ and $v_d = v_d(t)$, where τ is the model parameter.

The derivatives of drain current with respect to drain-source voltage and gate-source voltage individually, transconductance and output conductance are obtained and they are formulated below:

$$g_m = \tanh\left[\frac{\alpha V_{ds}}{(V_{gs} - V_T)}\right]\left[\frac{-2I_{dss}}{V_T}\left(1 - \frac{V_{gs}}{V_T}\right)\right]$$
$$- I_{dss}\left(1 - \frac{V_{gs}}{V_T}\right)^2 \sec h^2\left[\frac{\alpha V_{ds}}{(V_{gs} - V_T)}\right]\left[\frac{\alpha V_{ds}}{(V_{gs} - V_T)^2}\right] \quad (5.15)$$

$$g_{ds} = 2I_{dss}\left(1 - \frac{V_{gs}}{V_T}\right)\frac{\gamma V_{gs}}{V_T^2}\tanh\left[\frac{\alpha V_{ds}}{(V_{gs} - V_T)}\right]$$
$$+ I_{dss}\left(1 - \frac{V_{gs}}{V_T}\right)^2 \sec h^2\left[\frac{\alpha V_{ds}}{(V_{gs} - V_T)}\right]\frac{\alpha(V_{gs} - V_T) + \alpha\gamma V_{ds}}{(V_{gs} - V_T)^2} \quad (5.16)$$

The obtained results for Materka-Kacprzak large-signal model parameters are represented below:

Table 5–6 Results for Materka&Kacprzak large-signal model

	I_{dss}	V_{TO}	α	γ
2x50 MESFET	-0.00119	0.5067	4.2344	-0.0226
2x150 MESFET	-0.0028	0.4604	4.2347	-0.0208
4x50 MESFET	-0.0302	-1.1272	2.279	-0.1776
4x75 MESFET	0.003	0.472	4.01	-0.02
4x100 MESFET	-0.0037	0.4458	4.1955	-0.0194
4x125 MESFET	0.0723	-1.098	2.1839	-0.1759
4x150 MESFET	0.084	-1.0735	2.1388	-0.1744
4x175 MESFET	0.097	-1.0775	2.1614	-0.1817
6x50 MESFET	0.0143	-1.1555	2.1109	-0.1769
6x150 MESFET	0.1246	-1.0767	2.043	-0.1781

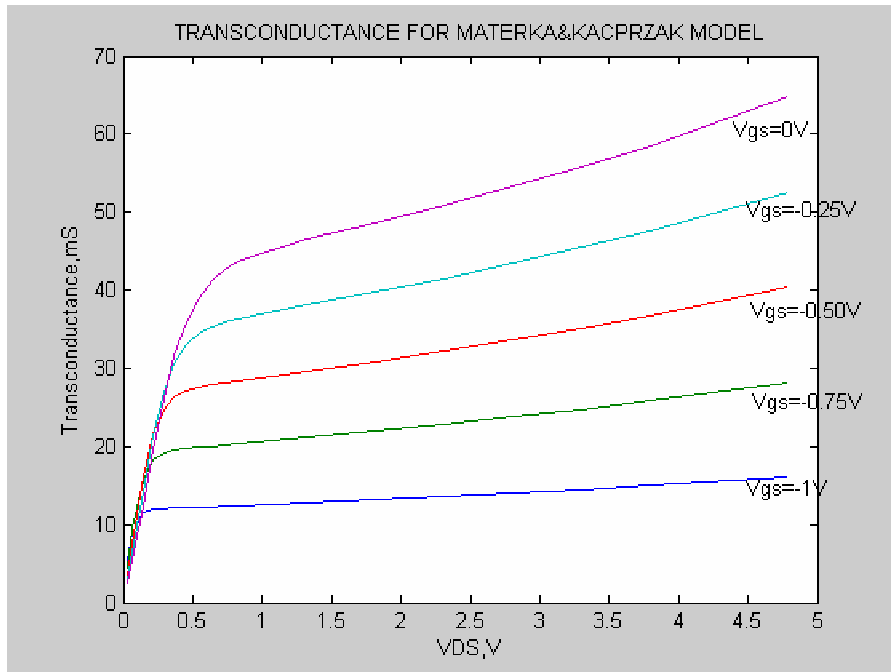

Figure 5-18 Transconductance of 4x150 MESFET for Materka&Kacprzak Large Signal Model

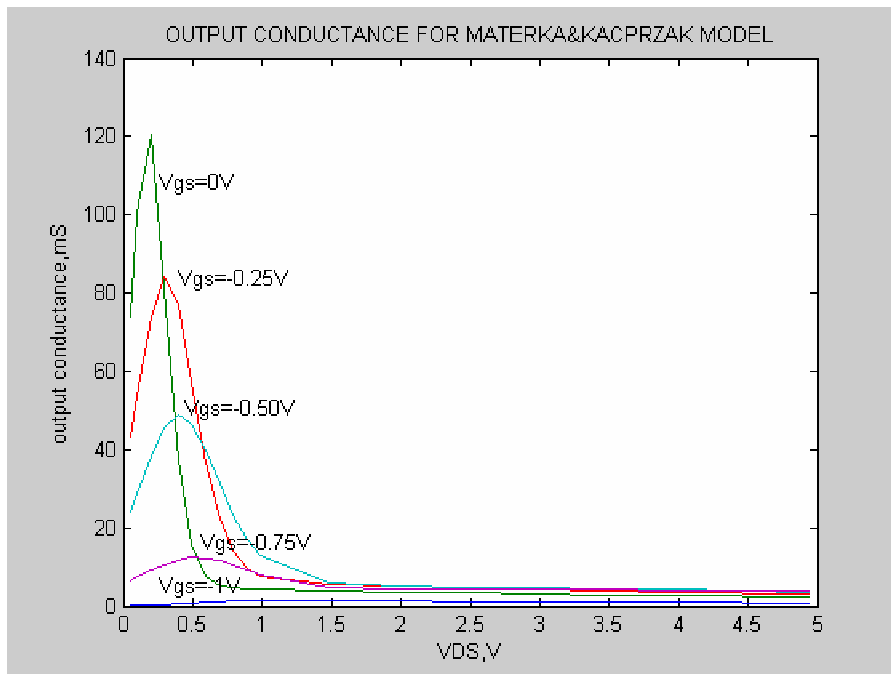

Figure 5-19 Output Conductance of 4x150 MESFET for Materka&Kacprzak Large Signal Model

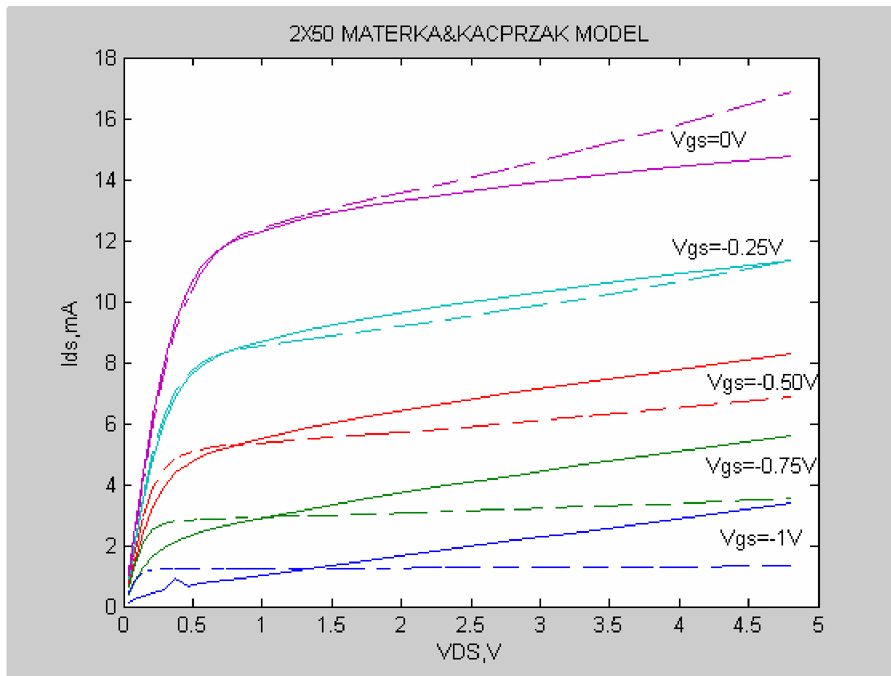

Figure 5-20 Comparison of Vds-Ids characteristics of Materka&Kacprzak Model with measured (solid lines) and theoretical values (dashed lines)

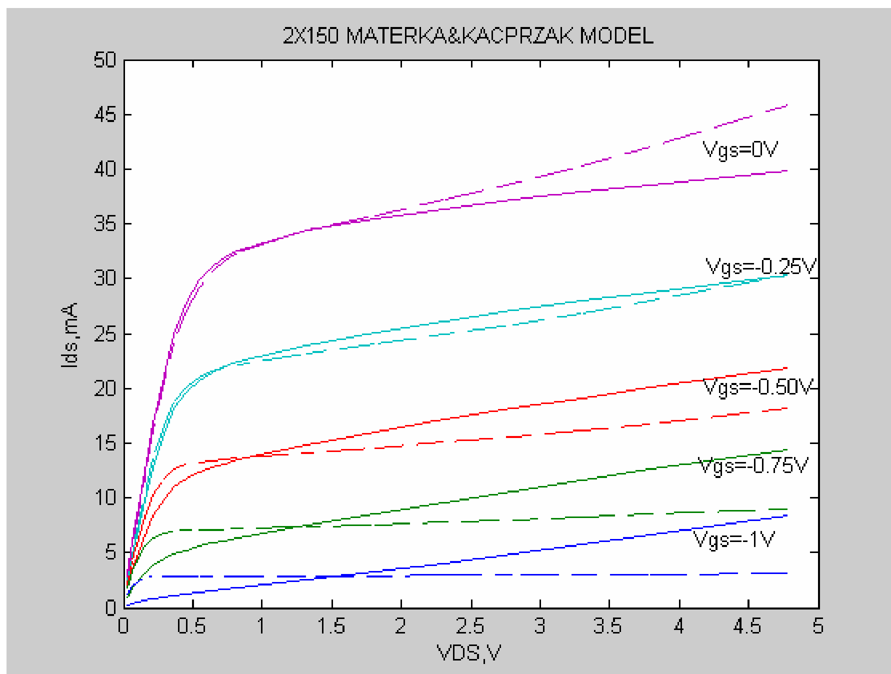

Figure 5-21 Comparison of Vds-Ids characteristics of Materka&Kacprzak Model with measured (solid lines) and theoretical values (dashed lines)

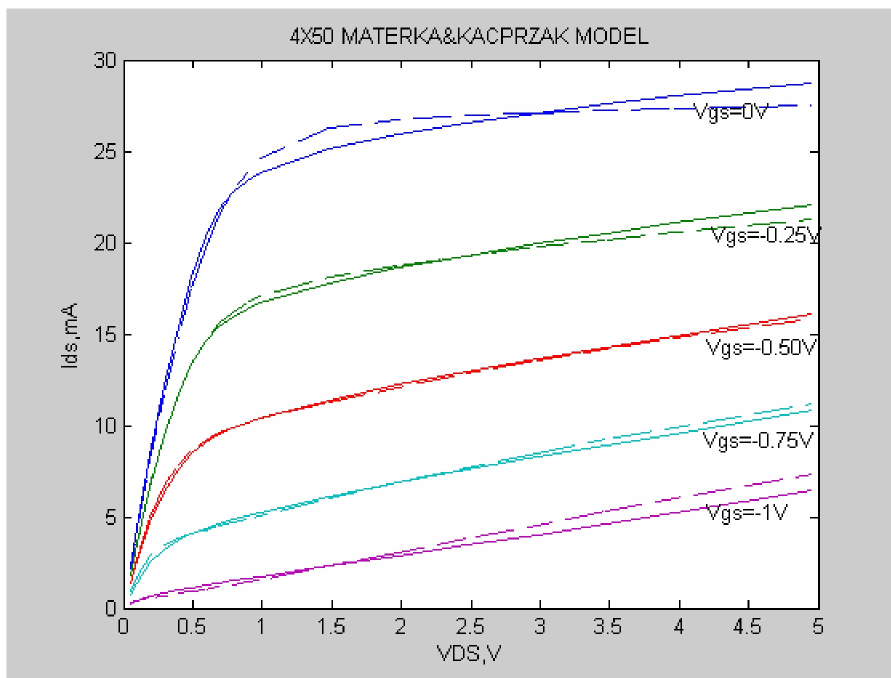

Figure 5-22 Comparison of Vds-Ids characteristics of Materka&Kacprzak Model with measured (solid lines) and theoretical values (dashed lines)

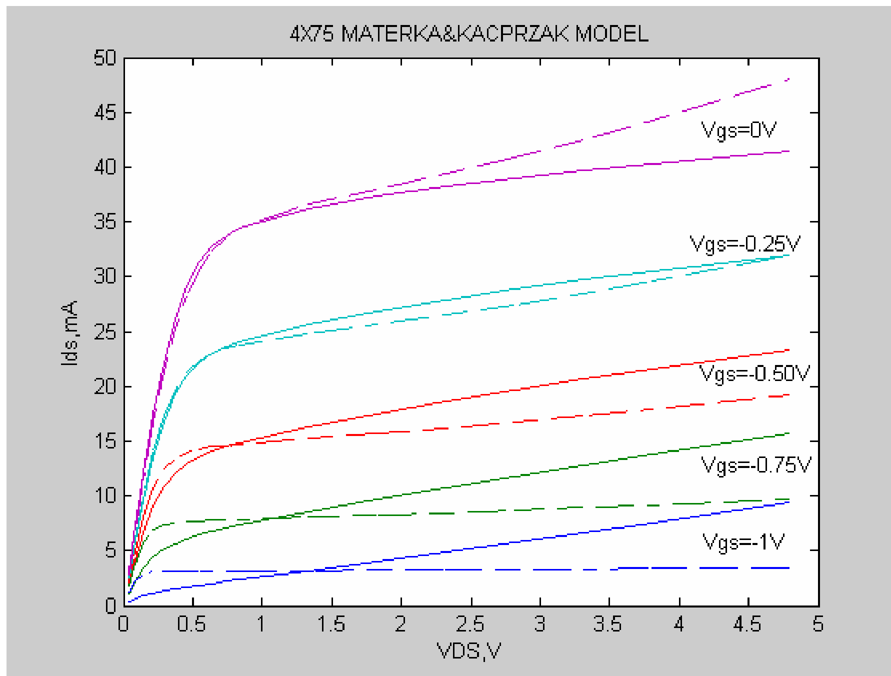

Figure 5-23 Comparison of Vds-Ids characteristics of Materka&Kacprzak Model with measured (solid lines) and theoretical values (dashed lines)

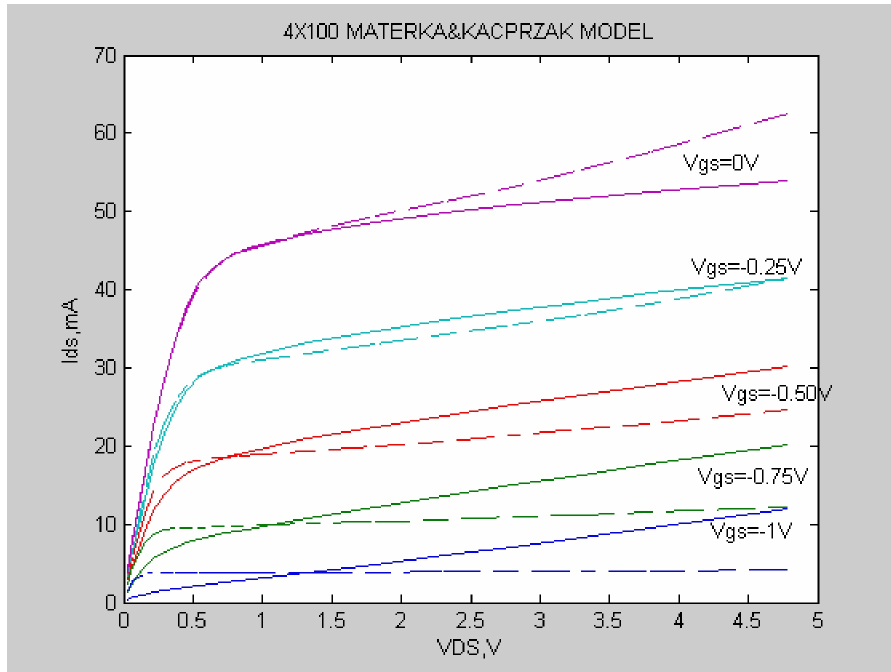

Figure 5-24 Comparison of Vds-Ids characteristics of Materka&Kacprzak Model with measured (solid lines) and theoretical values (dashed lines)

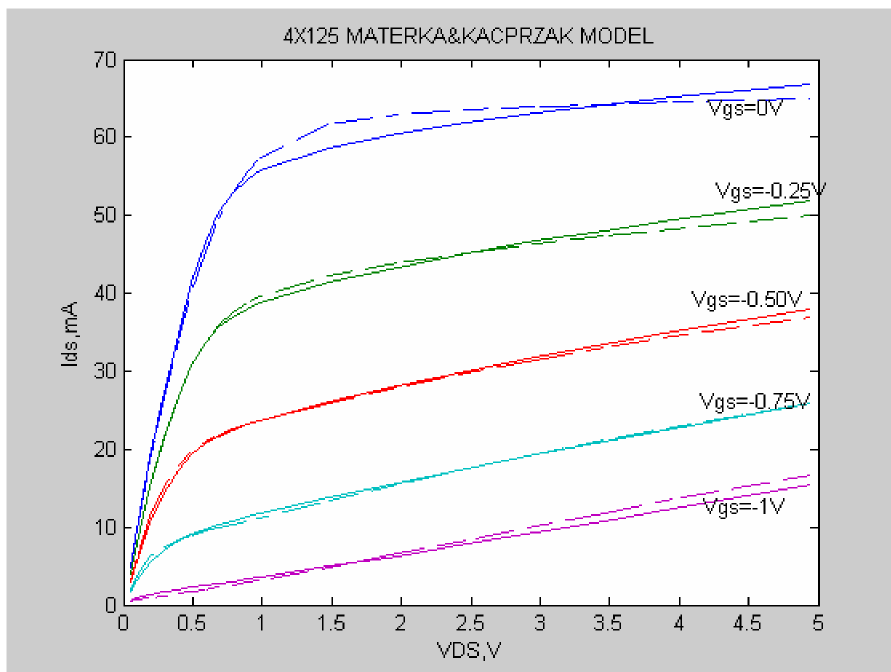

Figure 5-25 Comparison of Vds-Ids characteristics of Materka&Kacprzak Model with measured (solid lines) and theoretical values (dashed lines)

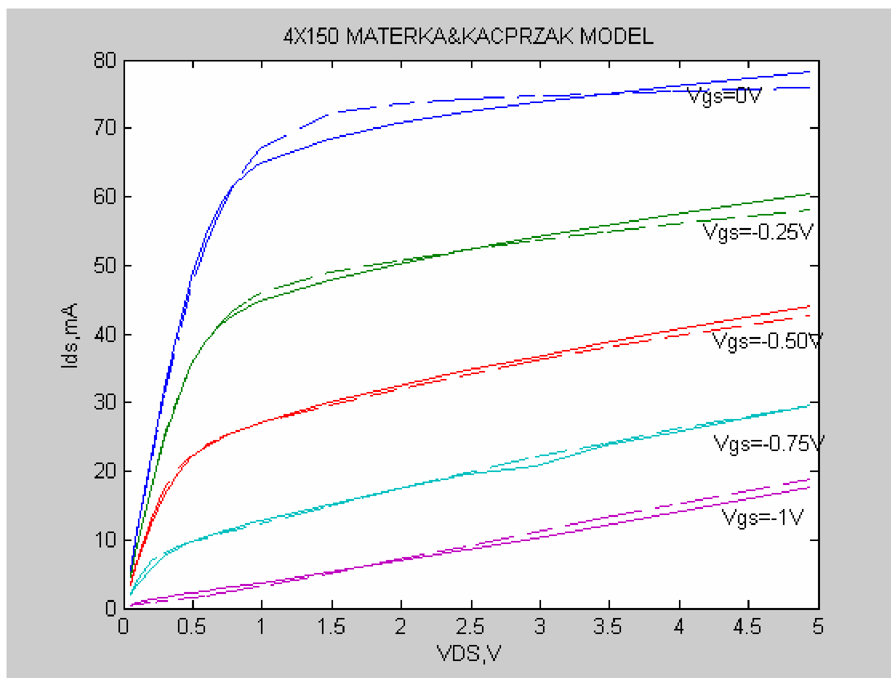

Figure 5-26 Comparison of Vds-Ids characteristics of Materka&Kacprzak Model with measured (solid lines) and theoretical values (dashed lines)

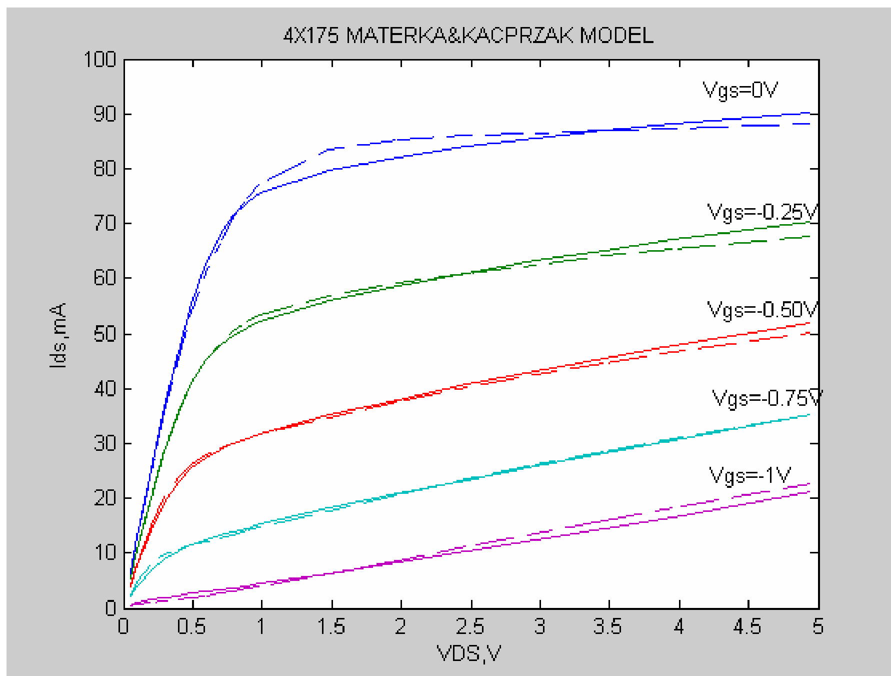

Figure 5-27 Comparison of Vds-Ids characteristics of Materka&Kacprzak Model with measured (solid lines) and theoretical values (dashed lines)

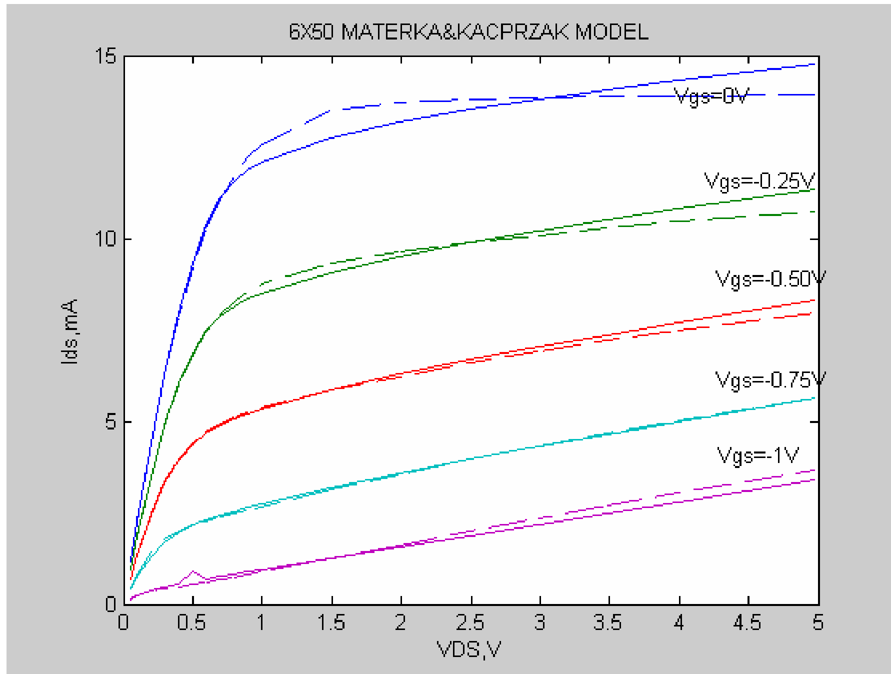

Figure 5-28 Comparison of Vds-Ids characteristics of Materka&Kacprzak Model with measured (solid lines) and theoretical values (dashed lines)

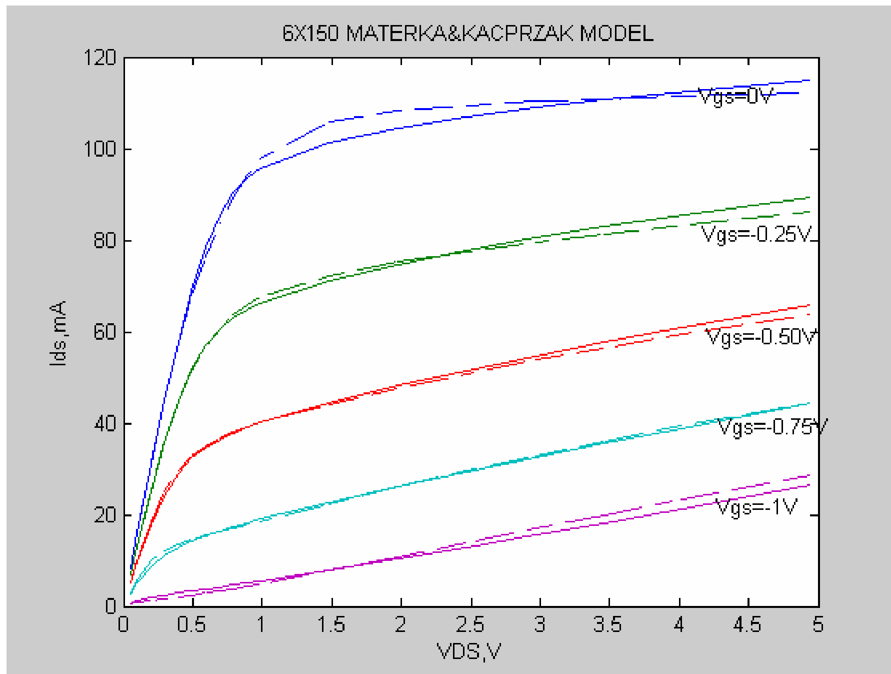

Figure 5-29 Comparison of Vds-Ids characteristics of Materka&Kacprzak Model with measured (solid lines) and theoretical values (dashed lines)

As discussed in Section 5.2.1, the same problems occurred again for Materka&Kacprzak Model. The MESFET types, which are 2x50, 2x150, 4x75, and 4x100, have less accurate results of drain-source current if compared with the other six types of MESFETs. The other six types altogether have better approximations to measured data than the four types of MESFETs and their parameter results tabulated in table 5.6 have close results to each other. The parameter values of the four types of MESFET also have different values with respect to the other six types.

For the four types of MESFETs as increasing the gate-source voltage towards pinch-off voltage, the error between the modeled data and measured data increases.

For the other six types of MESFETs, for $V_{gs} = 0V$ the error occurs at drain-source voltage of 0.5V and then up to 5V the modeled drain-source current deviates from the measured values.

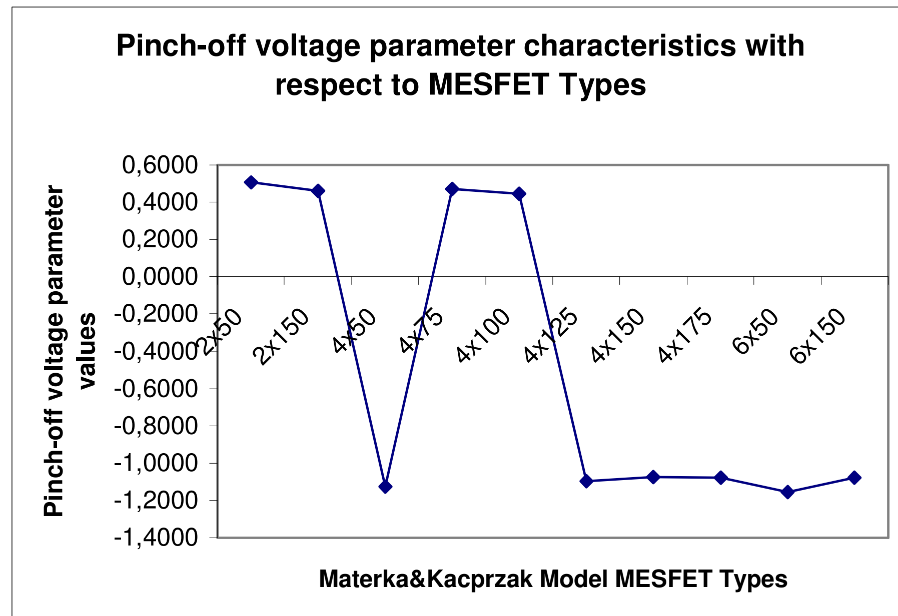

Figure 5-30 Parameter characteristics wih respect to MESFET Types

As represented in the figure, the evaluated parameter values are drawn with respect to MESFET types. This figure shows similar characteristics with Figure 5.16. As discussed before the figure represents two groups of parameter values; one for 4 of the types and one for the other 6 of the types. The first group of MESFET types

has the values between 0.4 and 0.5 and the second group has the values between -1.2 and -1.0.

5.2.3 Curtice&Ettenberg Model [12]

Figure 5.31 shows the equivalent circuit model assumed for Curtice and Ettenberg[12]. There are two new current sources used additionally to Curtice model. [4]. The drain-gate voltage-controlled current source represents the drain-gate avalanche current that can occur at large signal operation. The gate-source voltage controlled current source represents gate current that occurs when the gate-source junction is forward biased. The third current source, shown in the figure, $I_{ds}(V_{in}, V_{out})$ is the large signal form of the usual small signal transconductance.

Curtice assumed a square-law relationship between the (saturation) current and the gate-source voltage. Curtice and Ettenberg have shown that real devices did not exhibit such a relationship and they assumed that, it was more accurate to use a cubic approximation:

$$I_{ds} = (A_0 + A_1 V_1 + A_2 V_1^2 + A_3 V_1^3) \tanh(\gamma V_{ds}) \quad (5.17)$$

where V_1 is used to model the occurrence of pinch-off voltage increase with drain-source voltage. And it is assumed as:

$$V_1 = V_{gs}\left[1 + \beta(V_{dso} - V_{ds})\right] \quad (5.18)$$

where β is the parameter for pinch-off change, V_{dso} is the drain-source voltage (in saturation) at which the A_i parameters are evaluated.

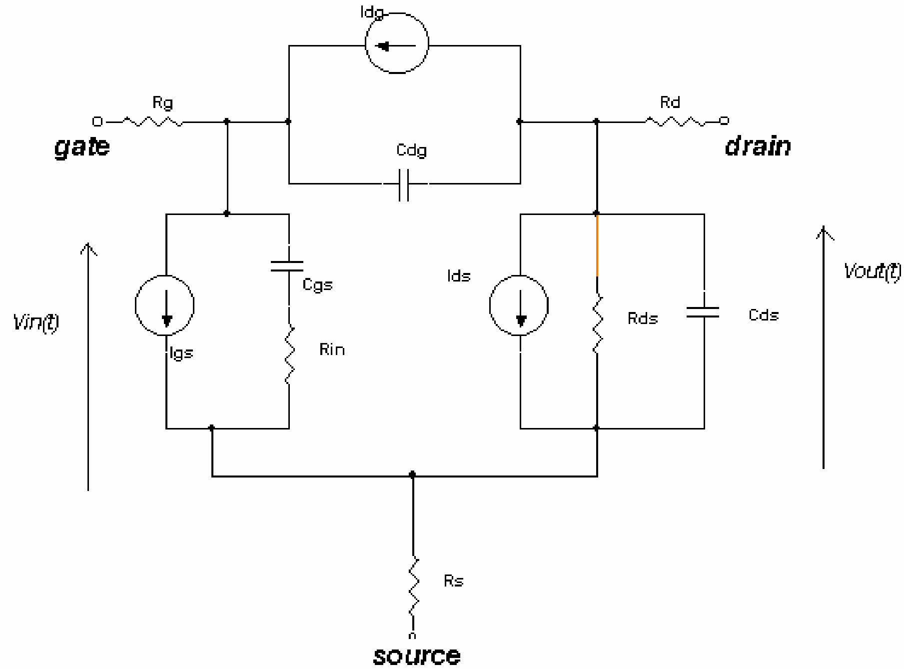

Figure 5-31 Equivalent circuit model of the Curtice&Ettenberg Model

Differentiation of the drain current in the model gives the following result for small signal output RF conductance:

$$g_{ds} = \left(A_0 + A_1V_1 + A_2V_1^2 + A_3V_1^3\right)\gamma \sec h^2\left[\gamma V_{ds}\right] - \beta V_{gs}\left(A_1 + 2A_2V_1 + 3A_3V_1^2\right)\tanh(\gamma V_{ds}) + \frac{1}{V_{dso}} \tag{5.19}$$

$$g_m = \tanh(\gamma V_{ds})\left(A_1V_2 + 2A_2V_1V_2 + 3A_3V_1^2V_2\right) \tag{5.20}$$

$$V_2 = \left[1 + \beta(V_{dso} - V_{ds})\right] \tag{5.21}$$

The results for this model type, which are evaluated by using the "fminsearch.m" optimization tool, are shown in table 5.7 and the $I_{ds} - V_{ds}$ caharateristics for all types of MESFETs are ploted in the figures in order. Transconductance and Output Conductance graphs for the type of 4x150 MESFET are shown below:

Table 5–7 Parameter results of Curtice and Ettenberg Large Signal Model

	β	A_0	A_1	A_2	A_3	γ	V_{dso}
2x50 MESFET	-0.0355	0.0008	-0.0121	0.0070	-0.000004	2.8933	11.353
2x150 MESFET	-0.041	0.0015	-0.0281	0.0151	0.000033	2.949	7.4773
4x50 MESFET	0.0934	0.0301	0.0364	0.0106	-0.000055	2.0869	3.0108
4x75 MESFET	-0.0523	0.0022	-0.0148	0.0434	0.0222	2.908	4.177
4x100 MESFET	-0.049	0.0025	-0.0248	0.0371	0.0154	2.870	3.809
4x125 MESFET	0.0330	0.0712	0.2648	0.2177	-0.046	2.0733	-17.54
4x150 MESFET	0.0335	0.0831	0.3126	0.2695	-0.0366	2.0745	-17.033
4x175 MESFET	0.0425	0.0964	0.2897	0.1866	-0.0427	2.0849	-11.141
6x50 MESFET	0.0312	0.0137	0.0313	-0.0416	-0.1077	1.8714	-17.441
6x150 MESFET	0.0401	0.1233	0.3749	0.2564	-.0332	1.929	-11.94

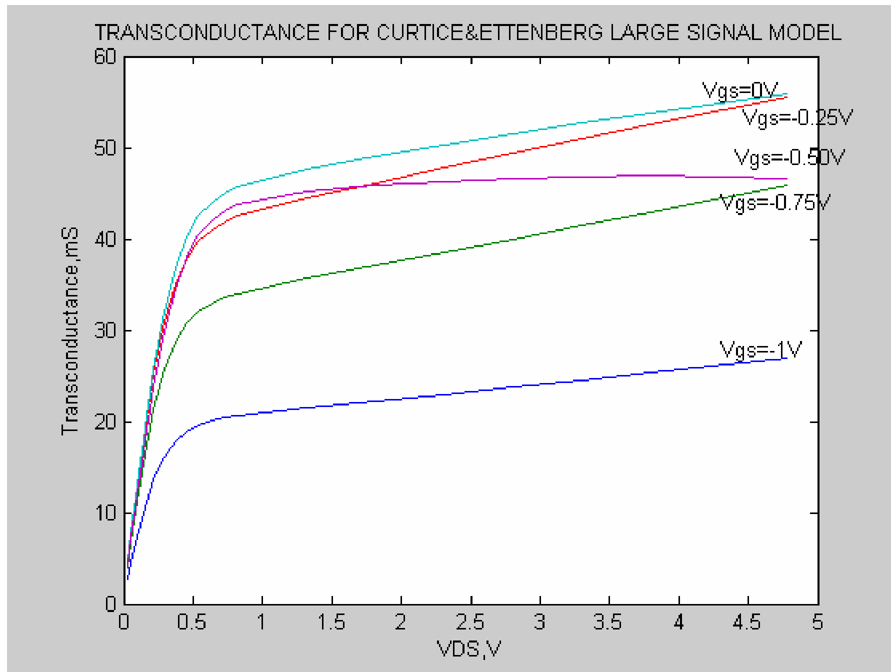

Figure 5-32 Transconductance of 4x150 MESFET for Curtice&Ettenberg Large Signal Model

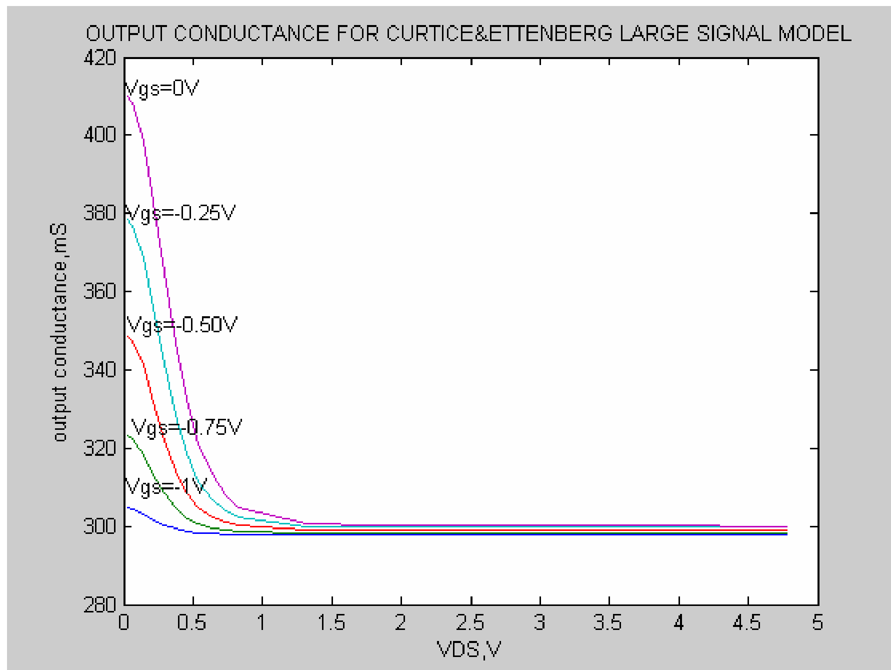

Figure 5-33 Output Conductance of 4x150 MESFET for Curtice&Ettenberg Large Signal Model

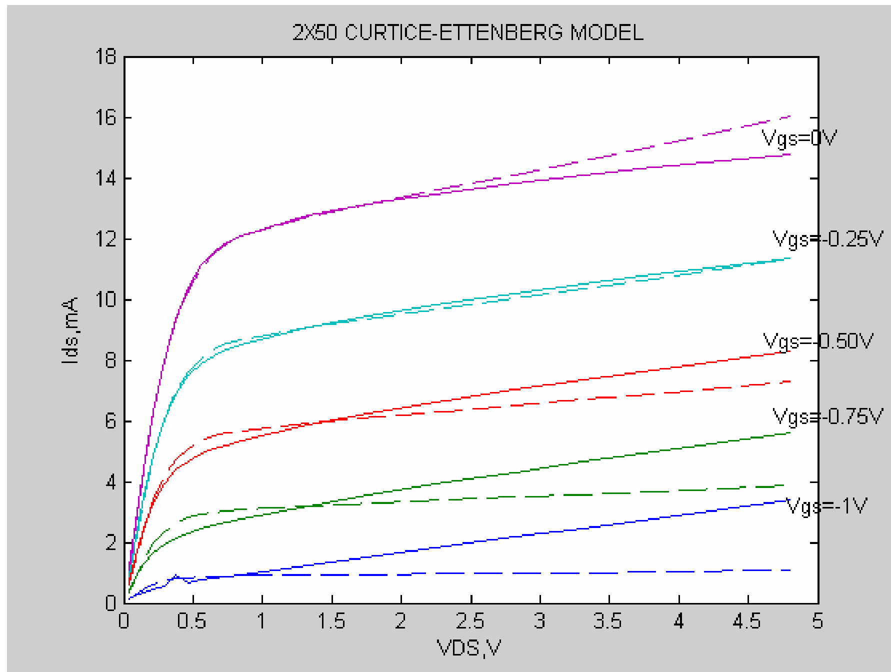

Figure 5-34Comparison of Vds-Ids characteristics of Curtice&Ettenberg Model with measured (solid lines) and theoretical values (dashed lines)

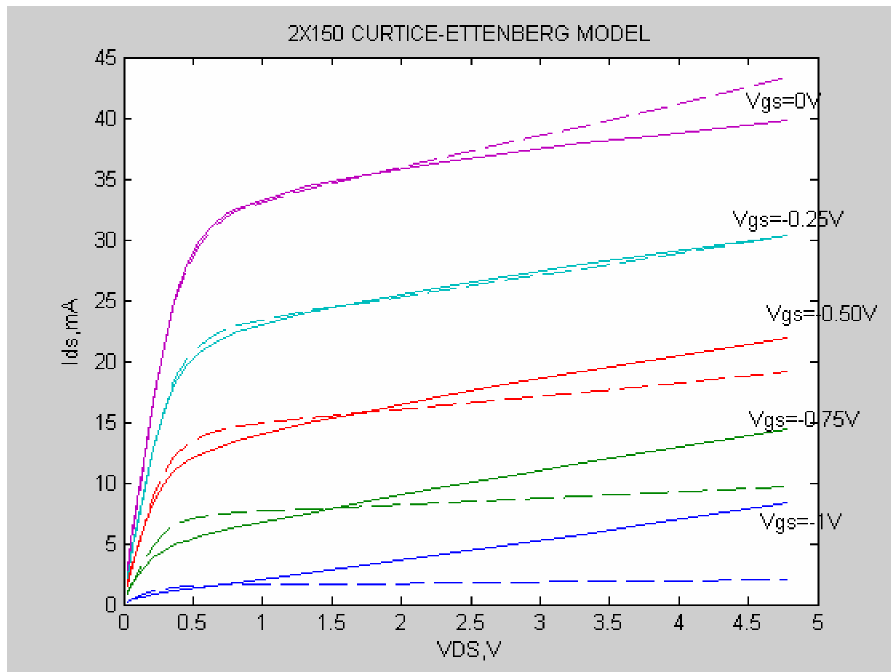

Figure 5-35 Comparison of Vds-Ids characteristics of Curtice&Ettenberg Model with measured (solid lines) and theoretical values (dashed lines)

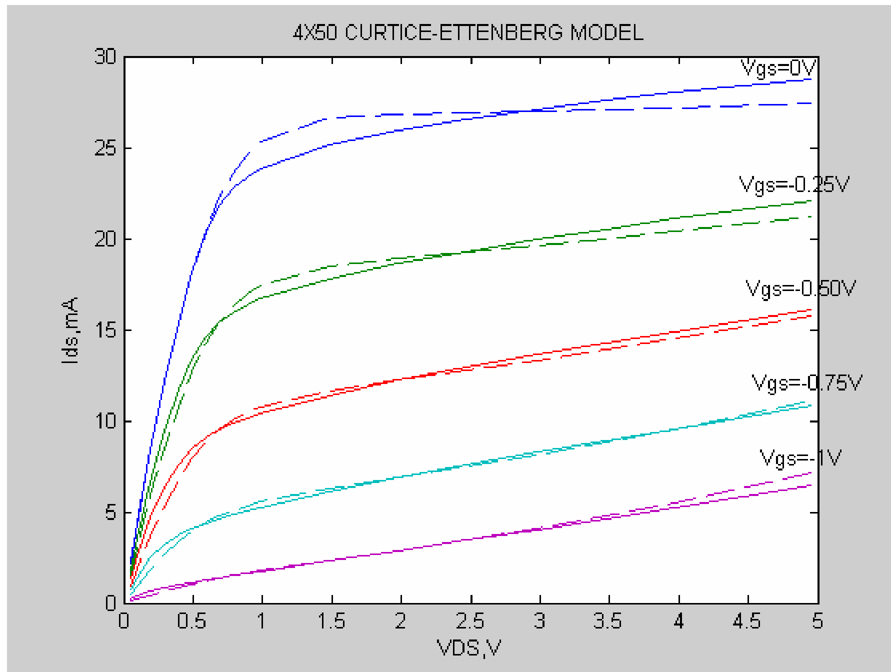

Figure 5-36 Comparison of Vds-Ids characteristics of Curtice&Ettenberg Model with measured (solid lines) and theoretical values (dashed lines)

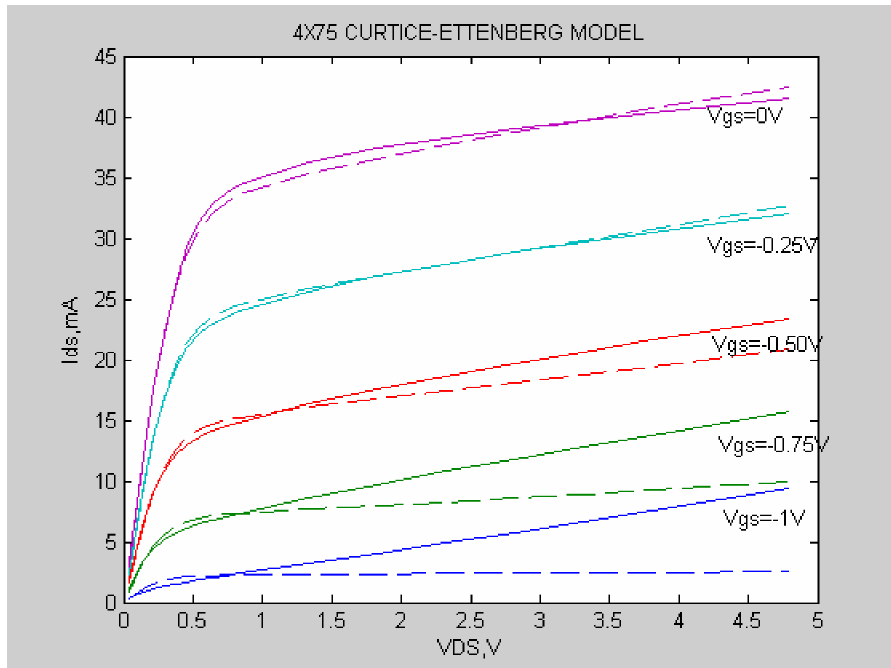

Figure 5-37 Comparison of Vds-Ids characteristics of Curtice&Ettenberg Model with measured (solid lines) and theoretical values (dashed lines)

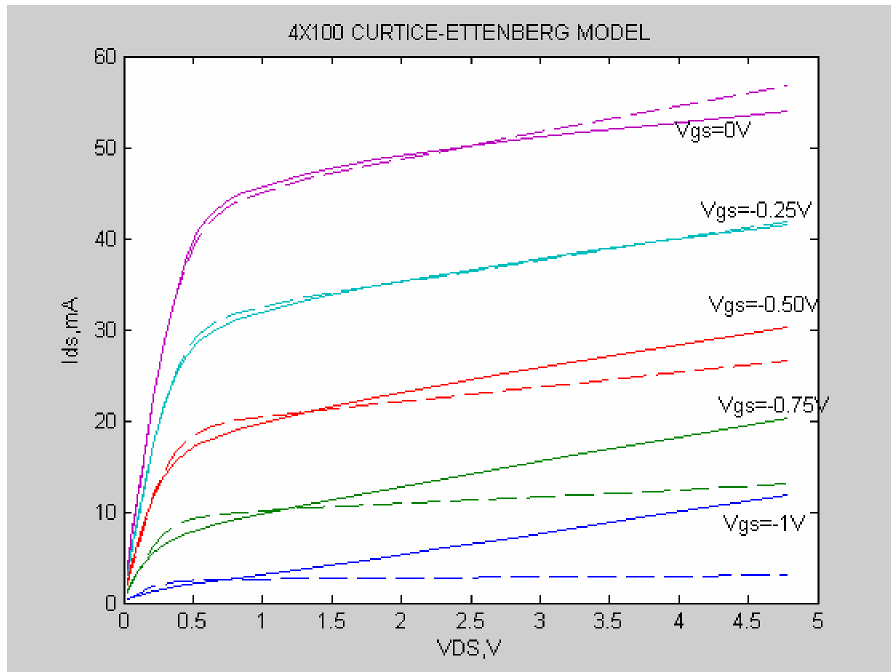

Figure 5-38 Comparison of Vds-Ids characteristics of Curtice&Ettenberg Model with measured (solid lines) and theoretical values (dashed lines)

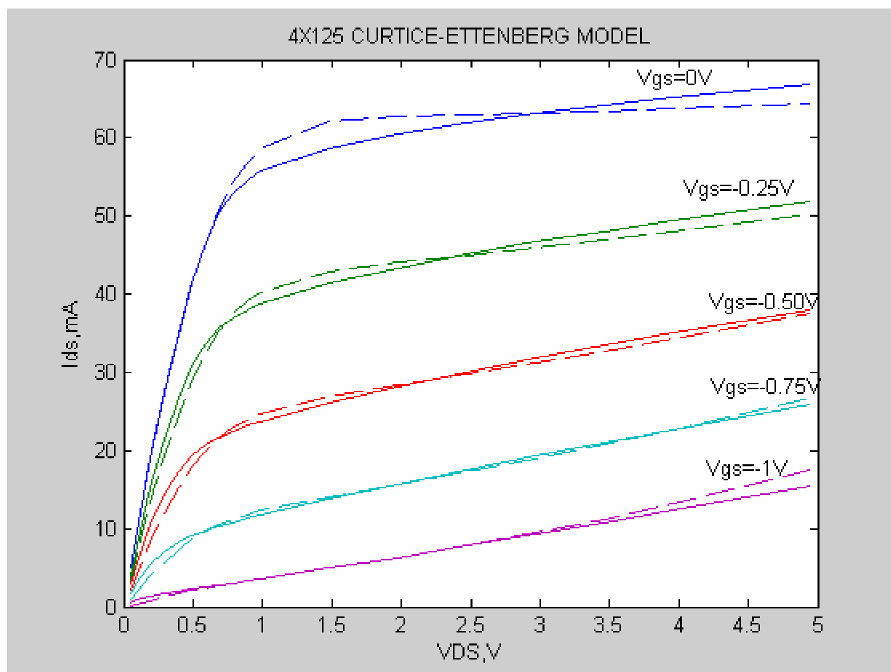

Figure 5-39 Comparison of Vds-Ids characteristics of Curtice&Ettenberg Model with measured (solid lines) and theoretical values (dashed lines)

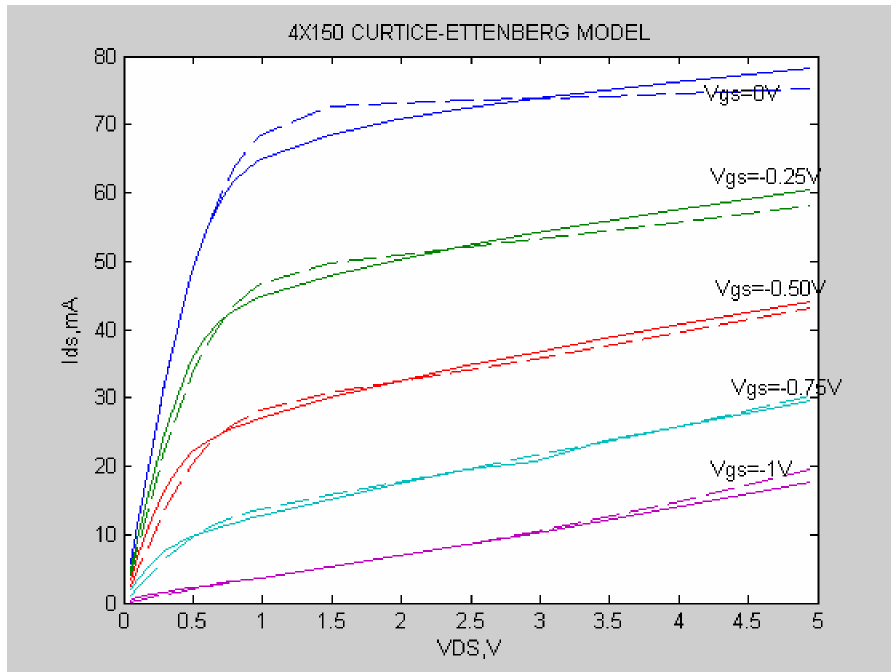

Figure 5-40 Comparison of Vds-Ids characteristics of Curtice&Ettenberg Model with measured (solid lines) and theoretical values (dashed lines)

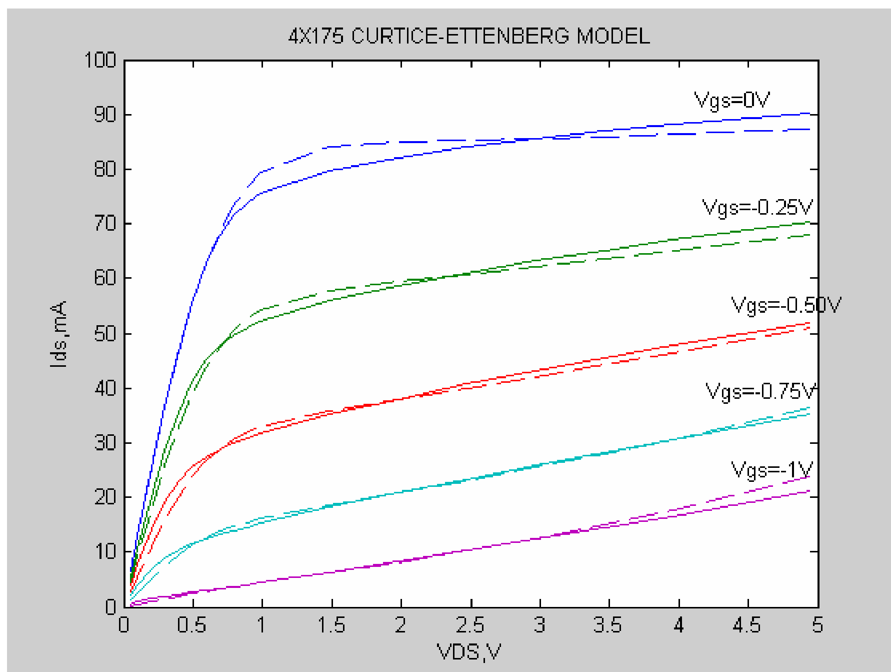

Figure 5-41 Comparison of Vds-Ids characteristics of Curtice&Ettenberg Model with measured (solid lines) and theoretical values (dashed lines)

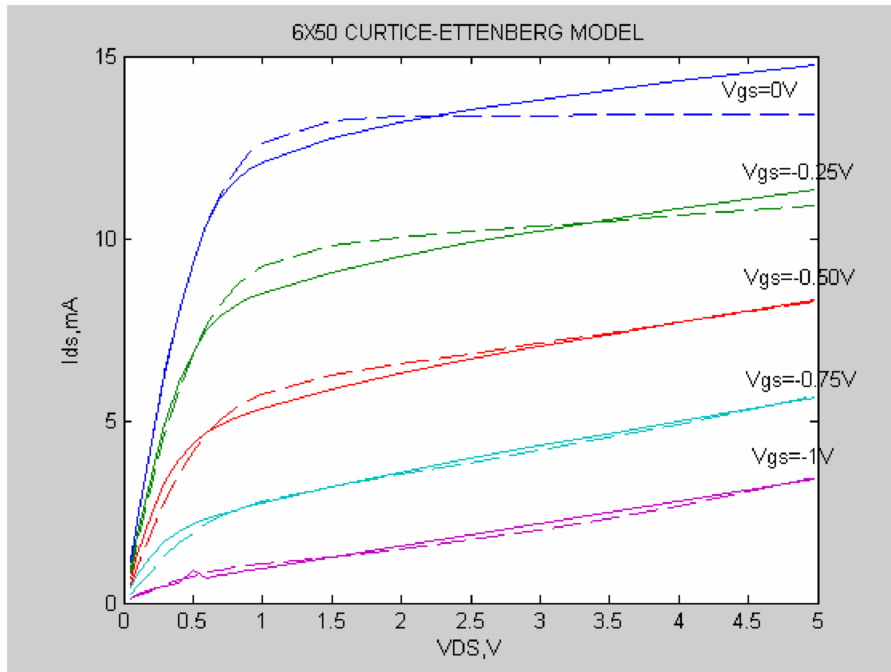

Figure 5-42 Comparison of Vds-Ids characteristics of Curtice&Ettenberg Model with measured (solid lines) and theoretical values (dashed lines)

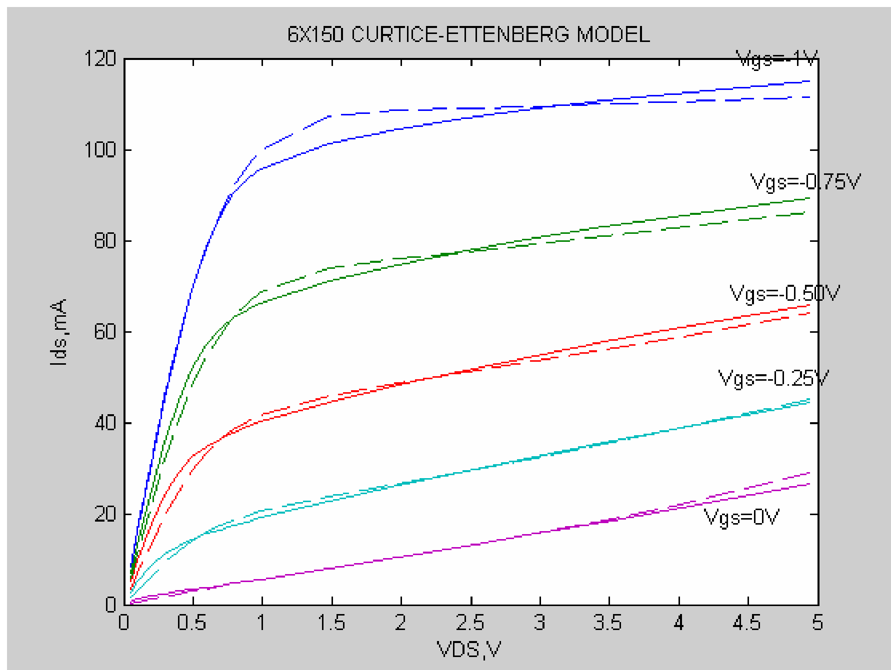

Figure 5-43 Comparison of Vds-Ids characteristics of Curtice&Ettenberg Model with measured (solid lines) and theoretical values (dashed lines)

As discussed in the previous sections, the $I_{ds} - V_{ds}$ characteristics of modeled data show similar properties. The modeled data, for the four types of MESFETs have only good approximations for $V_{gs} = -0.25V$, on the other hand, for the other six types of MESFETs the modeled data agrees for only $V_{gs} = -0.75V$ and $V_{gs} = -1.0V$. For other values than these, the modeled data are less accurate.

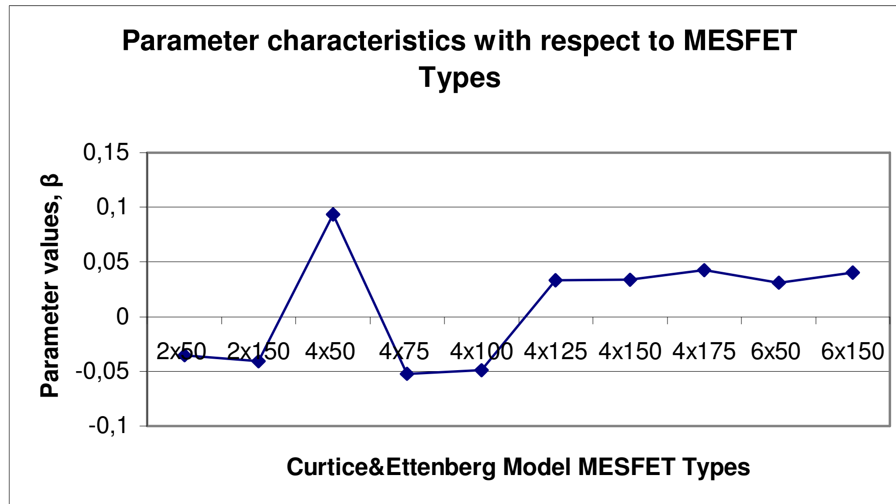

Figure 5-44 Parameter characteristics wih respect to MESFET Types

In the figure the parameter β is plotted with respect to MESFET types. As discussed before this figure represents two groups of parameter values; one for 4 of the types and one for the other 6 of the types.

5.2.4 Statz Model [10]

The researchers H. Statz, P. Newman, I. Smith, R. Pucel, and H.Haus were the members of Research Division of Raytheon Company. Therefore in literature Statz model can also be called as Raytheon Model. A model based on the Curtice model is developed [3]. Their research indicates that the square law approximation of drain-source current as a function of gate-source voltage is only valid for small $V_{gs} - V_{TO}$ values, where V_{TO} is the pinch-off potential. The drain-source current I_{ds} becomes almost linear for larger values of $V_{gs} - V_{TO}$. To model this behavior, the

original square law expression, $I_{ds} \sim \beta(V_{gs} - V_{TO})^2$ is modified:

$$I_{ds} \sim \frac{\beta(V_{gs} - V_{TO})^2}{1 + b(V_{gs} - V_{TO})} \tag{5.22}$$

for small values of $V_{gs} - V_{TO}$, the new expression is quadratic, while for large values, it becomes almost linear in $V_{gs} - V_{TO}$.

The hyperbolic tangent function tends to consume significant amounts of computer time and, therefore is modified using a polynomial of the form; $1 - [1 - (\alpha V_{ds}/n)]^n$ with n=3. Although this representation does not look similar to the tanh representation, it is simply a truncated series portrayal of the hyperbolic tangent. In the saturation region, the polynomial is replaced by unity. These modifications lead to a new form for the drain current and its derivatives.

For $0 < V_{ds} < 3/\alpha$,

$$I_{ds} = \frac{\beta(V_{gs} - V_{TO})^2}{1 + b(V_{gs} - V_{TO})}\left[1 - \left(1 - \frac{\alpha V_{ds}}{3}\right)^3\right](1 + \lambda V_{ds}) \tag{5.23a}$$

$$g_m = \left[1 - \left(1 - \frac{\alpha V_{ds}}{3}\right)^3\right](1 + \lambda V_{ds})\left[\frac{2\beta(V_{gs} - V_{TO})}{1 + b(V_{gs} - V_{TO})}\right] - \frac{b\beta(V_{gs} - V_{TO})^2}{[1 + b(V_{gs} - V_{TO})]^2} \tag{5.23b}$$

$$g_{ds} = \left[1 - \left(1 - \frac{\alpha V_{ds}}{3}\right)^3\right]\lambda + \alpha(1 + \lambda V_{ds})\left(1 - \frac{\alpha V_{ds}}{3}\right)^2 \frac{\beta(V_{gs} - V_{TO})^2}{1 + b(V_{gs} - V_{TO})} \tag{5.23c}$$

for $V_{ds} \geq 3/\alpha$,

$$I_{ds} = \frac{\beta(V_{gs} - V_{TO})^2(1 + \lambda V_{ds})}{1 + b(V_{gs} - V_{TO})} \tag{5.24a}$$

$$g_m = \frac{[1+b(V_{gs}-V_{TO})]2\beta(V_{gs}-V_{TO}) - b\beta(V_{gs}-V_{TO})^2}{1+b(V_{gs}-V_{TO})}(1+\lambda V_{ds}) \tag{5.24b}$$

$$g_{ds} = \frac{\lambda\beta(V_{gs}-V_{TO})^2}{1+b(V_{gs}-V_{TO})} \tag{5.24c}$$

new capacitance expressions replace the simple junction capacitance of the Curtice model. The simple Curtice model junction capacitance expression fails to predict accurate capacitance values for low drain-source voltages. The model also fails when the drain-source bias levels reverse. The capacitance-voltage expressions of Statz Model are:

$$C_{gs} = \left(\frac{C_{gs0}K2K1}{\left(1 - {V_n}/{V_{bi}}\right)^{1/2}} + C_{gd0}K3 \right) \tag{5.25}$$

$$C_{gd} = \left(\frac{C_{gs0}K3K1}{\left(1 - {V_n}/{V_{bi}}\right)^{1/2}} + C_{gd0}K2 \right) \tag{5.26}$$

where $V_{\max} = 0.5$, $\delta = 0.2$

$$K1 = \left\{1 + (V_e - V_{TO}) / \left[(V_e - V_{TO})^2 + \delta^2\right]^{1/2}\right\} / 2 \tag{5.27}$$

$$K2 = \left\{1 + (V_{gs} - V_{gd}) / \left[(V_{gs} - V_{gd})^2 + (1/\alpha)^2\right]^{1/2}\right\} / 2 \tag{5.28}$$

$$K3 = \left\{1 - (V_{gs} - V_{gd}) / \left[(V_{gs} - V_{gd})^2 + (1/\alpha)^2\right]^{1/2}\right\} / 2 \tag{5.29}$$

$$V_e = \left\{ V_{gs} + V_{gd} + \left[(V_{gs} - V_{gd})^2 + (1/\alpha)^2 \right]^{1/2} \right\} \Big/ 2 \qquad (5.30)$$

If: $\left\{ V_e + V_{TO} + \left[(V_e - V_{TO})^2 + \delta^2 \right]^{1/2} \right\} / 2 < V_{\max}$

$$V_n = \left\{ V_e + V_{TO} + \left[(V_e - V_{TO})^2 + \delta^2 \right]^{1/2} \right\} / 2 \qquad (5.31)$$

else: $V_n = V_{\max}$

The voltages V_{gs} and V_{gd} are intrinsic device voltages. The adjustable model parameters are C_{gs0}, C_{gd0}, and α, although α is usually determined by consideration of equations 5.23 and 5.24.

Transconductance and Output Conductance graphs for the type of 4x150 MESFET are shown below:

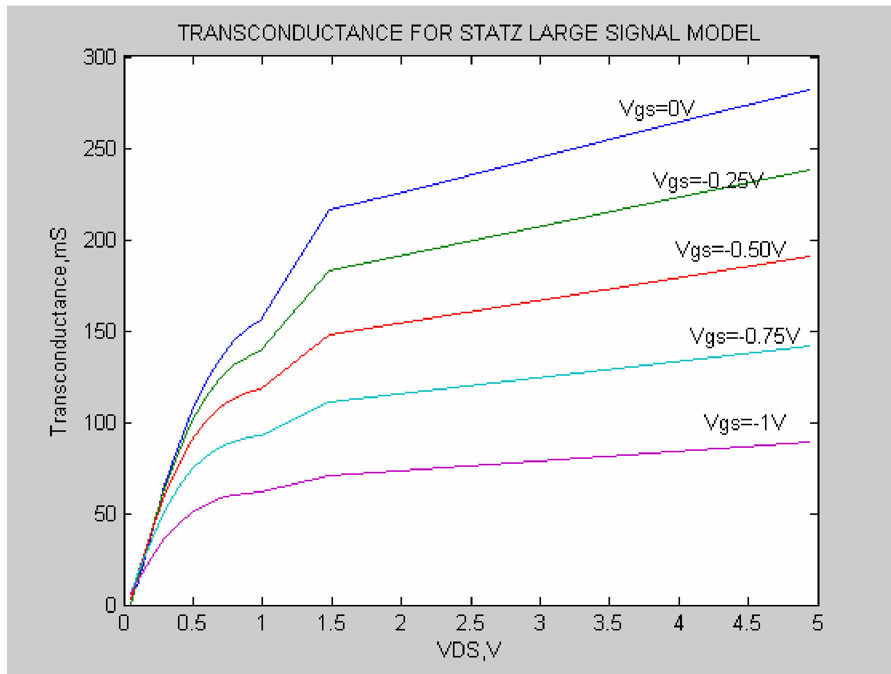

Figure 5-45 Transconductance of 4x150 MESFET for Statz Large-Signal Model

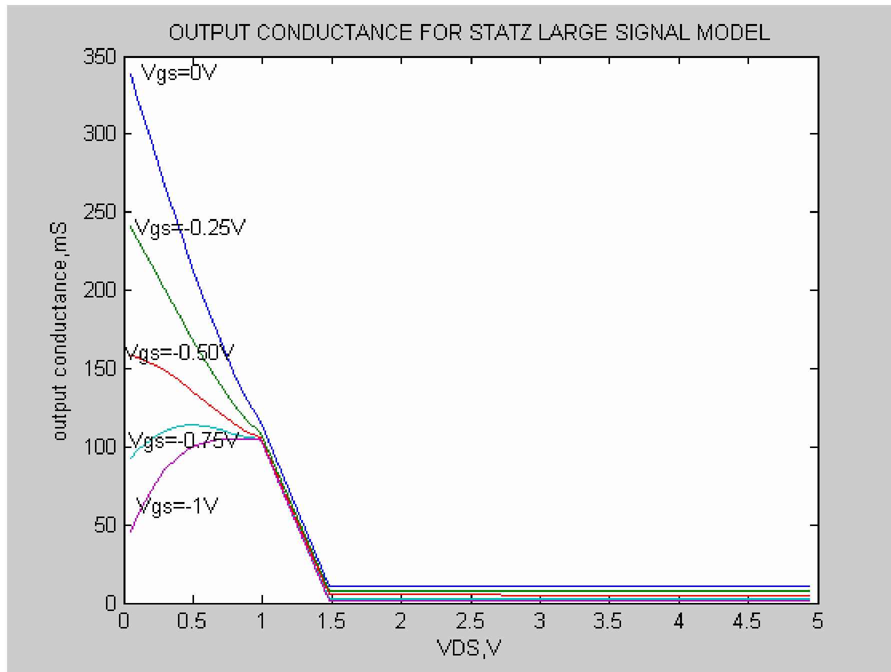

Figure 5-46 Output Conductance of 4x150 MESFET for Statz Large Signal Model

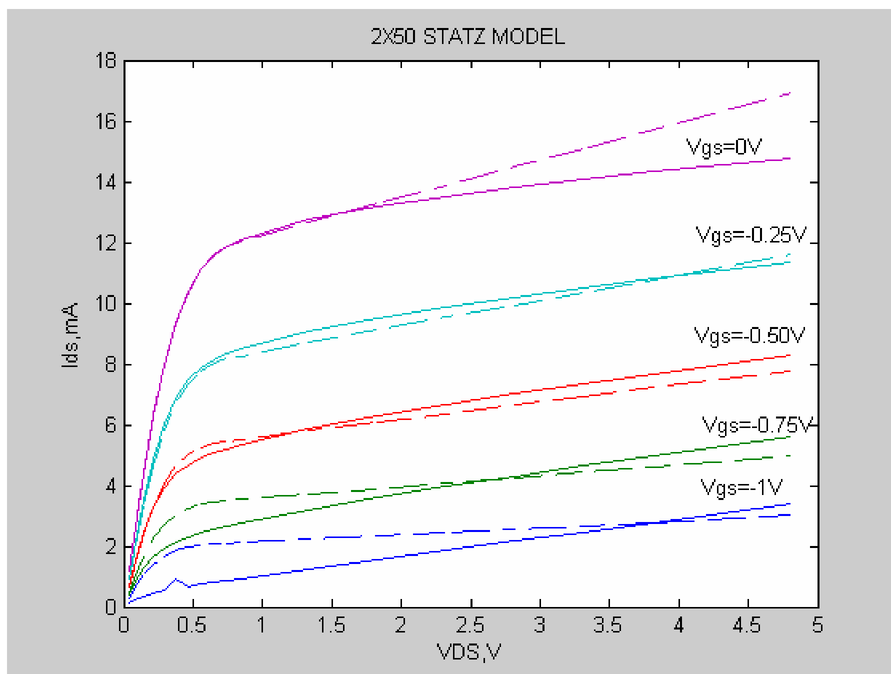

Figure 5-47 Comparison of Vds-Ids characteristics of Statz Model with measured (solid lines) and theoretical values (dashed lines)

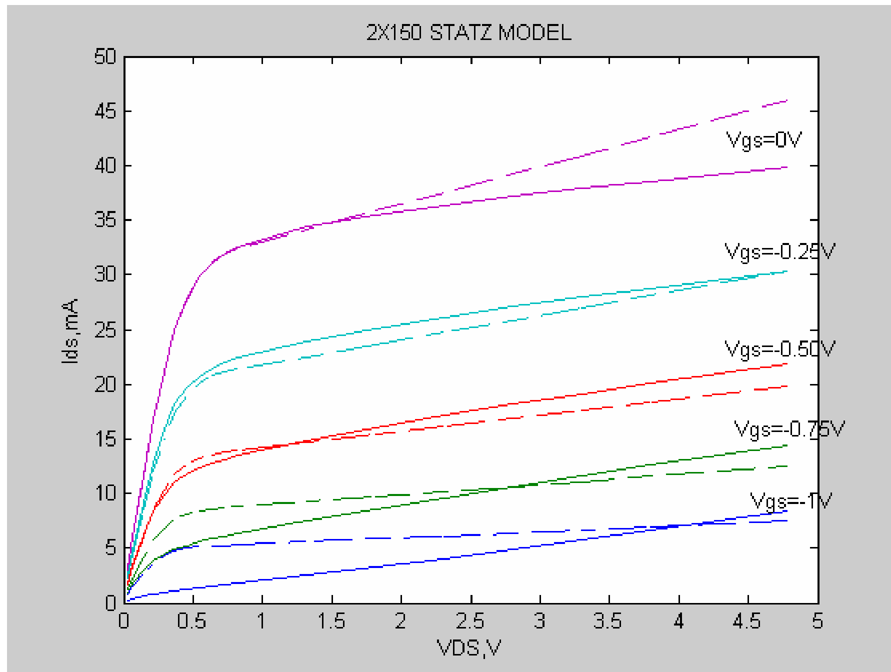

Figure 5-48 Comparison of Vds-Ids characteristics of Statz Model with measured (solid lines) and theoretical values (dashed lines)

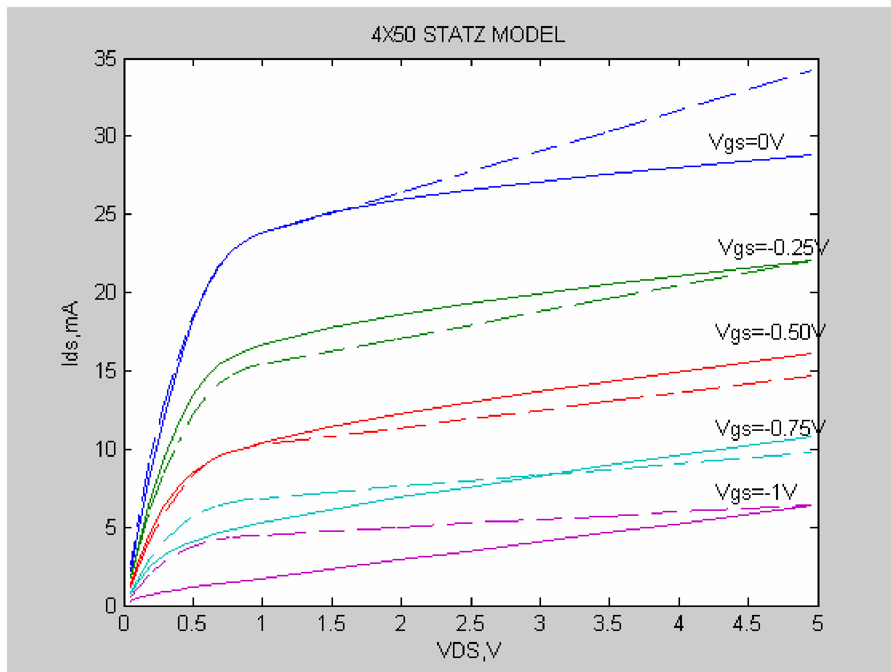

Figure 5-49 Comparison of Vds-Ids characteristics of Statz Model with measured (solid lines) and theoretical values (dashed lines)

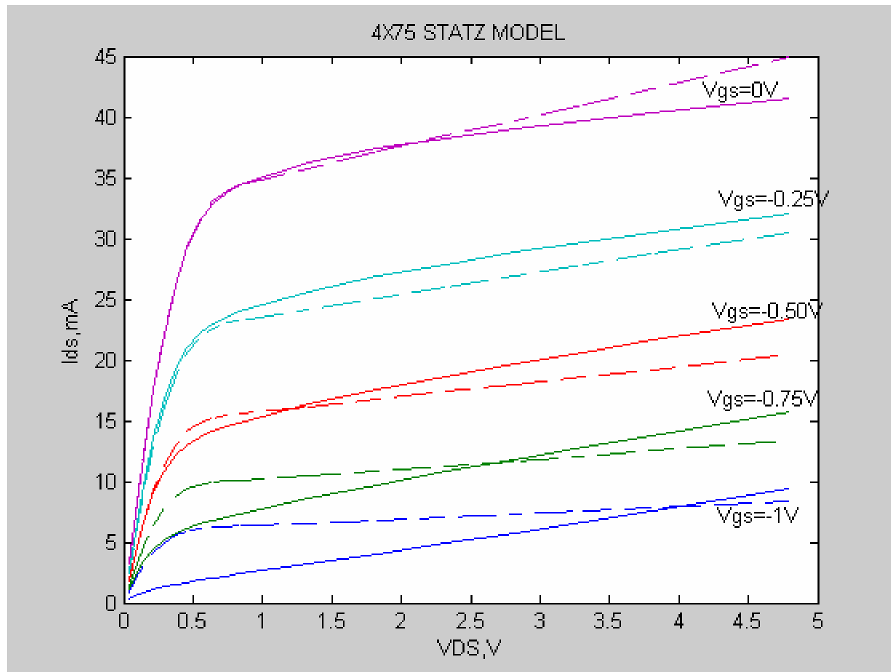

Figure 5-50 Comparison of Vds-Ids characteristics of Statz Model with measured (solid lines) and theoretical values (dashed lines)

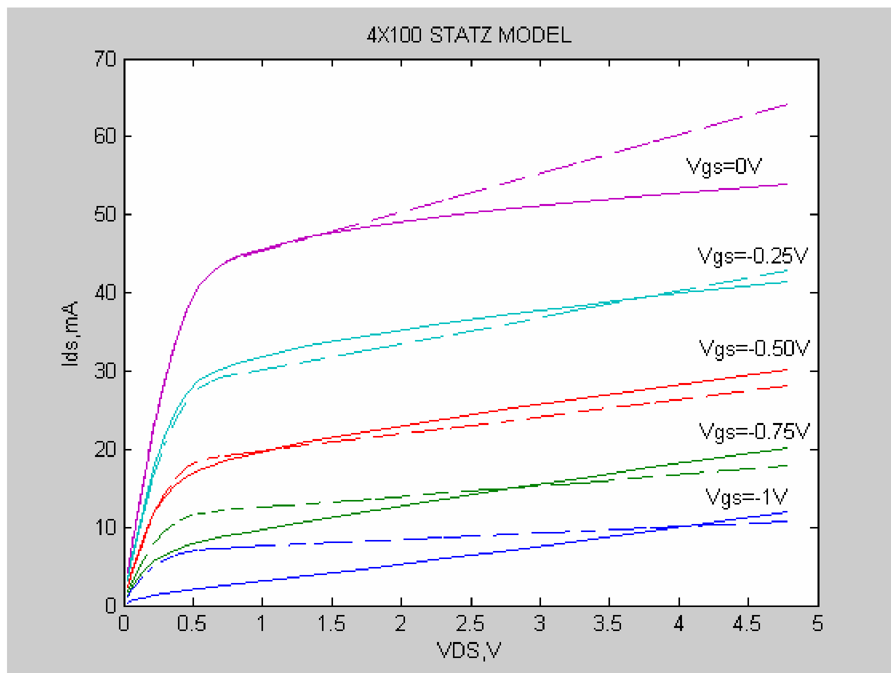

Figure 5-51 Comparison of Vds-Ids characteristics of Statz Model with measured (solid lines) and theoretical values (dashed lines)

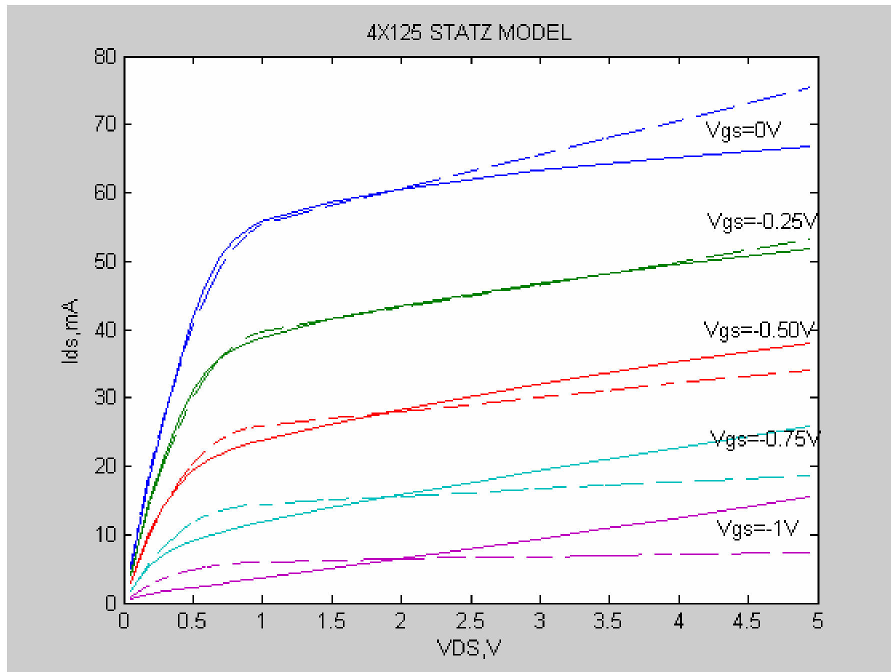

Figure 5-52 Comparison of Vds-Ids characteristics of Statz Model with measured (solid lines) and theoretical values (dashed lines)

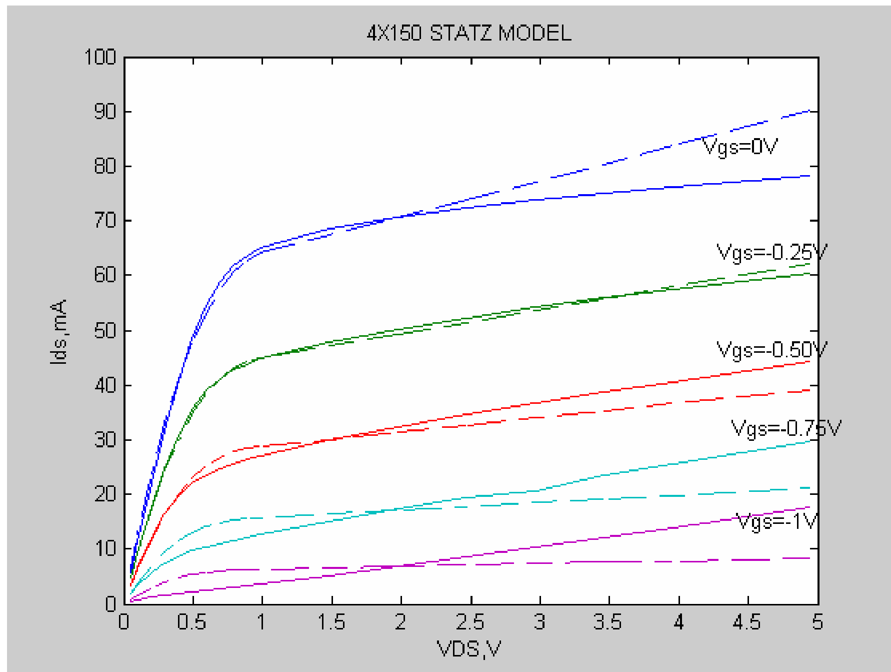

Figure 5-53 Comparison of Vds-Ids characteristics of Statz Model with measured (solid lines) and theoretical values (dashed lines)

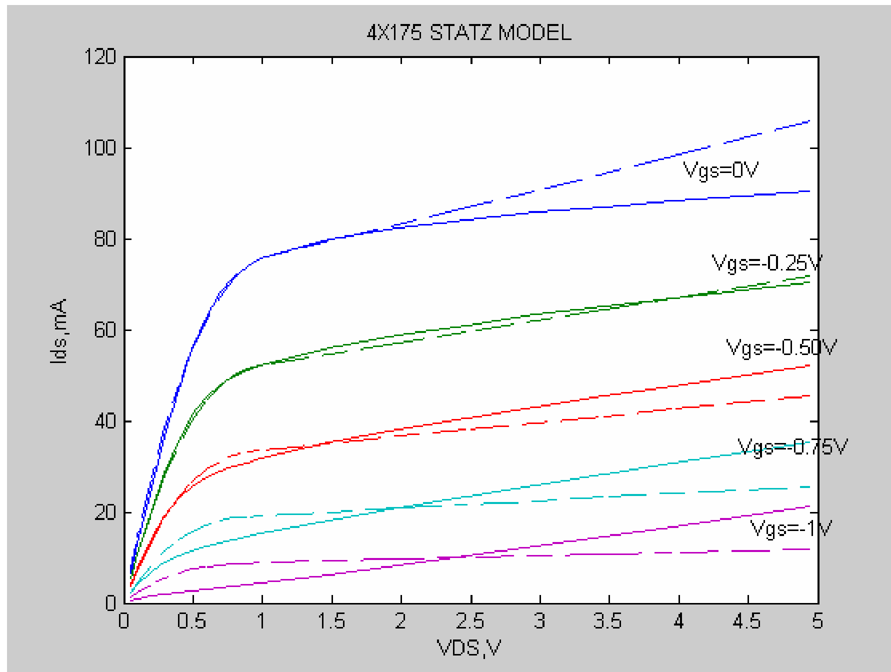

Figure 5-54 Comparison of Vds-Ids characteristics of Statz Model with measured (solid lines) and theoretical values (dashed lines)

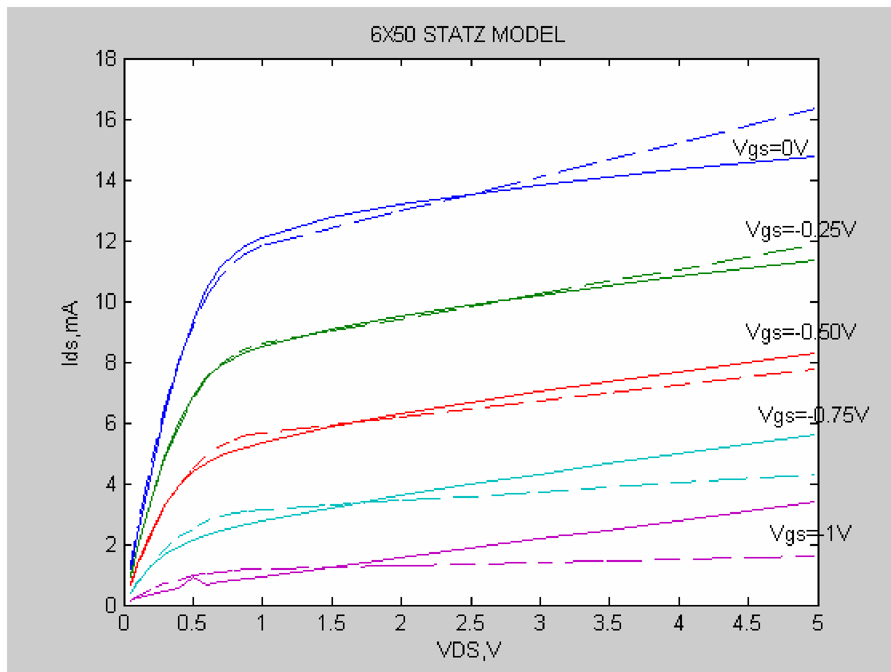

Figure 5-55 Comparison of Vds-Ids characteristics of Statz Model with measured (solid lines) and theoretical values (dashed lines)

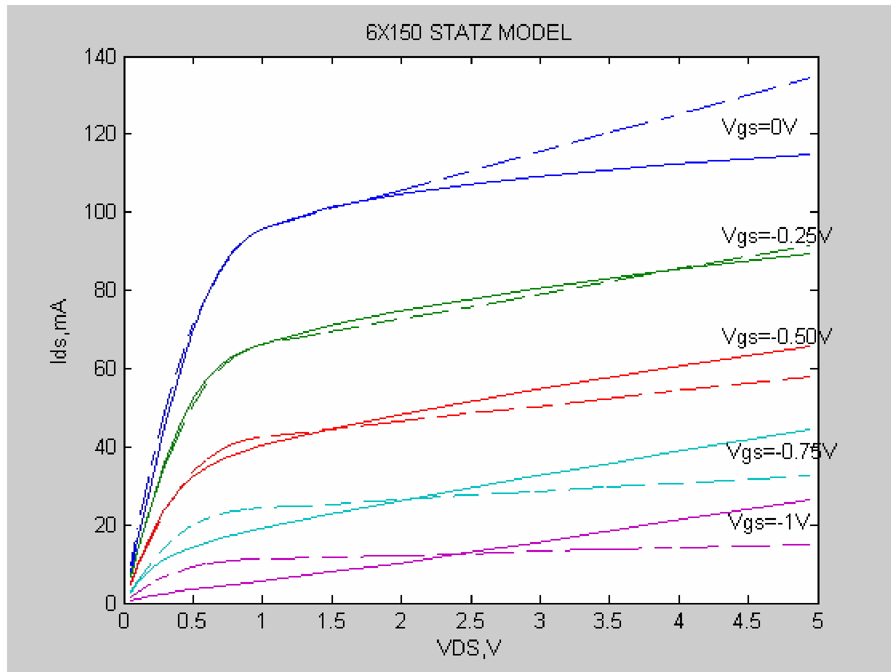

Figure 5-56 Comparison of Vds-Ids characteristics of Statz Model with measured (solid lines) and theoretical values (dashed lines)

The obtained results for Statz large-signal model are represented below:

Table 5–8 Results for Large-Signal Statz Model

	β	V_{TO}	λ	α	b
2x50 MESFET	-0.00013	1.0833	0.1023	3.52	-0.0244
2x150 MESFET	-0.00058	1.168	0.1041	3.5898	-0.0635
4x50 MESFET	0.0131	-2.6431	0.1355	3.1635	-5.2257
4x75 MESFET	-0.00096	1.2659	0.0739	3.3733	-0.094
4x100 MESFET	-0.00069	1.1356	0.1119	3.5561	-0.0481
4x125 MESFET	0.0698	-1.408	0.1043	2.89	0.2967
4x150 MESFET	0.0794	-1.4157	0.1205	3.082	0.054
4x175 MESFET	0.084	-1.5425	0.1189	3.052	-0.5259
6x50 MESFET	0.0144	-1.3376	0.1069	2.7869	0.8158
6x150 MESFET	0.106	-1.5420	0.1197	2.938	-0.5232

The results of Statz model as shown in the figures, are not as accurate as the models described in the previous sections. There are also two groups of MESFET types, which show different characteristics. The first group which includes four types of MESFETs, shows larger errors than the second group of MESFEts which includes six types. In the second group, the results give good approximation only for gate-source voltage of –0.25V.

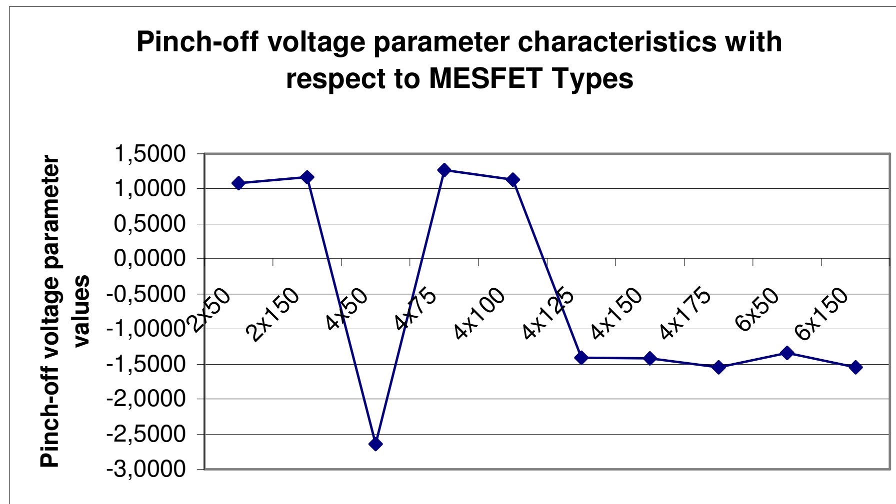

Figure 5-57 Parameter characteristics wih respect to MESFET Types

The figure shown above represents the Pinch-off parameter variation with respect to MESFET types. As discussed in the previous sections, the parameters' results form two groups; one group is for 4 types and the other is for the 6 types.

5.2.5 Curtice Model [3], [4], [5]

One of the first large signal MESFET models to be described in Large-signal circuit simulators was proposed by Van Tuyl and Liechti and later simplified by Curtice in 1980. The Curtice Model consists primarily of the voltage controlled current source I_{ds}, gate-source capacitance C_{gs}, gate-drain capacitance C_{gd}, and the clamping diode D_{gs}. The I_{ds} term is a function of the intrinsic gate-source and drain-source voltages and a time constant τ, which represents the electron transit

time under the gate.

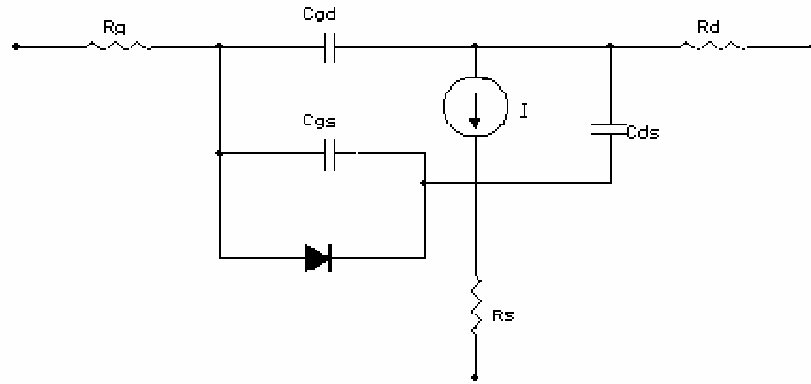

Figure 5-58 Equivalent Circuit for Large Signal Curtice Model of GaAs MESFET

The C_{gs} term is considered to be a function of the gate-source voltage, but the C_{gd} term is considered to be constant although today it is well known that this term is a function of gate-drain voltage.

The Curtice model describes the drain current with respect to the drain-source and gate-source voltages as;

$$I_{ds}(V_{gs},V_{ds}) = \beta(V_{gs}+V_{TO})^2(1+\lambda V_{ds})\tanh\alpha V_{ds} \qquad (5.32)$$

where V_{ds} and V_{gs} are the intrinsic drain-source and gate-source voltages and β, V_{TO}, α, and λ are the model parameters. The small signal transconductance and output conductance are derived by differentiating I_{ds} with respect to gate-source and drain-source voltages respectively:

$$g_m = \frac{\partial I_{ds}}{\partial V_{gs}} = 2\beta(V_{gs}-V_{TO})(1+\lambda V_{ds})\tanh(\alpha V_{ds}) \qquad (5.33)$$

$$g_{ds} = \frac{\partial I_{ds}}{\partial V_{ds}} = \beta\left(V_{gs} - V_{TO}\right)^2 \left\{ \frac{\alpha\left(1 + \lambda V_{ds}\right)}{\cosh^2(\alpha V_{ds})} + \lambda \tanh(\alpha V_{ds}) \right\} \tag{5.34}$$

For a complete large signal model the capacitance-voltage relationship must also be described. The Curtice model uses the following expression for both gate-source and gate-drain capacitances:

$$C_{gs} = C_{gs0} \left\{ 1 - \frac{V_{gs}}{V_{BI}} \right\}^{-\frac{1}{2}} \tag{5.35}$$

$$C_{gd} = C_{gd0} \left\{ 1 - \frac{V_{gd}}{V_{BI}} \right\}^{-\frac{1}{2}} \tag{5.36}$$

where V_{BI} is the built-in potential of the Schottky gate, C_{gs0} and C_{gd0} are the zero potential capacitances.

The parameters that have been shown in equation 5.32 are substituted and (I_{ds}, V_{ds}) characteristics for different V_{gs} values are drawn in figures below. In this analysis "fminsearch.m" algorithm is used. The values were compared with the measured values, which are also shown in the same figures. The transconductance (5.33) and output conductance (5.34) equations are drawn with respect to drain-source voltage V_{ds} for 4x150 type of MESFET, the other types of MESFETs have nearly the same results with 4x150, and therefore they are not drawn here.

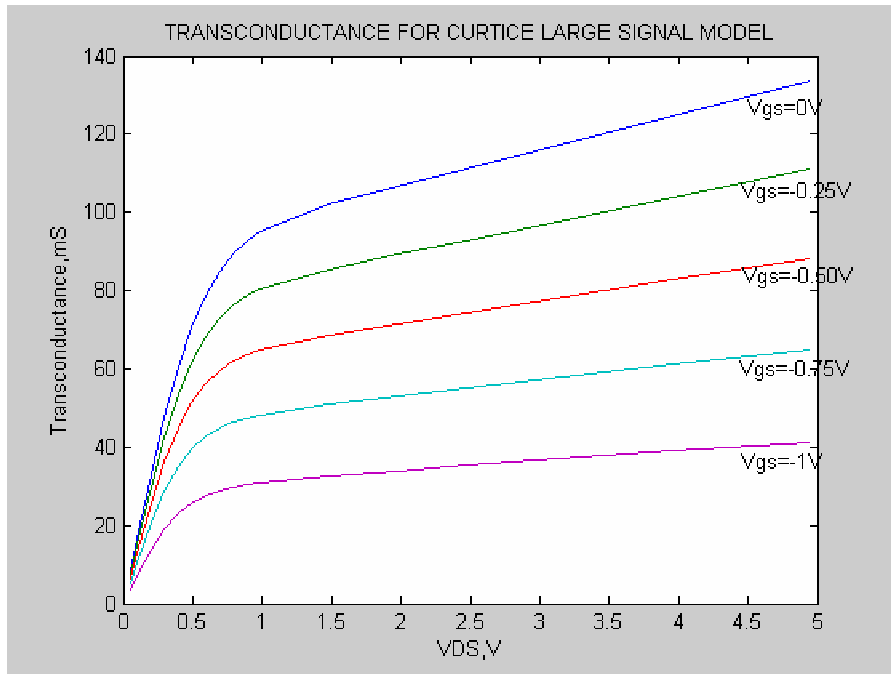

Figure 5-59 Transconductance of 4x150 MESFET for Curtice Large Signal Model

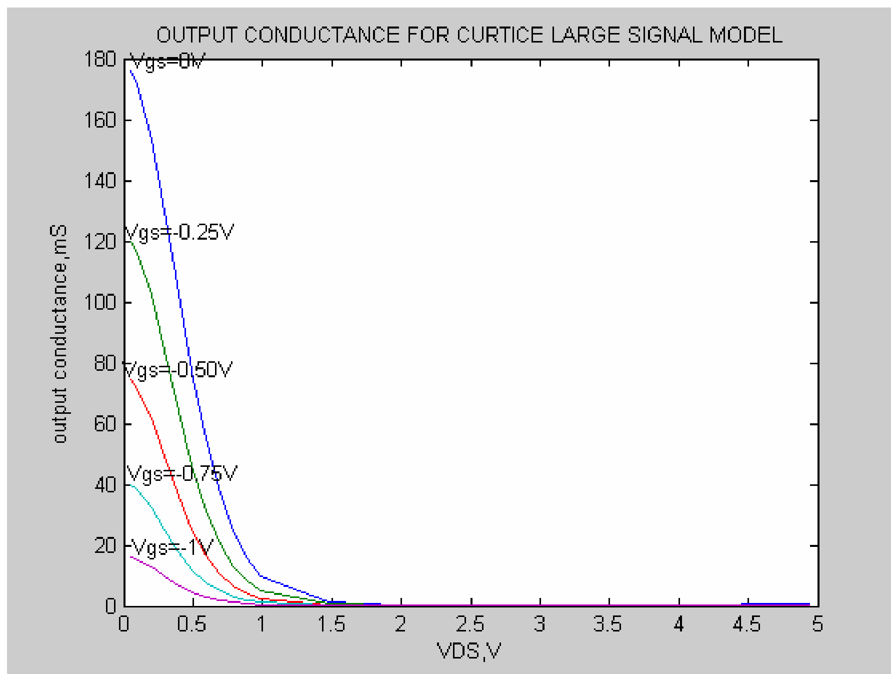

Figure 5-60 Output Conductance of 4x150 MESFET for Curtice Large Signal Model

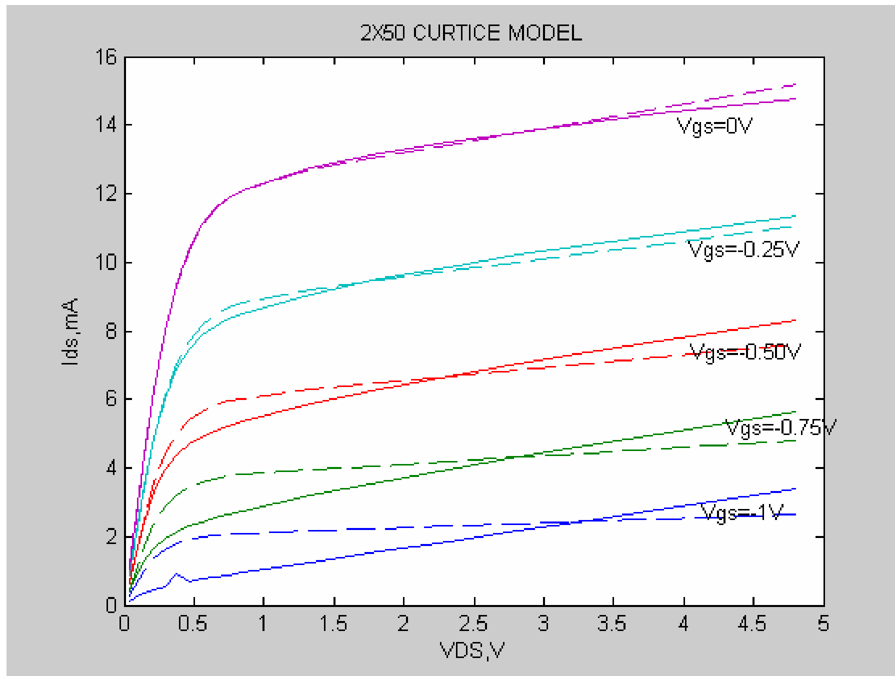

Figure 5-61 Comparison of Vds-Ids characteristics of Curtice Model with measured (solid lines) and theoretical values (dashed lines)

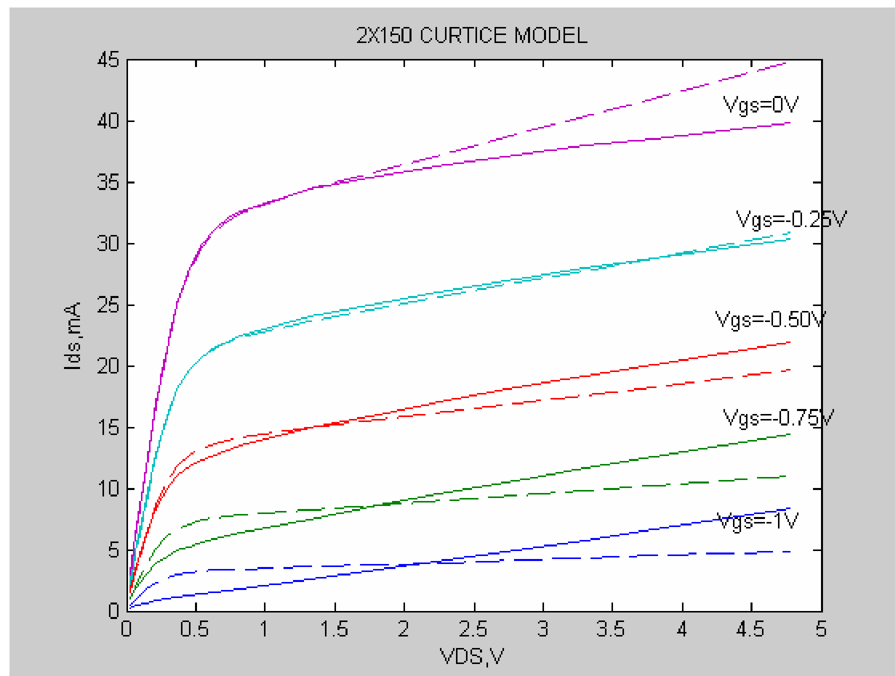

Figure 5-62 Comparison of Vds-Ids characteristics of Curtice Model with measured (solid lines) and theoretical values (dashed lines)

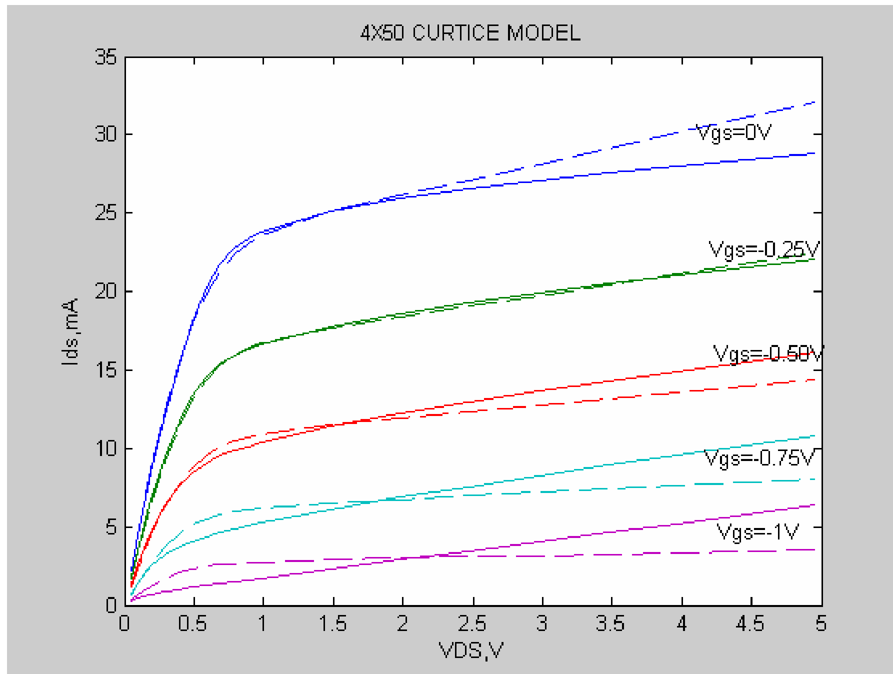

Figure 5-63 Comparison of Vds-Ids characteristics of Curtice Model with measured (solid lines) and theoretical values (dashed lines)

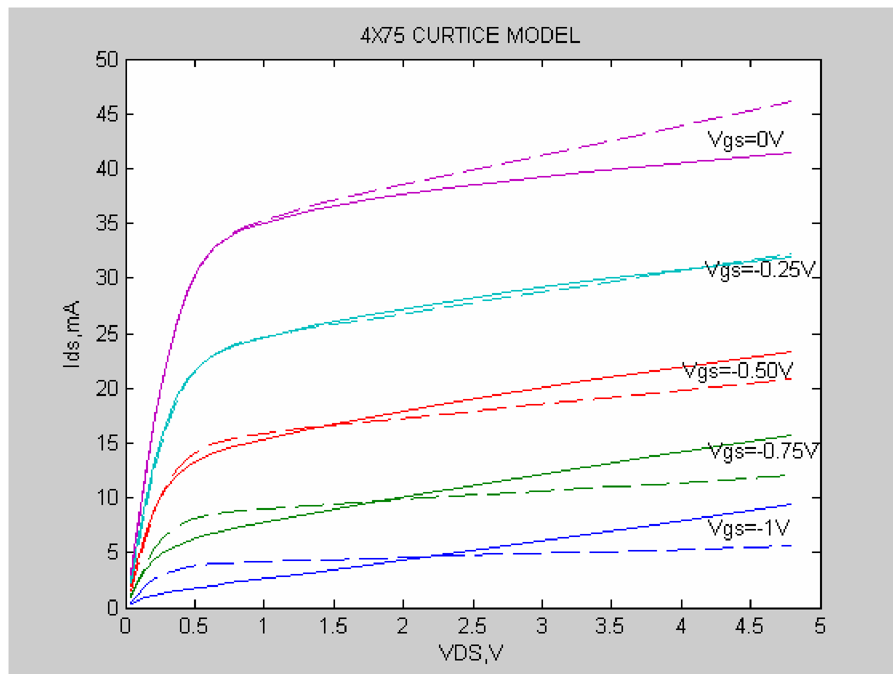

Figure 5-64 Comparison of Vds-Ids characteristics of Curtice Model with measured (solid lines) and theoretical values (dashed lines)

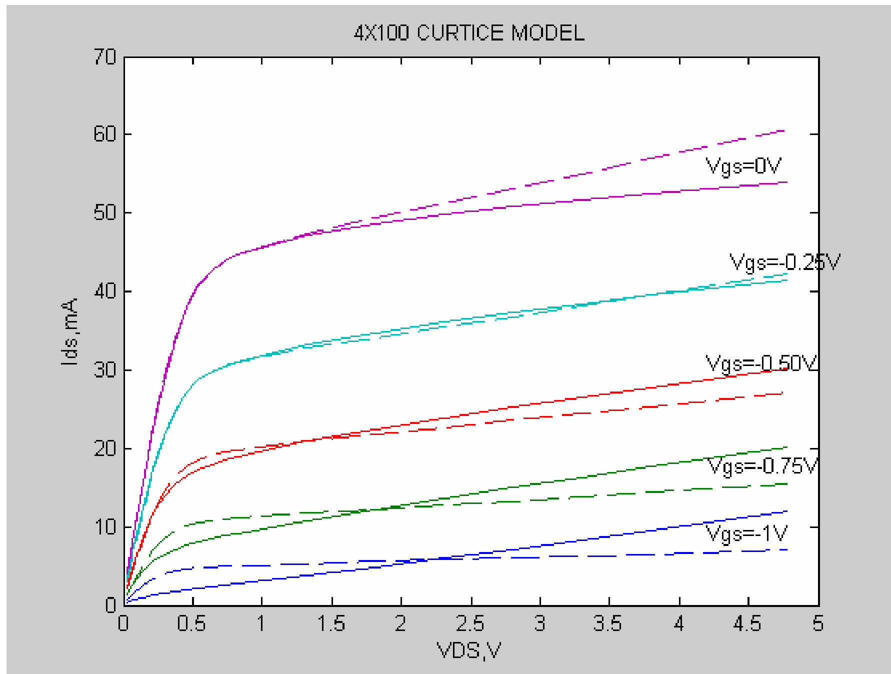

Figure 5-65 Comparison of Vds-Ids characteristics of Curtice Model with measured (solid lines) and theoretical values (dashed lines)

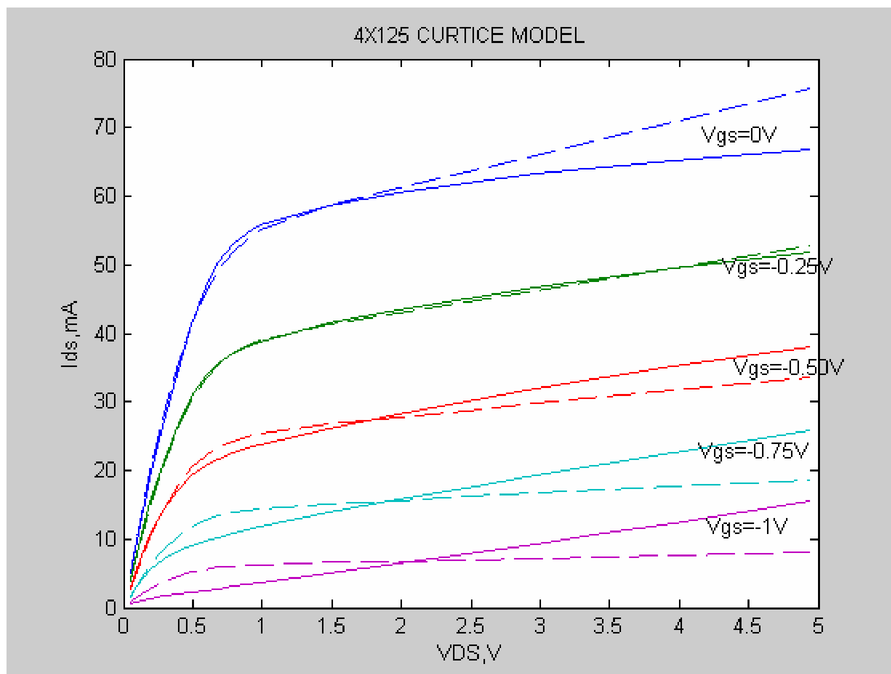

Figure 5-66 Comparison of Vds-Ids characteristics of Curtice Model with measured (solid lines) and theoretical values (dashed lines)

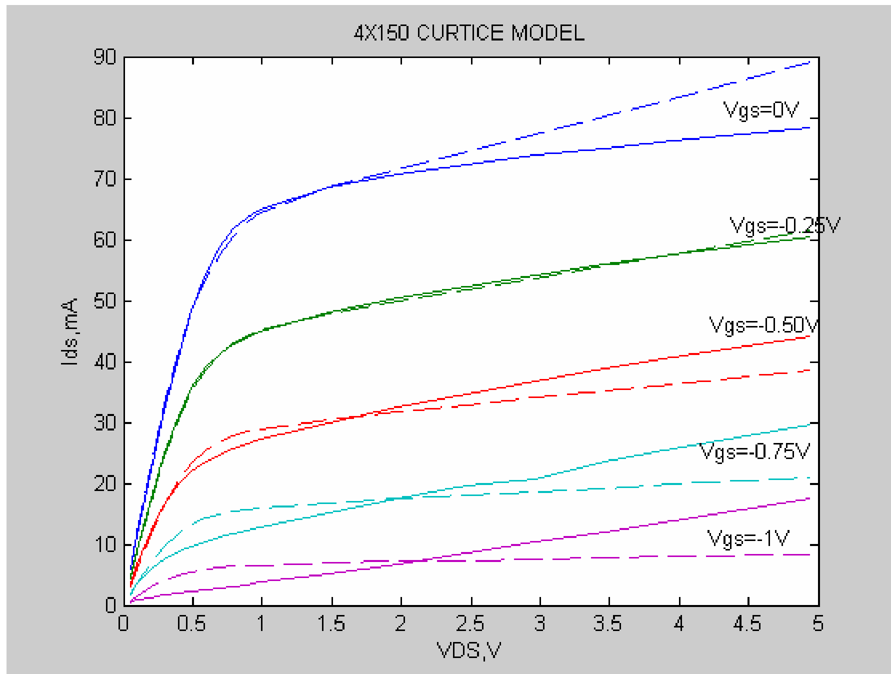

Figure 5-67 Comparison of Vds-Ids characteristics of Curtice Model with measured (solid lines) and theoretical values (dashed lines)

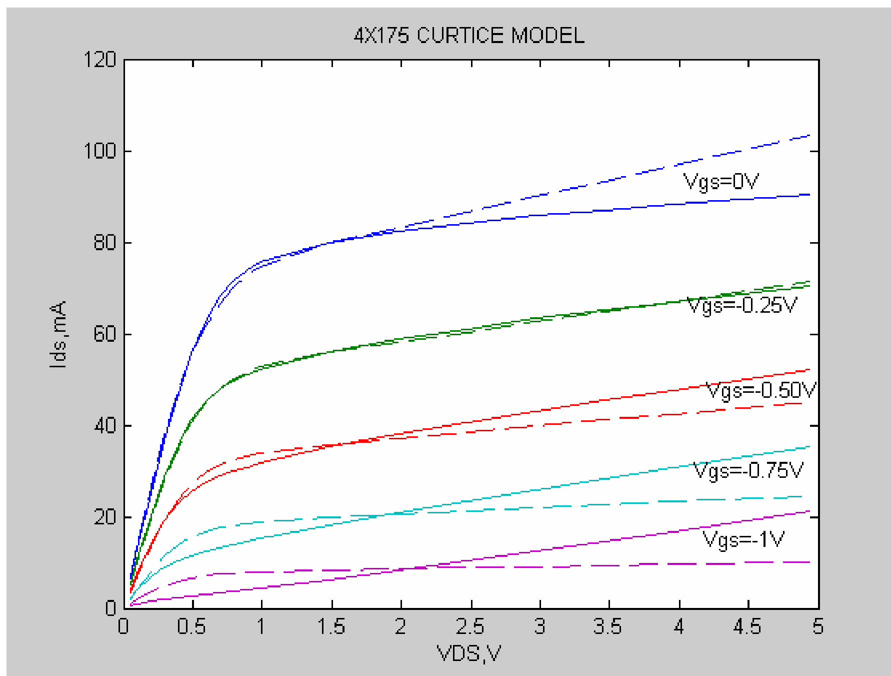

Figure 5-68 Comparison of Vds-Ids characteristics of Curtice Model with measured (solid lines) and theoretical values (dashed lines)

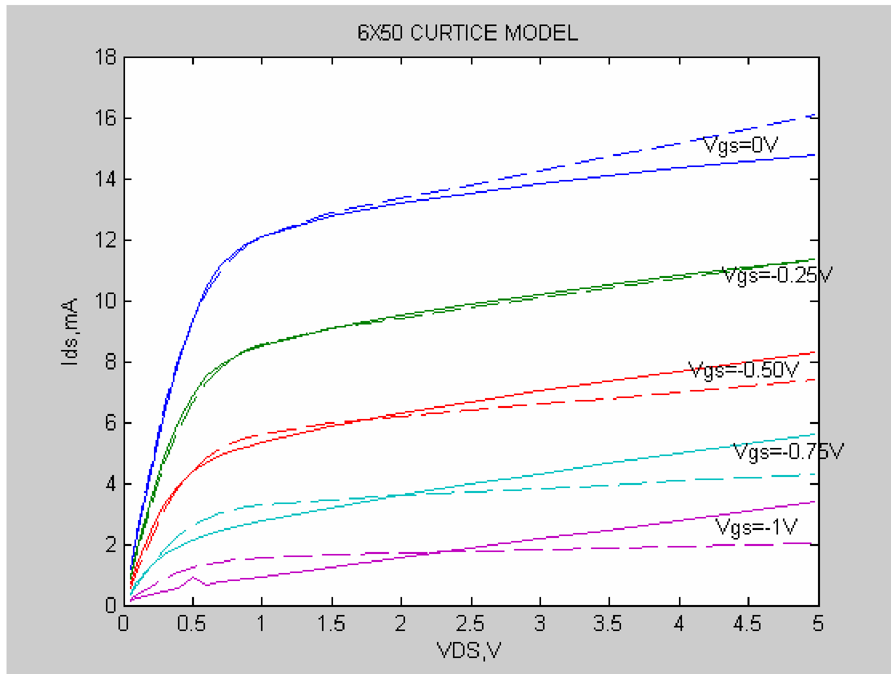

Figure 5-69 Comparison of Vds-Ids characteristics of Curtice Model with measured (solid lines) and theoretical values (dashed lines)

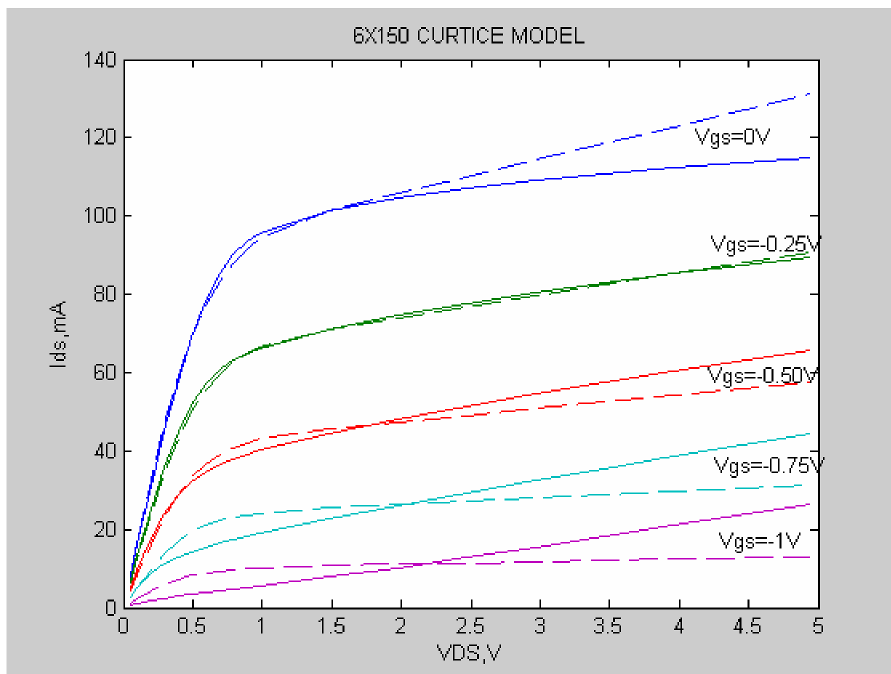

Figure 5-70 Comparison of Vds-Ids characteristics of Curtice Model with measured (solid lines) and theoretical values (dashed lines)

Table 5–9 The parameter values extracted by using MATLAB program for Curtice Model

	β	V_{TO}	λ	α
2x50 MESFET	0.0035436	0.74508	0.055316	2.8286
2x150 MESFET	0.012181	0.50374	0.090461	3.0925
4x50 MESFET	0.011424	-1.4767	0.096917	2.5932
4x75 MESFET	0.012476	0.55188	0.075182	2.7829
4x100 MESFET	0.016397	0.52995	0.083207	2.9538
4x125 MESFET	0.027419	-1.4633	0.10144	2.6057
4x150 MESFET	0.033503	-1.4286	0.10443	2.6145
4x175 MESFET	0.038647	-1.4378	0.10348	2.5972
6x50 MESFET	0.0050262	-1.542	0.081409	2.244
6x150 MESFET	0.04878	-1.4429	0.10233	2.4029

Similar to the discussions in section 5.2.4, the results for Curtice Model do not satisfy good approximation to measured data. The results for all ten types of MESFETs, the only accurate result is for $V_{gs} = -0.25V$, and for the other values of gate-source voltage the modeled data do not give good approximations to measured data.

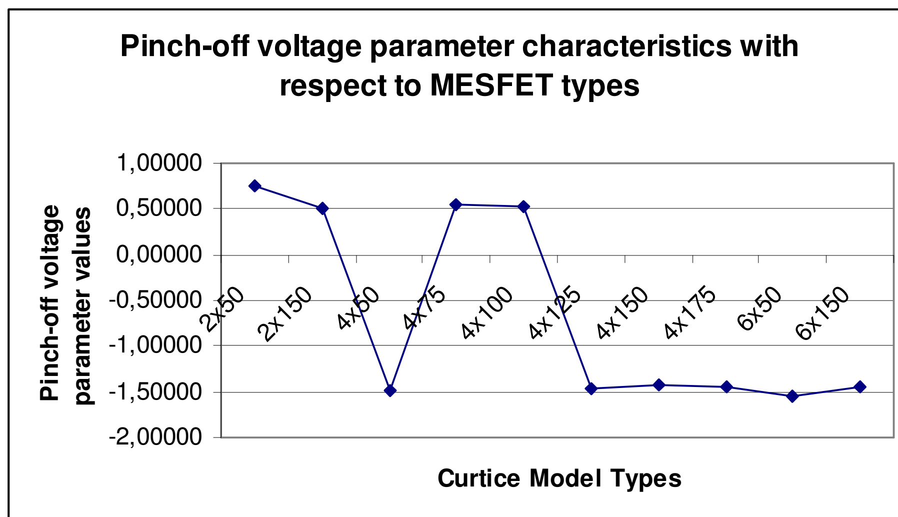

Figure 5-71 Parameter characteristics wih respect to MESFET Types

The pinch-off voltage parameter values are similar for all MESFET types shown in the figure above. The figures plotted for Curtice Model represents that the results are not grouped with respect to MESFET Types. Therefore the discussions for the other types, which are the groups of models of the MESFET types, is different for Curtice Model.

5.2.6 TriQuint's Own Model (TOM) [11]

This model is a modification of the Statz model. The first modification to the equation of Statz large signal model is designed to address the poor fit at near pinch-off values of V_{gs}. This is accomplished by making V_t a function of drain voltage:

$$V_t = V_{TO} - \gamma V_{ds} \tag{5.37}$$

This improves the drain conductance fit at low drain currents, where the statz model shows a cutoff independent of drain voltage. The utility of equation (5.37) has been noted by Materka&Kacprzak and Curtice&Ettenberg [8], [12].

The second modification relates to the way in which I_{ds} decreases at higher values of current and voltage, showing a smaller slope than would be predicted from the cited models, possibly even becoming negative. This model improved an equation which models this as a feedback effect:

For $0 < V_{ds} < 3/\alpha$,

$$I_{ds} = \frac{\beta(V_{gs} - V_T)^Q}{1 + \beta\delta V_{ds}(V_{gs} - V_T)^Q}\left[1 - \left(1 - \frac{\alpha V_{ds}}{3}\right)^3\right] \tag{5.37}$$

$$g_m = \left\{1 - \left[1 - \frac{\alpha V_{ds}}{3}\right]^3\right\}\left[\frac{Q\beta(V_{gs} - V_T)}{1 + \delta V_{ds} I_{dso}} - \frac{I_{dso} Q \delta V_{ds} \beta(V_{gs} - V_T)}{(1 + \delta V_{ds} I_{dso})^2}\right] \tag{5.38}$$

$$g_{ds} = \left\{1 - \left[1 - \frac{\alpha V_{ds}}{3}\right]^3\right\}$$

$$\left\{\frac{Q\beta\gamma(V_{gs} - V_T)(1 + \delta V_{ds} I_{dso})}{(1 + \delta V_{ds} I_{dso})^2} - \frac{I_{dso}\{\delta[I_{dso} + Q\beta\gamma V_{ds}(V_{gs} - V_T)]\}}{(1 + \delta V_{ds} I_{dso})^2}\right\} \quad (5.39)$$

$$+ I_{ds}\left\{\alpha\left[1 - \frac{\alpha V_{ds}}{3}\right]^2\right\}$$

for $V_{ds} \geq 3/\alpha$,

$$I_{ds} = \frac{\beta(V_{gs} - V_T)^Q}{1 + \beta\delta V_{ds}(V_{gs} - V_T)^Q} \quad (5.40)$$

$$g_m = \frac{Q\beta(V_{gs} - V_T)}{1 + \delta V_{ds} I_{dso}} - \frac{I_{dso} Q\delta V_{ds} \beta(V_{gs} - V_T)}{(1 + \delta V_{ds} I_{dso})^2} \quad (5.41)$$

$$g_{ds} = \frac{Q\beta\gamma(V_{gs} - V_T)(1 + \delta V_{ds} I_{dso}) - I_{dso}\{\delta[I_{dso} + Q\beta\gamma V_{ds}(V_{gs} - V_T)]\}}{(1 + \delta V_{ds} I_{dso})^2} \quad (5.42)$$

where,

$$I_{dso} = \beta(V_{gs} - V_T)^Q \quad (5.43)$$

Transconductance and Output Conductance graphs for the type of 4x150 MESFET are shown below.

Table 5–10 Results for TOM Large Signal Model

	α	β	δ	Q	V_{TO}	γ
2x50 MESFET	3.3820	0.00028	5.3179	4.00	1.4407	-0.0978
2x150 MESFET	3.7729	0.0009	2.1238	4.00	1.2850	-0.1014
4x50 MESFET	2.9185	0.0030	2.3209	3.3002	-1.9144	0.0807
4x75 MESFET	3.3657	0.0009	1.9824	4.00	1.3519	-0.1002
4x100 MESFET	3.3962	0.0013	1.6225	4.00	1.2901	-0.1026
4x125 MESFET	2.9145	0.0094	1.1067	3.1746	-1.8013	0.086
4x150 MESFET	2.9596	0.0099	1.0604	3.3533	-1.7975	0.0906
4x175 MESFET	2.8874	0.0210	0.9499	2.9267	-1.6041	0.0929
6x50 MESFET	2.7112	0.0087	1.9490	1.6261	-1.1947	0.0726
6x150 MESFET	2.7912	0.0085	0.7353	3.7057	-1.9699	0.0923

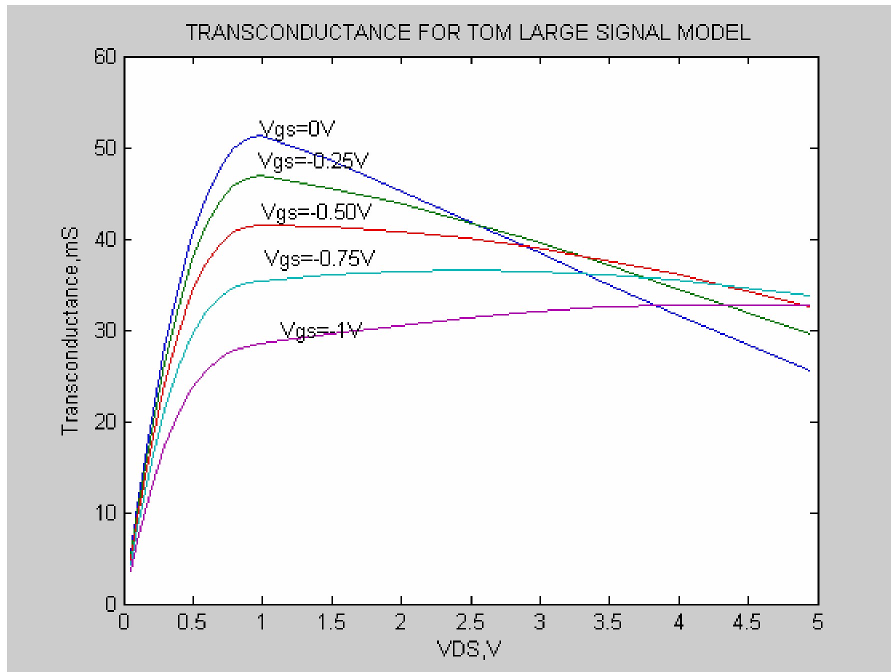

Figure 5-72 Transconductance of 4x150 MESFET for TOM Large Signal Model

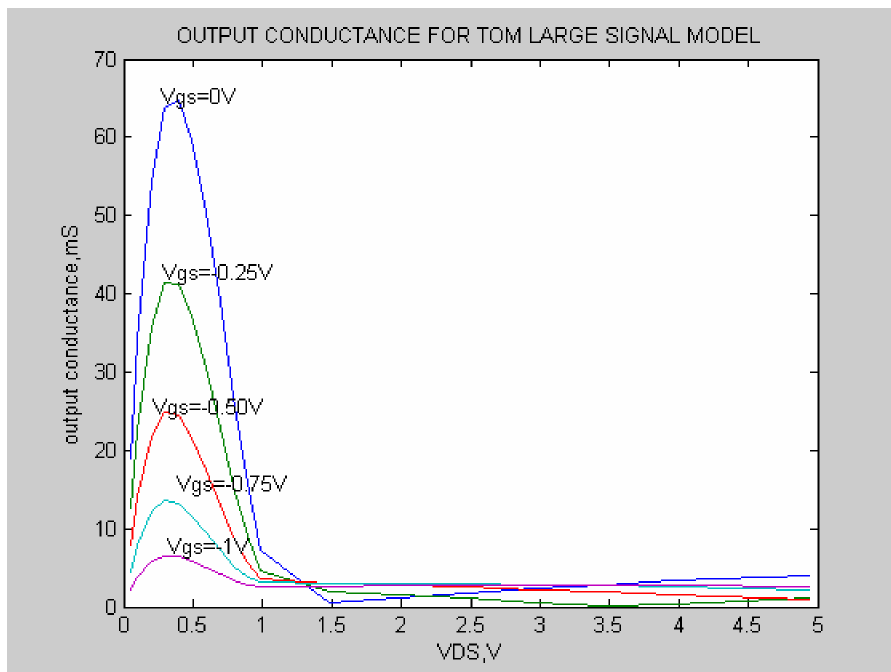

Figure 5-73 Output Conductance of 4x150 MESFET for TOM Large Signal Model

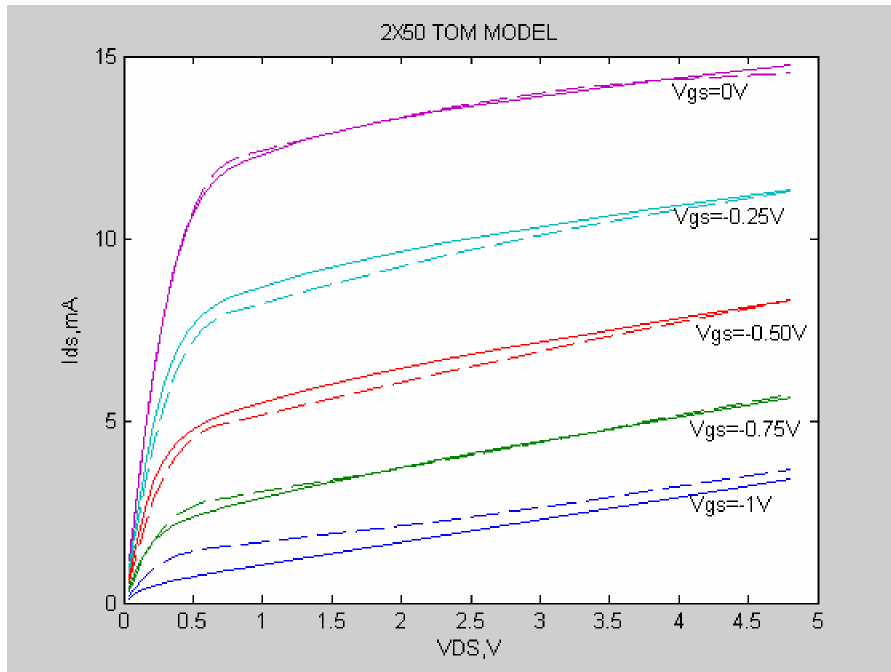

Figure 5-74 Comparison of Vds-Ids characteristics of TOM Model with measured (solid lines) and theoretical values (dashed lines)

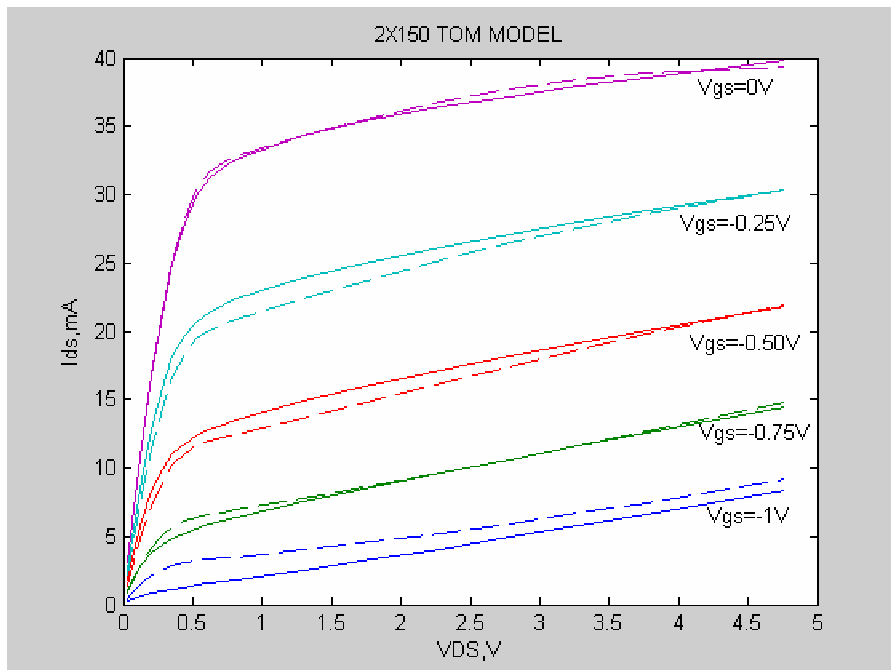

Figure 5-75 Comparison of Vds-Ids characteristics of TOM Model with measured (solid lines) and theoretical values (dashed lines)

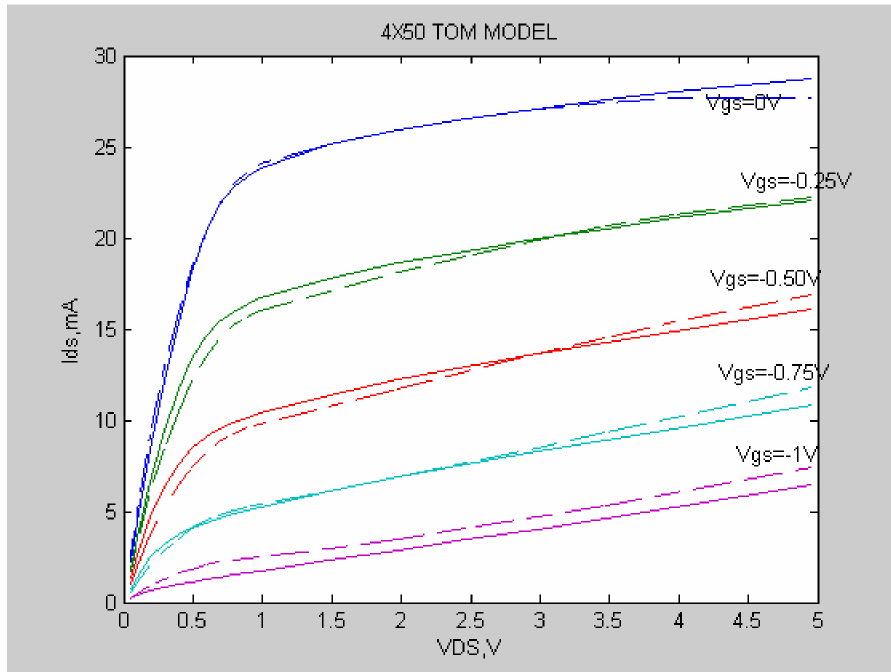

Figure 5-76 Comparison of Vds-Ids characteristics of TOM Model with measured (solid lines) and theoretical values (dashed lines)

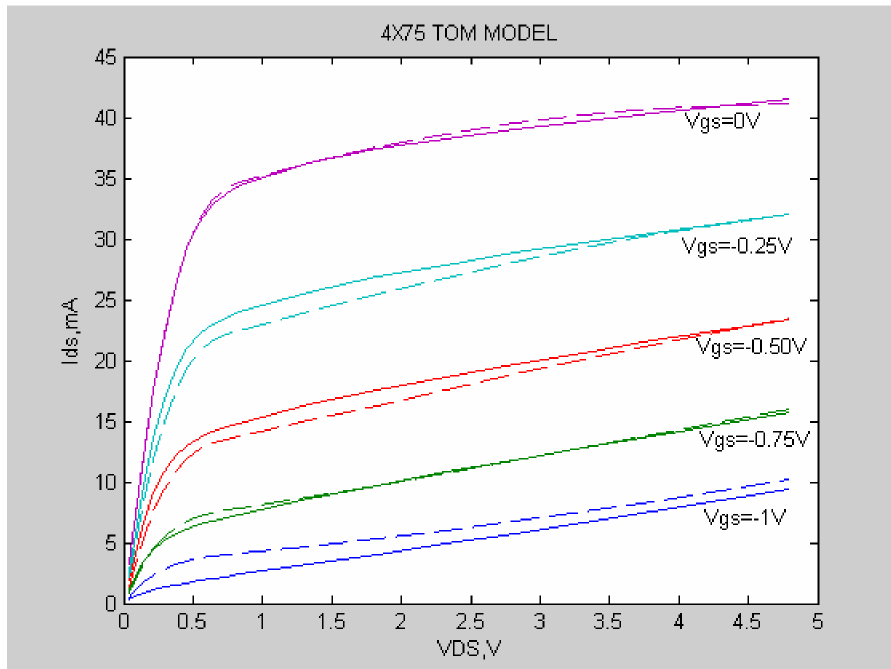

Figure 5-77 Comparison of Vds-Ids characteristics of TOM Model with measured (solid lines) and theoretical values (dashed lines)

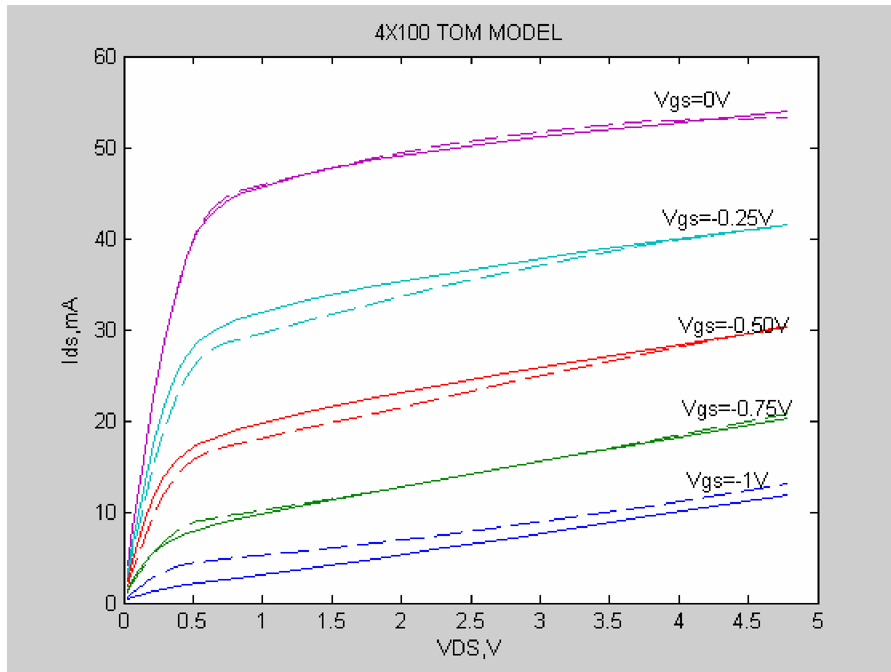

Figure 5-78 Comparison of Vds-Ids characteristics of TOM Model with measured (solid lines) and theoretical values (dashed lines)

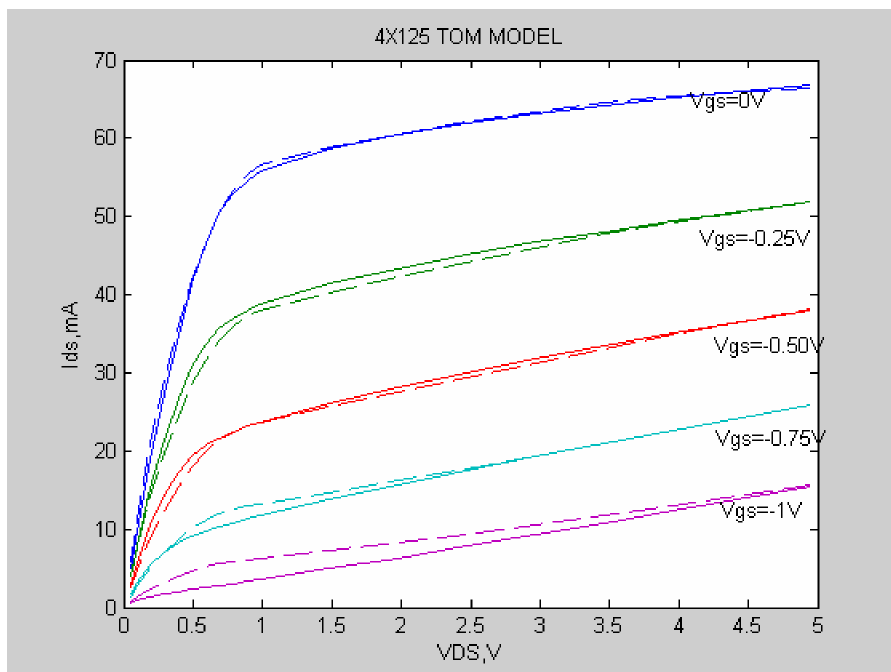

Figure 5-79 Comparison of Vds-Ids characteristics of TOM Model with measured (solid lines) and theoretical values (dashed lines)

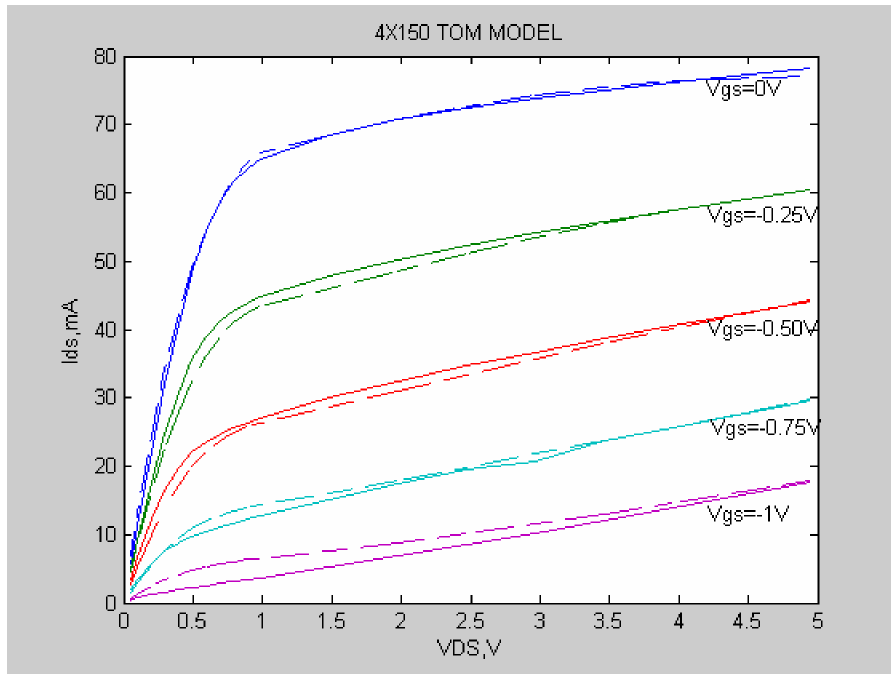

Figure 5-80 Comparison of Vds-Ids characteristics of TOM Model with measured (solid lines) and theoretical values (dashed lines)

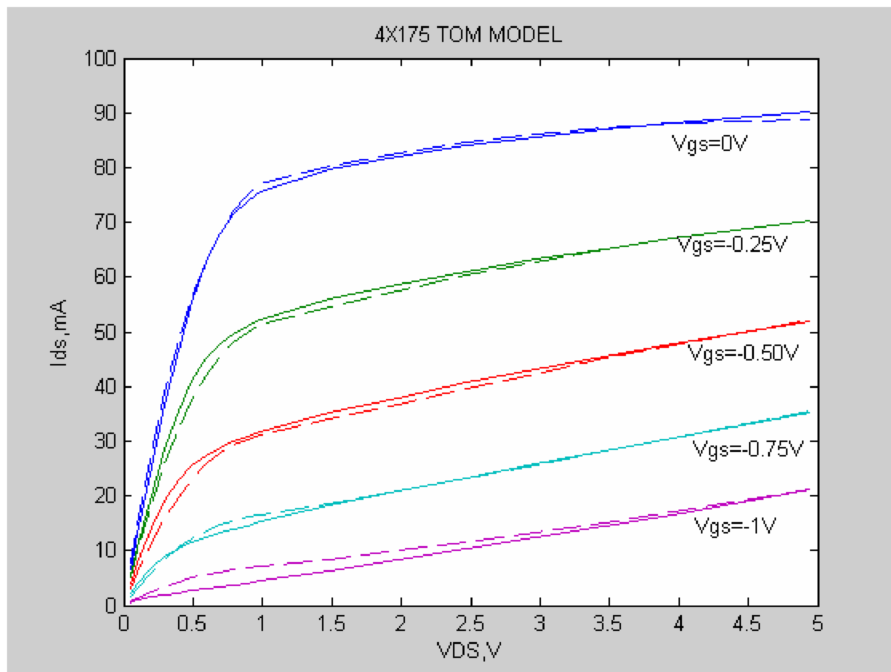

Figure 5-81 Comparison of Vds-Ids characteristics of TOM Model with measured (solid lines) and theoretical values (dashed lines)

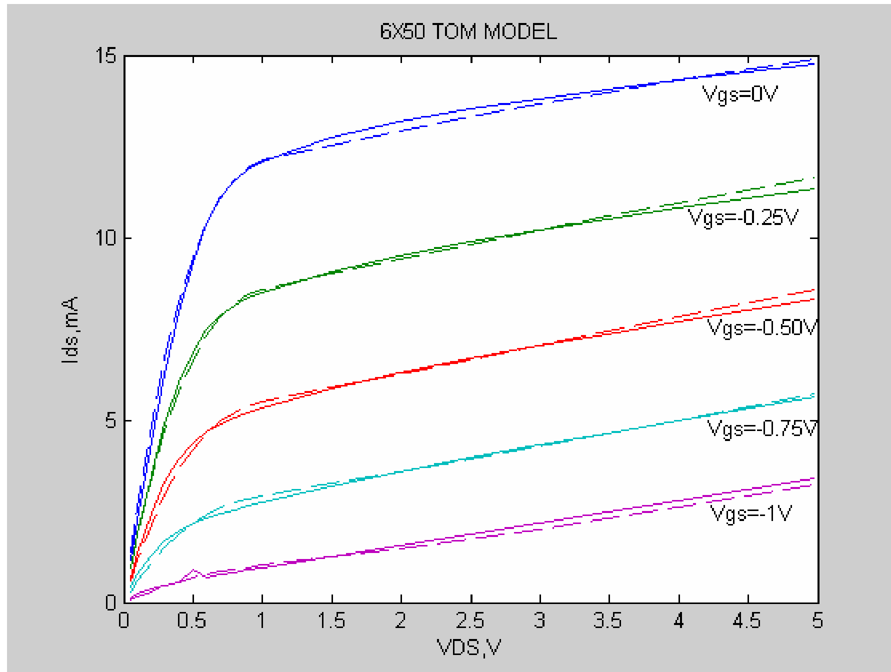

Figure 5-82 Comparison of Vds-Ids characteristics of TOM Model with measured (solid lines) and theoretical values (dashed lines)

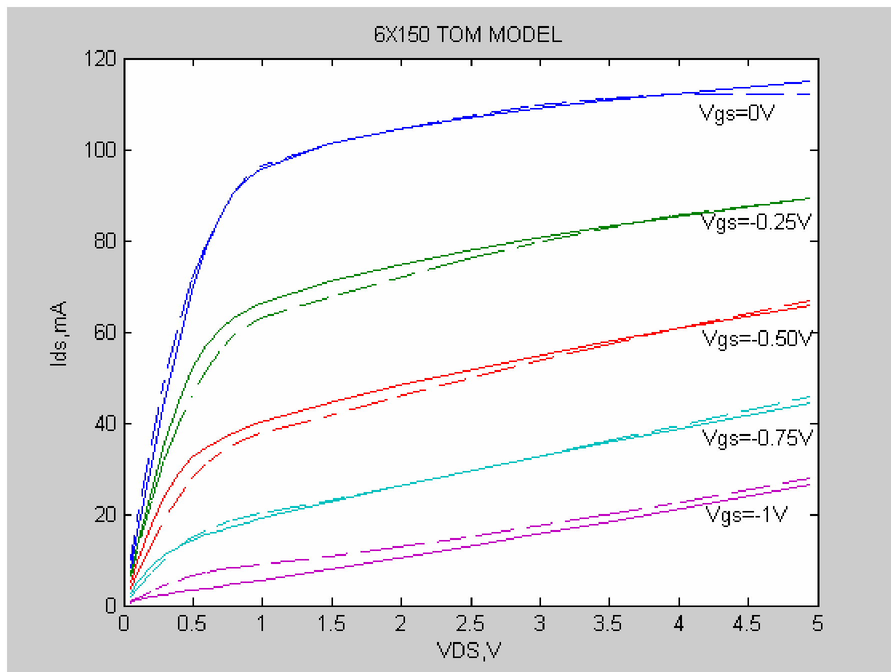

Figure 5-83 Comparison of Vds-Ids characteristics of TOM Model with measured (solid lines) and theoretical values (dashed lines)

The results for TOM, shows that the modeled drain-source current I_{ds} are nearly accurate for some values of gate-source voltage. And it can be easily realised that for from 2x50 through 4x100 types of MESFETs have good approximations for gate-source voltage of 0V and –0.75V. For the other values of gate-source voltages the results do not follow the measured data accurately. For other types of MESFETs better accuracy is obtained for the gate-source voltages of 0,-0.25,-0.50,-0.75V except -1.0V.

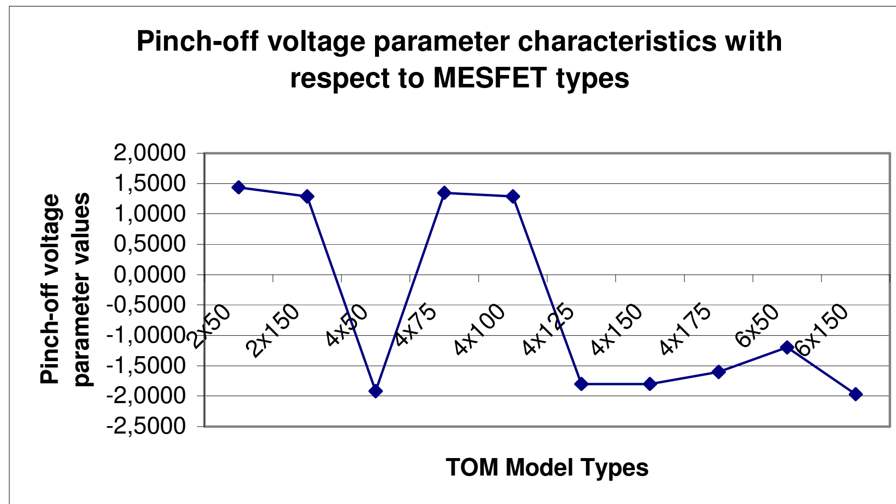

Figure 5-84 Parameter characteristics wih respect to MESFET Types

These results in figure above represents similar properties with the other models excep Curtice Model. Parameter characteristics again grouped to two, that each group has similar values of parameters in itself.

5.2.7 Angelov Model [14]

The drain current function is expressed in accordance with previous models as

$$I_{ds}[V_{gs}, V_{ds}] = I_{dA}[V_{gs}] I_{dB}[V_{ds}] \quad (5.44)$$

where the first factor is dependent only on the gate voltage and the second only on the drain voltage. The $I_{dB}[V_{ds}]$ term is the same as the one used in other models [2], [3], [4], [8], [9], [10], [12].

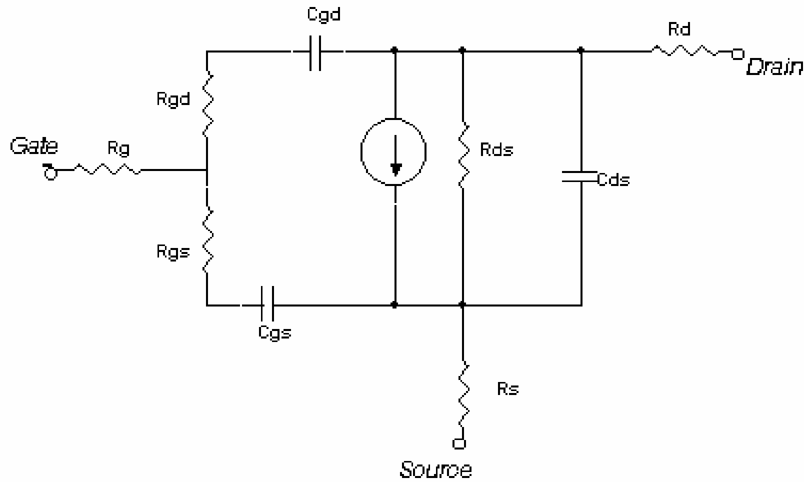

Figure 5-85 Equivalent Circuit model for Angelov Large Signal Model

For $I_{dA}[V_{gs}]$, Angelov proposed a function whose first derivative has the same 'bell shaped' structure as the measured transconductance function $g_m[V_{gs}]$. The hyperbolic tangent (tanh) function describes the gate voltage dependencies and its derivatives well and is normally available in commercial HB-simulators i.e.:

$$I_{ds} = I_{pk}(1+\tanh(\psi))(1+\lambda V_{ds})\tanh(\alpha V_{ds}) \quad (5.45)$$

where I_{pk} is the drain current at which the maximum transconductance is obtained. λ is the channel length modulation parameter and α is the saturation voltage parameter. The parameters α and λ are the same as those in the Statz and Curtice models. ψ is in general a power series function centered at V_{pk} with V_{gs} as a variable i.e.

$$\psi = P_1(V_{gs}-V_{pk}) + P_2(V_{gs}-V_{pk})^2 + P_3(V_{gs}-V_{pk})^3 +,... \quad (5.46)$$

where V_{pk} is the gate voltage for maximum transconductance g_{mpk}. The selected $I_{ds}[V_{gs},V_{ds}]$ function has well defined derivatives. An advantage of the selected model is its simplicity. The different parameters can as a first approximation be

easily obtained by inspection of the measured $I_{ds}[V_{gs}, V_{ds}]$ at a saturated channel condition as follows: all higher terms in ψ are assumed to be zero, λ is determined from the slope of the $I_{ds} - V_{ds}$ characteristic, I_{pk} and V_{pk} are determined at the peak transconductance g_{mpk}. V_{pk} is dependent on the drain voltage V_{ds} in the saturation region. This effect can be accounted for by:

$$V_{pk} = V_{pko} + \gamma V_{ds} \tag{5.47}$$

The intrinsic maximum transconductance g_{mpk} is calculated from the measured maximum transconductance g_{mpkm} by taking into account the feedback effect due to the source resistance, R_s, which can be obtained from DC-measurement:

$$g_{mpk} = \frac{g_{mpkm}}{(1 - R_s g_{mpkm})} \tag{5.48}$$

P_1 is obtained as:

$$P_1 = \frac{g_{mpk}}{I_{pk}(1 + \lambda V_d)} \approx \frac{g_{mpk}}{I_{pk}} \tag{5.49}$$

the same type of modeling functions were chosen to model the dependencies on gate and drain voltage of capacitances C_{gs} and C_{gd}:

$$C_{gs} = C_{gso}[1 + \tanh(\psi_1)][1 + \tanh(\psi_2)] \tag{5.50}$$

$$C_{gd} = C_{gdo}[1 + \tanh(\psi_3)][1 - \tanh(\psi_4)] \tag{5.51}$$

where

$$\psi_1 = P_{0gsg} + P_{1gsg}V_{gs} + P_{2gsg}V_{gs}^2 + P_{3gsg}V_{gs}^3 + \ldots \tag{5.52}$$

$$\psi_2 = P_{0gsd} + P_{1gsd}V_{ds} + P_{2gsd}V_{ds}^2 + P_{3gsd}V_{ds}^3 + ... \quad (5.53)$$

$$\psi_3 = P_{0gdg} + P_{1gdg}V_{gs} + P_{2gdg}V_{gs}^2 + P_{3gdg}V_{gs}^3 + ... \quad (5.54)$$

$$\psi_4 = P_{0gdd} + (P_{1gdd} + P_{1cc}V_{gs})V_{ds} + P_{2gdd}V_{ds}^2 + P_{3gdd}V_{ds}^3 + ... \quad (5.55)$$

the term $P_{1cc}V_{gs}V_{ds}$ reflects the cross-coupling of V_{gs} and V_{gd} on C_{gd}. When an accuracy on the order of 5-10% of C_{gd} and C_{gd} is sufficient 5.50-5.55 can be simplified to:

$$C_{gs} = C_{gso}[1 + \tanh(P_{1gsg}V_{gs})][1 + \tanh(P_{1gsd}V_{ds})] \quad (5.56)$$

$$C_{gd} = C_{gdo}[1 + \tanh(P_{1gdg}V_{gs})][1 - \tanh(P_{1gdd}V_{ds}) + P_{1cc}V_{gs}V_{ds}] \quad (5.57)$$

Equation 5.57 can be further simplified if cross coupling at large drain voltages $(V_{ds} > 1V)$ is neglected:

$$C_{gd} = C_{gdo}[1 + \tanh(P_{1gdg}V_{gs})][1 - \tanh(P_{1gdd}V_{ds})] \quad (5.58)$$

As described in previous sections, the transconductance and output conductance equations are written below:

$$g_m = I_{pk}(1 + \lambda V_{ds})\tanh(\alpha V_{ds})\frac{P_1 + 2P_2(V_{gs} - V_{pk}) + 3P_3(V_{gs} - V_{pk})^2}{\cosh^2[\psi]} \quad (5.59)$$

$$g_{ds} = I_{pk}\frac{-\gamma P_1 - 2\gamma P_2(V_{gs} - V_{pk}) - 3\gamma P_3(V_{gs} - V_{pk})^2}{\cosh^2[\psi]}(1 + \lambda V_{ds})\tanh(\alpha V_{ds})$$

$$+ I_{pk}(1 + \tanh(\psi))\left\{\lambda \tanh(\alpha V_{ds}) + (1 + \lambda V_{ds})\frac{\alpha}{\cosh^2[\alpha V_{ds}]}\right\} \quad (5.60)$$

Transconductance and Output Conductance graphs for the type of 4x150 MESFET are shown below:

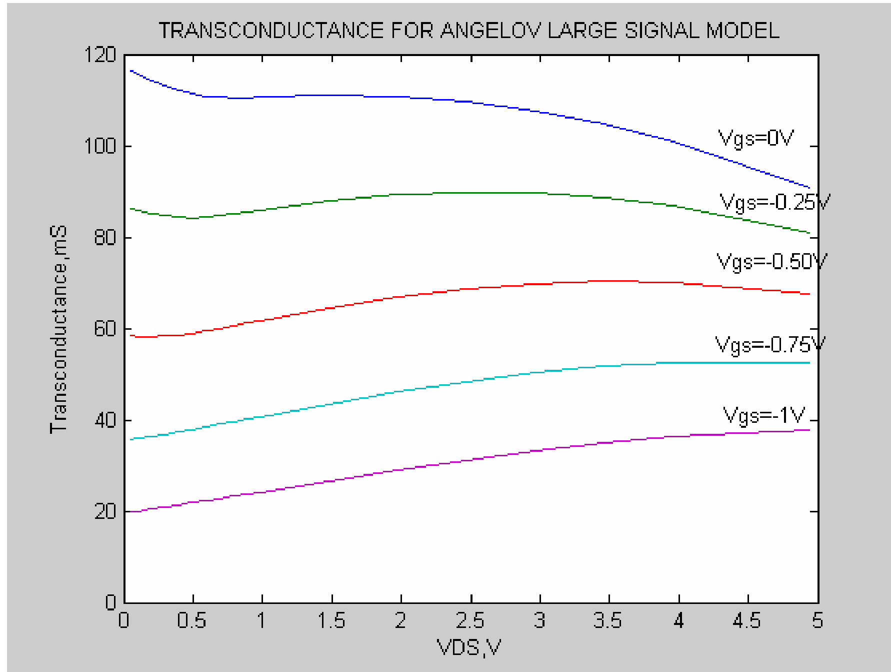

Figure 5-86 Transconductance of 4x150 MESFET for Angelov Large-Signal Model

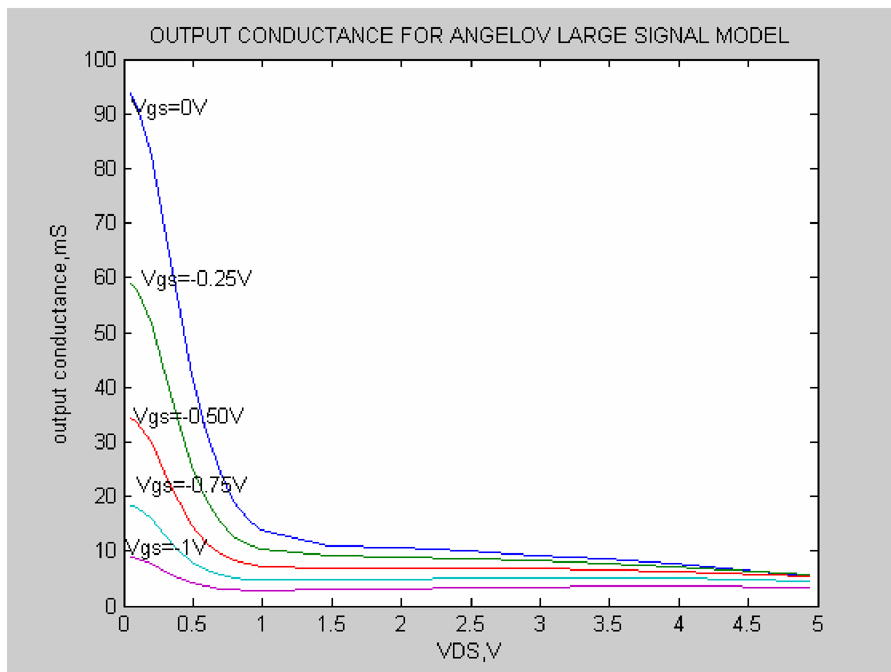

Figure 5-87 Output Conductance of 4x150 MESFET for Angelov Large Signal Model

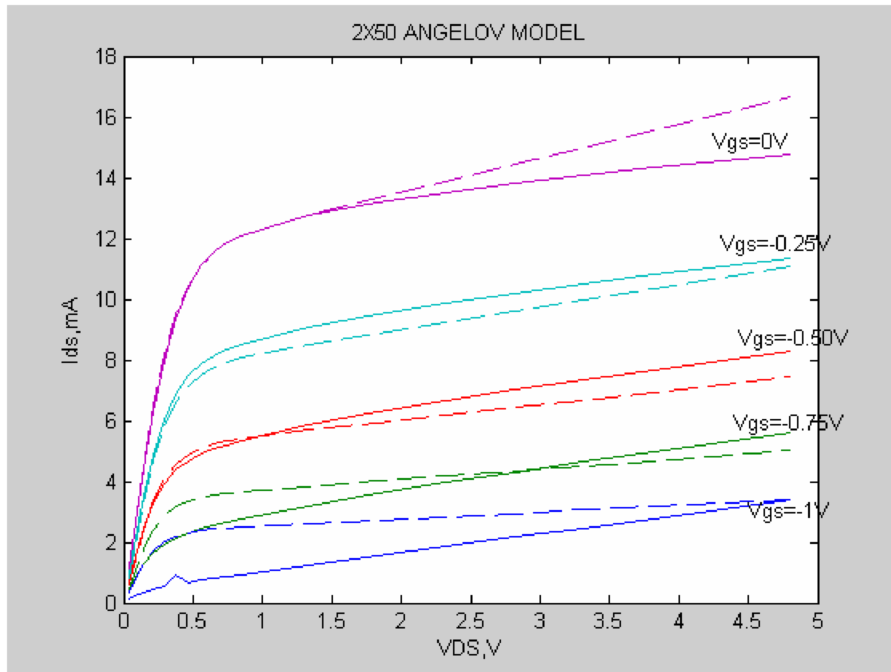

Figure 5-88 Comparison of Vds-Ids characteristics of Angelov Model with measured (solid lines) and theoretical values (dashed lines)

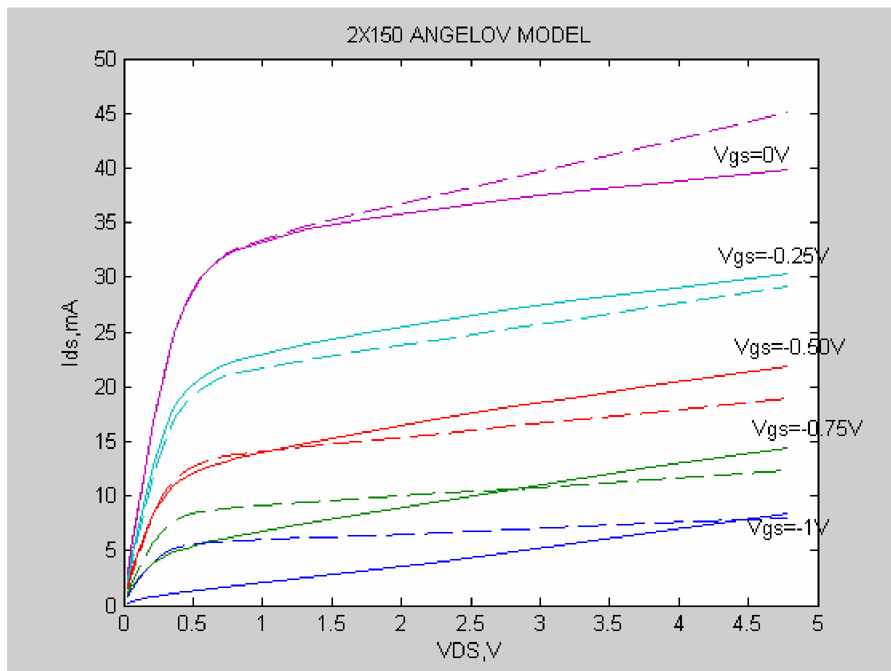

Figure 5-89 Comparison of Vds-Ids characteristics of Angelov Model with measured (solid lines) and theoretical values (dashed lines)

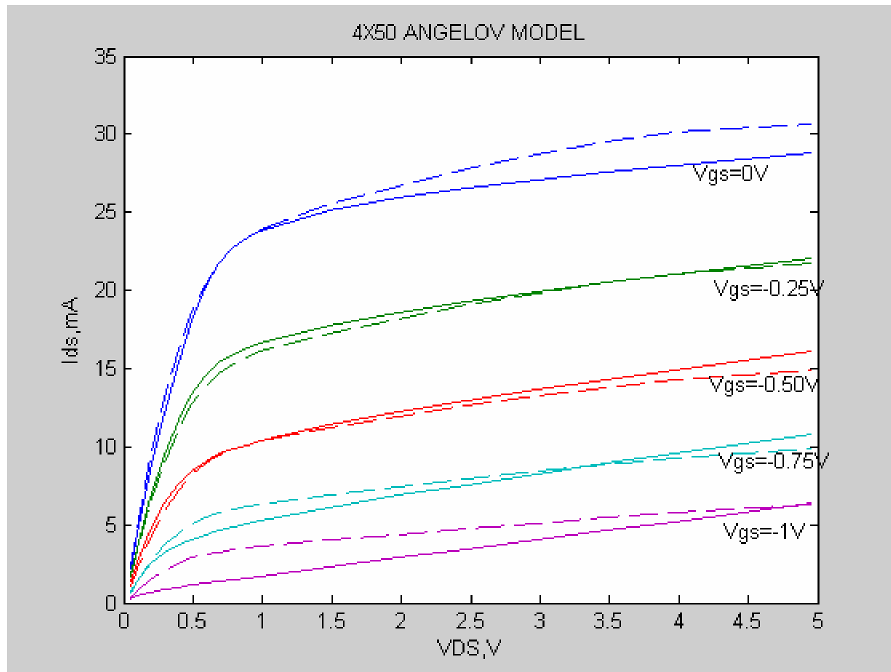

Figure 5-90 Comparison of Vds-Ids characteristics of Angelov Model with measured (solid lines) and theoretical values (dashed lines)

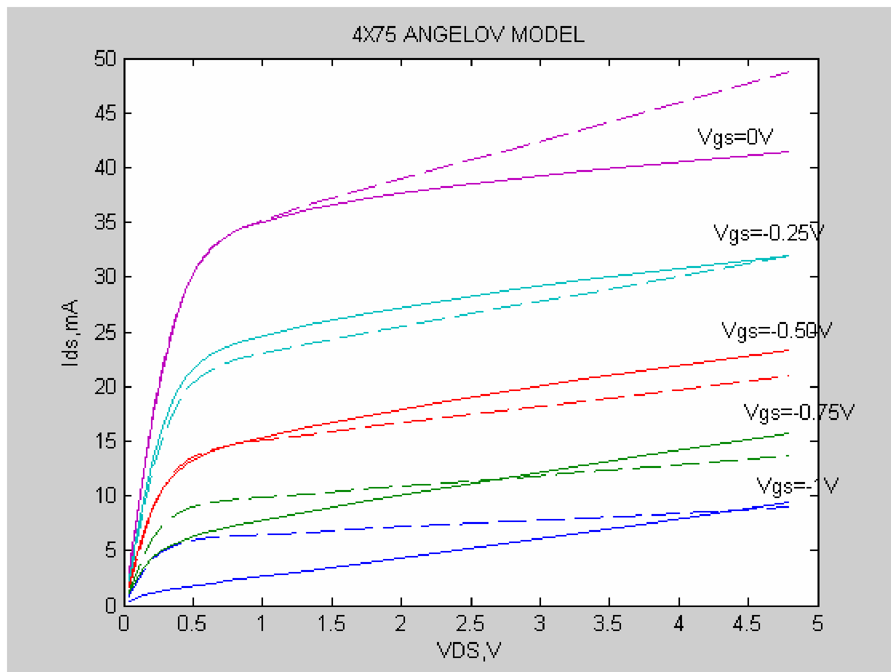

Figure 5-91 Comparison of Vds-Ids characteristics of Angelov Model with measured (solid lines) and theoretical values (dashed lines)

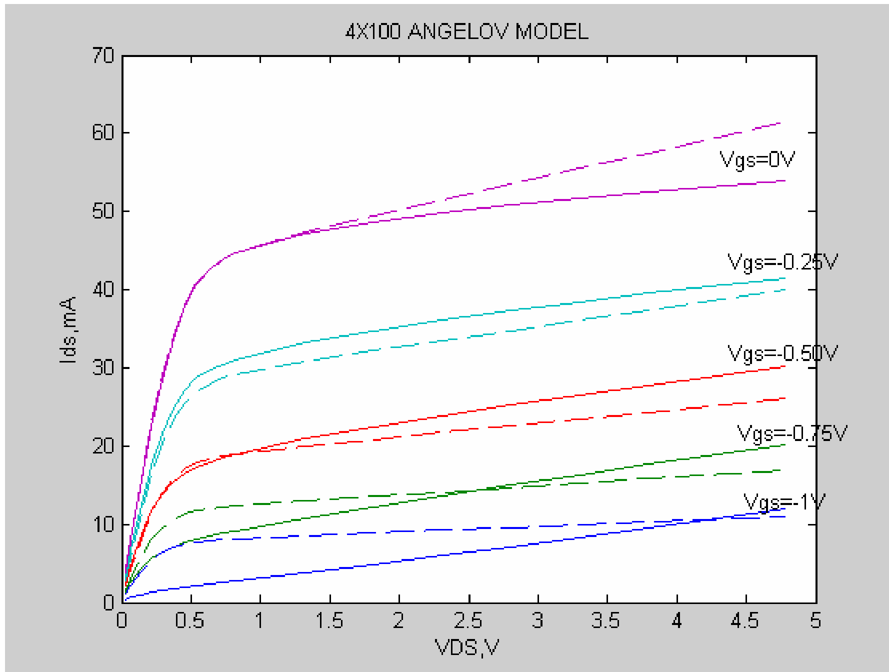

Figure 5-92 Comparison of Vds-Ids characteristics of Angelov Model with measured (solid lines) and theoretical values (dashed lines)

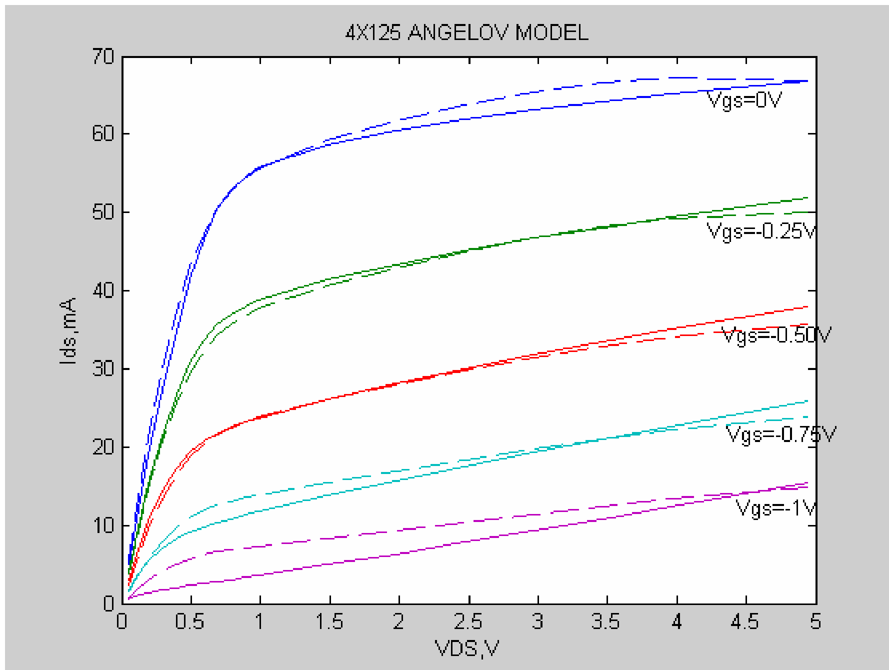

Figure 5-93 Comparison of Vds-Ids characteristics of Angelov Model with measured (solid lines) and theoretical values (dashed lines)

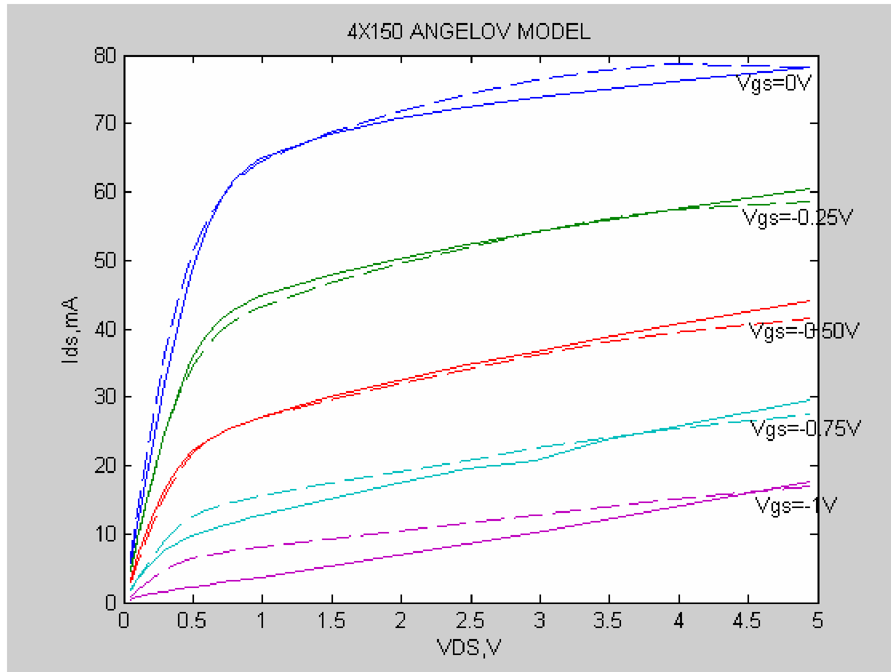

Figure 5-94 Comparison of Vds-Ids characteristics of Angelov Model with measured (solid lines) and theoretical values (dashed lines)

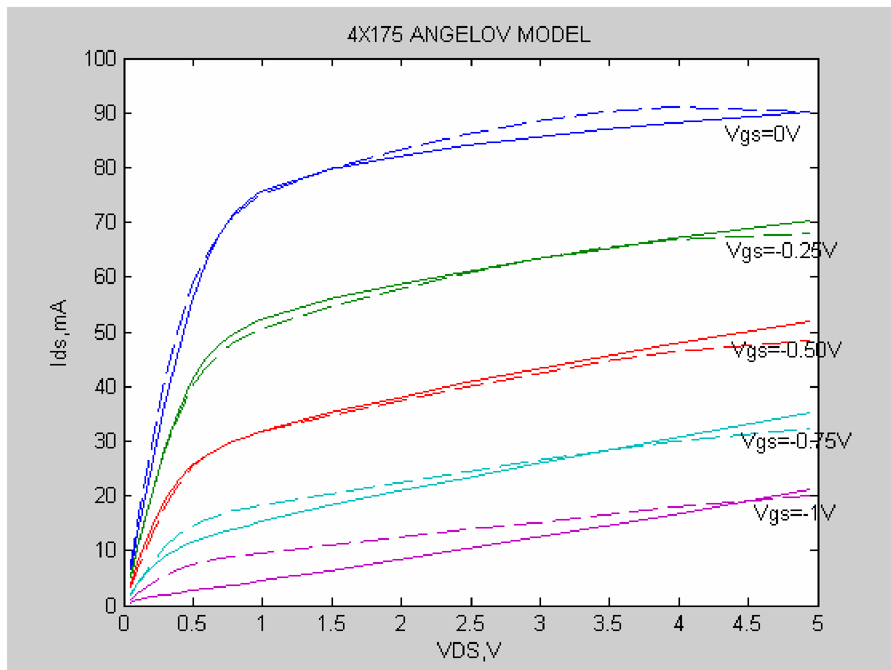

Figure 5-95 Comparison of Vds-Ids characteristics of Angelov Model with measured (solid lines) and theoretical values (dashed lines)

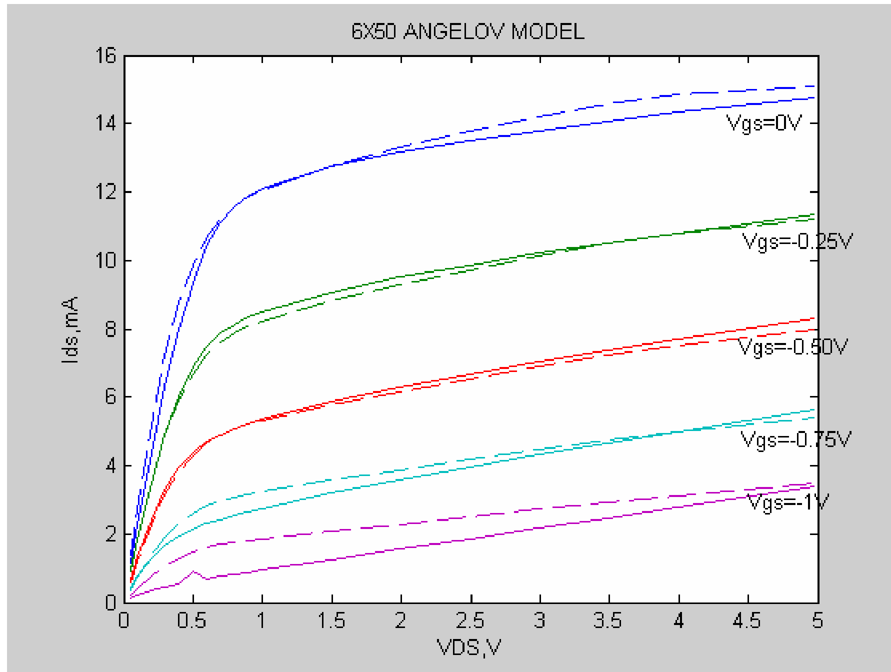

Figure 5-96 Comparison of Vds-Ids characteristics of Angelov Model with measured (solid lines) and theoretical values (dashed lines)

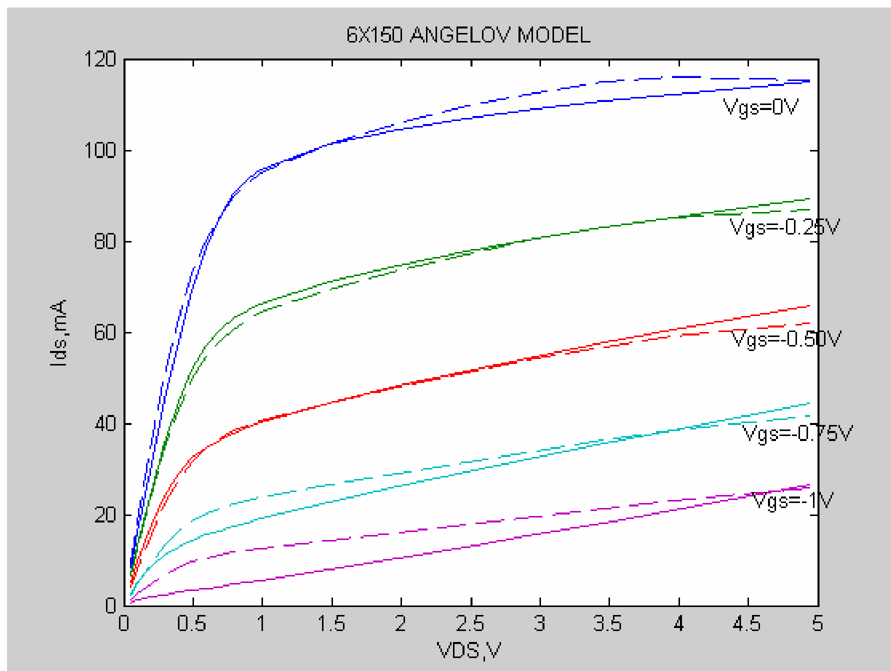

Figure 5-97 Comparison of Vds-Ids characteristics of Angelov Model with measured (solid lines) and theoretical values (dashed lines)

The Angelov large-signal modeled data of drain-source current as shown in the figures above, have good aproximations for the second group of MESFET types, for the gate-source voltage values of –0.25V, -0.50V and not so accurate for –0.75V.

Table 5–11 Parameter results of Angelov Large Signal Model

	P_1	P_2	P_3	V_{pko}	γ	I_{pk}	λ	α
2x50 MESFET	2.0973	0.1890	0.0041	13.7756	0.0014	3.0217	0.0863	3.1470
2x150 MESFET	2.2904	0.1891	0.0038	16.6278	0.0014	1.9866	0.1042	3.1828
4x50 MESFET	1.2456	0.2699	0.0424	3.372	-0.1272	3.145	-0.097	2.7728
4x75 MESFET	2.2857	0.1900	0.0038	16.6688	0.0026	2.2183	0.0934	3.0402
4x100 MESFET	2.2885	0.1903	0.0038	16.6043	0.0013	2.9427	0.0831	3.0182
4x125 MESFET	1.0057	0.3159	0.0403	4.9640	-0.1280	2.1973	-0.0947	2.7938
4x150 MESFET	0.9433	0.3056	0.0406	4.9004	-0.1309	2.1627	-0.0964	2.9552
4x175 MESFET	0.9287	0.3068	0.0411	4.8767	-0.1318	2.2098	-0.0968	2.9131
6x50 MESFET	1.2068	0.2745	0.0282	5.5821	-0.1260	2.86	-0.0828	2.6878
6x150 MESFET	0.8506	0.2821	0.0403	4.6854	-0.1301	2.4916	-0.0947	2.6845

The figure plotted below represents the similar characteristics with the previous models except Curtice model. The parameters have different values but the results can be divided into two groups with respect to evaluated values , which are described in the previous models.

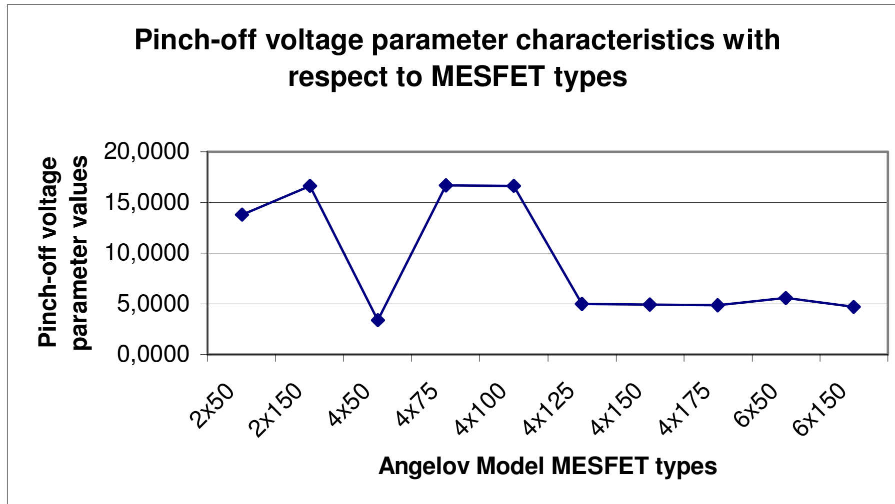

Figure 5-98 Parameter characteristics wih respect to MESFET Types

5.2.8 TriQuint's Own Model -2 (TOM-2) [13]

In this section we will describe an improved MESFET model developed at TriQuint Semiconductor, Inc. The model has been designated TOM-2 because this model is an incremental improvement based on TriQuint's original TOM model.[11]. It is based on the original TOM model with some refinements to improve accuracy in the knee region (V_{ds} of 1 volt or less) and subthreshold (V_{gs} , near cut-off) region.

Figure 5.99 shows a basic model for TOM-2.

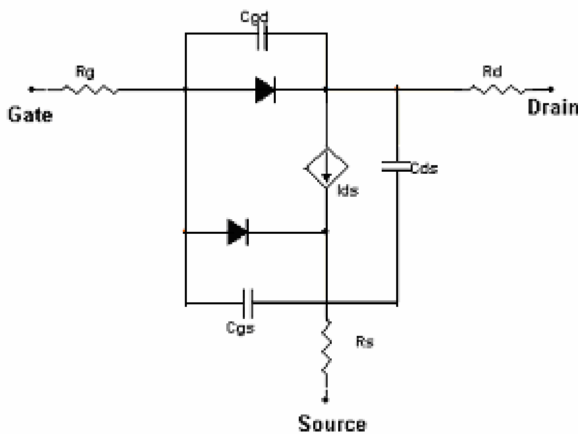

Figure 5-99 A simple Large Signal Equivalent Circuit of TOM-2 MESFET Model

The following equations are used to compute I_{ds} for the current source in figure 5.99.

$$I_{ds} = \frac{I_{ds0}}{1+\delta V_{ds} I_{ds0}} \tag{5.61}$$

where:

$$I_{ds0} = w\beta V_g^Q F_d(\alpha V_{ds}) \tag{5.62}$$

$$F_d(x) = \frac{x}{\sqrt{1+x^2}} \tag{5.63}$$

and V_g is given by:

$$V_g = QV_{st} \ln\left[\exp\left(\frac{V_{gs} - V_{to} - \gamma V_{ds}}{QV_{st}}\right) + 1\right] \tag{5.64}$$

The capacitance equations are based on the equations proposed by Statz.[10].

$$C_{gs} = \frac{C_{gso}}{\sqrt{1-\frac{V_n}{V_{bi}}}} \frac{1}{4}\left\{1+\frac{V_{eff}-V_{to}}{\sqrt{(V_{eff}-V_{to})^2+V_\delta^2}}\right\}\left\{1+\frac{V_{gs}-V_{gd}}{\sqrt{(V_{gs}-V_{gd})^2+\left(\frac{1}{\alpha}\right)^2}}\right\} + C_{gdo}\frac{1}{2}\left\{1-\frac{V_{gs}-V_{gd}}{\sqrt{(V_{gs}-V_{gd})^2+\left(\frac{1}{\alpha}\right)^2}}\right\} \tag{5.65}$$

$$C_{gd} = \frac{C_{gso}}{\sqrt{1-\frac{V_n}{V_{bi}}}}\frac{1}{4}\left\{1+\frac{V_{eff}-V_{to}}{\sqrt{\left(V_{eff}-V_{to}\right)^2+V_\delta^2}}\right\}\left\{1-\frac{V_{gs}-V_{gd}}{\sqrt{\left(V_{gs}-V_{gd}\right)^2+\left(\frac{1}{\alpha}\right)^2}}\right\}$$

$$+C_{gdo}\frac{1}{2}\left\{1+\frac{V_{gs}-V_{gd}}{\sqrt{\left(V_{gs}-V_{gd}\right)^2+\left(\frac{1}{\alpha}\right)^2}}\right\} \tag{5.66}$$

where:

$$V_{eff} = \left(V_{gs}+V_{gd}+\frac{1}{2}\sqrt{\left(V_{gs}-V_{gd}\right)^2+\left(\frac{1}{\alpha}\right)^2}\right) \tag{5.67}$$

$$V_n = \frac{1}{2}\left(V_{eff}+V_{to}+\sqrt{\left(V_{eff}-V_{to}\right)^2+V_\delta{}^2}\right) \tag{5.68}$$

The model parameters; V_t (VTO) is described as threshold voltage parameter, α (ALPHA) is knee-voltage parameter, β (BETA) is transconductance parameter, γ (GAMMA) is threshold shifting parameter, δ (DELTA) is output feedback parameter, *Q* is power-law parameter, *w* is device width and V_{st} is assumed to be the thermal voltage parameter.

The expressions for the conductances are derived directly from the equations 5.61 through 5.64.

To facilitate the computation, it is convenient to define a current reduction factor, *p*. *p* is defined with reference to equation 5.61 as follows:

$$p = \frac{1}{1+\delta V_{ds} I_{dso}} = 1-\delta V_{ds} I_{ds} \tag{5.69}$$

and g_{ds} and g_m are:

$$g_{ds} = \frac{\partial I_{ds}}{\partial V_{ds}} = g_{dso} p^2 - \delta I_{ds}^2 \tag{5.70}$$

$$g_m = \frac{\partial I_{ds}}{\partial V_{gs}} = g_{mo} p^2 \tag{5.71}$$

Differentiating equation 5.62 with respect to V_{gs} and V_{ds}, we obtain:

$$g_{mo} = \frac{\partial I_{dso}}{\partial V_{gs}} = \frac{I_{dso}}{V_g} \frac{Q}{\left[\exp - \left(\frac{V_{gs} - V_{to} + \gamma V_{ds}}{QV_{st}}\right) + 1\right]} \tag{5.72}$$

$$g_{dso} = \frac{\partial I_{dso}}{\partial V_{ds}} = g_m \left(\gamma - \frac{V_{gs} - V_{to} + \gamma V_{ds}}{V_{st}}\right) + \frac{QI_{dso}}{V_{st}} + \frac{\alpha \beta V_g^Q}{\left(1 + (\alpha V_{ds})^2\right)^{3/2}} \tag{5.73}$$

Transconductance and Output Conductance graphs for the type of 4x150 MESFET are shown below:

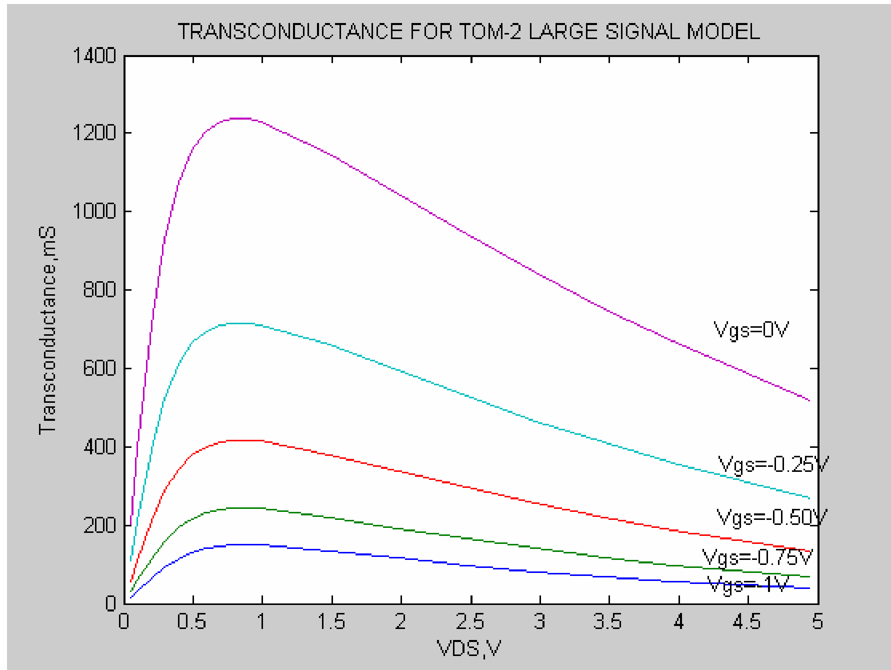

Figure 5-100 Transconductance of 4x150 MESFET for TOM-2 Large Signal Model

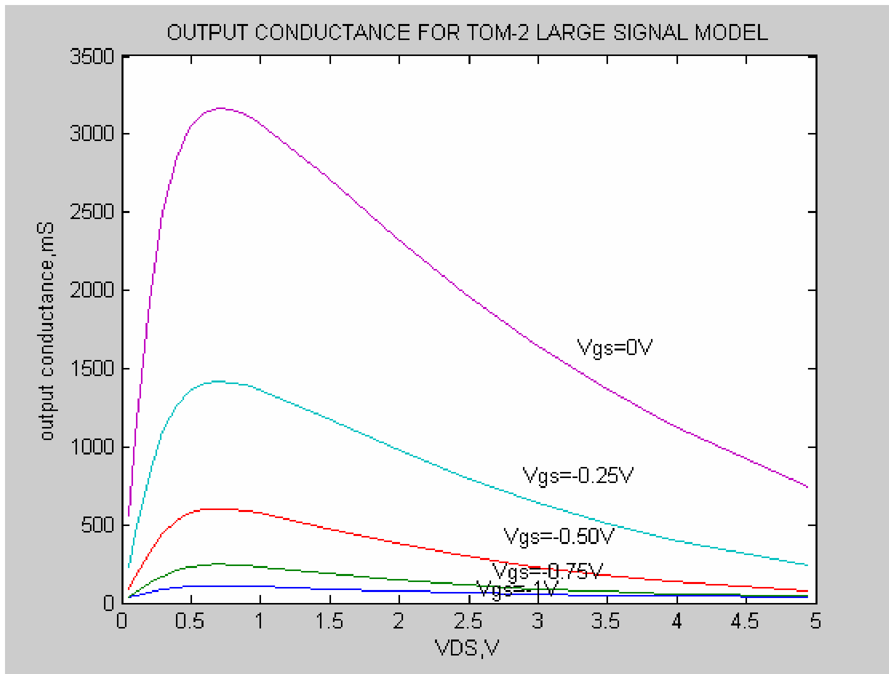

Figure 5-101 Output Conductance of 4x150 MESFET for TOM-2 Large Signal Model

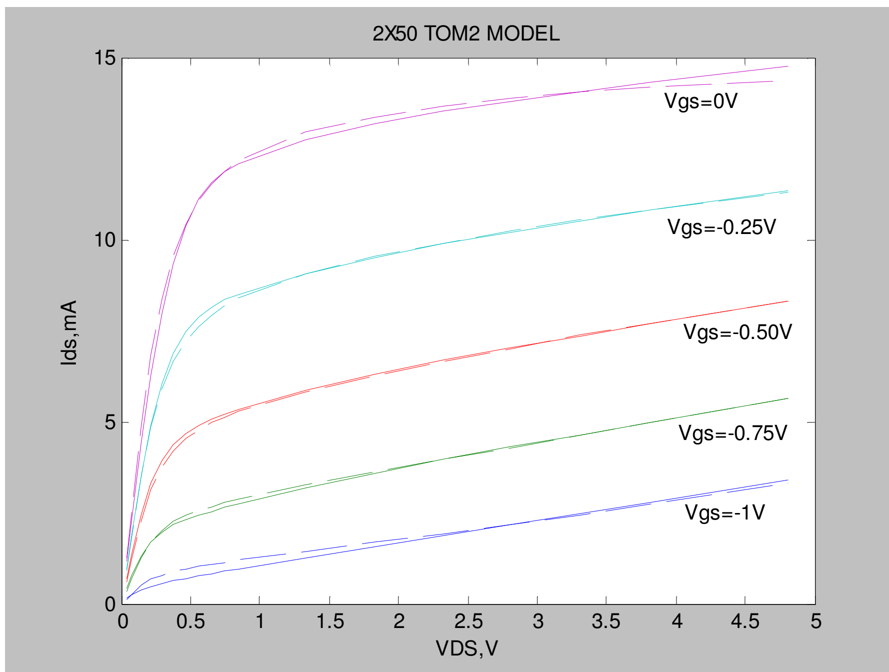

Figure 5-102 2x50 Comparison of Vds-Ids characteristics of TOM-2 Model with measured (solid lines) and theoretical values (dashed lines)

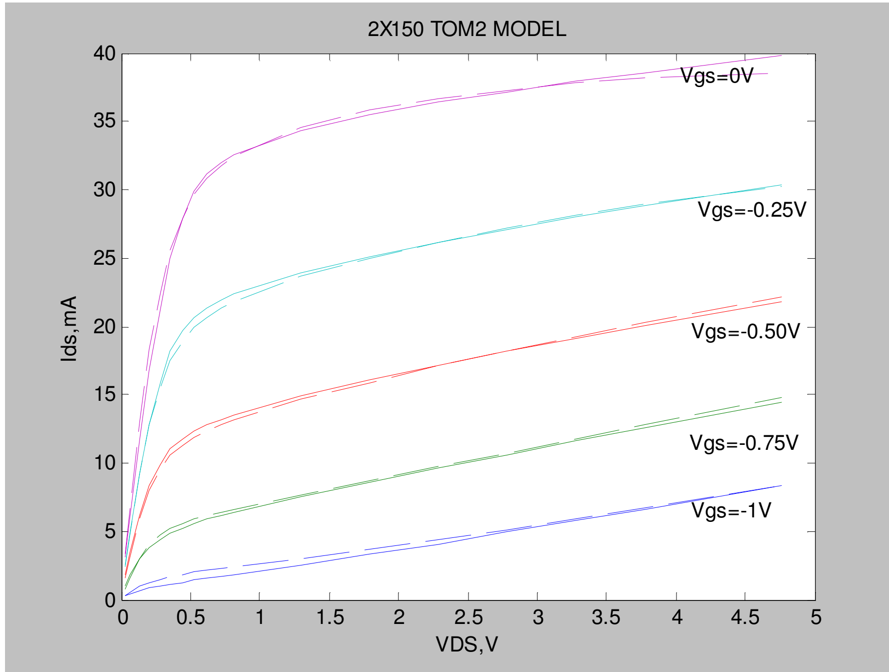

Figure 5-103 2x150 Comparison of Vds-Ids characteristics of TOM-2 Model with measured (solid lines) and theoretical values (dashed lines)

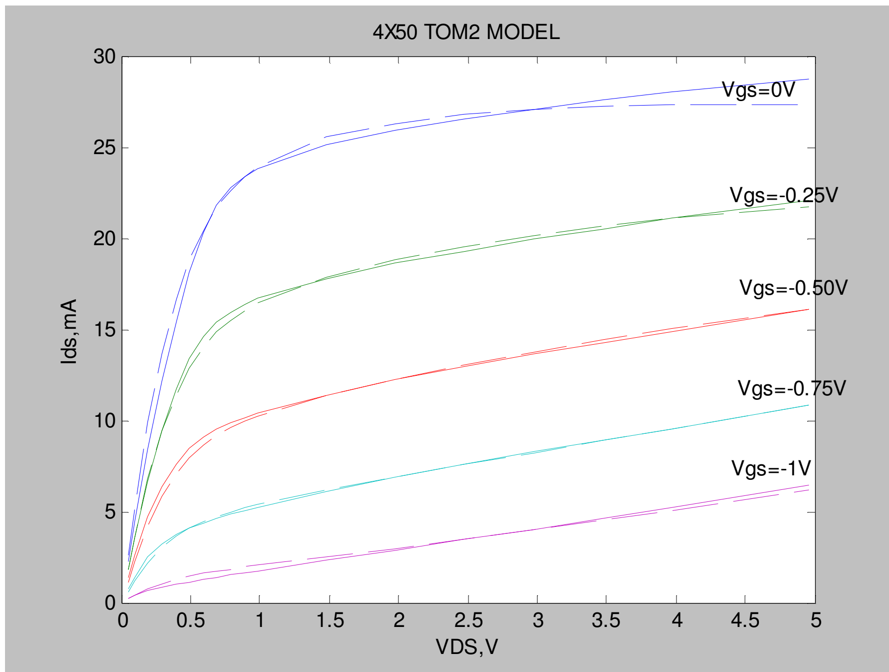

Figure 5-104 4x50 Comparison of Vds-Ids characteristics of TOM-2 Model with measured (solid lines) and theoretical values (dashed lines)

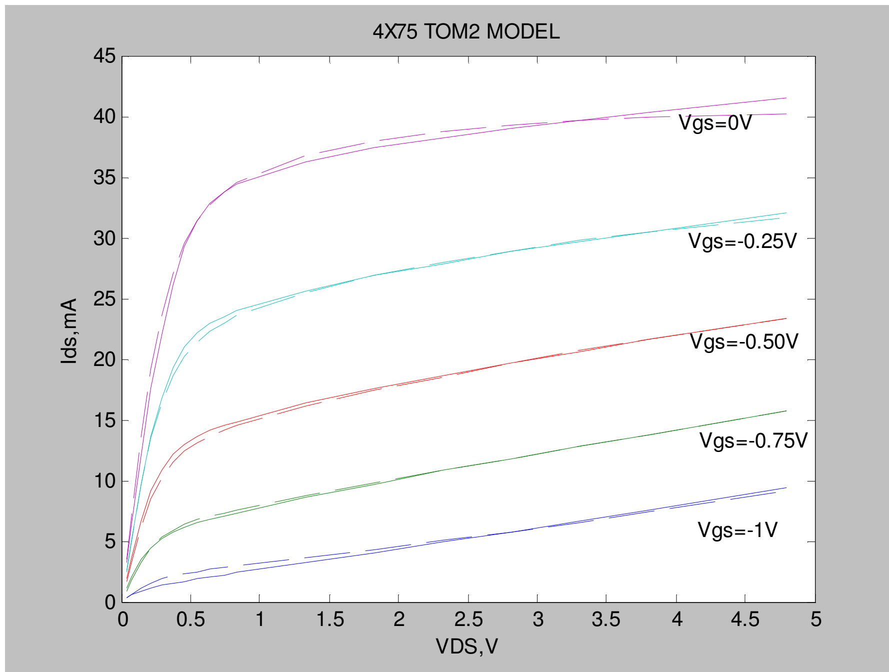

Figure 5-105 4x75 Comparison of Vds-Ids characteristics of TOM-2 Model with measured (solid lines) and theoretical values (dashed lines)

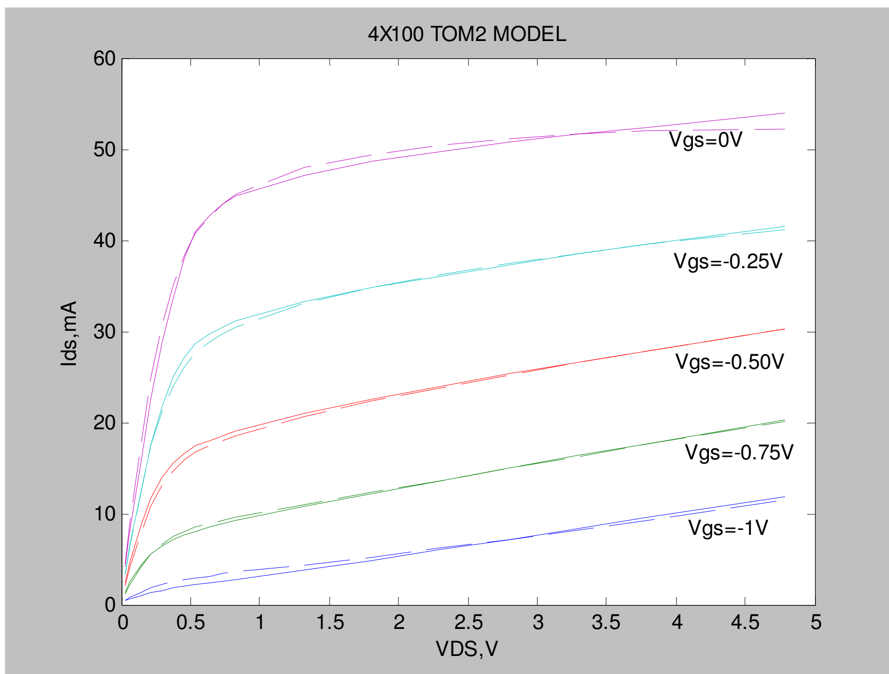

Figure 5-106 4x100 Comparison of Vds-Ids characteristics of TOM-2 Model with measured (solid lines) and theoretical values (dashed lines)

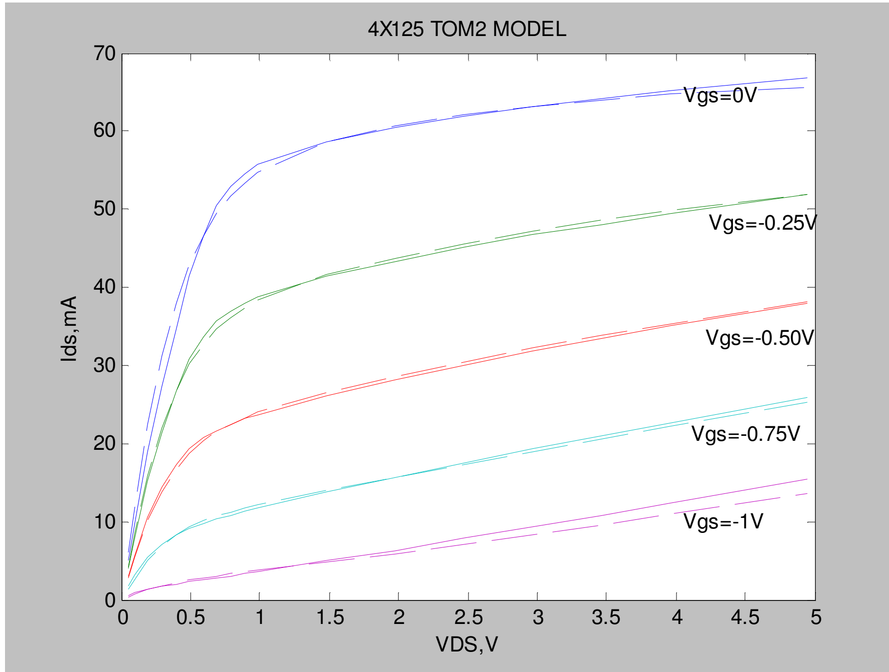

Figure 5-107 4x125 Comparison of Vds-Ids characteristics of TOM-2 Model with measured (solid lines) and theoretical values (dashed lines)

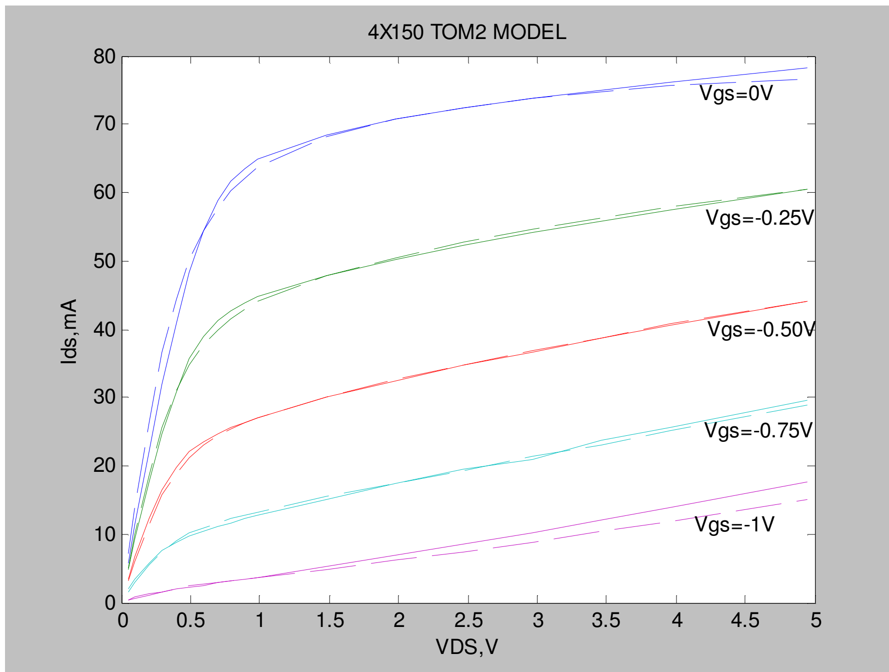

Figure 5-108 4x150 Comparison of Vds-Ids characteristics of TOM-2 Model with measured (solid lines) and theoretical values (dashed lines)

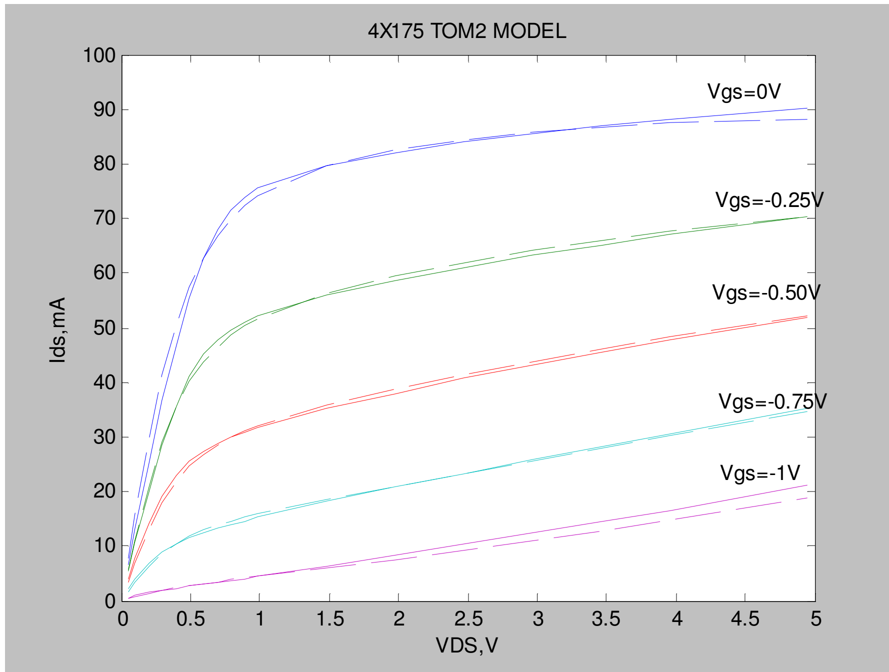

Figure 5-109 4x175 Comparison of Vds-Ids characteristics of TOM-2 Model with measured (solid lines) and theoretical values (dashed lines)

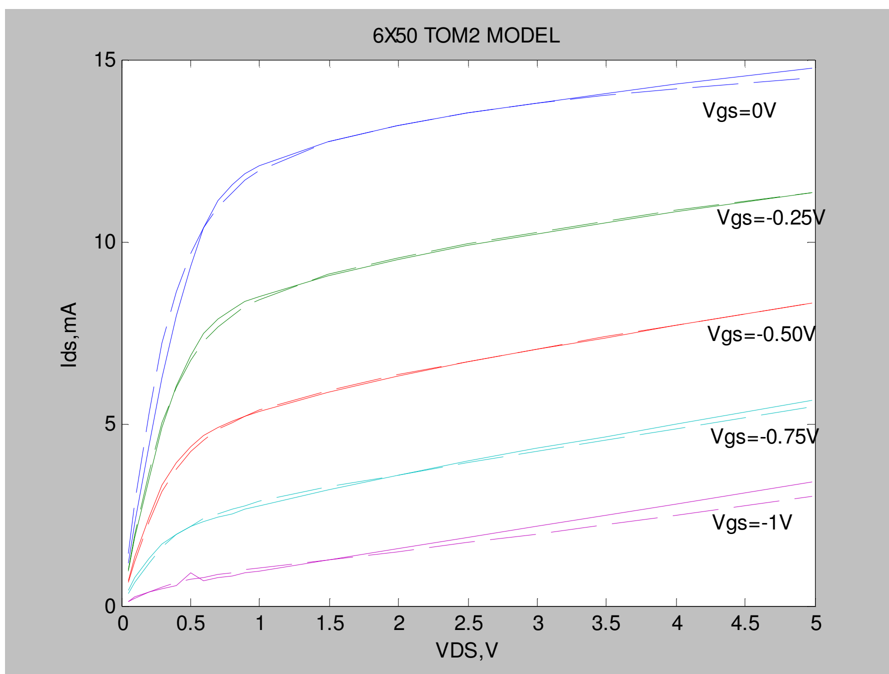

Figure 5-110 6x50 Comparison of Vds-Ids characteristics of TOM-2 Model with measured (solid lines) and theoretical values (dashed lines)

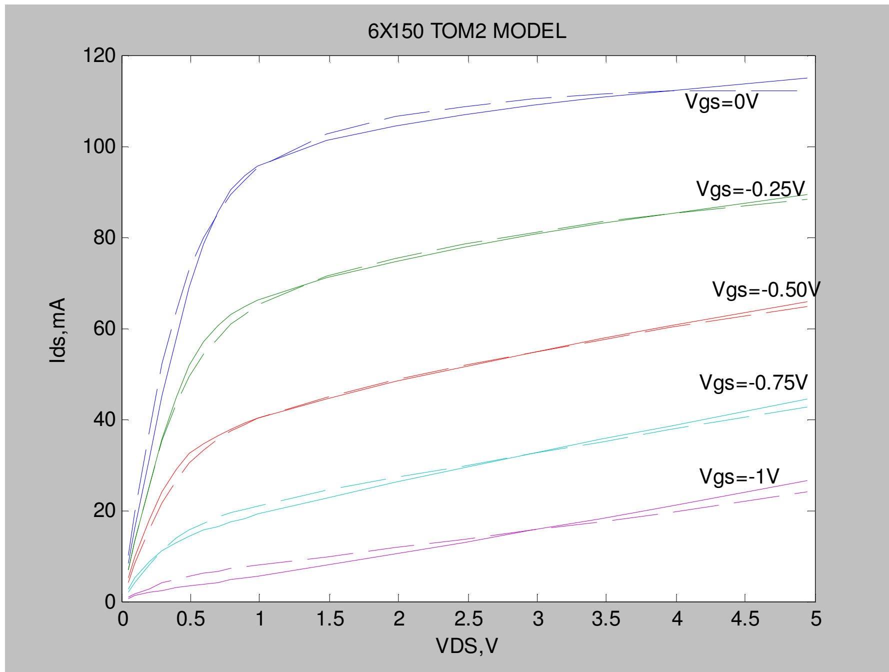

Figure 5-111 6x150 Comparison of Vds-Ids characteristics of TOM-2 Model with measured (solid lines) and theoretical values (dashed lines)

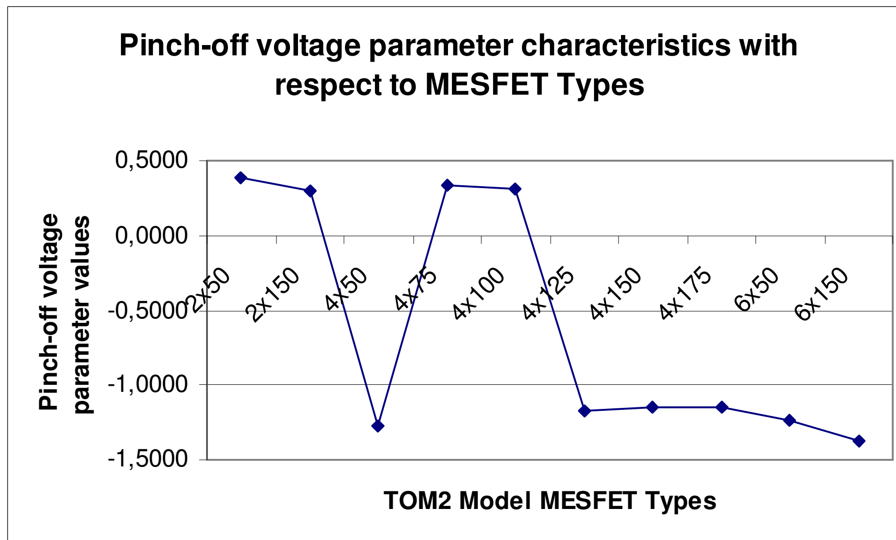

Figure 5-112 Parameter characteristics wih respect to MESFET Types

The figure represented above and the table below of results for the other parameters show that the parameters have values between some intervals, e.g. Pinch-off voltage parameter for TOM2 model differs from -1.5 to 0.5. The results are not

show the groups for MESFET types obvious, as shown in the previous models. But the groups can be distinguished with respect to parameter results.

The last model has shown that there is a big difference between the types of first and second groups. The first group includes four types of MESFETs and the results of modeled data have less accurate results than the second group.

Here are the results for the parameters.

Table 5–12 Results for TOM-2 Large Signal Model

	Q	V_{st}	V_{TO}	γ	w	β	α	δ
2x50 MESFET	2.000	-0.0387	0.3825	-0.0757	0.2214	0.0263	3.1660	3.9461
2x150 MESFET	2.000	-0.0321	0.2964	-0.0831	0.3839	0.0437	3.5956	1.6341
4x50 MESFET	2.1451	0.0196	-1.2706	0.0882	0.0353	1.1529	2.5412	1.5078
4x75 MESFET	2.000	-0.0033	-0.3355	-0.0782	-0.1334	0.1322	3.1644	1.5620
4x100 MESFET	2.000	-0.0030	-0.3126	-0.0782	-0.1445	0.1639	3.1996	1.2300
4x125 MESFET	1.7559	0.0425	-1.1726	0.0710	0.0365	1.3348	2.7835	0.8408
4x150 MESFET	1.7799	0.0152	-1.1525	0.0718	0.0302	1.9165	2.8408	0.7350
4x175 MESFET	1.7667	0.0267	-1.1499	0.0752	0.0526	1.3069	2.7236	0.7117
6x50 MESFET	1.7161	0.0104	-1.234	0.0641	0.0132	0.6701	2.5392	2.8093
6x150 MESFET	2.2770	0.0152	-1.3702	0.0735	0.0242	2.3270	2.4675	0.6309

CHAPTER 6

CONCLUSION

In this study, the primary MESFET models developed in different years of the last two decades are discussed and compared. As for a comparative analysis of the current MESFET models A. Çelebi's work carried out in year 2000 has a crucial role in this study because the MESFET measurement results obtained from his work emphasizes the primary approach in this thesis [1]. In this respect, having obtained 10 different types of MEFSET measurements, Çelebi applied all them to TOM GaAs MESFET model. Therefore, in this study 8 well-known MESFET models are compared in terms of their $I_{ds}[V_{ds}, V_{gs}]$ characteristics. By doing so, we have intended to compare those MESFET models as regard to their optimal results with the minimized errors.

Each model with different formulations and different number of parameters, defines $I_{ds}[V_{ds}, V_{gs}]$ characteristics. Within this study, the square of the difference between the modeled drain-source current $I_{ds\mathrm{mod}}$ and measured drain-source current I_{dsmeas}, is defined as the objective function. Equally, minimizing that difference value, the optimal parameters have been extracted. These parameters are the coefficients, which basically define the modeled $I_{ds\mathrm{mod}}$. What is more, these coefficients are different from one another for each model. In addition, the parameters extracted from each model, for each type, share essentially alike values excluding few exceptions.

In retrospect, as it was pointed out in chapter 5, each model has been examined specifically and hence the characteristics of $I_{ds}[V_{ds}, V_{gs}]$ have been indicated for each type. Moreover, for each model, firstly, output conductance,

g_{ds}, and transconductance, g_m, formulations have been derived and then illustrated in terms of V_{ds} and V_{gs}. The characteristics of g_{ds} and g_m for each model show similar properties for all types. Therefore each model is presented with only one graph of g_{ds} and g_m. On the other hand, the g_{ds} and g_m characterisctics shown in relevant figures, present nearly expected characteristics.

Besides, the optimization algorithm has been developed in a way that when it is run as a program on its own, it can be applied to all models and types. This algorithm is called as “program.m” and it is illustrated in Appendix-B. In this program, “fminsearch.m” tool has been utilized. “fminsearch.m” is a multidimensional unconstrained nonlinear minimization tool. It starts at an initial point and finds a local minimizer at some value of the objective function to be optimized. When the algorithm is run, MESFET model and type are initially applied as ‘input’. In this respect, each model has different numbers of parameters. For this reason, parameter values of each model are entered as vectors within the input. By taking all these input values into consideration, optimization algorithm is run and after a number of iterations, which is sufficiently high enough to minimize the difference between the modelled I_{ds} characteristics and measured I_{ds} data. Then, the modelled I_{ds} characteristics are illustrated along with measured I_{ds} data as output within the same graph. Finally, the optimal parameter values for the modelled I_{ds} characteristic, are presented as output.

On the other hand, during the optimization process, which is mentioned above, some problems appeared which is worth of mentioning here: One of the problems encountered during the optimization procedure is about the accuracy of I_{ds} with respect to measured values. The obtained I_{ds} values were not in accordance with some types of MESFETs for each model. This problem occurred specifically, for the types of 2x50, 2x150, 4x75 and 4x100µm in comparison to the other types.

Within the optimization process of these models, the results obtained in relation to initial parameter values, did not match with the expected measured values. Under normal circumstances, all model parameters were taken initially as “1.0”. However, these initially entered parameters do not give good

approximations for modeled data with measured data. Therefore, initial parameter values were exchanged with some random values. Because of this fact we dealt with the matter in some different ways. In this respect, first of all, “fminunc.m” tool, which is an unconstrained optimization tool just like fminsearch, was applied. “Fminunc” finds the minimum of a function of several variables, starts at defined initial values and finds a minimum of a function.” Even though the similar results with fminsearch were obtained when “fminunc.m” tool was applied; it took too much computer time to finalize the optimization process. Consequently, in this study fminsearch was regarded as a better means for the optimization process.

Furthermore, with Prof. Dr. Gönül Turhan Sayan’s supervisory guidance Genetic Algorithm code (GAcode) as an alternate optimization algorithm was developed and adopted with MESFET modeling algorithm. It is illustrated in the Appendix-B as “mesgencode” within the framework of MESFET Genetic Algorithm. The primary facility of this alternate algorithm is that, it lets each initially determined parameter to be defined in some definite intervals. In other words, when the Genetic Algorithm is run, each parameter is defined initially in certain intervals and as a result of these intervals the optimal values for each parameter are extracted through which the optimization process is accomplished.

The number of the iterations in Genetic Algorithm is determined by the user. In this sense, according to the number of iterations and the dimensions of the intervals the algorithm parameter values are obtained more accurately. In other words, the larger the range of the interval dimensions and the iteration are, the better the values become. However, it is necessary to emphasize that when compared to MESFET model code “program.m” (including fminsearch tool), the Genetic Algorithm code takes too much computer time to be accomplished. Hence, it was used only when the optimization did not come up with proper results.Therefore, it was run only when we come across with initial parameter problems.

To sum up, when the results are viewed altogether, one observes that each model leads to optimal results for different V_{gs} values. As for some V_{gs} values optimization could not be achieved. At this point, for example if the Curtice model (includes 4 parameters) is taken into account, the I_{ds} values for $V_{gs} = 0V$

deviated from the normal conditions when the V_{ds} voltage exceeds 2 volt. On the other hand, until the V_{ds} values reach at the 2 volt they seemed to keep their stances close to measured data. In addition, for $V_{gs} = -0.25V$ in Curtice model, modelled data, in any type, is close to measured data for all values of drain-source voltage. As for the other V_{gs} values the results presents nearly similar properties as for $V_{gs} = 0V$, some deviations occur after exceeding certain values.

Tajima model (includes 8 parameters) results for all types have been plotted in Chapter-5. The results constitute two groups of MESFET types, one includes 4 types of MESFET and the other one includes 6 types of MESFET. These two groups can be distinguished with respect to the parameter results and the model optimization with measured data. The latter one of the two groups has more accurate results than the former one. Therefore the latter one has good approximations if compared with the other models, for the same types of MESFETs.

Materka&Kacprzak Model (includes 4 parameters) shows nearly same characteristics with Tajima Model, but the accuracy is lesser than the Tajima Model. The groups can be easily determined for all MESFET types. For the second group of types the current deviates a little at $V_{gs} = 0V$ and at $V_{gs} = -1.0V$. The first group of MESFET types have nearly good approximations of current only at $V_{gs} = -0.25V$.

Curtice&Ettenberg Model (includes 7 parameters) have similar characteristics with Materka&Kacprzak Model. If all types are taken into account, the results will represent that the model can be divided into two groups, as described previously. For the first group the results are optimized better only for $V_{gs} = 0V$ and $V_{gs} = -0.25V$. Besides for the second group the results are optimized more accurately except for $V_{gs} = 0V$, at this voltage level the modeled current deviates from the measured data with small errors.

Statz Model (includes 5 parameters) results are not as accurate as the other models. The comparison with other models showed that the accuracy is not satisfied for the first group of MESFET types. For the second group of MESFET types the

only accuracy is satisfied for $V_{gs} = -0.25V$.

TriQuint's Own Model (includes 6 parameters), in literature, is mostly discussed model. The results are optimized more accurately than the other models discussed before if all types of MESFET results are taken into account. However the results do not satisfy the measured data accurately. The model can be divided into two groups, as discussed previously. The second group of MESFET types is approximated to measured data more accurately than the first group.

Angelov Model (includes 8 parameters) results show that the MESFET types are divided into two groups with respect to the accuracy of optimized data to measured data. The second group optimizes to measured data more accurately than the first group. For the second group the accuracy deviates at $V_{gs} = -0.75V$ and $V_{gs} = -1.0V$. Besides the first group has good approximation only at $V_{gs} = -0.25V$.

The last model for this study, TriQuint's Own Model-2 (includes 8 parameters), have two groups of MESFET types characterizing the model. As compared with the other models, TOM-2 shows the most accuracy to the measured data. If all types of MESFET and the consumed computer time for each model are considered, it can be said taht the TOM-2 Large Signal MESFET Model has the best representation among the others.

A full large-signal model requires the inclusion of the other elements of the large-signal model such as C_{gs} and C_{gd}. Therefore, the work can be extended to the other elements of the models provided that the relevant measurements are done.

For future studies, to obtain good approximation of I-V characteristics, one should take the measured data for more types of MESFETs. The modeled function can be approximated to the measured data or the objective function can be minimized by considering the saturation points of I_{ds} current accurately at each V_{gs} voltage level seperately. This saturation point may help the searcher to divide the I_{ds} function into two parts with respect to V_{ds} voltage, one for V_{ds} voltage of below saturation point and the other for above.

As described in chapter 5, some workers assumed or described V_{ds} voltage at this saturation point as $3/\alpha$. And they defined I_{ds} characteristics with respect to V_{ds} of below $3/\alpha$ and above. But α represents a constant value for a type of MESFET, therefore $3/\alpha$ also represents a constant value, this means that the saturation point is same for all V_{gs} values. Actually this is not true as can be seen in the graphs. If the saturation point can be defined and formulated accurately, this will definitely lead to better optimization results.

REFERENCES

[1] Abdullah Çelebi, "Extraction and Scaling of TOM Model Parameters of GaAs MESFETs," M.Sc. Thesis, METU, August 2000

[2] Matlab 7 Guide

[3] Walter R. Curtice, "A MESFET model for use in the design of GaAs integrated circuits," IEEE Trans. Mirowave Theory and Tech., vol. MTT-28, pp. 448-456, May 1980

[4] W. R. Curtice and R. L. Camisa, "Self-consistent GaAs FET models for amplifier design and device diagnostics," IEEE Trans. Mirowave Theory and Tech., vol.MTT-32, pp.1573-1578, Dec. 1984

[5] Walter R. Curtice, "GaAs MESFET Modeling and Nonlinear CAD," IEEE Trans. Mirowave Theory and Tech., vol. 28, pp. 220-230, Feb. 1980

[6] J. A Nelder and R. Mead, "A Simplex Method for function minimization," Computer Journal 7 pp. 308-313, 1965

[7] Y. Tajima, B. Wrona, and K. Mishima, "GaAs FET Large-Signal Model and its Application to Circuit Designs," IEEE Transactions on Electron Devices, vol. ED-28, pp. 171-175, Feb. 1981

[8] A. Materka and T. Kacprzak, "Computer Calculation of Large-Signal GaAs FET Amplifier Characteristics," IEEE Trans. Microwave Theory and Tech., vol.MTT-33, pp. 129-135, Feb. 1985

[9] T. Kacprzak and A. Materka, "Compact dc model of GaAs FET's for large-signal computer calculation," IEEE J. Solid-State Circuits, vol. SC-18, pp. 211–213, Apr. 1983.

[10] H. Statz, P. Newman, I. Smith, R. Pucel, and H.Haus, "GaAs FET Device and Circuit Simulatin in Spice," IEEE Trans. Electron Devices, Vol. ED-34, pp. 160-169, 1987

[11] A. J. McCamant, G. D. McCormack, and D. H. Smith, "An Improved MESFET Model for Spice," IEEE Transactions on Microwave Theory and Techniques, Vol. 38, pp. 822-824, June 1990

[12] W. R. Curtice and M. Ettenberg, "A Nonlinear GaAs FET Model for Use in the Design of Output Circuits for Power Amplifiers," IEEE Transactions on Microwave Theory and Techniques, Vol. MTT-33, pp.1383-1393, Dec. 1985

[13] David H. Smith, “TOM-2: An Improved Model for GaAs MESFETs,” TriQuint Semiconductor, Inc., TriQuint Properietary-3, Feb. 1995

[14] I. Angelov, H. Zirath, and N. Rorsman, “a New Empirical Nonlinear Model for HEMT and MESFET Devices,” IEE Transactions on Microwave Theory and Techniques, Vol. 40, Dec. 1992

[15] R. Cumhur Kasımcan, “Evaluation of DC Parameters of MESFET TOM Equivalent Circuit,” M.Sc. Thesis, METU, September 1999

[16] Charles A. Liechti “Microwave Field-Effect Transistors” IEEE Transactions on Microwave Theory and Techniques, Vol. MTT-24, No. 6, June 1976, pp. 279-300

[17] J. M. Golio, “Microwave MESFETs and HEMTs” Artech House, Boston – London

[18] Y. A. Khalaf, “Systematic Optimization Technique for MESFET Modeling” Ph.D. Dissertation, Faculty of the Virginia Polytechnic Institute and State University, July, 2000

[19] S. Y Liao, “Micowave Devices and Circuits” Prentice Hall, Englewood Cliffs, New Jersey, 1990

[20] I. Yüksel, “MATLAB ile Mühendislik Sistemlerinin Analizi ve Çözümü,” Uludağ Üniversitesi, Bursa, 1996

[21] T. Taki, “Approximation of Junction Field-effect Transistor Characteristics by a hyperbolic function,” IEEE J. Solid-State Circuits, vol.SC-13, pp. 724-726, Oct. 1978.

APPENDIX A

RESULTS OF DC I-V MEASUREMENTS

A-1 V_{ds}- I_{ds} data of 2x50 MESFET [1]

2x50	I_d , mA				
V_{ds}, V	V_{gs}=0V	V_{gs}=-0.25V	V_{gs}=-0.5V	V_{gs}=-0.75V	V_{gs}=-1.0V
0.05	1.16	0.94	0.69	0.40	0.13
0.1	2.27	1.87	1.34	0.76	0.23
0.2	4.39	3.48	2.43	1.29	0.36
0.3	6.27	4.88	3.30	1.67	0.46
0.4	7.96	6.03	3.94	1.94	0.54
0.5	9.32	6.88	4.38	2.15	0.62
0.6	10.39	7.48	4.68	2.30	0.68
0.7	11.11	7.86	4.90	2.43	0.76
0.8	11.57	8.13	5.07	2.54	0.82
0.9	11.88	8.34	5.21	2.65	0.88
1.0	12.10	8.50	5.34	2.75	0.94
1.5	12.76	9.07	5.86	3.19	1.24
2.0	13.17	9.50	6.29	3.59	1.55
2.5	13.51	9.87	6.67	3.96	1.85
3.0	13.80	10.20	7.03	4.31	2.16
3.5	14.06	10.50	7.36	4.64	2.47
4.0	14.32	10.79	7.68	4.97	2.78
5.0	14.75	11.33	8.30	5.62	3.40

A-2 V_{ds}- I_{ds} data for 2x150 MESFET [1]

2x150	I_d, mA				
V_{ds}, V	V_{gs}=0V	V_{gs}=-0.25V	V_{gs}=-0.5V	V_{gs}=-0.75V	V_{gs}=-1.0V
0.05	3.06	2.50	1.78	0.96	0.24
0.1	6.06	4.82	3.42	1.78	0.40
0.2	11.69	9.18	6.19	2.98	0.64
0.3	16.77	12.81	8.34	3.83	0.83
0.4	21.19	15.80	9.92	4.43	0.99
0.5	24.99	18.13	11.00	4.89	1.13
0.6	27.90	19.68	11.75	5.23	1.27
0.7	29.88	20.69	12.31	5.56	1.42
0.8	31.13	21.40	12.75	5.85	1.56
0.9	31.99	21.95	13.14	6.12	1.69
1.0	32.60	22.38	13.48	6.38	1.84
1.5	34.36	23.95	14.87	7.50	2.55
2.0	35.46	25.13	16.04	8.62	3.29
2.5	36.38	26.16	17.14	9.63	4.09
3.0	37.18	27.10	18.16	10.64	4.92
3.5	37.90	27.98	19.12	11.62	5.77
4.0	38.55	28.80	20.08	12.58	6.63
5.0	39.80	30.33	21.85	14.41	8.37

A-3 V_{ds}- I_{ds} data for 4x50 MESFET [1]

4x50	I_d, mA				
V_{ds}, V	V_{gs}=0V	V_{gs}=-0.25V	V_{gs}=-0.5V	V_{gs}=-0.75V	V_{gs}=-1.0V
0.05	2.24	1.80	1.34	0.78	0.24
0.1	4.42	3.54	2.57	1.40	0.42
0.2	8.42	6.66	4.70	2.48	0.67
0.3	12.12	9.45	6.35	3.18	0.85
0.4	15.38	11.68	7.63	3.71	1.00
0.5	18.11	13.39	8.49	4.08	1.14
0.6	20.30	14.60	9.09	4.38	1.27
0.7	21.77	15.40	9.53	4.63	1.39
0.8	22.72	15.95	9.87	4.86	1.51
0.9	23.36	16.34	10.13	5.06	1.62
1.0	23.82	16.67	10.39	5.25	1.73
1.5	25.10	17.78	11.38	6.10	2.31
2.0	25.90	18.60	12.22	6.86	2.87
2.5	26.54	19.29	12.93	7.57	3.45
3.0	27.08	19.95	13.64	8.28	4.03
3.5	27.56	20.52	14.28	8.91	4.62
4.0	28.01	21.08	14.90	9.55	5.20
5.0	28.77	22.08	16.09	10.82	6.44

A-4 V_{ds}- I_{ds} data for 4x75 MESFET [1]

4x75	**I_d , mA**				
V_{ds}, V	**V_{gs}=0V**	**V_{gs}=-0.25V**	**V_{gs}=-0.5V**	**V_{gs}=-0.75V**	**V_{gs}=-1.0V**
0.05	3.18	2.6	1.92	1.09	0.32
0.1	6.32	5.12	3.68	2.01	0.56
0.2	12.1	9.64	6.67	3.45	0.9
0.3	17.52	13.58	9.12	4.44	1.13
0.4	22.09	16.76	10.91	5.16	1.34
0.5	26.07	19.3	12.12	5.67	1.53
0.6	29.22	21.03	12.95	6.09	1.71
0.7	31.39	22.16	13.59	6.45	1.88
0.8	32.8	22.96	14.08	6.78	2.04
0.9	33.73	23.55	14.49	7.07	2.21
1.0	34.39	24.02	14.86	7.35	2.43
1.5	36.23	25.65	16.33	8.58	3.21
2.0	37.38	26.86	17.54	9.72	4.05
2.5	38.25	27.89	18.65	10.8	4.91
3.0	39.03	28.82	19.68	11.82	5.78
3.5	39.71	29.69	20.64	12.82	6.67
4.0	40.33	30.51	21.58	13.79	7.56
5.0	41.49	31.98	23.35	15.67	9.36

A-5 V_{ds}- I_{ds} data for 4x100 MESFET [1]

4x100	**I_d , mA**				
V_{ds}, V	**V_{gs}=0V**	**V_{gs}=-0.25V**	**V_{gs}=-0.5V**	**V_{gs}=-0.75V**	**V_{gs}=-1.0V**
0.05	4.11	3.32	2.45	1.37	0.37
0.1	8.08	6.60	4.70	2.54	0.64
0.2	15.68	12.43	8.65	4.32	1.01
0.3	22.48	17.40	11.69	5.54	1.28
0.4	28.63	21.63	13.91	6.42	1.55
0.5	33.66	24.92	15.53	7.09	1.77
0.6	37.91	27.17	16.57	7.61	1.98
0.7	40.90	28.67	17.37	8.06	2.18
0.8	42.70	29.69	17.99	8.48	2.39
0.9	43.93	30.45	18.52	8.86	2.60
1.0	44.78	31.08	19.00	9.19	2.79
1.5	47.18	33.17	20.90	10.80	3.83
2.0	48.63	34.74	22.49	12.26	4.89
2.5	49.78	36.10	23.94	13.67	6.00
3.0	50.78	37.33	25.30	15.04	7.15
3.5	51.63	38.45	26.60	16.37	8.33
4.0	52.43	39.51	27.83	17.68	9.50
5.0	53.88	41.46	30.20	20.18	11.90

A-6 V_{ds}- I_{ds} data for 4x125 MESFET [1]

4x125	I_d , mA				
V_{ds}, V	V_{gs}=0V	V_{gs}=-0.25V	V_{gs}=-0.5V	V_{gs}=-0.75V	V_{gs}=-1.0V
0.05	4.97	4.08	2.98	1.73	0.48
0.1	9.82	7.97	5.73	3.20	0.83
0.2	18.88	15.21	10.62	5.47	1.29
0.3	27.33	21.47	14.45	7.06	1.67
0.4	34.78	26.70	17.28	8.19	1.97
0.5	41.37	30.81	19.31	9.01	2.26
0.6	46.63	33.75	20.70	9.69	2.53
0.7	50.40	35.68	21.67	10.27	2.78
0.8	52.90	37.01	22.49	10.79	3.06
0.9	54.53	37.98	23.17	11.28	3.32
1.0	55.68	38.76	13.74	11.74	3.59
1.5	58.71	41.43	26.18	13.81	4.93
2.0	60.52	43.39	28.22	15.70	6.32
2.5	61.95	45.11	30.08	17.51	7.79
3.0	63.17	46.69	31.85	19.25	9.30
3.5	64.24	48.08	33.47	20.98	10.81
4.0	65.18	49.44	35.09	22.65	12.35
5.0	66.78	51.89	38.04	25.85	15.45

A-7 V_{ds}- I_{ds} data for 4x150 MESFET [1]

4x150	I_d , mA				
V_{ds}, V	V_{gs}=0V	V_{gs}=-0.25V	V_{gs}=-0.5V	V_{gs}=-0.75V	V_{gs}=-1.0V
0.05	5.81	4.72	3.48	1.89	0.46
0.1	11.44	9.21	6.62	3.45	0.79
0.2	22.14	17.60	12.22	5.82	1.26
0.3	31.85	24.77	16.54	7.56	1.63
0.4	40.75	30.87	19.75	8.76	1.95
0.5	48.28	35.63	21.99	9.68	2.26
0.6	54.44	38.99	23.52	10.40	2.55
0.7	58.90	41.19	24.70	11.09	2.83
0.8	61.73	42.70	25.62	11.68	3.12
0.9	63.61	43.85	26.40	12.20	3.42
1.0	64.95	44.76	27.11	12.78	3.71
1.5	68.53	47.90	29.98	15.19	5.22
2.0	70.65	50.28	32.41	17.40	6.83
2.5	72.34	52.33	34.62	19.55	8.50
3.0	73.78	54.17	36.69	21.64	10.28
3.5	75.00	55.88	38.69	23.68	12.02
4.0	76.13	57.49	40.58	25.69	13.90
5.0	78.19	60.41	44.20	29.56	17.58

A-8 V_{ds}- I_{ds} data for 4x175 MESFET [1]

4x175	I_d, mA				
V_{ds}, V	V_{gs}=0V	V_{gs}=-0.25V	V_{gs}=-0.5V	V_{gs}=-0.75V	V_{gs}=-1.0V
0.05	6.63	5.43	4.00	2.22	0.54
0.1	13.08	10.60	7.69	4.08	0.93
0.2	25.20	20.17	14.06	6.95	1.48
0.3	36.58	28.50	19.11	8.95	1.91
0.4	46.78	35.58	22.88	10.40	2.28
0.5	55.53	41.16	25.58	11.50	2.66
0.6	62.70	45.20	27.44	12.40	3.02
0.7	68.08	47.83	28.80	13.20	3.37
0.8	71.54	49.65	29.92	13.93	3.72
0.9	73.84	50.99	30.85	14.60	4.06
1.0	75.44	52.09	31.72	15.21	4.43
1.5	79.71	55.85	35.15	17.14	6.25
2.0	82.16	58.67	38.00	20.79	8.19
2.5	84.10	61.05	40.66	23.30	10.24
3.0	85.66	63.17	43.12	25.77	12.37
3.5	86.99	65.15	45.46	28.23	14.50
4.0	88.20	66.98	47.67	30.63	16.66
5.0	90.29	70.33	52.03	35.20	21.19

A-9 V_{ds}- I_{ds} data for 6x50 MESFET [1]

6x50	I_d, mA				
V_{ds}, V	V_{gs}=0V	V_{gs}=-0.25V	V_{gs}=-0.5V	V_{gs}=-0.75V	V_{gs}=-1.0V
0.05	3.28	2.69	2.00	1.18	0.38
0.1	6.52	5.25	3.86	2.19	0.66
0.2	12.47	9.98	7.11	3.77	1.06
0.3	17.99	14.08	9.63	4.90	1.34
0.4	22.83	17.52	11.56	5.70	1.59
0.5	27.03	20.23	12.91	6.28	1.81
0.6	30.35	22.09	13.84	6.73	2.02
0.7	32.69	23.32	14.53	7.12	2.21
0.8	34.20	24.17	15.01	7.46	2.39
0.9	35.19	24.78	15.45	7.77	2.57
1.0	35.90	25.27	15.82	8.06	2.74
1.5	37.80	26.94	17.32	9.36	3.64
2.0	38.95	28.16	18.56	10.52	4.53
2.5	39.86	29.20	19.66	11.61	5.43
3.0	40.65	30.14	20.71	12.64	6.34
3.5	41.33	31.02	21.68	13.65	7.25
4.0	41.99	31.82	22.61	14.61	8.16
5.0	43.16	33.29	24.38	16.53	10.02

A-10 V_{ds}- I_{ds} data for 6x150 MESFET [1]

6x150	I_d, mA				
V_{ds}, V	**V_{gs}=0V**	**V_{gs}=-0.25V**	**V_{gs}=-0.5V**	**V_{gs}=-0.75V**	**V_{gs}=-1.0V**
0.05	8.15	6.74	4.99	2.75	0.68
0.1	16.05	13.19	9.62	5.09	1.16
0.2	31.09	25.24	17.75	8.62	1.84
0.3	45.19	35.67	24.08	11.12	2.38
0.4	57.83	44.68	28.95	12.93	2.87
0.5	69.08	51.87	32.30	14.31	3.32
0.6	78.47	57.11	34.70	15.45	3.76
0.7	85.46	60.63	36.47	16.44	4.20
0.8	90.43	63.06	37.88	17.34	4.63
0.9	93.54	64.80	39.08	18.19	5.07
1.0	95.70	66.20	40.14	18.98	5.50
1.5	101.33	71.04	44.51	22.62	7.78
2.0	104.50	74.59	48.13	25.99	10.21
2.5	106.94	77.62	51.48	29.24	12.75
3.0	108.97	80.40	54.62	32.39	15.44
3.5	110.72	82.86	57.57	35.48	18.14
4.0	112.26	85.20	60.41	38.53	20.94
5.0	115.01	89.44	65.78	44.34	26.56

APPENDIX B

MATLAB SCRIPTS

B.1 “program.m”

```
format long
global model type IDS IDSMEAS Vdsintrinsic Vgsintrinsic min IDN IDM gm gds Idso Vt

%The aim of this program is to compare the models, which are described by
%formulas and parameters,with the measured data.
%The parameters are obtained by using an optimization algorithm that minimizes
%the difference between modeled(or described by formulation) Ids and measured Ids data.
%There are 8 different models and 10 different types of MESFETs exist.
%The algorithm needs the MESFET type, MESFET model and because of the model the initial
%parameter values:

disp('1 for 2x50')
disp('2 for 2x150')
disp('3 for 4x50')
disp('4 for 4x75')
disp('5 for 4x100')
disp('6 for 4x125')
disp('7 for 4x150')
disp('8 for 4x175')
disp('9 for 6x50')
disp('10 for 6x150')
disp('EACH NUMBER REFERS TO A MESFET TYPE')
disp('ENTER THE NUMBER FOR THE TYPE OF THE MESFET STRUCTURE:')
type=input('TYPE=')
disp('CURTICE MODEL(4 PARAMETERS)=1')
disp('MATERKA&KACPRZAK MODEL(4 PARAMETERS)=2')
disp('TOM-2 MODEL(8 PARAMETERS)=3')
disp('CURTICE-ETTENBERG MODEL (7 PARAMETERS) =4')
disp('TAJIMA MODEL(8 PARAMETERS)=5')
disp('TOM MODEL( 4 PARAMETERS )=6')
disp('STATZ MODEL( 5 PARAMETERS )=7')
disp('ANGELOV MODEL(8 PARAMETERS)=8')
disp('EACH MODEL INCLUDES DIFFERENT NUMBER OF PARAMETERS')
model=input('ENTER THE NUMBER FOR MODEL=');
disp('ENTER THE INITIAL PARAMETER VALUES AS A VECTOR BELOW ')
if model==1
 %CURTICE MODEL, model=1
    disp('CURTICE MODEL CONSISTS OF 4 DIFFERENT PARAMETERS')
    x0=input('ENTER THE INITIAL PARAMETERS AS A 1x4 VECTOR=')

 elseif model==2
```

```
   %MATERKA&KACPRZAKmodel; model=2
    disp('MATERKA&KACPRZAK MODEL CONSISTS OF 4 DIFFERENT PARAMETERS')
    x0=input('ENTER THE INITIAL PARAMETERS AS A 1x4 VECTOR=')

elseif model==3
   %tom2model;
    disp('TOM-2 MODEL CONSISTS OF 8 DIFFERENT PARAMETERS')
    x0=input('ENTER THE INITIAL PARAMETERS AS A 1x8 VECTOR=')

elseif model==4
   %curticeettenbergmodel;
    disp('CURTICE&ETTENBERG MODEL CONSISTS OF 7 DIFFERENT PARAMETERS')
    x0=input('ENTER THE INITIAL PARAMETERS AS A 1x7 VECTOR=')

elseif model==5
   %tajimamodel;
    disp('TAJIMA MODEL CONSISTS OF 8 DIFFERENT PARAMETERS')
    x0=input('ENTER THE INITIAL PARAMETERS AS A 1x8 VECTOR=')

elseif model==6
   %Tommodel;
    disp('TOM MODEL CONSISTS OF 6 DIFFERENT PARAMETERS')
    x0=input('ENTER THE INITIAL PARAMETERS AS A 1x6 VECTOR=')

 elseif model==7
   %statzmodel;
    disp('STATZ MODEL CONSISTS OF 5 DIFFERENT PARAMETERS')
    x0=input('ENTER THE INITIAL PARAMETERS AS A 1x5 VECTOR=')

elseif model==8
   %Angelov Model
   disp('ANGELOV MODEL CONSISTS OF 8 DIFFERENT PARAMETERS')
    x0=input('ENTER THE INITIAL PARAMETERS AS A 1x8 VECTOR=')
end
options = optimset('MaxFunEvals',10^8,'MaxIter',10^8,'TolX',1e-14,'TolFun',1e-14);
[x,fval,exitflag,output]=fminsearch('modelling',x0,options);
%options = optimset('GradConstr','on','MaxFunEvals',10^7,'MaxIter',10^7,'TolX',1e-10,'TolFun',1e-
10);
%[x,fval,exitflag,output]=fminunc('modelling',x0,options);
figure;
plot(Vdsintrinsic,IDSMEAS*1000)
hold on
plot(Vdsintrinsic,IDS*1000,'--')
hold on
if model==1
      %CURTICE MODEL
      hold on
      xlabel('VDS,V')
      ylabel('Ids,mA')
      hold on
   if type==1
      title('2X50 CURTICE MODEL')
      elseif type==2
      title('2X150 CURTICE MODEL')
      elseif type==3
      title('4X50 CURTICE MODEL')
      elseif type==4
      title('4X75 CURTICE MODEL')
      elseif type==5
      title('4X100 CURTICE MODEL')
```

```
      elseif type==6
      title('4X125 CURTICE MODEL')
      elseif type==7
      title('4X150 CURTICE MODEL')
      elseif type==8
      title('4X175 CURTICE MODEL')
      elseif type==9
      title('6X50 CURTICE MODEL')
      elseif type==10
      title('6X150 CURTICE MODEL')
    end
      gtext('Vgs=0V')
      gtext('Vgs=-0.25V')
      gtext('Vgs=-0.50V')
      gtext('Vgs=-0.75V')
      gtext('Vgs=-1V')
elseif model==2
      %MATERKA&KACPRZAKmodel;
      hold on
      xlabel('VDS,V')
      ylabel('Ids,mA')
      hold on
    if type==1
      title('2X50 MATERKA&KACPRZAK MODEL')
      elseif type==2
      title('2X150 MATERKA&KACPRZAK MODEL')
      elseif type==3
      title('4X50 MATERKA&KACPRZAK MODEL')
      elseif type==4
      title('4X75 MATERKA&KACPRZAK MODEL')
      elseif type==5
      title('4X100 MATERKA&KACPRZAK MODEL')
      elseif type==6
      title('4X125 MATERKA&KACPRZAK MODEL')
      elseif type==7
      title('4X150 MATERKA&KACPRZAK MODEL')
      elseif type==8
      title('4X175 MATERKA&KACPRZAK MODEL')
      elseif type==9
      title('6X50 MATERKA&KACPRZAK MODEL')
      elseif type==10
      title('6X150 MATERKA&KACPRZAK MODEL')
    end
    gtext('Vgs=0V')
    gtext('Vgs=-0.25V')
    gtext('Vgs=-0.50V')
    gtext('Vgs=-0.75V')
    gtext('Vgs=-1V')
elseif model==3
      %tom2model;
      hold on
      xlabel('VDS,V')
      ylabel('Ids,mA')
      hold on
    if type==1
      title('2X50 TOM2 MODEL')
      elseif type==2
      title('2X150 TOM2 MODEL')
      elseif type==3
      title('4X50 TOM2 MODEL')
```

```
      elseif type==4
      title('4X75 TOM2 MODEL')
      elseif type==5
      title('4X100 TOM2 MODEL')
      elseif type==6
      title('4X125 TOM2 MODEL')
      elseif type==7
      title('4X150 TOM2 MODEL')
      elseif type==8
      title('4X175 TOM2 MODEL')
      elseif type==9
      title('6X50 TOM2 MODEL')
      elseif type==10
      title('6X150 TOM2 MODEL')
    end
    gtext('Vgs=0V')
    gtext('Vgs=-0.25V')
    gtext('Vgs=-0.50V')
    gtext('Vgs=-0.75V')
    gtext('Vgs=-1V')
  elseif model==4
    %curticeettenbergmodel;
    hold on
    xlabel('VDS,V')
    ylabel('Ids,mA')
    hold on
    if type==1
      title('2X50 CURTICE-ETTENBERG MODEL')
      elseif type==2
      title('2X150 CURTICE-ETTENBERG MODEL')
      elseif type==3
      title('4X50 CURTICE-ETTENBERG MODEL')
      elseif type==4
      title('4X75 CURTICE-ETTENBERG MODEL')
      elseif type==5
      title('4X100 CURTICE-ETTENBERG MODEL')
      elseif type==6
      title('4X125 CURTICE-ETTENBERG MODEL')
      elseif type==7
      title('4X150 CURTICE-ETTENBERG MODEL')
      elseif type==8
      title('4X175 CURTICE-ETTENBERG MODEL')
      elseif type==9
      title('6X50 CURTICE-ETTENBERG MODEL')
      elseif type==10
      title('6X150 CURTICE-ETTENBERG MODEL')
    end
    gtext('Vgs=0V')
    gtext('Vgs=-0.25V')
    gtext('Vgs=-0.50V')
    gtext('Vgs=-0.75V')
    gtext('Vgs=-1V')
  elseif model==5
    %tajimamodel;
    hold on
    xlabel('VDS,V')
    ylabel('Ids,mA')
    hold on
    if type==1
      title('2X50 TAJIMA MODEL')
```

```
      elseif type==2
      title('2X150 TAJIMA MODEL')
      elseif type==3
      title('4X50 TAJIMA MODEL')
      elseif type==4
      title('4X75 TAJIMA MODEL')
      elseif type==5
      title('4X100 TAJIMA MODEL')
      elseif type==6
      title('4X125 TAJIMA MODEL')
      elseif type==7
      title('4X150 TAJIMA MODEL')
      elseif type==8
      title('4X175 TAJIMA MODEL')
      elseif type==9
      title('6X50 TAJIMA MODEL')
      elseif type==10
      title('6X150 TAJIMA MODEL')
   end
   gtext('Vgs=0V')
   gtext('Vgs=-0.25V')
   gtext('Vgs=-0.50V')
   gtext('Vgs=-0.75V')
   gtext('Vgs=-1V')
elseif model==6
   %Tommodel;
    hold on
   xlabel('VDS,V')
   ylabel('Ids,mA')
   hold on
   if type==1
      title('2X50 TOM MODEL')
      elseif type==2
      title('2X150 TOM MODEL')
      elseif type==3
      title('4X50 TOM MODEL')
      elseif type==4
      title('4X75 TOM MODEL')
      elseif type==5
      title('4X100 TOM MODEL')
      elseif type==6
      title('4X125 TOM MODEL')
      elseif type==7
      title('4X150 TOM MODEL')
      elseif type==8
      title('4X175 TOM MODEL')
      elseif type==9
      title('6X50 TOM MODEL')
      elseif type==10
      title('6X150 TOM MODEL')
   end
   gtext('Vgs=0V')
   gtext('Vgs=-0.25V')
   gtext('Vgs=-0.50V')
   gtext('Vgs=-0.75V')
   gtext('Vgs=-1V')
elseif model==7
   %statzmodel;
   hold on
   xlabel('VDS,V')
```

```
    ylabel('Ids,mA')
    hold on
    if type==1
        title('2X50 STATZ MODEL')
        elseif type==2
        title('2X150 STATZ MODEL')
        elseif type==3
        title('4X50 STATZ MODEL')
        elseif type==4
        title('4X75 STATZ MODEL')
        elseif type==5
        title('4X100 STATZ MODEL')
        elseif type==6
        title('4X125 STATZ MODEL')
        elseif type==7
        title('4X150 STATZ MODEL')
        elseif type==8
        title('4X175 STATZ MODEL')
        elseif type==9
        title('6X50 STATZ MODEL')
        elseif type==10
        title('6X150 STATZ MODEL')
    end
    gtext('Vgs=0V')
    gtext('Vgs=-0.25V')
    gtext('Vgs=-0.50V')
    gtext('Vgs=-0.75V')
    gtext('Vgs=-1V')
elseif model==8
    %Angelov Model
    hold on
    xlabel('VDS,V')
    ylabel('Ids,mA')
    hold on
    if type==1
        title('2X50 ANGELOV MODEL')
        elseif type==2
        title('2X150 ANGELOV MODEL')
        elseif type==3
        title('4X50 ANGELOV MODEL')
        elseif type==4
        title('4X75 ANGELOV MODEL')
        elseif type==5
        title('4X100 ANGELOV MODEL')
        elseif type==6
        title('4X125 ANGELOV MODEL')
        elseif type==7
        title('4X150 ANGELOV MODEL')
        elseif type==8
        title('4X175 ANGELOV MODEL')
        elseif type==9
        title('6X50 ANGELOV MODEL')
        elseif type==10
        title('6X150 ANGELOV MODEL')
    end
    gtext('Vgs=0V')
    gtext('Vgs=-0.25V')
    gtext('Vgs=-0.50V')
    gtext('Vgs=-0.75V')
    gtext('Vgs=-1V')
```

```
end
figure;
plot(Vdsintrinsic,abs(gm)*1000)
%plot(Vdsintrinsic,gm*1000)
hold on
xlabel('VDS,V')
ylabel('Transconductance,mS')
if model==1
title('TRANSCONDUCTANCE FOR CURTICE LARGE SIGNAL MODEL')
elseif model==2
title('TRANSCONDUCTANCE FOR MATERKA&KACPRZAK MODEL')
elseif model==3
title('TRANSCONDUCTANCE FOR TOM-2 LARGE SIGNAL MODEL')
elseif model==4
title('TRANSCONDUCTANCE FOR CURTICE&ETTENBERG LARGE SIGNAL MODEL')
elseif model==5
title('TRANSCONDUCTANCE FOR TAJIMA LARGE SIGNAL MODEL')
elseif model==6
title('TRANSCONDUCTANCE FOR TOM LARGE SIGNAL MODEL')
elseif model==7
title('TRANSCONDUCTANCE FOR STATZ LARGE SIGNAL MODEL')
elseif model==8
title('TRANSCONDUCTANCE FOR ANGELOV LARGE SIGNAL MODEL')
end
gtext('Vgs=0V')
gtext('Vgs=-0.25V')
gtext('Vgs=-0.50V')
gtext('Vgs=-0.75V')
gtext('Vgs=-1V')
figure;
plot(Vdsintrinsic,abs(gds)*1000)
hold on
xlabel('VDS,V')
ylabel('output conductance,mS')
if model==1
title('OUTPUT CONDUCTANCE FOR CURTICE LARGE SIGNAL MODEL')
elseif model==2
title('OUTPUT CONDUCTANCE FOR MATERKA&KACPRZAK MODEL')
elseif model==3
title('OUTPUT CONDUCTANCE FOR TOM-2 LARGE SIGNAL MODEL')
elseif model==4
title('OUTPUT CONDUCTANCE FOR CURTICE&ETTENBERG LARGE SIGNAL MODEL')
elseif model==5
title('OUTPUT CONDUCTANCE FOR TAJIMA LARGE SIGNAL MODEL')
elseif model==6
title('OUTPUT CONDUCTANCE FOR TOM LARGE SIGNAL MODEL')
elseif model==7
title('OUTPUT CONDUCTANCE FOR STATZ LARGE SIGNAL MODEL')
elseif model==8
title('OUTPUT CONDUCTANCE FOR ANGELOV LARGE SIGNAL MODEL')
end
hold on
gtext('Vgs=0V')
gtext('Vgs=-0.25V')
gtext('Vgs=-0.50V')
gtext('Vgs=-0.75V')
gtext('Vgs=-1V')

x
min
```

B.2 "modelling.m"

```
function min = modelling(x);
global model type IDS IDSMEAS Vdsintrinsic Vgsintrinsic min IDN IDM gm gds Idso Vt
%This function includes the measured results for each type of MESFET
%These results are obtained from A.Çelebi's study.
%in this function Vto, gammadc are used for TOM model
%The resistances are obtained again from Çelebi, and these resistances are constants for this function
if type==1
   %type2x50;
  IDSMEAS=1e-3*[.13 .23 .36 .46 .54 .62 .68 .76 .82 .88 .94 1.24 1.55 1.85 2.16 2.47 2.78 3.40;...
        .4 .76 1.29 1.67 1.94 2.15 2.30 2.43 2.54 2.65 2.75 3.19 3.59 3.96 4.31 4.64 4.97 5.62;...
        .69 1.34 2.43 3.30 3.94 4.38 4.68 4.9 5.07 5.21 5.34 5.86 6.29 6.67 7.03 7.36 7.68 8.3;...
        .94 1.87 3.48 4.88 6.03 6.88 7.48 7.86 8.13 8.34 8.5 9.07 9.5 9.87 10.2 10.5 10.79 11.33;...
        1.16 2.27 4.39 6.27 7.96 9.32 10.39 11.11 11.57 11.88 12.10 12.76 13.17 13.51 13.8 14.06
14.32 14.75];
  VDS=[.05 .1 .2 .3 .4 .5 .6 .7 .8 .9 1 1.5 2 2.5 3 3.5 4 5];
  VGS=[0; -0.25; -.50; -.75; -1];
      Rs=6.4; Rd=6.6;
elseif type==2
   %type2x150;
  IDSMEAS=1e-3*[.24 .40 .64 .83 .99 1.13 1.27 1.42 1.56 1.69 1.84 2.55 3.29 4.09 4.92 5.77 6.63
8.37;...
            .96 1.78 2.98 3.83 4.43 4.89 5.23 5.56 5.85 6.12 6.38 7.50 8.62 9.63 10.64 11.62 12.58
14.41;...
            1.78 3.42 6.19 8.34 9.92 11.00 11.75 12.31 12.75 13.14 13.48 14.87 16.04 17.14 18.16
19.12 20.08 21.85;...
            2.5 4.82 9.18 12.81 15.80 18.13 19.68 20.69 21.40 21.95 22.38 23.95 25.13 26.16 27.10
27.98 28.80 30.33;...
            3.06 6.06 11.69 16.77 21.19 24.99 27.90 29.88 31.13 31.99 32.60 34.36 35.46 36.38 37.18
37.90 38.55 39.80];
  VDS=[.05 .1 .2 .3 .4 .5 .6 .7 .8 .9 1 1.5 2 2.5 3 3.5 4 5];
  VGS=[0; -0.25; -.50; -.75; -1];
   Rs=3.00;  Rd=2.80;%Rs=2.45;  Rd=2.82;
elseif type==3
   %type4x50;
   IDSMEAS=1e-3*[2.24 4.42 8.42 12.12 15.38 18.11 20.30 21.77 22.72 23.36 23.82 25.10 25.90
26.54 27.08 27.56 28.01 28.77;...
               1.80 3.54 6.66 9.45 11.68 13.39 14.60 15.40 15.95 16.34 16.67 17.78 18.60 19.29 19.95
20.52 21.08 22.08;...
               1.34 2.57 4.70 6.35 7.63 8.49 9.09 9.53 9.87 10.13 10.39 11.38 12.22 12.93 13.64 14.28
14.9 16.09;...
               .78 1.40 2.48 3.18 3.71 4.08 4.38 4.63 4.86 5.06 5.25 6.1 6.86 7.57 8.28 8.91 9.55
10.82;...
               .24 .42 .67 .85 1.00 1.14 1.27 1.39 1.51 1.62 1.73 2.31 2.87 3.45 4.03 4.62 5.2 6.44];

   VDS=[.05 .1 .2 .3 .4 .5 .6 .7 .8 .9 1 1.5 2 2.5 3 3.5 4 5];
   VGS=[0 -0.25 -.50 -.75 -1];
    Rs=3.2;  Rd=3.5;
elseif type==4
   %type4x75;
   IDSMEAS=1e-3*[.32 .56 .9 1.13 1.34 1.53 1.71 1.88 2.04 2.21 2.43 3.21 4.05 4.91 5.78 6.67 7.56
9.36;
       1.09 2.01 3.45 4.44 5.16 5.67 6.09 6.45 6.78 7.07 7.35 8.58 9.72 10.80 11.82 12.82 13.79
15.67;
```

```
        1.92 3.68 6.67 9.12 10.91 12.12 12.95 13.59 14.08 14.49 14.86 16.33 17.54 18.65 19.68 20.64
21.58 23.35;
        2.6 5.12 9.64 13.58 16.76 19.30 21.03 22.16 22.96 23.55 24.02 25.65 26.86 27.89 28.82 29.69
30.51 31.98;
        3.18 6.32 12.10 17.52 22.09 26.07 29.22 31.39 32.8 33.73 34.39 36.23 37.38 38.25 39.03
39.71 40.33 41.49];
  VGS=[0 -0.25 -.50 -.75 -1];
  VDS=[.05 .1 .2 .3 .4 .5 .6 .7 .8 .9 1 1.5 2 2.5 3 3.5 4 5];
  Rs=2.3;    Rd=2.5;%they are found by s/c and o/c measurements
elseif type==5
  %type4x100;
  IDSMEAS=1e-3*[.37 .64 1.01 1.28 1.55 1.77 1.98 2.18 2.39 2.60 2.79 3.83 4.89 6.0 7.15 8.33 9.5
11.90;...
            1.37 2.54 4.32 5.54 6.42 7.09 7.61 8.06 8.48 8.86 9.19 10.8 12.26 13.67 15.04 16.37 17.68
20.18;...
            2.45 4.7 8.65 11.69 13.91 15.53 16.57 17.37 17.99 18.52 19.0 20.9 22.49 23.94 25.30
26.60 27.83 30.2;...
            3.32 6.60 12.43 17.40 21.63 24.92 27.17 28.67 29.69 30.45 31.08 33.17 34.74 36.10 37.33
38.45 39.51 41.46;...
            4.11 8.08 15.68 22.48 28.63 33.66 37.91 40.90 42.70 43.93 44.78 47.18 48.63 49.78 50.78
51.63 52.43 53.88];
  VDS=[.05 .1 .2 .3 .4 .5 .6 .7 .8 .9 1 1.5 2 2.5 3 3.5 4 5];
  VGS=[0; -0.25; -.50; -.75; -1];
  Rs=1.8;     Rd=2.08;
elseif type==6
  %type4x125;
  IDSMEAS=1e-3*[4.97 9.82 18.88 27.33 34.78 41.37 46.63 50.40 52.90 54.53 55.68 58.71 60.52
61.95 63.17 64.24 65.18 66.78;...
          4.08 7.97 15.21 21.47 26.70 30.81 33.75 35.68 37.01 37.98 38.76 41.43 43.39 45.11 46.69
48.08 49.44 51.89;...
          2.98 5.73 10.62 14.45 17.28 19.31 20.70 21.67 22.49 23.17 23.74 26.18 28.22 30.08 31.85
33.47 35.09 38.04;...
          1.73 3.20 5.47 7.06 8.19 9.01 9.69 10.27 10.79 11.28 11.74 13.81 15.70 17.51 19.25 20.98
22.65 25.85;...
          .48 .83 1.29 1.67 1.97 2.26 2.53 2.78 3.06 3.32 3.59 4.93 6.32 7.79 9.30 10.81 12.35 15.45];
  VDS=[.05 .1 .2 .3 .4 .5 .6 .7 .8 .9 1 1.5 2 2.5 3 3.5 4 5];
  VGS=[0; -0.25; -.50; -.75; -1];
  Rs=1.5;    Rd=1.75;
elseif type==7
  %type4x150;
  IDSMEAS=1e-3*[5.81 11.44 22.14 31.85 40.75 48.28 54.44 58.90 61.73 63.61 64.95 68.53 70.65
72.34 73.78 75.0 76.13 78.19;...
            4.72 9.21 17.60 24.77 30.87 35.63 38.99 41.19 42.70 43.85 44.76 47.90 50.28 52.33 54.17
55.88 57.49 60.41;...
            3.48 6.62 12.22 16.54 19.75 21.99 23.52 24.70 25.62 26.40 27.11 29.98 32.41 34.62 36.69
38.69 40.58 44.20;...
            1.89 3.45 5.82 7.56 8.76 9.68 10.40 11.09 11.68 12.20 12.78 15.19 17.40 19.55 21.05
23.68 25.69 29.56;...
            .46 .79 1.26 1.63 1.95 2.26 2.55 2.83 3.12 3.42 3.71 5.22 6.83 8.50 10.28 12.02 13.90
17.58];
  VDS=[.05 .1 .2 .3 .4 .5 .6 .7 .8 .9 1 1.5 2 2.5 3 3.5 4 5]; %21=20.64
  VGS=[0; -0.25; -.50; -.75; -1];
  Rs=1.25;    Rd=1.55;
elseif type==8
  %type4x175;
  IDSMEAS=1e-3*[6.63 13.08 25.20 36.58 46.78 55.53 62.70 68.08 71.54 73.84 75.44 79.71 82.16
84.10 85.66 86.99 88.20 90.29;...
            5.43 10.60 20.17 28.50 35.58 41.16 45.20 47.83 49.65 50.99 52.09 55.85 58.67 61.05
63.17 65.15 66.98 70.33;...
            4.0 7.69 14.06 19.11 22.88 25.58 27.44 28.80 29.92 30.85 31.72 35.15 38.0 40.66 43.12
```

```
45.46 47.67 52.03;...
              2.22 4.08 6.95 8.95 10.40 11.50 12.40 13.20 13.93 14.60 15.21 18.14 20.79 23.30 25.77
28.23 30.63 35.20;...
              .54 .93 1.48 1.91 2.28 2.66 3.02 3.37 3.72 4.06 4.43 6.25 8.19 10.24 12.37 14.50 16.66
21.19];
   VDS=[.05 .1 .2 .3 .4 .5 .6 .7 .8 .9 1 1.5 2 2.5 3 3.5 4 5];
   VGS=[0; -0.25; -.50; -.75; -1];
   Rs=1.1;   Rd=1.45;
elseif type==9
   %type6x50;
   IDSMEAS=1e-3*[1.16 2.27 4.39 6.27 7.96 9.32 10.39 11.11 11.57 11.88 12.10 12.76 13.17 13.51
13.8 14.06 14.32 14.75;...
              0.94 1.87 3.48 4.88 6.03 6.88 7.48 7.86 8.13 8.34 8.5 9.07 9.5 9.87 10.2 10.5 10.79
11.33;...
              .69 1.34 2.43 3.30 3.94 4.38 4.68 4.9 5.07 5.21 5.34 5.86 6.29 6.67 7.03 7.36 7.68 8.3;...
              .4 .76 1.29 1.67 1.94 2.15 2.30 2.43 2.54 2.65 2.75 3.19 3.59 3.96 4.31 4.64 4.97 5.62;...
              .13 .23 .36 .46 .54 .92 .68 .76 .82 .88 .94 1.24 1.55 1.85 2.16 2.47 2.78 3.40];
   VDS=[.05 .1 .2 .3 .4 .5 .6 .7 .8 .9 1 1.5 2 2.5 3 3.5 4 5];
   VGS=[0; -0.25; -.50; -.75; -1];
   Rs=2.15;     Rd=2.50;
elseif type==10
   %type6x150;
   IDSMEAS=1e-3*[8.15 16.05 31.09 45.19 57.83 69.08 78.47 85.46 90.43 93.54 95.70 101.33
104.50 106.94 108.97 110.72 112.26 115.01;...
              6.74 13.19 25.24 35.67 44.68 51.87 57.11 60.60 63.06 64.80 66.2 71.04 74.59 77.62 80.40
82.86 85.20 89.44;...
              4.99 9.62 17.75 24.08 28.95 32.30 34.70 36.47 37.88 39.08 40.14 44.51 48.13 51.48 54.62
57.57 60.41 65.78;...
              2.75 5.09 8.62 11.12 12.93 14.31 15.45 16.44 17.34 18.19 18.98 22.62 25.99 29.24 32.39
35.48 38.53 44.34;...
              .68 1.16 1.84 2.38 2.87 3.32 3.76 4.20 4.63 5.07 5.50 7.78 10.21 12.75 15.44 18.14 20.94
26.56];
   VDS=[.05 .1 .2 .3 .4 .5 .6 .7 .8 .9 1 1.5 2 2.5 3 3.5 4 5];
   VGS=[0; -0.25; -.50; -.75; -1];
   Rs=0.86;     Rd=1.0;
end
[IDM,IDN]=size(IDSMEAS);
if model==1
 %CURTICE MODEL
%*****************************************************************************
 for ii=1:IDM
   for jj=1:IDN
      Vdsintrinsic(jj)=VDS(jj)-(Rs+Rd)*IDSMEAS(ii,jj);
      Vgsintrinsic(ii)=VGS(ii)-Rs*IDSMEAS(ii,jj);
      IDS(ii,jj)=x(1)*(Vgsintrinsic(ii)-x(2))^2*(1+x(3)*Vdsintrinsic(jj))*tanh(x(4)*Vdsintrinsic(jj));
      gm(ii,jj)=abs(2*x(1)*(Vgsintrinsic(ii)-
x(2))*(1+x(3)*Vdsintrinsic(jj))*(tanh(x(4)*Vdsintrinsic(jj))));
      gds(ii,jj)=x(1)*((Vgsintrinsic(ii)-
x(2))^2)*(1+x(3)*Vdsintrinsic(jj))*((x(4)/((cosh(x(4)*Vdsintrinsic(jj)))^2))+x(1)*((Vgsintrinsic(ii)-
x(2))^2)*x(3)*tanh(x(4)*Vdsintrinsic(jj)));
      %x(1)=beta x(2)=Vto x(3)=lambda x(4)=alpha
   end;
end;
%*****************************************************************************
elseif model==2
   %MATERKA&KACPRZAKmodel;

%*****************************************************************************
    for ii=1:IDM
     for jj=1:IDN
```

```
        Vdsintrinsic(jj)=VDS(jj)-(Rs+Rd)*IDSMEAS(ii,jj);
        Vgsintrinsic(ii)=VGS(ii)-Rs*IDSMEAS(ii,jj);
        Vt=x(2)+x(4)*Vdsintrinsic(jj);
        IDS(ii,jj)=x(1).*(1-Vgsintrinsic(ii)/Vt)^2.*tanh(x(3).*Vdsintrinsic(jj)/(Vgsintrinsic(ii)-Vt));
        gm(ii,jj)=abs(tanh(x(3)*Vdsintrinsic(jj)/(Vgsintrinsic(ii)-Vt))*(-2*x(1)/Vt)*(1-
Vgsintrinsic(ii)/Vt)-x(1)*((1-Vgsintrinsic(ii)/Vt)^2)*((sech(x(3)*Vdsintrinsic(jj)/Vgsintrinsic(ii)-
Vt))^2)*((x(3)*Vdsintrinsic(jj)))/(Vgsintrinsic(ii)-Vt)^2));
        gds(ii,jj)=2*x(1)*(1-
Vgsintrinsic(ii)/Vt)*(x(4)*Vgsintrinsic(ii)/Vt^2)*tanh(x(3)*Vdsintrinsic(jj)/(Vgsintrinsic(ii)-
Vt))+x(1)*((1-Vgsintrinsic(ii)/Vt)^2)*((sech(x(3)*Vdsintrinsic(jj)/Vgsintrinsic(ii)-
Vt))^2)*(x(3)*(Vgsintrinsic(ii)-Vt)+x(3)*x(4)*Vdsintrinsic(jj))/(Vgsintrinsic(ii)-Vt)^2;
        %x(1)=IDSS, x(2)=Vto, x(3)=alpha, x(4)=gamma
    end
 end

%*****************************************************************************
elseif model==3
  %tom2model;

%*****************************************************************************
for ii=1:IDM
  for jj=1:IDN
      Vdsintrinsic(jj)=VDS(jj)-(Rs+Rd)*IDSMEAS(ii,jj);
      Vgsintrinsic(ii)=VGS(ii)-Rs*IDSMEAS(ii,jj);
      Vg(ii,jj)=x(1)*x(2)*log(exp((Vgsintrinsic(ii)-x(3)+x(4)*Vdsintrinsic(jj))/(x(1)*x(2)))+1);
      IDSO(ii,jj)=x(5)*x(6)*Vg(ii,jj)^x(1)*x(7)*Vdsintrinsic(jj)/sqrt(1+x(7)^2*Vdsintrinsic(jj)^2);
      IDS(ii,jj)=IDSO(ii,jj)/(1+x(8)*Vdsintrinsic(jj)*IDSO(ii,jj));
      p(ii,jj)=1-x(8)*Vdsintrinsic(jj)*IDS(ii,jj);
      gmo(ii,jj)=(IDSO(ii,jj)/Vg(ii,jj))*x(1)/(exp(-(Vgsintrinsic(ii)-
x(3)+x(4)*Vdsintrinsic(jj))/x(1)*x(2))+1);
      gm(ii,jj)=gmo(ii,jj)*p(ii,jj)^2;
      %gdso(ii,jj)=(x(4)-(Vgsintrinsic(ii)-
x(3)+x(4)*Vdsintrinsic(jj))/x(2))+x(1)*IDSO(ii,jj)/x(2)+(x(7)*x(6)*Vg(ii,jj)^2)/(1+(x(7)*Vdsintrinsic
(jj))^2)^(3/2);
      gdso(ii,jj)=gm(ii,jj)*(x(4)-(Vgsintrinsic(ii)-
x(3)+x(4)*Vdsintrinsic(jj))/x(2))+x(1)*IDSO(ii,jj)/x(2)+(x(7)*x(6)*Vg(ii,jj)^2)/(1+(x(7)*Vdsintrinsic
(jj))^2)^(3/2);
      gds(ii,jj)=gdso(ii,jj)*p(ii,jj)^2-x(8)*IDS(ii,jj)^2;
      %x(1)=Q, x(2)=Vst, x(3)=Vto, x(4)=gamma, x(5)=w, x(6)=beta, x(7)=alpha, x(8)=delta
  end;
end;
 %*****************************************************************************
elseif model==4
  %curticeettenbergmodel;
 %*****************************************************************************
for ii=1:IDM
  for jj=1:IDN
      Vdsintrinsic(jj)=VDS(jj)-(Rs+Rd)*IDSMEAS(ii,jj);
      Vgsintrinsic(ii)=VGS(ii)-Rs*IDSMEAS(ii,jj);
      V1(ii,jj)=Vgsintrinsic(ii)*(1+x(1)*(x(7)-Vdsintrinsic(jj)));
      V2(ii,jj)=(1+x(1)*(x(7)-Vdsintrinsic(jj)));

IDS(ii,jj)=(x(2)+x(3)*V1(ii,jj)+x(4)*(V1(ii,jj))^2+x(5)*(V1(ii,jj))^3)*tanh(x(6)*Vdsintrinsic(jj));

gm(ii,jj)=abs(tanh(x(6)*Vdsintrinsic(jj))*(x(3)*V2(ii,jj)+2*x(4)*V1(ii,jj)*V2(ii,jj)+3*x(5)*(V1(ii,jj)^
2)*V2(ii,jj)));

gds(ii,jj)=(x(2)+x(3)*V1(ii,jj)+x(4)*(V1(ii,jj))^2+x(5)*(V1(ii,jj))^3)*x(6)*((sech(x(6)*Vdsintrinsic(jj
)))^2)-
x(1)*Vgsintrinsic(ii)*(x(3)+2*x(4)*V1(ii,jj)+3*x(5)*(V1(ii,jj)^2))*tanh(x(6)*Vdsintrinsic(jj))+1/x(7)
```

```
      %x(1)=beta, x(2)=A0, x(3)=A1, x(4)=A2, x(5)=A3, x(6)=gamma,
      %x(7)=Vdso, x(8)=Vto
   end
end
%******************************************************************************
elseif model==5
   %tajimamodel;
%******************************************************************************
for ii=1:IDM
    for jj=1:IDN
      Vdsintrinsic(jj)=VDS(jj)-(Rs+Rd)*IDSMEAS(ii,jj);
      Vgsintrinsic(ii)=VGS(ii)-Rs*IDSMEAS(ii,jj);
      VGS1(ii)=Vgsintrinsic(ii)-x(1);
      Vp(jj)=x(2)+x(3)*Vdsintrinsic(jj)+x(1);
      k=1-(1/x(4))*(1-exp(-x(4)));
      IDS2(ii,jj)=x(5)*(1-exp((-Vdsintrinsic(jj)/x(6))-x(7)*(Vdsintrinsic(jj)/x(6))^2-
x(8)*(Vdsintrinsic(jj)/x(6))^3));
      IDS1(ii,jj)=(1/k)*(1+(VGS1(ii)/Vp(jj))-(1/x(4))+((1/x(4))*exp(-x(4)*(1+(VGS1(ii)/Vp(jj))))));
      IDS(ii,jj)=IDS1(ii,jj)*IDS2(ii,jj);
      gm(ii,jj)=abs((IDS2(ii,jj)/k*Vp(jj))*(1-exp(-x(4)*(1+VGS1(ii)/Vp(jj)))));
      gds(ii,jj)=abs(((IDS2(ii,jj)*x(3)*VGS1(ii))/(k*Vp(jj)^2))*(1-exp(-x(4)*(1+VGS1(ii)/Vp(jj))))-
IDS1(ii,jj)*x(5)*((1/x(6))+2*x(7)*Vdsintrinsic(jj)/(x(6)^2)+(3*x(8)*Vdsintrinsic(jj)^2)/(x(6)^3))*exp
(-Vdsintrinsic(jj)/x(6)-x(7)*(Vdsintrinsic(jj)/x(6))^2-x(8)*(Vdsintrinsic(jj)/x(6))^3));
      %x(1)=VBI, x(2)=Vpo, x(3)=p, x(4)=m, x(5)=IDSP, x(6)=VDSS, x(7)=a, x(8)=b
    end
end
%******************************************************************************
elseif model==6
   %Tommodel;
%******************************************************************************
   for ii=1:IDM
    for jj=1:IDN
       Vdsintrinsic(jj)=VDS(jj)-(Rs+Rd)*IDSMEAS(ii,jj);
       Vgsintrinsic(ii)=VGS(ii)-Rs*IDSMEAS(ii,jj);
       Vt(jj)=x(5)-x(6)*Vdsintrinsic(jj);
       Idso(ii,jj)=x(2)*(Vgsintrinsic(ii)-Vt(jj))^x(4);
      if Vdsintrinsic(jj)<(3/x(1))
          IDS1(ii,jj)=x(2).*(Vgsintrinsic(ii)-Vt(jj)).^x(4).*(1-(1-x(1).*Vdsintrinsic(jj)/3).^3);
          IDS(ii,jj)=IDS1(ii,jj)./(1+x(3).*Vdsintrinsic(jj).*IDS1(ii,jj));
          gm(ii,jj)=abs(1-(1-x(1)*Vdsintrinsic(jj)/3)^3)*((x(4)*x(2)*(Vgsintrinsic(ii)-
Vt(jj)))/(1+x(3)*Vdsintrinsic(jj)*Idso(ii,jj))-
Idso(ii,jj)*x(4)*x(3)*Vdsintrinsic(jj)*x(2)*(Vgsintrinsic(ii)-
Vt(jj))/((1+x(3)*Vdsintrinsic(jj)*Idso(ii,jj))^2));
          gds(ii,jj)=(x(4)*x(2)*x(6)*(Vgsintrinsic(ii)-Vt(jj))*(1+x(3)*Vdsintrinsic(jj)*Idso(ii,jj))-
Idso(ii,jj)*x(3)*(Idso(ii,jj)+x(4)*x(2)*x(6)*Vdsintrinsic(jj)*(Vgsintrinsic(ii)-Vt(jj))))*(1-(1-
x(1)*Vdsintrinsic(jj)/3)^3)/(1+x(3)*Vdsintrinsic(jj)*Idso(ii,jj))^2+IDS(ii,jj)*(x(1)*(1-
x(1)*Vdsintrinsic(jj)/3)^2);
          %gds(ii,jj)=(x(4)*x(2)*gamma*(Vgsintrinsic(ii)-Vt(jj))*(1+x(3)*Vdsintrinsic(jj)*Idso(ii,jj))-
Idso(ii,jj)*x(3)*(Idso(ii,jj)+x(4)*x(2)*gamma*Vdsintrinsic(jj)*(Vgsintrinsic(ii)-Vt(jj))))*(1-(1-
x(1)*Vdsintrinsic(jj)/3)^3)/(1+x(3)*Vdsintrinsic(jj)*Idso(ii,jj))^2+IDS(ii,jj)*(x(1)*(1-
x(1)*Vdsintrinsic(jj)/3)^2);
      elseif Vdsintrinsic(jj)>=(3/x(1))
          IDS1(ii,jj)=x(2).*(Vgsintrinsic(ii)-Vt(jj)).^x(4);
          IDS(ii,jj)=IDS1(ii,jj)./(1+x(3).*Vdsintrinsic(jj).*IDS1(ii,jj));
          gm(ii,jj)=abs((x(4)*x(2)*(Vgsintrinsic(ii)-Vt(jj)))/(1+x(3)*Vdsintrinsic(jj)*Idso(ii,jj))-
Idso(ii,jj)*x(4)*x(3)*Vdsintrinsic(jj)*x(2)*(Vgsintrinsic(ii)-
Vt(jj))/((1+x(3)*Vdsintrinsic(jj)*Idso(ii,jj))^2));
          gds(ii,jj)=(x(4)*x(2)*x(6)*(Vgsintrinsic(ii)-Vt(jj))*(1+x(3)*Vdsintrinsic(jj)*Idso(ii,jj))-
Idso(ii,jj)*x(3)*(Idso(ii,jj)+x(4)*x(2)*x(6)*Vdsintrinsic(jj)*(Vgsintrinsic(ii)-
Vt(jj))))/(1+x(3)*Vdsintrinsic(jj)*Idso(ii,jj))^2;
```

```
          %gds(ii,jj)=(x(4)*x(2)*gamma*(Vgsintrinsic(ii)-Vt(jj))*(1+x(3)*Vdsintrinsic(jj)*Idso(ii,jj))-
Idso(ii,jj)*x(3)*(Idso(ii,jj)+x(4)*x(2)*gamma*Vdsintrinsic(jj)*(Vgsintrinsic(ii)-
Vt(jj)))))/(1+x(3)*Vdsintrinsic(jj)*Idso(ii,jj))^2;
        end
           %x(1)=alpha, x(2)=beta, x(3)=delta, x(4)=Q
           % x(5)=Vto, x(6)=gamma
    end
  end
  %***************************************************************************
elseif model==7
  %statzmodel;
  %************************************************************************
  for ii=1:IDM
    for jj=1:IDN
        Vdsintrinsic(jj)=VDS(jj)-(Rs+Rd)*IDSMEAS(ii,jj);
        Vgsintrinsic(ii)=VGS(ii)-Rs*IDSMEAS(ii,jj);
        if 0<Vdsintrinsic(jj) & Vdsintrinsic(jj)<(3/x(4))
          IDS(ii,jj)=[(x(1)*((Vgsintrinsic(ii)-x(2))^2))/(1+(x(5)*Vgsintrinsic(ii)-x(2)))]*[1-(1-
(x(4)*Vdsintrinsic(jj)/3))^3]*(1+x(3)*Vdsintrinsic(jj));
          gm(ii,jj)=abs((1-(1-
x(4)*Vdsintrinsic(jj)/3)^3)*(1+x(3)*Vdsintrinsic(jj))*(2*x(1)*(Vgsintrinsic(ii)-
x(2))/(1+x(5)*(Vgsintrinsic(ii)-x(2))))-(x(5)*x(1)*((Vgsintrinsic(ii)-
x(2))^2)/((1+x(5)*(Vgsintrinsic(ii)-x(2)))^2)));
          gds(ii,jj)=(1-(1-x(4)*Vdsintrinsic(jj)/3)^3)*x(3)+x(4)*(1+x(3)*Vdsintrinsic(jj))*((1-
x(4)*Vdsintrinsic(jj)/3)^2)*(x(1)*((Vgsintrinsic(ii)-x(2))^2)/(1+x(5)*(Vgsintrinsic(ii)-x(2))));
        elseif Vdsintrinsic(jj)>(3/x(4))
          IDS(ii,jj)=[(x(1)*((Vgsintrinsic(ii)-x(2))^2))/(1+(x(5)*Vgsintrinsic(ii)-
x(2)))]*(1+x(3)*Vdsintrinsic(jj));
          gm(ii,jj)=abs(((1+x(5)*(Vgsintrinsic(ii)-x(2)))*2*x(1)*(Vgsintrinsic(ii)-x(2))-
x(5)*x(1)*((Vgsintrinsic(ii)-x(2))^2))*(1+x(3)*Vdsintrinsic(jj))/(1+x(5)*(Vgsintrinsic(ii)-x(2))));
          gds(ii,jj)=x(3)*x(1)*((Vgsintrinsic(ii)-x(2))^2)/(1+x(5)*(Vgsintrinsic(ii)-x(2)));
        else
        end
        % beta=x(1) Vto=x(2) Lambda=x(3) alpha=x(4) b=x(5)
    end
 end
  %************************************************************************
elseif model==8
  %Angelov Model
  %****************************************************************************
   for ii=1:IDM
    for jj=1:IDN
        Vdsintrinsic(jj)=VDS(jj)-(Rs+Rd)*IDSMEAS(ii,jj);
        Vgsintrinsic(ii)=VGS(ii)-Rs*IDSMEAS(ii,jj);
        Vpk(jj)=x(4)+x(5)*Vdsintrinsic(jj);
        Phi(ii,jj)=x(1)*(Vgsintrinsic(ii)-Vpk(jj))+x(2)*(Vgsintrinsic(ii)-
Vpk(jj))^2+x(3)*(Vgsintrinsic(ii)-Vpk(jj))^3;
        IDS(ii,jj)=x(6)*(1+tanh(Phi(ii,jj)))*(1+x(7)*Vdsintrinsic(jj))*tanh(x(8)*Vdsintrinsic(jj));
        gm(ii,jj)=abs(x(6)*(1+x(7)*Vdsintrinsic(jj))*(x(1)+2*x(2)*(Vgsintrinsic(ii)-
Vpk(jj))+3*x(3)*(Vgsintrinsic(ii)-Vpk(jj))^2)/(cosh(Phi(ii,jj)))^2);
        gds(ii,jj)=x(6)*(1+x(7)*Vdsintrinsic(jj))*tanh(x(8)*Vdsintrinsic(jj))*(-x(1)*x(5)-
2*x(2)*x(5)*(Vgsintrinsic(ii)-Vpk(jj))-3*x(3)*x(5)*(Vgsintrinsic(ii)-
Vpk(jj))^2)/(cosh(Phi(ii,jj)))^2+(1+tanh(Phi(ii,jj)))*(x(7)*tanh(x(8)*Vdsintrinsic(jj))+(1+x(7)*Vdsint
rinsic(jj))*x(8)/(cosh(x(8)*Vdsintrinsic(jj)))^2);
        %x(1)=P1, x(2)=P2, x(3)=P3, x(4)=Vpko, x(5)=gamma, x(6)=Ipk, x(7)=lambda, x(8)=alpha
    end
   end
  %****************************************************************************
end
min=(sum(sum(abs(IDS-IDSMEAS))))^2;
```

B.3 "fminsearch.m"

FMINSEARCH Multidimensional unconstrained nonlinear minimization (Nelder-Mead).
X = FMINSEARCH(FUN,X0) starts at X0 and attempts to find a local minimizer
X of the function FUN. FUN accepts input X and returns a scalar function
value F evaluated at X. X0 can be a scalar, vector or matrix.

X = FMINSEARCH(FUN,X0,OPTIONS) minimizes with the default optimization
parameters replaced by values in the structure OPTIONS, created
with the OPTIMSET function. See OPTIMSET for details. FMINSEARCH uses
these options: Display, TolX, TolFun, MaxFunEvals, MaxIter, FunValCheck,
and OutputFcn.

[X,FVAL]= FMINSEARCH(...) returns the value of the objective function,
described in FUN, at X.

[X,FVAL,EXITFLAG] = FMINSEARCH(...) returns an EXITFLAG that describes
the exit condition of FMINSEARCH. Possible values of EXITFLAG and the
corresponding exit conditions are

1 FMINSEARCH converged to a solution X.
0 Maximum number of function evaluations or iterations reached.
-1 Algorithm terminated by the output function.

[X,FVAL,EXITFLAG,OUTPUT] = FMINSEARCH(...) returns a structure
OUTPUT with the number of iterations taken in OUTPUT.iterations, the
number of function evaluations in OUTPUT.funcCount, the algorithm name
in OUTPUT.algorithm, and the exit message in OUTPUT.message.

Examples
FUN can be specified using @:

```
X = fminsearch(@sin,3)
```

finds a minimum of the SIN function near 3.
In this case, SIN is a function that returns a scalar function value
SIN evaluated at X.

FUN can also be an anonymous function:

```
X = fminsearch(@(x) norm(x),[1;2;3])
```

returns a point near the minimizer [0;0;0].

If FUN is parameterized, you can use anonymous functions to capture the
problem-dependent parameters. Suppose you want to optimize the objective
given in the function MYFUN, which is parameterized by its second argument A.
Here MYFUN is an M-file function such as

```
function F = myfun(x,a)
f = x(1)^2 + a*x(2)^2;
```

To optimize for a specific value of A, first assign the value to A. Then
create a one-argument anonymous function that captures that value of A
and calls MYFUN with two arguments. Finally, pass this anonymous function
to FMISEARCH:

```
a = 1.5; % define parameter first
x = fminsearch(@(x) myfun(x,a),[0.3;1])
```

B.4 optimset (foptions)

```
OPTIMSET Create/alter OPTIM OPTIONS structure.
   OPTIONS = OPTIMSET('PARAM1',VALUE1,'PARAM2',VALUE2,...) creates an
   optimization options structure OPTIONS in which the named parameters have
   the specified values.  Any unspecified parameters are set to [] (parameters
   with value [] indicate to use the default value for that parameter when
   OPTIONS is passed to the optimization function). It is sufficient to type
   only the leading characters that uniquely identify the parameter.  Case is
   ignored for parameter names.
   NOTE: For values that are strings, correct case and the complete string
   are required; if an invalid string is provided, the default is used.

   OPTIONS = OPTIMSET(OLDOPTS,'PARAM1',VALUE1,...) creates a copy of OLDOPTS
   with the named parameters altered with the specified values.

   OPTIONS = OPTIMSET(OLDOPTS,NEWOPTS) combines an existing options structure
   OLDOPTS with a new options structure NEWOPTS.  Any parameters in NEWOPTS
   with non-empty values overwrite the corresponding old parameters in
   OLDOPTS.

   OPTIMSET with no input arguments and no output arguments displays all
   parameter names and their possible values, with defaults shown in {}
   when the default is the same for all functions that use that option -- use
   OPTIMSET(OPTIMFUNCTION) to see options for a specific function.).

   OPTIONS = OPTIMSET (with no input arguments) creates an options structure
   OPTIONS where all the fields are set to [].

   OPTIONS = OPTIMSET(OPTIMFUNCTION) creates an options structure with all
   the parameter names and default values relevant to the optimization
   function named in OPTIMFUNCTION. For example,
           optimset('fminbnd')
   or
           optimset(@fminbnd)
   returns an options structure containing all the parameter names and
   default values relevant to the function 'fminbnd'.

 OPTIMSET PARAMETERS for MATLAB
 Display - Level of display [ off | iter | notify | final ]
 MaxFunEvals - Maximum number of function evaluations allowed
                    [ positive integer ]
 MaxIter - Maximum number of iterations allowed [ positive scalar ]
 TolFun - Termination tolerance on the function value [ positive scalar ]
 TolX - Termination tolerance on X [ positive scalar ]
 FunValCheck - Check for invalid values, such as NaN or complex, from
              user-supplied functions [ {off} | on ]
 OutputFcn - Name of installable output function  [ function ]
          This output function is called by the solver after each
          iteration.

   Note: To see OPTIMSET parameters for the OPTIMIZATION TOOLBOX
         (if you have the Optimization Toolbox installed), type
             help optimoptions
    Examples
     To create options with the default options for fzero
       options = optimset('fzero');
     To create an options structure with TolFun equal to 1e-3
       options = optimset('TolFun',1e-3);
     To change the Display value of options to 'iter'
       options = optimset(options,'Display','iter');
```

B.5 “fminunc”

```
FMINUNC finds the minimum of a function of several variables.
   X=FMINUNC(FUN,X0) starts at X0 and attempts to find a local minimizer X
   of the function FUN. FUN accepts input X and returns a scalar function
   value F evaluated at X. X0 can be a scalar, vector or matrix.
    X=FMINUNC(FUN,X0,OPTIONS) minimizes with the default optimization
   parameters replaced by values in the structure OPTIONS, an argument
   created with the OPTIMSET function.  See OPTIMSET for details.  Used
   options are Display, TolX, TolFun, DerivativeCheck, Diagnostics,
   FunValCheck GradObj, HessPattern, Hessian, HessMult, HessUpdate,
   InitialHessType, InitialHessMatrix, MaxFunEvals, MaxIter,
   DiffMinChange and DiffMaxChange, LargeScale, MaxPCGIter,
   PrecondBandWidth, TolPCG, TypicalX. Use the GradObj option to specify
   that FUN also returns a second output argument G that is the partial
   derivatives of the function df/dX, at the point X. Use the Hessian
   option to specify that FUN also returns a third output argument H that
   is the 2nd partial derivatives of the function (the Hessian) at the
   point X. The Hessian is only used by the large-scale method, not the
   line-search method.

   [X,FVAL]=FMINUNC(FUN,X0,...) returns the value of the objective
   function FUN at the solution X.

   [X,FVAL,EXITFLAG]=FMINUNC(FUN,X0,...) returns an EXITFLAG that describes
   the exit condition of FMINUNC. Possible values of EXITFLAG and the
   corresponding exit conditions are

     1  FMINUNC converged to a solution X.
     2  Change in X smaller than the specified tolerance.
     3  Change in the objective function value smaller than the specified
        tolerance (only occurs in the large-scale method).
     0  Maximum number of function evaluations or iterations reached.
    -1  Algorithm terminated by the output function.
    -2  Line search cannot sufficiently decrease the objective function along
        the current search direction (only occurs in the medium-scale method).

   [X,FVAL,EXITFLAG,OUTPUT]=FMINUNC(FUN,X0,...) returns a structure OUTPUT
   with the number of iterations taken in OUTPUT.iterations, the number
   of function evaluations in OUTPUT.funcCount, the algorithm used in
   OUTPUT.algorithm, the number of CG iterations (if used) in
   OUTPUT.cgiterations, the first-order optimality (if used) in
   OUTPUT.firstorderopt, and the exit message in OUTPUT.message.

   [X,FVAL,EXITFLAG,OUTPUT,GRAD]=FMINUNC(FUN,X0,...) returns the value
   of the gradient of FUN at the solution X.

   [X,FVAL,EXITFLAG,OUTPUT,GRAD,HESSIAN]=FMINUNC(FUN,X0,...) returns the
   value of the Hessian of the objective function FUN at the solution X.

   Examples
     FUN can be specified using @:
        X = fminunc(@myfun,2)

   where MYFUN is a MATLAB function such as:

       function F = myfun(x)
       F = sin(x) + 3;
```

```
   To minimize this function with the gradient provided, modify
   the MYFUN so the gradient is the second output argument:
     function [f,g]= myfun(x)
      f = sin(x) + 3;
      g = cos(x);
   and indicate the gradient value is available by creating an options
   structure with OPTIONS.GradObj set to 'on' (using OPTIMSET):
     options = optimset('GradObj','on');
     x = fminunc('myfun',4,options);

   FUN can also be an anonymous function:
     x = fminunc(@(x) 5*x(1)^2 + x(2)^2,[5;1])

  If FUN is parameterized, you can use anonymous functions to capture the problem-
  dependent parameters. Suppose you want to minimize the objective given in the
  function MYFUN, which is parameterized by its second argument A. Here MYFUN is
  an M-file function such as

   function [f,g] = myfun(x,a)

   f = a*x(1)^2 + 2*x(1)*x(2) + x(2)^2; % function
   g = [2*a*x(1) + 2*x(2)               % gradient
        2*x(1) + 2*x(2)];

  To optimize for a specific value of A, first assign the value to A. Then
  create a one-argument anonymous function that captures that value of A
  and calls MYFUN with two arguments. Finally, pass this anonymous function
  to FMINUNC:

   a = 3;                        % define parameter first
   options = optimset('GradObj','on'); % indicate gradient is provided
   x = fminunc(@(x) myfun(x,a),[1;1],options)
```

B.6 mesgencode.m

```
% SPRING 2004 - for thesis of Mirkan ALTAY
%it is refered from Efe YARDIMCI&Taner OKTAR project of 1998
% Modified by Gonul TURHAN SAYAN (June'99)
% MAIN PROGRAM FOR A GENETIC PROBLEM SOLVING ALGORITHM
%Modified for Mirkan Altay by G. Turhan-Sayan (March'04)
report=0;
mesfettype;
mesfetmodel;
 QZ = 0;
 QG = 0;
 clc;
 popsize = input('Population size: ');
 varnum = input('Number of variables: ');
 varsize = input('Bits per variable: ');
 pause;
  %Specify the lower and upper limits of variables
  for in=1:varnum;
 lowerv(in)=input('Enter lower limit for variable');
 upperv(in)=input('Enter upper limit for variable');
 cofa(in)=lowerv(in);
 cofb(in)=(upperv(in)-lowerv(in))/(pow2(varsize)-1);
 end;
```

```
 turnnum = input('Number of runs: ');
 chromsize = varnum*varsize;
 turns = 1;
 ef = input('Elitism (1/0): ');
 maximum = zeros(turnnum,10);
 clf;
mutcoeff = linspace(0.1,0.01,turnnum);

hold on;
  % POPULATION INITIALIZATION
pop = rand(popsize,chromsize+2);
   for  i = linspace(1,popsize,popsize);
   for  j = linspace(1,chromsize,chromsize);
    if  pop(i,j) < 0.5
         pop(i,j)=0;
     else pop(i,j) = 1;
    end;
   end;
  end;

  for  i = linspace(1,popsize,popsize);
   for  j = linspace(chromsize+1,chromsize+2,2);
    pop(i,j) = 0;
   end;
  end;
  % INITIAL EVALUATION
  for  ii = linspace(1,popsize,popsize)
   nch = pop(ii,1:chromsize+2);
   optim
   pop(ii,1:chromsize+2) = nch;
  end;
   turnin=1;
for turns = turnin:turnnum ;
 finished_turns = turns-1
 mutation_coefficient = mutcoeff(turns)
 pause(0.75);
 tic
% PLOT POPULATION FITNESSES
for  p = linspace(1,popsize,popsize);
 px(p) = pop(p,chromsize+2);
end;
px = sort(px);
p = linspace(1,popsize,popsize);
if rem(turns,6) == 0
     plot(p,px,'w')
  elseif rem(turns,6) == 1
     plot(p,px,'c')
  elseif rem(turns,6) == 2
     plot(p,px,'b')
  elseif rem(turns,6) == 3
     plot(p,px,'m')
  elseif rem(turns,6) == 4
     plot(p,px,'y')
  elseif rem(turns,6) == 5
     plot(p,px,'g')
   else end;
xlabel ('n');
ylabel ('Fitness of the (n)th chrom. in the population')
title ('CHROMOSOME FITNESSES IN ASCENDING ORDER')
% ROULETTE WHEEL PARENT SELECTION TECHNIQUE
```

```
 % First, sumation of the fitnesses:
Fitsum = 0;
for  i = linspace(1,popsize,popsize);
 Fitsum = Fitsum + pop(i,chromsize+2);
end;
  % Select best chromosome for copying into next generation
 % ( If Elitism factor ef = 1)
 %**************************
 if (ef==1)
  float = 0;
  for q = linspace(1,popsize,popsize)
   if pop(q,chromsize+2) > float
    float = pop(q,chromsize+2);
    place1 = q;
   else end;
  end;
 end
 %***************************
 % Initialize target population:
targpop = zeros(popsize,chromsize+2);
count = 0;
 while (count<popsize);
 % Select a reproducing Chromosome (first, generate n (0<n<Fitsum) )
 Fitsum = 0;
 for  i = linspace(1,popsize,popsize);
  Fitsum = Fitsum + pop(i,chromsize+2);
 end;
 n = rand*(Fitsum);
 flag1 = 0;
 dummysum = 0;
 i = 1;
 while flag1 ~= 1;
  dummysum = dummysum + pop(i,chromsize+2);
  if dummysum < n;
    i = i+1;
   else
   parent1 = pop(i,1:chromsize);
   pop(i,chromsize+1) = pop(i,chromsize+1) + 1;
   flag1 = 1;
  end;
 end;
 count = count + 1;
  % Select second reproducing Chromosome the same way:
  Fitsum = 0;
 for  i = linspace(1,popsize,popsize);
  Fitsum = Fitsum + pop(i,chromsize+2);
 end;
 n = rand*(Fitsum);
 flag2 = 0;
 dummysum = 0;
 i = 1;
 while flag2 ~= 1;
  dummysum = dummysum + pop(i,chromsize+2);
  if dummysum < n;
   i = i+1;
  else
   parent2 = pop(i,1:chromsize+2);
   pop(i,chromsize+1) = pop(i,chromsize+1) + 1;
   flag2 = 1;
  end;
```

```
 end;
 % One point Crossover:
 r = rand*(chromsize);
 n = ceil(r);
 for k = linspace(1,n,n)
  child1(k) = parent1(k);
  child2(k) = parent2(k);
 end;
 for k = linspace(n,chromsize,chromsize-n+1)
  child1(k) = parent2(k);
  child2(k) = parent1(k);
 end;
  % Applying Mutation to the Offspring Chromosomes:
 mch = child1;
 mut4n;
 child1 = mch;
 mch = child2;
 mut4n;
 child2 = mch;
 targpop(count,1:chromsize) = child1(1:chromsize);
 targpop(count+1,1:chromsize) = child2(1:chromsize);
 count=count+1;
end;
  % 10 MOSTLY SELECTED  CHROMOSOMES
   nthch = 1;
   for j = 1:10
       max = 0;
       for i = 1:popsize
           if max < pop(i,chromsize+1);
                max = pop(i,chromsize+1);
                nthch = i;
           else end;
       end;
       maximum(turns,j) =pop(nthch,chromsize+1);
       pop(nthch,chromsize+1) = 0;
   end;
 % APPLICATION OF ELITISM :
 s = ceil(rand*popsize);
 if (ef ==1 )
  targpop(s,1:chromsize+2) = pop(place1,1:chromsize+2);
  else end;
pop = targpop;
 % CLOSENESS EVALUATION-
for  f = linspace(1,popsize,popsize);
 nch = pop(f,1:chromsize+2);
 optim;
 pop(f,1:chromsize+2) = nch;
end
 % -AND STORE BEST RESULTS
 float = 0;
 for v = linspace(1,popsize,popsize)
  if pop(v,chromsize+2) > float
   float = pop(v,chromsize+2);
   place = v;
  else end;
 end;
  %The BEST CHROMOSOME of the current iteration
  nch = pop(place,1:chromsize+2);
  if turns==turnnum
    report=1;
```

```
   % Summarize the results at the end of each turn
 end;
  optim
  if turns==turnnum
   % Summarize the results at the end of each turn
   turns
   place
   uact
   pop(place,chromsize+2)
 end;
 for g=1:varnum
   QZ(g,turns) = U(g);
   QG(g,turns) = uact(g);
 end;
toc
end;
% PLOT FINAL POPULATION FITNESSES
pause(1.90);
%turns = turns +1;
for  p = linspace(1,popsize,popsize);
 px(p) = abs(pop(p,chromsize+2));
end;
px = sort(px);
p = linspace(1,popsize,popsize);
plot(p,px,'r')
xlabel ('n');
ylabel ('Fitness of the (n)th chrom. in the population')
title ('CHROMOSOME FITNESSES IN ASCENDING ORDER')
QG
```

B.7 optim.m

```
k=nch;
U=zeros(varnum,1);
for jj=1:varnum
 for jjj=linspace((jj*varsize),((jj-1)*varsize)+1,varsize)
  U(jj)=U(jj)+pow2(rem((jjj+varsize-1),varsize))*k( (( (2*jj)-1 )*varsize)+1-jjj);
 end;
end;
if (gf > 0)
 for i = 1:varnum
   U(i) =grey(U(i));
 end;
else end;
%****************************************
for ig=1:varnum
   uact(ig)=cofa(ig)+cofb(ig)*U(ig);
end;
% ****************************************
%
%  This code assumes that the followings are available:
%  # of variables = VARNUM
%  actual values of variables = UACT Array of size VARNUM
%  The variables (in order) are: ALFA,GAMMA,LAMDA,VT0 etc.
%  IDSMEAS: Measurement Data Matrix of size (IDM,IDN)
%mod=1;
%modelling;
[IDM,IDN]=size(IDSMEAS);
cost=0;
if model==1
```

```
 %CURTICE MODEL
%*****************************************************************
for ii=1:IDM
   for jj=1:IDN
       Vdsintrinsic(jj)=VDS(jj)-(Rs+Rd)*IDSMEAS(ii,jj);
       Vgsintrinsic(ii)=VGS(ii)-Rs*IDSMEAS(ii,jj);
       %if (Vgsintrinsic(ii)+uact(2))>=0
       IDS(ii,jj)=uact(1)*(Vgsintrinsic(ii)-
uact(2))^2*(1+uact(3)*Vdsintrinsic(jj))*tanh(uact(4)*Vdsintrinsic(jj));
       %uact(1)=beta uact(2)=Vto uact(3)=lambda uact(4)=alpha
       %elseif (Vgsintrinsic(ii)+uact(2))<0
       %IDS(ii,jj)=0;
       %end
      cost=cost+(IDS(ii,jj)-IDSMEAS(ii,jj))^2;
  end;
end;
%*****************************************************************elseif model==2
   %MATERKA&KACPRZAK model;
%*****************************************************************
    for ii=1:IDM
     for jj=1:IDN
        Vdsintrinsic(jj)=VDS(jj)-(Rs+Rd)*IDSMEAS(ii,jj);
        Vgsintrinsic(ii)=VGS(ii)-Rs*IDSMEAS(ii,jj);
        Vt=uact(2)+uact(4)*Vdsintrinsic(jj); %uact(2)=Vto uact(4)=gamma
        IDS(ii,jj)=uact(1).*(1-Vgsintrinsic(ii)/Vt)^2.*tanh(uact(3).*Vdsintrinsic(jj)/(Vgsintrinsic(ii)-
Vt)); %uact(1)=IDSS uact(3)=alpha
        cost=cost+(IDS(ii,jj)-IDSMEAS(ii,jj))^2;
     end
 end
 %*****************************************************************
elseif model==3
   %tom2model;
%*****************************************************************
   for ii=1:IDM
   for jj=1:IDN
      Vdsintrinsic(jj)=VDS(jj)-(Rs+Rd)*IDSMEAS(ii,jj);
      Vgsintrinsic(ii)=VGS(ii)-Rs*IDSMEAS(ii,jj);
      %if Vf>0  IDSO(ii,jj)=a*beta*(Vf^Q)*alpha*Vdsintrinsic(jj)/sqrt(1+alpha^2*Vdsintrinsic(jj)^2);
       %elseif Vf<0
      %    IDSO(ii,jj)=0;
      %end
      %IDS(ii,jj)=IDSO(ii,jj)/(1+delta*Vdsintrinsic(jj)*IDSO(ii,jj));
      Vg=uact(1)*uact(2)*log(exp((Vgsintrinsic(ii)-
uact(3)+uact(4)*Vdsintrinsic(jj))/(uact(1)*uact(2)))+1); %uact(1)=Q  uact(2)=Vst uact(3)=Vto
uact(4)=gamma

IDSO=uact(5)*uact(6)*Vg^uact(1)*uact(7)*Vdsintrinsic(jj)/sqrt(1+uact(7)^2*Vdsintrinsic(jj)^2);
%uact(5)=w uact(6)=beta uact(7)=alpha
      IDS(ii,jj)=IDSO/(1+uact(8)*Vdsintrinsic(jj)*IDSO); %uact(8)=delta
      cost=cost+(IDS(ii,jj)-IDSMEAS(ii,jj))^2;
  end;
end;
  %*****************************************************************
  elseif model==4
   %curticeettenbergmodel;
  %*****************************************************************
    for ii=1:IDM
   for jj=1:IDN
      Vdsintrinsic(jj)=VDS(jj)-(Rs+Rd)*IDSMEAS(ii,jj);
      Vgsintrinsic(ii)=VGS(ii)-Rs*IDSMEAS(ii,jj);
```

```
      V1(ii,jj)=Vgsintrinsic(ii)*(1+uact(1)*(uact(7)-Vdsintrinsic(jj))); %uact(1)=beta uact(7)=Vdso

IDS(ii,jj)=(uact(2)+uact(3)*V1(ii,jj)+uact(4)*V1(ii,jj)^2+uact(5)*V1(ii,jj)^3)*tanh(uact(6)*Vdsintrin
sic(jj));
      %uact(2)=A0 uact(3)=A1 uact(4)=A2 uact(5)=A3 uact(6)=gamma
      cost=cost+(IDS(ii,jj)-IDSMEAS(ii,jj))^2;
   end
  end
    %*****************************************************************
elseif model==5
   %tajimamodel;
   %*****************************************************************
   for ii=1:IDM
    for jj=1:IDN
    Vdsintrinsic(jj)=VDS(jj)-(Rs+Rd)*IDSMEAS(ii,jj);
    Vgsintrinsic(ii)=VGS(ii)-Rs*IDSMEAS(ii,jj);
    VGS1(ii)=Vgsintrinsic(ii)-uact(1);  %VBI=uact(1);
    Vp(jj)=uact(2)+uact(3)*Vdsintrinsic(jj)+uact(1); %Vpo=uact(2) - p=uact(3);
    k=1-(1/uact(4))*(1-exp(-uact(4))); %m=uact(4);
    IDS2(ii,jj)=uact(5)*(1-exp((-Vdsintrinsic(jj)/uact(6))-uact(7)*(Vdsintrinsic(jj)/uact(6))^2-
uact(8)*(Vdsintrinsic(jj)/uact(6))^3)); %IDSP=uact(5)  VDSS=uact(6)  a=uact(7)  b=uact(8);
    IDS1(ii,jj)=(1/k)*(1+(VGS1(ii)/Vp(jj))-(1/uact(4))+((1/uact(4))*exp(-
uact(4)*(1+(VGS1(ii)/Vp(jj))))));
    IDS(ii,jj)=IDS1(ii,jj)*IDS2(ii,jj);
    cost=cost+(IDS(ii,jj)-IDSMEAS(ii,jj))^2;
    end
 end
   %*****************************************************************
elseif model==6
   %Tommodel;
   %*****************************************************************
   for ii=1:IDM
    for jj=1:IDN
       Vdsintrinsic(jj)=VDS(jj)-(Rs+Rd)*IDSMEAS(ii,jj);
       Vgsintrinsic(ii)=VGS(ii)-Rs*IDSMEAS(ii,jj);
       Vt(ii,jj)=Vto-gammadc*Vdsintrinsic(jj);
       if Vdsintrinsic(jj)<(3/uact(1))
          IDS1(ii,jj)=uact(2).*(Vgsintrinsic(ii)-Vt(ii,jj)).^uact(4).*(1-(1-
uact(1).*Vdsintrinsic(jj)/3).^3);
          %uact(1)=alpha   uact(2)=beta  uact(3)=delta  uact(4)=Q
       else
          IDS1(ii,jj)=uact(2).*(Vgsintrinsic(ii)-Vt(ii,jj)).^uact(4);
       end
      IDS(ii,jj)=IDS1(ii,jj)./(1+uact(3).*Vdsintrinsic(jj).*IDS1(ii,jj));
      cost=cost+(IDS(ii,jj)-IDSMEAS(ii,jj))^2;
    end
 end
  %*****************************************************************
  elseif model==7
   %statzmodel;
   %*******************************************************************
   for ii=1:IDM
    for jj=1:IDN
       Vdsintrinsic(jj)=VDS(jj)-(Rs+Rd)*IDSMEAS(ii,jj);
       Vgsintrinsic(ii)=VGS(ii)-Rs*IDSMEAS(ii,jj);
       if 0<Vdsintrinsic(jj) & Vdsintrinsic(jj)<(3/uact(4))
       IDS(ii,jj)=[(uact(1)*((Vgsintrinsic(ii)-uact(2))^2))/(1+(uact(5)*Vgsintrinsic(ii)-uact(2)))]*[1-(1-
(uact(4)*Vdsintrinsic(jj)/3))^3]*(1+uact(3)*Vdsintrinsic(jj));
    elseif Vdsintrinsic(jj)>(3/uact(4))
       IDS(ii,jj)=[(uact(1)*((Vgsintrinsic(ii)-uact(2))^2))/(1+(uact(5)*Vgsintrinsic(ii)-
```

```
uact(2)))]*(1+uact(3)*Vdsintrinsic(jj));
      else
      end
  cost=cost+(IDS(ii,jj)-IDSMEAS(ii,jj))^2;
      end
    end
    %*****************************************************************
elseif model==8
    %Angelov Model
    %*****************************************************************
     for ii=1:IDM
      for jj=1:IDN
          Vdsintrinsic(jj)=VDS(jj)-(Rs+Rd)*IDSMEAS(ii,jj);
          Vgsintrinsic(ii)=VGS(ii)-Rs*IDSMEAS(ii,jj);
          Vpk=uact(4)+uact(5)*Vdsintrinsic(jj);   %Vpko=uact(4)   gamma=uact(5)
          Phi=uact(1)*(Vgsintrinsic(ii)-Vpk)+uact(2)*(Vgsintrinsic(ii)-Vpk)^2+uact(3)*(Vgsintrinsic(ii)-
Vpk)^3;
          %uact(1)=P1 uact(2)=P2 uact(3)=P3
          IDS(ii,jj)=uact(6)*(1+tanh(Phi))*(1+uact(7)*Vdsintrinsic(jj))*tanh(uact(8)*Vdsintrinsic(jj));
          %uact(6)=Ipk uact(7)=lambda uact(8)=alpha;
          cost=cost+(IDS(ii,jj)-IDSMEAS(ii,jj))^2;
       end
  end
     %*****************************************************************
end
% Map the cost-to be minimized to a fitness-to be maximized
% The parameters fmin and fmax MUST be pre-defined.
% Assuming costmin=0  and  costmax=1, a linear mapping is:
fitness=1/(cost+0.00000001);
% Now, keep the fitness in the last entry of the chromosome
 nch(1,chromsize+2) = fitness;
```

B.8 mut4n.m

```
k=mch;
for q=1:chromsize;
   c=rand;
   if c <= mutcoeff(turns)
      if k(1,q) == 0
         mch(1,q) = 1;
      else
         mch(1,q) = 0;
      end;
    else end;
end;
```